Research Progress and Accomplishments

2000 – 2001

A Selection of Papers Chronicling Technical Achievements of the Multidisciplinary Center for Earthquake Engineering Research

The Multidisciplinary Center for Earthquake Engineering Research

The Multidisciplinary Center for Earthquake Engineering Research (MCEER) is a national center of excellence in advanced technology applications that is dedicated to the reduction of earthquake losses nationwide. Headquartered at the University at Buffalo, State University of New York, the Center was originally established by the National Science Foundation (NSF) in 1986, as the National Center for Earthquake Engineering Research (NCEER).

Comprising a consortium of researchers from numerous disciplines and institutions throughout the United States, the Center's mission is to reduce earthquake losses through research and the application of advanced technologies that improve engineering, pre-earthquake planning and post-earthquake recovery strategies. Toward this end, the Center coordinates a nationwide program of multidisciplinary team research, education and outreach activities.

Funded principally by NSF, the State of New York and the Federal Highway Administration (FHWA), the Center derives additional support from the Federal Emergency Management Agency (FEMA), other state governments, academic institutions, foreign governments and private industry.

Research Progress and Accomplishments

2000 - 2001

Multidisciplinary Center for Earthquake Engineering Research
University at Buffalo, State University of New York

May 2001

MCEER-01-SP01
Red Jacket Quadrangle, Buffalo, New York 14261
Tel: (716) 645-3391; Fax: (716) 645-3399; Email: *mceer@acsu.buffalo.edu*
World Wide Web: *http://mceer.buffalo.edu*

Foreword

by George C. Lee, Director,
Multidisciplinary Center for Earthquake Engineering Research

The vision of the Multidisciplinary Center for Earthquake Engineering Research (MCEER) is to help foster activities that will lead to more earthquake resilient communities. Its mission is to discover, nurture, develop, promote, help implement, and in some instances pilot test, innovative measures and advanced and emerging technologies to reduce losses in future earthquakes in a cost-effective manner. Research findings show that relatively new buildings and infrastructure that are designed and constructed to the current state-of-practice in earthquake engineering perform significantly better than older ones during earthquakes, and that the largest threat to society lies in the seismically vulnerable infrastructure designed and constructed at a time when earthquake-resistant design had not yet matured.

With that knowledge in mind, it is MCEER's view that the best way of achieving the stated vision of earthquake resilient communities in the short term is to invest in two focused system-integrated endeavors: the rehabilitation of critical infrastructure facilities that society will need and expect to be operational following an earthquake, more specifically hospitals and lifelines; and the improvement of emergency response and crisis management capabilities to ensure efficient response and appropriate recovery strategies following earthquakes.

MCEER works with the entire earthquake loss reduction community, which consists of practicing engineers and other design professionals, policy makers, regulators and code officials, facility and building owners, governmental entities, and other stakeholders who have responsibility for loss reduction decision making, to ensure that research results are implemented to improve safety and advance earthquake loss reduction for government, private industry, and the public-at-large.

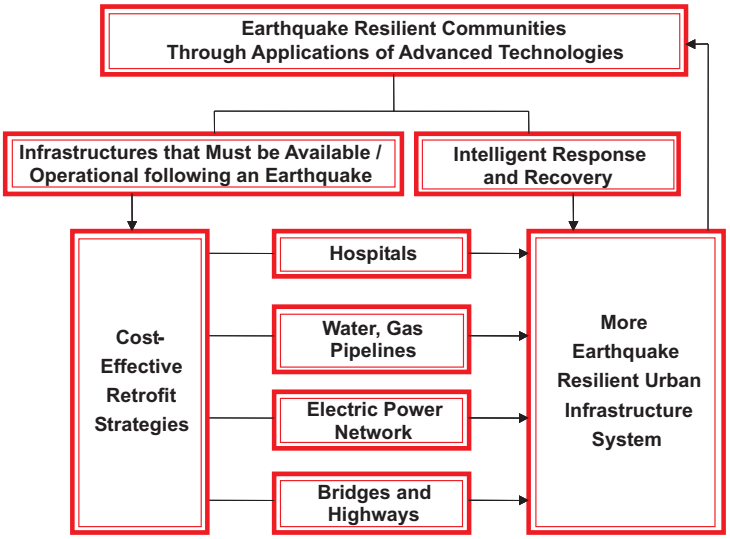

The flowchart above schematically shows how the Center's research interests contribute collectively to achieve the vision of more earthquake resilient communities. The papers in this volume

highlight efforts in intelligent response and recovery, hospitals, water and gas pipelines, electric power networks, and bridges and highways. These studies involve many different disciplines, whose work will cohesively join together toward successful implementation of design and retrofit techniques to protect urban infrastructures from earthquake damage.

This report is the third in our annual compilation of research progress and accomplishments. It is available in both printed and electronic form (on our web site in PDF format at *http://mceer.buffalo.edu/publications/default.asp*, under Special Publications).

If you would like more information on any of the studies presented herein, or on other MCEER research or educational activities, you are encouraged to contact us by telephone at (716) 645-3391, facsimile (716) 645-3399, or email at *mceer@acsu.buffalo.edu.*

Contents

Contributors

Tarek H. Abdoun, Research Assistant Professor, Civil and Environmental Engineering Department, Rensselaer Polytechnic Institute

Daniel J. Alesch, Professor, Department of Public and Environmental Affairs, University of Wisconsin – Green Bay

Michael Augustyniak, Supervising Planner, New Jersey State Police Office of Emergency Management

Timothy Bond, Laboratory Manager, Department of Civil and Environmental Engineering, Cornell University

Michel Bruneau, Deputy Director, Multidisciplinary Center for Earthquake Engineering Research and Professor, Department of Civil, Structural and Environmental Engineering, University at Buffalo

Ian G. Buckle, Professor, Department of Civil Engineering, University of Nevada, Reno

Sungbin Cho, Research Associate, School of Policy, Planning and Development, University of Southern California

Michael C. Constantinou, Professor and Chair, Department of Civil, Structural and Environmental Engineering, University at Buffalo

Chris Cyr, Undergraduate Student, Wharton Risk Management and Decision Processes Center, The Wharton School, University of Pennsylvania

Andrea S. Dargush, Associate Director for Education and Research Administration, Multidisciplinary Center for Earthquake Engineering Research

Gary F. Dargush, Associate Professor, Department of Civil, Structural and Environmental Engineering, University at Buffalo

George Deodatis, Professor, Civil Engineering & Operations Research Department, Princeton University

Ricardo Dobry, Professor, Civil and Environmental Engineering Department, Rensselaer Polytechnic Institute

Gang Dong, Post-Doctoral Research Associate, Department of Civil, Structural and Environmental Engineering, University at Buffalo

Ronald T. Eguchi, President, ImageCat, Inc.

Selahattin Ersoy, Graduate Student, Department of Civil and Environmental Engineering, New Jersey Institute of Technology

Maria Q. Feng, Associate Professor, Civil and Environmental Engineering Department, University of California, Irvine

Ian. M. Friedland, Associate Director for Development, Applied Technology Council

Patricia M. Gallagher, Assistant Professor, Department of Civil and Architectural Engineering, Drexel University

Siang-Huat Goh, Research Assistant, Department of Civil and Environmental Engineering, Cornell University

Juan Gomez, Graduate Student, Department of Civil, Structural and Environmental Engineering, University at Buffalo

Patricia Grossi, Post-Doctoral Researcher, Wharton Risk Management and Decision Processes Center, The Wharton School, University of Pennsylvania

Benedikt Halldorsson, Graduate Student, Department of Civil, Structural and Environmental Engineering, University at Buffalo

Masanori Hamada, Professor, Department of Civil Engineering, Waseda University, Japan

Wilhelm Hammel, Senior Consultant, KPMG, Germany

Charles K. Huyck, Vice President, ImageCat, Inc.

Klaus H. Jacob, Senior Reserch Scientist, Seismology Department, Geology and Tectonics, Lamont-Doherty Earth Observatory

Sang-Soo Jeon, Graduate Research Assistant, Department of Civil and Environmental Engineering, Cornell University

Yasuo Kitane, Graduate Student, Department of Civil, Structural and Environmental Engineering, University at Buffalo

Howard Kunreuther, Co-director, Wharton Risk Management and Decision Processes Center, The Wharton School, University of Pennsylvania

George C. Lee, Director, Multidisciplinary Center for Earthquake Engineering Research and Samuel P. Capen Professor of Engineering, Department of Civil, Structural and Environmental Engineering, University at Buffalo

Li Lin, Associate Professor, Department of Industrial Engineering, University at Buffalo

Wei Liu, Ph.D. Candidate, Department of Civil, Structural and Environmental Engineering, University at Buffalo

James Mason, Graduate Research Assistant, Department of Civil and Environmental Engineering, Cornell University

Ronald L. Mayes, Independent Consultant, Moraga, California

Laura McGinty, GIS Specialist, Westchester County Geographic Information Systems, Department of Information Technology

James K. Mitchell, University Distinguished Professor Emeritus, Department of Civil Engineering, Virginia Polytechnic Institute and State University

James E. Moore, III, Associate Professor, Departments of Civil Engineering and Public Policy and Management, University of Southern California

Nobuo Murota, Bridgestone Company, Japan

George Mylonakis, Assistant Professor, Department of Civil Engineering, City University of New York

Guy J.P. Nordenson, Associate Professor, Civil Engineering & Operations Research Department, Princeton University

Daniel O'Brien, Earthquake Program Manager, New York State Emergency Management Office

Yasuhide Okuyama, Assistant Professor, Department of Architecture and Planning, University at Buffalo

Thomas D. O'Rourke, Thomas R. Briggs Professor of Engineering, Department of Civil and Environmental Engineering, Cornell University

Apostolos Papageorgiou, Professor, Department of Civil, Structural and Environmental Engineering, University at Buffalo

William J. Petak, Professor, School of Policy, Planning and Development, University of Southern California

Rajesh Radhakrishnan, Graduate Student, Department of Civil, Structural and Environmental Engineering, University at Buffalo

Oscar Ramirez, Graduate Student, Department of Civil, Structural and Environmental Engineering, University at Buffalo

Ricardo Ramos, Graduate Student, Civil and Environmental Engineering Department, Rensselaer Polytechnic Institute

Andrei Reinhorn, Professor, Department of Civil, Structural and Environmental Engineering, University at Buffalo

M. Ala Saadeghvaziri, Associate Professor, Department of Civil and Environmental Engineering, New Jersey Institute of Technology

Ramesh Sant, Ph.D. Candidate, Department of Civil, Structural and Environmental Engineering, University at Buffalo

Masanobu Shinozuka, Fred Champion Chair in Civil Engineering, Department of Civil Engineering, University of Southern California

Ani N. Sigaher, Ph.D. Candidate, Department of Civil, Structural and Environmental Engineering, University at Buffalo

Mettupalayam Sivaselvan, Ph.D. Candidate, Department of Civil, Structural and Environmental Engineering, University at Buffalo

Scott Stanford, Geologist, New Jersey Geological Survey

Ernest Sternberg, Associate Professor, Department of Architecture and Planning, University at Buffalo

Bruce Swiren, Natural Hazards Program Specialist, Federal Emergency Management Agency, Region II

Michael W. Tantala, Ph.D. Candidate, Civil Engineering & Operations Research Department, Princeton University

Wendy Tao, Undergraduate Student, Wharton Risk Management and Decision Processes Center, The Wharton School, University of Pennsylvania

Craig E. Taylor, President, Natural Hazards Management, Inc.

Mai Tong, Senior Research Scientist, Multidisciplinary Center for Earthquake Engineering Research and the Department of Civil, Structural and Environmental Engineering, University at Buffalo

Panos Tsopelas, Assistant Professor, Catholic University of America

Emmanuel Velivasakis, Senior Vice President, LZA Technology

Darren Vian, Ph.D. Candidate, Department of Civil, Structural and Environmental Engineering, University at Buffalo

Jon S. Walton, Vice President, MacFarland Walton Enterprises

Yinjuang Wang, Graduate Student, Civil and Environmental Engineering Department, Rensselaer Polytechnic Institute

Sam Wear, GIS Manager, Westchester County Geographic Information Systems, Department of Information Technology

Stuart D. Werner, Principal, Seismic Systems and Engineering Consultants

Andrew S. Whittaker, Associate Professor, Department of Civil, Structural and Environmental Engineering, University at Buffalo

Katrin Winkelmann, Visiting Research Associate, Department of Civil, Structural and Environmental Engineering, University at Buffalo, from the University of Darmstadt

Eric Wolff, Graduate Research Assistant, Department of Civil, Structural and Environmental Engineering, University at Buffalo

Yihui Wu, Research Scientist, Multidisciplinary Center for Earthquake Engineering Research and the Department of Civil, Structural and Environmental Engineering, University at Buffalo

Tony Yang, Undergraduate Student, Department of Civil, Structural and Environmental Engineering, University at Buffalo

Koji Yoshizaki, Pipeline Engineer, Fundamental Technology Laboratory, Tokyo Gas Company, Ltd., Japan

Earthquake Motion Input and Its Dissemination Via the Internet

by Apostolos S. Papageorgiou (Principal Author), Benedikt Halldorsson and Gang Dong

Research Objectives

The objectives of this task are to conduct research on seismic hazards, and provide relevant input on the expected levels of these hazards to other tasks. Other tasks requiring this input include those dealing with inventory, fragility curves, rehabilitation strategies and demonstration projects. The corresponding input is provided in various formats depending on the intended use: as peak ground motion parameters and/or response spectral values for a given magnitude, epicentral distance and site conditions; or as time histories for scenario earthquakes that are selected based on the disaggregated seismic hazard mapped by the U.S. Geological Survey and used in the *NEHRP Recommended Provisions for the Development of Seismic Regulations for New Buildings* (BSSC, 1998).

Sponsors

National Science Foundation, Earthquake Engineering Research Centers Program

Research Team

***Apostolos S. Papageorgiou**, Professor, **Gang Dong**, Post-Doctoral Research Associate, and **Benedikt Halldorsson**, Graduate Student, Department of Civil, Structural and Environmental Engineering, University at Buffalo*

Prediction of the seismic hazard in tectonic regions of moderate-to-low seismicity is a difficult task because of the paucity of data that are available regarding such regions. Specifically, the problem of earthquake ground motion prediction in Eastern North America (ENA) is hindered by two factors: (1) the causative structures of seismicity in ENA are largely unknown, and (2) the recorded strong motion database is very limited (if at all existent), especially for moderate to large magnitude ($M_W \geq 6$) events virtually for all epicentral distances. For these reasons, prediction of strong ground motion in ENA makes the use of well-founded physical models imperative. These models should, among other things, provide the means to make extrapolations to large magnitudes and/or short distances with confidence. (This is contrast to the western U.S. (WUS), where the abundance of recorded strong motion data makes prediction of ground motion by empirical methods a viable procedure.)

Strong Motion Synthesis Techniques

Our task is the synthesis of strong ground motion input over the entire frequency range of engineering interest. There are two approaches for modeling earthquake strong motion:

Links to Current Research

Program 1: Seismic Evaluation and Retrofit of Lifeline Systems

Program 2: Seismic Retrofit of Hospitals

(1) The *Stochastic (Engineering) Approach*, according to which, earthquake motion (acceleration) is modeled as Gaussian noise with a spectrum that is either empirical, or a spectrum that is based on a physical model (such as the *Specific Barrier Model*) of the earthquake source. This approach is expedient and therefore cost-effective, and has been extensively used in the past by engineers (using empirical spectra) and recently by seismologists (using spectra derived from physical models of the source). The intent of this approach to strong motion simulation is to capture the essential characteristics of high-frequency motion at an average site from an average earthquake of specified size. Phrasing this differently, the accelerograms artificially generated using the *Engineering Approach* do not represent any specific earthquake but embody certain average properties of past earthquakes of a given magnitude.

(2) The *Kinematic Modeling Approach* was developed by seismologists. In this approach, the rupture process is modeled by postulating a slip function on a fault plane and then using the Elastodynamic Representation Theorem to compute the motion (e.g., Aki and Richards, 1980). There are several variant forms of this approach depending on whether the slip function (i.e., the function that describes the evolution of slip on the fault plane) and/or the Green functions are synthetic or empirical. The *Kinematic Modeling Approach* involves the prediction of motions from a fault that has specific dimensions and orientation in a specified geologic setting. As such, this approach more accurately reflects the various wave propagation phenomena and is useful for site-specific simulations.

Stochastic (Engineering) Approach

Recognizing that the *Stochastic Approach* for synthesizing earthquake strong motion time histories is the most expedient method, ground motion synthesis efforts were initiated with this approach. The following computer codes have been developed, and are available to any interested user via the Internet:

1. *SGMP_ENA - Stochastic Ground Motion Prediction for Eastern North America: Random Vibration Theory (RVT):* is used to estimate the mean/expected values of peak ground motion parameters (i.e., peak acceleration, peak velocity and peak

The user community for this research is both academic researchers and practicing engineers who may use the seismic input generated by the synthesis techniques that are developed under this task for a variety of applications. These include ground motions for scenario earthquakes, for developing fragility curves and in specifying ground motion input for critical facilities (such as hospitals) located in the eastern U.S.

displacement), and spectral response amplitudes (e.g., Rice, 1944, 1945; Cartwright and Longuet-Higgins, 1956; Shinozuka and Yang, 1971; Soong and Grigoriu, 1993).

2. *SGMS_ENA - Stochastic Ground Motion Simulation for Eastern North America:* Synthetic ground motions are generated using the *Stochastic (Engineering) Approach* briefly described above (e.g., Shinozuka and Jan, 1972; Shinozuka and Deodatis, 1991; Boore, 1983; Grigoriu, 1995).
3. *RSCTHS – Response Spectrum Compatible Time Histories:* Synthesis of ground motion time histories that are compatible with prescribed response spectra using the *Spectral Representation Method* (Deodatis, 1996).

Various earthquake source models that have been proposed in the published literature [such as the *Specific Barrier Model* (Papageorgiou and Aki, 1983a,b; 1985; 1988) and the ω^2-model (Brune, 1970; Frankel et al., 1996)], have been implemented (and are provided as options) in computer codes *SGMP_ENA* and *SGMS_ENA*. [Both computer codes predict/synthesize ground motions that are compatible with the site classifications of the 1997 NEHRP Provisions (BSSC, 1998).]

Of all the source models, the *Specific Barrier Model* is favored because it provides the most complete, yet parsimonious, self-consistent description of the faulting processes that are responsible for the generation of the high frequencies, and at the same time provides a clear and unambiguous way of how to distribute the seismic moment on the fault plane. The latter requirement is necessary for the implementation of the *Kinematic Modeling Approach* described above. We calibrated the *Specific Barrier Model* using the available strong motion data base of ENA earthquakes, as well as inferred source spectra for the 25 November 1988 Saguenay earthquake (M_w 5.8) and 19 October 1990 Mont Laurier earthquake (M_w 4.5) Quebéc, Canada. The estimates of the global and local stress drops that resulted from the calibration are believed to be representative of earthquake sources in ENA. Thus, a "scaling law" of the source spectra of ENA earthquakes has been established. Such a "scaling law" allows the prediction/synthesis of ground motion at magnitude-distance ranges that currently are not cov-

Web Sites

Engineering Seismology Laboratory:
http://civil.eng.buffalo.edu/engseislab/

USGS National Seismic Hazards Project of the Earthquake Hazards Program:
http://geohazards.cr.usgs.gov/eq/

■ Table 1. Scenario Earthquake Events for Six Oscillator Periods for New York, NY

Period (s)	0.1	0.2	0.33	0.5	1.0	2.0
M_w	4.8	4.8	5.7	5.7	6.2	6.2
R (km)	12	12	33	33	34	34
(factor)	0.712	1.253	1.458	1.692	1.170	1.999

Notes:

M_w = Moment Magnitude
R (km) = Epicentral Distance
(factor) = scaling factor used to adjust/scale the synthetic ground motions of the modal event so that they are compatible with the Uniform Hazard Spectrum

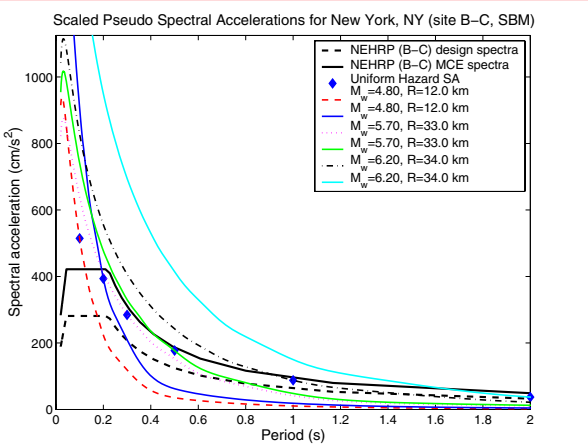

■ Figure 1. This figure displays: (1) The Pseudo-Spectral Acceleration (PSA) spectra of the *scenario events* tabulated in Table 1; (2) the *Uniform Hazard Spectrum*, which is obtained from the PSHA; (3) the *Maximum Considered Earthquake (MCE)* spectrum as specified by the 1997 NEHRP Provisions on the basis of the "Uniform Hazard Spectrum"; (4) the *Design Basis Earthquake* spectrum, which is obtained by multiplying the amplitudes of the MCE spectrum by the factor (2/3).

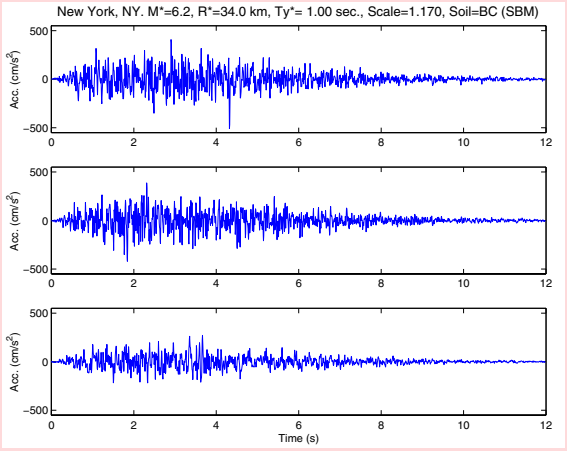

■ Figure 2. Scaled synthetic ground accelerations of the *scenario events* corresponding to oscillator periods 1.0 and 2.0 seconds. The soil conditions correspond to the boundary B-C of site classes of the 1997 NEHRP Provisions (BSSC, 1998).

ered by the existing strong motion database of ENA.

In order to make it more convenient for the practicing engineer/designer, the ground motion synthesis capabilities described above are linked with estimates of the seismic hazard produced by the US Geological Survey (USGS), the *National Seismic Hazards Project of the Earthquake Hazards Program (http://geohazards.cr.usgs.gov/eq)*. Specifically, the disaggregated seismic hazard (Frankel, 1995; Frankel et al., 1996; Harmsen et al., 1999; Harmsen and Frankel, 2001) for five cities in the eastern U.S. (Boston, MA; Buffalo, NY; Charleston, SC; Memphis, TN; and New York, NY) was obtained from the above USGS website. For each city/site, the disaggregated seismic hazard is expressed in the form of a *"modal event"* for each one of six selected oscillator periods (0.1, 0.2, 0.33, 0.5, 1.0 and 2.0 seconds) ["*modal event*" is the seismic event that makes the most significant contribution to the seismic hazard at a site for a specified oscillator period; each "*modal event*" is characterized/specified by a moment magnitude M_w and a distance R]. The spectral amplitude of the "*modal event*" at the corresponding oscillator period usually does not agree with the spectral amplitude of the *Uniform Hazard Spectra* that are produced by the *Probabilistic Seismic Hazard Analysis (PSHA)* and are incorporated in building codes. [Usually, for eastern North America, the amplitudes of the modal events are higher than the Uniform Hazard Spectra, while in the western U.S. the reverse is true]. Current practice recommends (Shome et al., 1998) to adjust/scale the entire spectrum of the "*modal event*" so that its spectral amplitude matches that of the *Uniform Hazard Spectrum* at the oscillator period to which it corresponds.

For each one of the selected five eastern North America cities, following the procedure briefly described above, we generated and posted on the web (*http://civil.eng.buffalo.edu/engseislab/*) a suite of ground motion realizations (*scenario earthquake* motions). [The site class used for these simulations is the B-C NEHRP site class (BSSC, 1998), which is the reference site condition for the USGS seismic hazard maps.] Furthermore, the ground motion synthesis computer codes discussed above are accessible and may be used to generate additional time histories, possibly for different soil conditions, if the user deems it necessary.

As an example, consider New York, NY. Table 1 shows the six "scenario earthquake events" that have been selected (based on the disaggregated seismic hazard provided by USGS) for New York, corresponding to the six oscillator periods that were mentioned above and essentially cover the frequency range of interest for most practical applications.

Figure 1 displays the following: (1) the Pseudo-Spectral Acceleration (PSA) spectra of the abovementioned scenario events (the *Specific Barrier Model* was used as the source model); (2) the *Uniform Hazard Spectrum*, which is obtained from the PSHA; (3) the *Maximum Considered Earthquake (MCE)* spectrum as specified by the 1997 NEHRP Provisions (BSSC, 1998) on the basis of the *Uniform Hazard Spectrum*; (4) the *Design Basis Earthquake* spectrum, which is obtained by multiplying the amplitudes of the MCE spectrum by the factor (2/3). Note that a scenario event for a specific oscillator period has the same PSA value as the uniform hazard spectrum at that period.

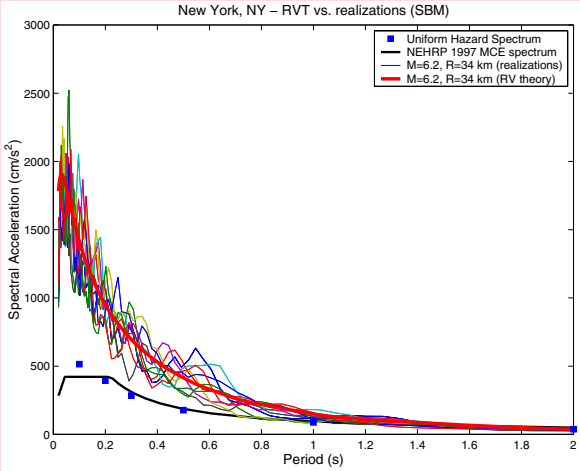

Figure 3. The PSA spectra of ten realizations of a *scenario event* are compared with the predictions of Random Vibration Theory

The scaled synthetic ground accelerations (two horizontal and one vertical components) of the *scenario events* corresponding to oscillator periods 1.0 and 2.0 seconds are displayed in Figure 2. The soil conditions correspond to the boundary B-C of site classes of the 1997 NEHRP Provisions (BSSC, 1998).

The consistency between the predictions of RVT with the synthetic ground motions are demonstrated, as seen in Figure 3. The agreement, as anticipated, is very satisfactory.

Development of Kinematic Modeling Approach

Having completed the work related to the implementation of the *Stochastic (Engineering) Approach* of strong motion synthesis, efforts are now focused on the development of the *Kinematic Modeling Approach*. As discussed in

"The objective is to propose simple analytical functions to describe near source pulses. These descriptions will be readily useful to engineers and may be included in future versions of the building code."

previous research progress reports (Papageorgiou, 2000), two important elements are necessary for this method of ground motion synthesis: (1) *Sub-event models* which are used to synthesize composite earthquake events; (2) *Scattering effects of the lithosphere* which are very important for stable tectonic environments such as that of Eastern North America. We have made substantial progress regarding the first element. Specifically, we have derived closed form solutions for the seismic radiation of a new class of kinematic models (asymmetrical circular and elliptical crack models) that will be used to simulate sub-events in the synthesis of strong ground motion generated by large earthquake events. These results have been recently presented in a forum consisting primarily of seismologists (*"International Workshop on the Quantitative Prediction of Strong-Motion and the Physics of Earthquake Sources"* held in Tsukuba, Japan, Oct. 23 - 25, 2000) and were very well received. These results have been presented in papers recently submitted to the *Bulletin of the Seismological Society*.

Conclusions – Future Research

The efforts regarding the development and implementation of the *Kinematic Modeling Approach* to strong motion synthesis focus on the following aspects of the method:

- *Scattering effects of the lithosphere*: Scattering effects are a very important consideration in the synthesis of ground motion in ENA. We have initiated the collection of seismograms of small events that have been recorded in ENA (US and Canada) by various networks (including broadband, short period and strong motion networks) with the intention of performing analysis that will provide values of important parameters (e.g., quality factor, Q, and scattering coefficient g) of the scattering characteristics of the lithosphere in ENA. The objective is to synthesize results developed in the field of *Stochastic Seismology* with techniques for the generation of evolutionary stochastic processes developed in the field of *Probability Theory* [such as the *Spectral Representation* (Shinozuka and Deodatis, 1991, see also *Applied Non-Gaussian Processes* (Grigoriu, 1995)].
- *Variable size sub-events*: We have collected all the necessary literature related to Poisson Random Pulse Processes and are well positioned to investigate the consequences of using variable size sub-events on synthetic motions.
- *Sub-event Models*: We have made substantial progress in developing closed-form mathematical expressions of the far-field radiation of new kinematic models to represent the sub-events. We want to extent this line of research to other models of sub-events such as *asperity models*. We thus aim at creating a "library" of models of sub-events adequate to simulate the various modes of rupture of real faults.
- *Validation*: Any simulation method should be validated by comparing the synthetic seismograms against the recorded ones for as many earthquake events as possible. We have initiated

such validation comparisons using the 1988 Saguenay earthquake event as a case study.

- We intend to address also the issue of *near source* ground motions. In particular, there are two competing physical effects that would affect near-source ground motions in ENA: Earthquake sources in ENA are characterized by higher *stress drops* and shorter *rise times* as compared to corresponding motions in California. Thus ENA near-source "*killer pulses*" are expected to be stronger and of higher frequency (i.e., shorter duration). On the other hand, ENA earthquake sources appear to occur at greater depths and thus the source-to-station distance (and consequently geometric attenuation) is greater. It is of great practical significance to investigate which one of the above two effects dominates. The ultimate objective of such an investigation is to propose simple analytical functions to describe near source pulses. Such simple descriptions will be readily useful to engineers and may be included in future versions of the building code.
- Finally, in response to the needs of various MCEER investigators, we intend to provide ground motion synthesis capabilities for sites in the western U.S. (e.g., California). For this, we need to calibrate the *Specific Barrier Model* using the extensive strong motion database that exists for the above tectonic region. For this calibration, we plan to exploit some recent developments regarding the improved mathematical description of the geometric attenuation of ground motion in the vicinity of an extended earthquake source.

References

Aki, K. and Richards, P., (1980), *Quantitative Seismology: Theory and Methods,* Volume I, II, W. H. Freeman and Company, San Francisco, 948 pp.

Boore, D. M., (1983), "Stochastic Simulation of High-Frequency Ground Motions Based on Seismological Models of the Radiated Spectra," *Bull. Seism. Soc. Am.*, Vol. 73, pp. 1865-1894.

Brune, J. N., (1970), "Tectonic Stress and the Spectra of Seismic Shear Waves from Earthquakes," *J. Geophys. Res.*, Vol. 75, pp. 4997–5009.

Building Seismic Safety Council (BSSC) (1998), *1997 NEHRP Recommended Provisions for the Development of Seismic Regulation for New Buildings*, Federal Emergency Management Agency, Washington, D.C., FEMA 302.

Cartwright, D. E. and Longuet-Higgins, M. S., (1956), "The Statistical Distribution of the Maxima of a Random Function," *Proceedings of the Royal Statistical Society,* Vol. 237, pp. 212–232.

Deodatis, G., (1996), "Non-stationary Stochastic Vector Processes: Seismic Ground Motion Applications," *Prob. Eng. Mech.*, Vol. 11, pp. 149–167.

Frankel, A., (1995), "Mapping Seismic Hazard in the Central and Eastern United States," *Seism. Res. Lett.*, Vol. 66, pp. 8–21.

References (Con't)

Frankel, A., Mueller, C., Barnhard, T., Perkins, D., Leyendecker, E.V., Dickman, N., Hanson, S. and Hopper, M., (1996), *National Seismic-Hazard Maps: Documentation*, U.S. Geological Survey, Open-File Report 96-532, 110 pp.

Grigoriu, M., (1995), *Applied Non-Gaussian Processes*, Prentice Hall, Englewood Cliffs, NJ, 442 pp.

Harmsen, S. and Frankel, A., (2001), "Geographic Deaggregation of Seismic Hazard in the United States," Bull. Seism. Soc. Am., Vol. 91, pp. 13–26.

Harmsen, S., Perkins, D. and Frankel, A., (1999), "Deaggregation of Probabilistic Ground Motions in the Central and Eastern United States," Bull. Seism. Soc. Am., Vol. 89, pp. 1–13.

Papageorgiou, A. S., (2000), "Ground Motion Prediction Methodologies for Eastern North America," Research Progress and Accomplishments: 1999-2000, Multidisciplinary Center for Earthquake Engineering Research, University at Buffalo, pp. 63-69.

Papageorgiou, A. S., (1988), "On Two Characteristic Frequencies of Acceleration Spectra: Patch Corner Frequency and fmax," *Bull. Seism. Soc. Am.*, Vol. 78, pp. 509–529.

Papageorgiou, A. S. and Aki, K., (1983a), "A Specific Barrier Model for the Quantitative Description of Inhomogeneous Faulting and the Prediction of Strong Ground Motion. I. Description of the Model," Bull. Seism. Soc. Am., Vol. 73, pp. 693–722.

Papageorgiou, A. S. and Aki, K., (1983b), "A Specific Barrier Model for the Quantitative Description of Inhomogeneous Faulting and the Prediction of Strong Ground Motion. Part II. Applications of the Model," *Bull. Seism. Soc. Am.*, Vol. 73, pp. 953–978.

Papageorgiou, A. S. and Aki, K., (1985), "Scaling Law of Far-field Spectra Based on Observed Parameters of the Specific Barrier Model," *Pure Appl. Geophys.*, Vol. 123, pp. 354–374.

Rice, S. O., (1944), "Mathematical Analysis of Random Noise," *Bell Syst. Tech. J.*, Vol. 23, pp. 282–332.

Rice, S. O., (1945), "Mathematical Analysis of Random Noise (concluded)," *Bell Syst. Tech. J.*, Vol. 24, pp. 46–156.

Shinozuka, M. and Deodatis, G., (1991), "Simulation of Stochastic Processes by Spectral Representation," *Appl. Mech. Rev.*, ASME, Vol. 44, pp. 191–204.

Shinozuka, M. and Jan, C., (1972), "Digital Simulation of Random Processes and Its Applications," *J. Sound. Vib.*, Vol. 25, pp. 111–128.

Shinozuka, M. and Yang, J.-N., (1971), "Peak Structural Response to Non-stationary Random Excitations," *J. Sound Vib.*, Vol. 16, pp. 505–517.

Shome, N., Cornell, A., Bazzurro, P. and Carballo, J. E., (1998), "Earthquakes, Records and Nonlinear Response," *Earthquake Spectra*, Vol. 14, pp. 469–500.

Soong, T. T. and Grigoriu, M., (1993), *Random Vibration of Mechanical and Structural Systems*, Prentice-Hall, Englewood Cliffs, NJ, 402 pp.

Overcoming Obstacles to Implementation: Addressing Political, Institutional and Behavioral Problems in Earthquake Hazard Mitigation Policies

by Daniel J. Alesch and William J. Petak

Research Objectives

This project is aimed at bridging the three planes, from basic research, through enabling processes, to engineered systems. At the basic research plane, we have been working to improve our collective understanding about obstacles to implementing mitigation practices, owner decision processes (in connection with other MCEER projects), and public policy processes. At the level of enabling processes, we have been seeking to develop an understanding of how obstacles to greater mitigation can be overcome by improved policy design and processes. At the engineered systems plane, our work is intended to result in practical guidelines for devising policies and programs with appropriate motivation and incentives for implementing policies and programs once adopted.

This phase of the research has been aimed, first, at a thorough, multidisciplinary review of the literature concerning obstacles to implementation. Second, the research has focused on advancing the state of the art by developing means for integrating the insights offered by diverse perspectives on the implementation process from the several social, behavioral, and decision sciences. The research establishes a basis for testing our understanding of these processes in the case of hospital retrofit decisions.

Sponsors

National Science Foundation, Earthquake Engineering Research Centers Program

Research Team

***William J. Petak**, Professor, School of Policy, Planning, and Development, University of Southern California*

***Daniel J. Alesch**, Professor, Department of Public and Environmental Affairs, University of Wisconsin-Green Bay*

As development continues to concentrate in high risk earthquake areas, the probability increases that disastrous earthquakes will occur. Public officials face the prospect of dealing with earthquake crises that could have been reduced significantly with the application of known technologies. Although earthquakes are an uncontrollable force of nature, unnecessary losses in life and property and social disruptions are generally the result of not having implemented precautions that we know could have mitigated the losses.

The primary research emphasis in earthquake hazard mitigation has been on developing increased knowledge about the earthquake phenomena, increasing understanding of structural performance under earthquake conditions, developing advanced design methods and standards, and improving building codes. Improved knowledge about the

Collaborative Partners

- *The International Institute for Applied Systems Analysis, Vienna, Austria, provided Professor Petak with extended use of its research links and materials during his recent sabbatic leave so that he was able to initiate and develop the literature review.*
- *Representatives from the San Francisco Department of Building and Safety, structural engineers (Degenkolb Engineering, Comartin and Reis, Daniel Shapiro), the Applied Technology Council, California Seismic Safety Commission, and urban planning consultants reviewed the draft document.*
- *Social Science scholars from MAE, PEER, and MCEER reviewed early draft documents.*

physical and technical aspects of the problem has led to the adoption of public policies intended to reduce the probability of loss, but they must be implemented appropriately to actually reduce risk. Today, there remains an inadequate understanding of the barriers, impediments, disincentives, and issues associated with implementing appropriate earthquake hazard mitigation technologies and strategies, much less with overcoming those barriers. This research was undertaken because no complete conceptual model or empirically validated model exists to explain mitigation adoption processes for the rehabilitation of existing structures, either across or within specific stakeholder groups.

Background

Our broadly-based assessment of barriers to policy implementation resulted in a background working paper entitled *Barriers to Successful Implementation of Earthquake Hazard Mitigation Policies*. In it, we address three questions that are central to implementation:

- First, what constitutes appropriate, successful implementation of public policies concerning earthquake hazard mitigation? That is, how can we determine whether a policy has been implemented appropriately or successfully?
- Second, what are the key variables thought to affect the success of implementation? Which of those variables can be controlled to help ensure successful implementation?
- Third, how can mitigation advocates help to ensure that public policies adopted in an attempt to reduce the probability of losses to life and property from earthquakes are implemented successfully? How can we help ensure that the resources devoted to hazard reduction in pursuit of these policies are used effectively?

Our first paper is based on a review of the implementation literature that has developed over the past three decades. A rich body of research on implementation exists within the social and behavioral sciences, but very little of it addresses natural hazards risk reduction. Consequently, we've drawn on a broad base of literature to draw inferences about implementing earthquake hazard mitigation. The 75 page draft report cuts across the

The primary audience for our reports comprises two groups. One group includes architects, engineers, developers, builders, building owners, and organizations whose actions or inactions are the targets of policies intended to get them to reduce risks to themselves and other members of the community from natural hazard events. The second group consists of policy and program designers and public and private program managers with responsibilities in earthquake hazard risk reduction and mitigation.

social and behavioral sciences, drawing on more than three dozen significant studies, and resulting in 37 basic propositions concerning impediments to effective implementation. The propositions are organized around a model we developed that attempts to identify key inter-institutional nexuses in the implementation process.

The Implementation Web

We view organizations as open systems, comprising elements related to one another in ways such that perturbations of one element have ramifications for the others. Organizations exist within environments of varying complexity with which they inexorably interact. Organizational systems, we believe, are inherently unstable, requiring continual resources from the environment to survive and requiring continual adjustment simply to maintain their relative position. Our model enables us to examine multiple organizations embracing all the levels of government within the systems framework.

In our work, we examined organizational variables, including policy makers, the program designers, the program implementing agency, staff assigned to implement the program, and the target population. We were unable to find a model in the literature that embraces the contributions of the various social and behavioral science concepts, constructs, and analysis. We chose, therefore, to create a model based on general systems theory to try to embrace the breadth of implementation research. The original model was not intended as a conceptual breakthrough; it is simply the most convenient, useful way we know to organize this diverse, complex body of research. Our model also contains non-organizational variables that give it substance: the problem giving rise to the policy, the policy itself, the characteristics of the system, and characteristics of the system's environment. Each of these is thought to affect implementation. Finally, the model incorporates dynamic elements. These are characteristics of the system that affect in the model. Four points about the model are particularly important. First, the entire process is dynamic and, typically, iterative; policies are often revisited after having been enacted. Second, policy gets defined and redefined at each step in the implementation process as it is interpreted and reality-checked by the participants in that organizational node. Third, obstacles to implementation can arise at each link in the implementation process. They can also arise at the points at which organizations and processes are joined with one another. Fourth, the nature of the entire process itself may engender obstacles to implementation, particularly if the process is long and complex, involving lots of actors and transactions.

To guide our work, we conceptualized a simple model to embrace the processes that extend from policy adoption through implementation by operating agencies (see figures 1 and 2). We describe this as a complex web of expectations and actions. The model extends to include organizations with implementation roles as well as the characteristics of the implementation

Links to Current Research

- *Our efforts to seek greater understanding of how to ensure increased application of methods for earthquake hazard risk reduction by public and private organizations cuts across the program focuses in lifelines, hospitals, and response and recovery, including community sustainability and community resilience.*

- *Hospital retrofit cases are being used as a test bed for furthering our knowledge and for developing practical guides to improving mitigation practice, coordinating our work closely with that of von Winterfelt, Tierney, and others. Since the MCEER agenda is aimed at the application of new technologies to the reduction of risk, implementation necessarily cuts across all programs and is relevant to each.*

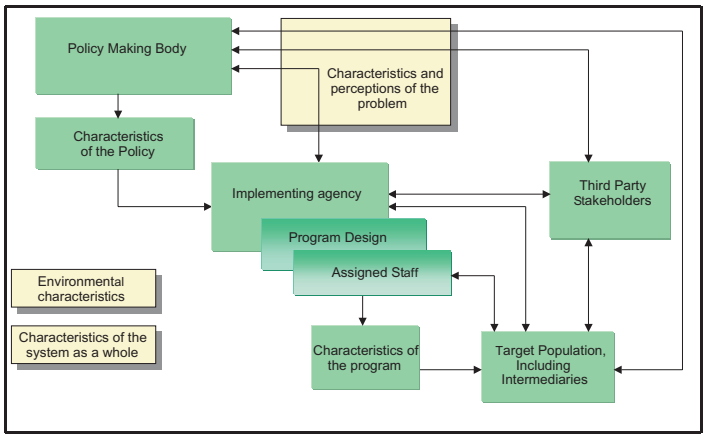

■ Figure 1. Implementation Within a Single Jurisdiction

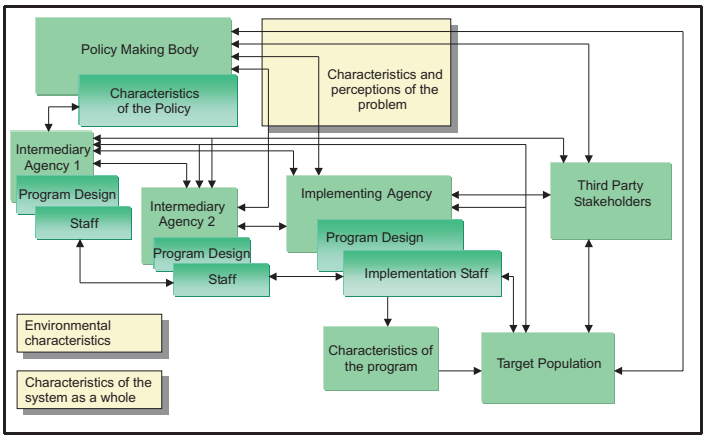

■ Figure 2. Implementation in a Multi-Level Governmental Setting

process itself. Our focus is on sets of organizations and the systemic setting within which they play their implementation roles. We call these different sets of organizations primary target organizations, market intermediaries, front line implementors, indirect implementors, nongovernmental policymaking participants, and public policymaking organizations.

Primary Actors in the Implementation Process

We define **Primary Target Organizations** as architects, engineers, developers, builders, building owners, and organizations whose actions or inactions are the targets of policies intended to get them to reduce risks to themselves and other members of the community from natural hazard events. **Market Intermediary Organizations** are defined as private organizations and public agencies that provide mortgage monies, mortgage insurance, or insurance against losses from natural hazard events including, especially, those whose policies and practices affect the behavior of **Primary Target Organizations**.

We have defined **Front Line Implementing Organizations** as agencies, typically public agencies, such as building and safety and code enforcement agencies, that are charged with program implementation. That is, they are organizations that are expected to allocate resources, including time and personnel, to bring about the desired effects in the target organizations. We include the individuals within those organizations assigned to take action. **Indirect Implementing Organizations**, on the other hand, are those organizations charged with designing implementation programs which mandate others, like local departments of building and safety, to take action, inflict sanctions for not taking action, or provide incentives to take action. Typically, these are viewed as federal or state agencies responsible for ensuring that municipalities administer mitigation programs.

Nongovernmental Policymaking Participants are an important element in the implementation web. They comprise private organizations that participate in policy development, such as professional associations (SEAOC, BSSC), and private interest

groups that seek to influence policy (ICBO, trade organizations). Some participants are fully engaged in public policy formation to the extent that they are almost indistinguishable from authorized public policymakers in their sphere of influence.

Policy Making Organizations are defined for our purposes as public legislative, executive (or occasionally judicial) entities that adopt and authoritatively state a policy intended to reduce risk to life and property from natural hazard events

What Constitutes Successful Policy Implementation?

At the simplest level, "implementation represents the faithful fulfillment of policy intentions by public servants"(Calista, 1994, p. 117). Newcomers to business and government often assume that a policy, once adopted, will be implemented in accord with the policy makers' intent. An increasingly rich body of research confirms what old hands know – that is just not the case. Practitioners and scholars have come to understand that policy adoption is simply one milestone in a continuing process of addressing an issue. Researchers have concluded, however, that implementation is a critical part of policy making process. Policy is adopted and adapted and drifts, morphs, and mutates through the implementation process. The extent of drift and mutation depends on a myriad of variables, only some of which can be controlled by policy makers. Calista's assessment of the field of study is that it has evolved from one of viewing implementation as simply the process of carrying out policy directives to where implementation "is now integral to the field of policy intervention, including recognizing its influence on policy formulation" (Calista, 1994, p. 117). Evidence continues to mount demonstrating that, often, policies are not implemented in accord with the policy makers' intent. Indeed, it may be that successful implementation is the exception rather than the rule. Calista reports that the most prevalent finding in implementation research is that outcomes are either disappointing or unwitting (Calista, 1994, citing Derthick, 1990). Others suggest that policy implementation is "the continuation of politics with other means" (Majone and Wildavsky, 1978).

We have concluded that successful implementation is not the same as solving the problem. It is entirely possible that a program could be implemented exactly as intended and that the program is ineffective because the problem transformed during the implementation period or because the program was flawed conceptually. If a local government provides incentives for action by private actors, some will choose to participate and others will not. It is possible that an overwhelming majority act in such a way as to convince even the most jaded skeptic that the policy has been implemented. Suppose, however, that only 10 percent of those targeted by the policy and eligible to participate actually volunteer to participate in the program or implement the policy. Is policy implementation successful? Presumably not, because such a small proportion of the target was reached. Careful di-

"A rich body of research on implementation exists within the social and behavioral sciences, but very little of it addresses natural hazards risk reduction."

agnosis of the implementation process might focus attention on a specific aspect of the program designed to implement the policy, such as providing greater incentive or engaging in more effective campaigns to make members of the target audience more aware of the program. If each of the organizations in the implementation net does precisely what is called for in an agency's program plan, but, still, the private citizens or organizations targeted for action fail to take the steps that bring about clear intent of the public policy, is implementation successful or has it failed?

We concluded, too, that successful implementation is a matter of degree. Consider the fanning out of responsibility for implementation. A federal agency looks to fifty states, each of which looks to a hundred or more municipalities, each of which looks to several employees, each of whom tries to affect the behavior of a dozen or more individuals or firms. What proportion of the several hundred thousand potential "implementations" in this example has to "take" for implementation to be judged successful? Successful implementation is clearly, then, a relative concept. We have to think of it in terms of the extent to which it has occurred rather than whether it has occurred. Success, in the case of implementation, is not a matter of absolutes.

Criteria for Evaluating Implementation

We have identified six criteria for evaluating the extent to which implementation has been successful:

- Did the policy have the nominally intended effect on the intended target population?
- To what extent were there unintended side effects and were those side effects adverse?
- To what extent did the various elements of the implementation network comply with policy directives?
- What proportion of the target was reached?
- Did implementation take place within a reasonable time frame? That is, if one expected implementation of a retrofit to be completed within five years and it has been fifteen and the job is not yet completed, how effective has the implementation been?
- Were the costs of implementation acceptable and reasonable?

Barriers to Implementation

We developed 37 propositions concerning obstacles to implementation, including obstacles throughout the policy development and implementation process. For Year 4, we focused our attention on examining reasons private organizations might not implement risk reduction measures. We summarized those impediments into four barriers.

Barrier 1. The organization does not perceive itself at risk.

The first barrier to successful implementation of earthquake risk reduction is that the organization facing the risk does not perceive itself at risk. Most practitioners in the earthquake hazard field may find it difficult to comprehend there are organizations that are not

fully aware of their exposure and vulnerability, many are not, even in seismically active areas. In such cases, appropriate means for overcoming the ignorance barrier by efforts to communicate the hazard along with improving the target organization's perceptions of exposure, vulnerability, and probable effects.

Barrier 2. The organization may perceive itself to be at risk, but does not perceive that it can do something to reduce the risk.

Organizations may see themselves as having both exposure and vulnerability, but not know what to do to reduce the probability of loss when the event occurs. This condition can exist when there is a small inventory of acceptable risk reducing actions or when no means have yet been devised to mitigate the potential loss. The organizational decision makers may have a fatalistic mind set that dictates against attempts at risk reduction. Or, the problem may be viewed as intractable by organizational decision makers.

Barrier 3. The organization sees the risk and possible actions, but doesn't see taking risk-reducing actions as in being in its best interest.

This barrier is not at all unlikely. Decision makers must weigh the sure costs of risk reduction against the possible benefits and, then, compare those costs and returns against those of other possible investments. Earthquake hazard mitigation does not always win those comparisons. Second, any risk reduction measures must be congruent with organizational culture, goals, and priorities; if they are not, then the investment is directed toward other goals. Similarly, the proposed mitigations must be congruent with organizational motivation.

Barrier 4. The individual organization may be aware of the problem and risk reduction measures and be eager to reduce its risks, but find that it is impossible to take action at this time.

Any of several reasons can keep an organization from acting when it knows the risk, understands there are ways to reduce risk, and is willing to move ahead. There may not be space on the organizational agenda right now. The organization may not have the capacity at present in terms of financial strength or available skills. Or, it may be that the organizational environment presents sufficient ambiguity to cause the organization to defer action.

Overcoming Barriers to Implementation

In Year 4, we also worked to develop a document useful to the decision making community and to integrate our work with other MCEER tasks. Our second working draft, entitled *Overcoming Barriers To Implementing Earthquake Hazard Mitigations: A Practical Guide*, is an attempt to develop practical means for overcoming

"We have concluded that successful implementation is not the same as solving the problem."

barriers that occur throughout the implementation network. The guidelines on which the draft is based are summarized below.

Guideline 1: If a basic obstacle to taking precautions is an inaccurate assessment of risks by the target organization, then the hazards professional, if he or she expects to have any impact, must provide the organization with a clear, compelling statement of the risks to the organization.

Guideline 2: Risk reduction measures are more likely when the **Primary Target Organizations** see a clear link between the potential hazardous event and adverse effects on them and their businesses. Prudent hazard mitigators work to make the linkage clear to those organizations.

Guideline 3:The probability of successful implementation of a policy (in either a multi-organizational setting or in a single organization) increases when both those involved in policy making and implementation have a similar perception of the problem. It is sensible, then, to help ensure similar perceptions by active communication among the two parties.

Guideline 4: Problems often shift out from under solutions, rendering policies obsolete, ineffective, or dysfunctional. Prudent implementors work to ensure that policies are modified as necessary to ensure they are both effective and appropriate, so that efforts at implementing the policy will not diminish.

Guideline 5: For an organization to take steps to reduce its exposure or vulnerability to earthquakes, key decision makers in the organization must believe that practical steps exist to reduce the risks associated with the event or condition and that those steps are congruent with the problem. To increase the probability of implementation, design professionals and public officials must ensure that decision makers see the link between the risk and the solution.

Guideline 6: The prudent implementor does not assume that the **Primary Target Organization** understands the availability of a range of solutions and the possibility of modifying solutions to match the specific needs of the individual organization.

Guideline 7: The more a problem is viewed intractable, the less likely it is that implementation will be successful. Hazard mitigators must work to reduce ignorance about the phenomenon, reduce diversity in specific target populations, work with reasonably sized target populations, and become more skilled in understanding means for changing perceptions and behavior in the target population.

Guideline 8: Successful implementation of new policies and approaches is more likely to occur promptly in organizations that are traditionally amendable to change or have a culture that embraces innovation.

Guideline 9: : The probability of successful implementation increases to the extent that actors in the implementation process perceive congruence between means and ends; that is, they will work harder to ensure implementation if they perceive that the policy and the programs designed to implement the policy are appropriate, given their perception of the problem.

Guideline 10: The probability of successful implementation in either a multi-organizational setting or in a single organization increases to

the extent that various actors in the organization have similar goals with respect to risk reduction and buy into the means selected for risk reduction.

Guideline 11: Risk reduction measures are more likely to be faithfully implemented when the organizational leadership's support is unambiguous, the order is widely publicized, the people charged with implementation have everything needed to implement the measures, and those charged with implementation have no doubt of the authority of the leadership to issue the decision.

Guideline 12: Unless the interests of the various stakeholders, especially those of the **Primary Target Organizations**, are accommodated at some minimally acceptable level, it is likely that mitigation policies and programs will face guerilla action, be subject to subsequent watering down, and face court challenges.

Guideline 13: "Hazard mitigation is not a technical exercise; it is inherently and often intensely political because mitigation usually involves placing cost burdens on some stakeholders, and may involve a redistribution of resources. Hazard mitigators must, therefore, develop political as well as technical solutions" (Alesch and Petak, 1986).

Guideline 14: Policies are more likely to be implemented successfully when they are entrusted for implementation to organizations that embrace the same goals and values as those implicit or explicit in the policy.

Guideline 15: Organizations will work toward achieving successful implementation to the extent that they believe they can implement the policy, that implementing the policy will achieve desired program objectives, and that achieving the program objectives is consistent with and supportive of the organization's primary objectives.

Guideline 16: Private organizations are more likely to implement risk reduction practices when they see that the risk poses a clear and present danger to their enterprise. Coupling risk reduction with routine business concerns, such as property and casualty insurance and related risk management concerns, helps bring it to the attention of the organizational decision makers.

Guideline 17: Public policies intended to induce private parties to reduce natural hazard risks to the organization and to the public at large are more likely to be implemented when the financial concerns of the private parties are acknowledged explicitly in the policy and provisions are made to alleviate financial burdens associated with implementation.

Guideline 18: Other things being equal, successful implementation depends on entrusting implementation to organizations with sufficient capacity to administer the program. If local government agencies are called upon to implement risk reduction programs, they should be provided with the resources necessary to do the job.

Guideline 19: Implementation proceeds more effectively when "the leaders of the implementing agencies possess substantial managerial and political skill and are committed to statutory objectives (Sabatier and Mazmanian, 1979).

Guideline 20: Smaller organizations may need technical assistance, in the form of consultants or self-help instructional materials, to augment their staffs so they are capable

"Case studies involving seismic retrofit of hospitals are planned to evaluate and extend the propositions concerning barriers to implementation and a means to overcome them."

of making prudent choices concerning risk reduction for buildings and structures.

Guideline 21: In complex organizational environments characterized by instability and change, it may be useful to test implement public risk reduction programs aimed at private organizations in pilot projects in a variety of settings. This will help avoid implementation pitfalls that could come from immediate, widespread implementation.

Guideline 22: If the purpose of a public program is to induce private organizations to implement risk reduction policies and practices, governmental organizations should work to make it easy for the private organizations to understand the requirements and to facilitate implementation by the private organizations.

Conclusions and Further Research

In February 2001, we distributed both drafts to a select group of fourteen practicing structural engineers, public officials, and members of the earthquake hazard community who agreed to read both documents and to participate in a one day session in San Francisco to critique our work and our products. The session, held in March, was extremely successful. Because the reviewers were practitioners, the focus was primarily on the second working draft. The participants pointed out what was useful and what was not, helped us clarify our target audience, and provided guidance on how we could make the draft more useful. At this writing, we are working to integrate their critique into the document.

We have also distributed our first draft — the synthesis of the prior research on implementation — to a half dozen scholars drawn from the social and behavioral sciences. Each of these scholars is associated with one of the three engineering research centers (MCEER, MAE, or PEER) and is actively engaged in earthquake hazard research. The group of scholars collectively decided it would be appropriate to meet in a central location to review their work. The group will have assembled by the time this report is published and will have provided a substantive critique of our draft report. Along with the critiques by the practitioners, this review will guide our development of final documents.

Several tasks dominate our current research activities. The first is completing our review of the state of the art in understanding obstacles to implementation and means for overcoming them. We have essentially completed our assessment of policy, intergovernmental, interorganizational, political, and process variables. We still have work to complete on obstacles to implementation associated with organizational behavior and decision making. Second, we will revise our drafts based on critique from the scholars and practitioners who have reviewed our work. Third, we will begin case studies involving seismic retrofits of hospitals as a means for evaluating and extending our set of propositions concerning barriers to implementation and means for overcoming them. Fourth, we will continue the development of our conceptual model

concerning the implementation process. Development of the conceptual models has been guided by the existing research literature, but refining and specifying the model is dependent on the data elicited in our stakeholder studies.

Beyond this year, we hope to expand our hospital retrofit case studies. Second, we will continue our current efforts to integrate our work with other MCEER researchers, Detlof von Winterfelt (University Southern California) and Kathleen Tierney (Disaster Research Center, University of Delaware). Third, we will complete the development of our conceptual model of the implementation process. Finally, we expect to complete two monographs for publication by MCEER focusing on means for overcoming barriers to implementation both in the public and private sectors.

References

Alesch, Daniel J., (1998), "Adopting And Implementing Performance-Based Seismic Design Standards," paper prepared for the Earthquake Engineering Research Institute, Oakland, CA.

Alesch, D.J., and Petak, W.J., (1986), *The Politics and Economics of Earthquake Hazard Mitigation*, Natural Hazard Research and Application Center, University of Colorado, Boulder, CO.

Bardach, Eugene, (1977), *The Implementation Game: What Happens After a Bill Becomes Law*, Cambridge, Mass.: The MIT Press.

Calista, Donald, (1994), "Policy Implementation," *Encyclopedia of Policy Studies* (ed. Stuart Nagel), Marcel Dekker, New York, NY., pp 117-155.

Calista, Donald, (1986), *Linking Policy Intention and Policy Implementation: The Role of the Organization in the Integration of Human Resources, Administration and Society*, Vol. 18, pp. 263-286.

Drabeck, Thomas E., Mushkatel, Alvin H. and Kilijanek, Thomas S., (1983), *Earthquake Mitigation Policy: The Experience of Two States*, University of Colorado, Boulder, Institute of Behavioral Science, Monograph 37.

Earthquake Engineering Research Institute, (1988), *Incentives and Impediments to Improving the Seismic Performance of Buildings*, Oakland, CA.

Godschalk, David R., Beatley, Timothy, Berke, Philip, Brower, David J., Kaiser, Edward J., Bohl, Charles C., and Goebel, R. Matthew, (1999), *Natural Hazard Mitigation: Recasting Disaster Policy and Planning*, Island Press, Washington, D. C.

Lipsky, M., (1971), "Street Level Bureaucracy and the Analysis of Urban Reform," *Urban Affairs Quarterly*, Vol. 6, pp. 391-409.

Mazmanian, D. A. and Sabatier, P.A., (1989), *Effective Policy Implementation*, Lexington Books, Lexington, MA.

Majone, G. and Wildavsky, A., (1978), "Implementation as Evolution," *Policy Studies Annual Review*, Vol. 2. H. E. Freeman (ed.), Sage, Beverly Hills. CA

May, Peter J. and Williams, Walter, (1986), *Disaster Policy Implementation: Managing Programs Under Shared Governance*, Plenum Press, New York.

References (Con't)

Pressman and Wildavsky, (1984), 3rd edition, *Implementation*, University of California Press, Berkeley, California

Sabatier, P. and Mazmanian, D., (1979), "The Conditions of Effective Implementation; a Guide to Accomplishing Policy Objectives," *Policy Analysis*, No. 5, pp. 481-504.

Sabatier, P. and Mazmanian, D., (1981), "The Implementation of Public Policy: A Framework of Analysis," *in Effective Policy Implementation,* (eds. D. A. Mazmanian and P. A. Sabatier), Heath, Lexington, MA.

Sabatier, P. A., (1986), "Top-Down and Bottom-Up Approaches to Implementation Research: A Critical Analysis and Suggested Synthesis," *Journal of Public Policy*, Vol. 6, pp. 21-48.

Taylor, Craig, Mittler, Elliot, and Lund, LeVal, (1998), *Overcoming Barriers: Lifeline Seismic Improvement Programs*, Monograph No. 13, American Society of Civil Engineers, Reston, VA.

Large Scale Experiments of Permanent Ground Deformation Effects on Steel Pipelines

by Koji Yoshizaki, Thomas D. O'Rourke, Timothy Bond, James Mason and Masanori Hamada

Research Objectives

The objectives of the research are to: 1) simulate in the laboratory full-scale permanent ground deformation (PGD) effects on steel pipelines with elbows, 2) develop an extensive and detailed experimental database on pipeline and soil reactions triggered by earthquake-induced PGD, and 3) refine and validate analytical models so that complex soil-pipeline interactions can be numerically simulated with the precision and reliability necessary for planning and design. To accomplish these objectives, an international partnership was organized, involving the Tokyo Gas Company, Ltd., MCEER, and NSF through its program for US/Japan Cooperative Research in Urban Earthquake Disaster Mitigation. The project combines experimental and analytical research performed at Tokyo Gas facilities with experimental and analytical work undertaken at Cornell University. The experiments at Cornell represent the largest simulations of PGD effects on pipelines ever performed in the laboratory.

During earthquakes, permanent ground deformation (PGD) can damage buried pipelines. Earthquake-induced PGD can occur as surface fault deformation, liquefaction-induced soil movements, and landslides. There is substantial evidence from previous earthquakes, such as the 1983 Nihonkai-chubu (Hamada and O'Rourke, 1992), the 1994 Northridge (O'Rourke and Palmer, 1996), and the 1995 Hyogoken-Nanbu (Oka, 1996) earthquakes, of gas and water supply pipeline damage caused by earthquake-induced PGD. More recent earthquakes, including the 1999 Kocaeli and Duzce earthquakes in Turkey, and the 1999 Chi-chi earthquake in Taiwan, have provided additional evidence of the importance of liquefaction, fault rupture, and landslides through their effects on a variety of highway, electrical, gas, and water supply lifelines.

Gas and other types of pipelines must often be constructed to change direction rapidly. In such cases, the pipeline is installed with an elbow that can be fabricated for a change in direction from 90 to a few degrees. Because elbows are locations where flexural and axial pipeline

Sponsors

National Science Foundation, Earthquake Engineering Research Centers Program
Tokyo Gas Company, Ltd.
National Science Foundation, U.S.- Japan Cooperative Research for Mitigation of Urban Earthquake Disasters

Research Team

Koji Yoshizaki, *Pipeline Engineer, Fundamental Technology Laboratory, Tokyo Gas Company, Ltd.*
Thomas D. O'Rourke, *Thomas R. Briggs Professor of Engineering,* ***Timothy Bond,*** *Laboratory Manager, and* ***James Mason,*** *Graduate Research Assistant, Department of Civil and Environmental Engineering, Cornell University*
Masanori Hamada, *Professor, Department of Civil Engineering, Waseda University*

Collaborative Partners

- *Cambridge University*
- *Kyoto University*
- *Rensselaer Polytechnic Institute*
- *University of Southern California*
- *University of Tokyo*
- *Yamaguchi University*

deformations are restrained, concentrated strains can easily accumulate at elbows in response to PGD.

The response of a pipeline elbow, deformed by adjacent ground rupture and subject to the constraining effects of surrounding soil, is a complex interaction problem. A comprehensive and reliable solution to this problem requires laboratory experiments on elbows to characterize their three-dimensional response to axial and flexural loading, an analytical model that embodies soil-structure interaction combined with three-dimensional elbow response, and full-scale experimental calibration and validation of the analytical model.

To resolve this problem, an international team was organized. The principal participants are Tokyo Gas Company, Cornell and Waseda Universities. The research also involves the University of Cambridge, UK, Rensselaer Polytechnic Institute, and the University of Southern California. Waseda University leads a consortium of Japanese university participants that include Kyoto and Yamaguchi Universities and the University of Tokyo. The work was performed as part of MCEER Program 1 on the Seismic Retrofit and Rehabilitation of Lifelines and the NSF program for U.S./Japan Cooperative Research in Urban Earthquake Disaster Mitigation.

MCEER has a long history of productive collaboration with the Japanese earthquake engineering research community. Seven U.S./Japan workshops on the earthquake performance of lifeline facilities and countermeasures against liquefaction have been co-sponsored by MCEER, and the proceedings of these workshops have been published and distributed by MCEER. The latest in this series of workshops (O'Rourke, et al., 1999) was held in Seattle, WA in conjunction with the *5th U.S. Conference on Lifeline Earthquake Engineering*. The next workshop is planned during the forthcoming year in Tokyo, Japan. U.S. participants in the workshops include MAE, MCEER, and PEER researchers.

Experimental and Analytical Models

One of the deformation conditions of interest is illustrated in Figure 1a that shows a pipeline

The users of this research include: public and private utility companies, including gas distribution companies, such as Tokyo Gas and Memphis Gas, Light and Water; and water distribution companies, such as the Los Angeles Department of Water and Power (LADWP), and the East Bay Municipal Utility District (EBMUD). The research is also of interest to engineering design and consulting companies. The experimental data and analytical modeling procedures developed for this project are of direct relevance for underground gas, water, petroleum and electrical conduits.

with an elbow subjected to PGD consistent with lateral spread and/or landslides. Although lateral spreads and landslides involve complex patterns of soil movement, the most severe deformation associated with these phenomena occurs at the elbows and near the margins between the displaced soil mass and adjacent, more stable ground. The deformation along this boundary can be simplified as abrupt, planar soil displacement. Pipelines that can be sited and designed for abrupt lateral displacement will be able to accommodate complex patterns of deformation that frequently involve a more gradual distribution of movement across the pipeline. Abrupt soil displacement also represents the principal mode of deformation at fault crossings.

Figure 1b illustrates the concept of the large-scale experiments. A steel pipeline with an elbow is installed under the actual soil, using fabrication and compaction procedures encountered in practice, and then subjected to abrupt lateral soil displacement. The scale of the experimental facility is chosen so that large soil movements are generated, inducing soil-pipeline interaction unaffected by the boundaries of the test facility in which the pipeline is buried. The ground deformation simulated by the experiment represents deformation conditions associated with lateral spread, landslides, and fault crossings, and therefore applies to many different geotechnical scenarios. In addition, the experimental data and analytical modeling products are of direct relevance for underground gas, water, petroleum, and electrical conduits.

A modeling technique, named HYBRID MODEL, was developed for simulating large-scale pipeline and elbow response to PGD (Yoshizaki et al., 1999 and 2001). The model uses shell elements for the elbow where large, localized strains occur. Shell elements are located over a distance of 20 times the pipe diameter from the center point of the elbow. The shell elements are linked to beam elements that extend beyond this

Links to Current Research

Program 1: Seismic Evaluation and Retrofit of Lifeline Networks

Program 2: Seismic Retrofit of Hospitals, Task 2.7a, Cost Benefit Studies of Rehabilitation Using Advanced Technologies

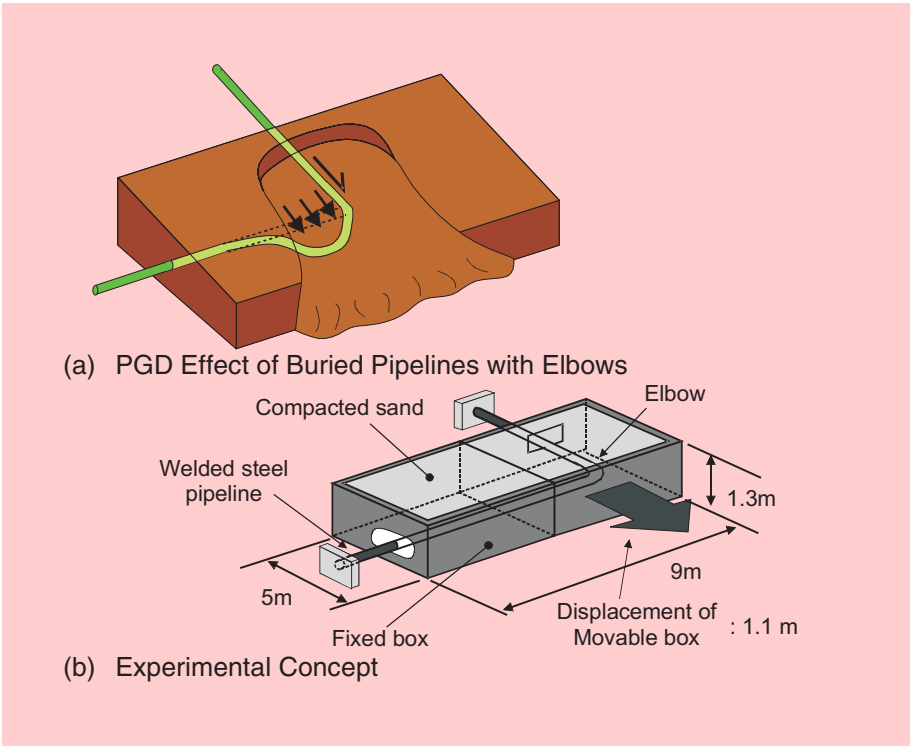

Figure 1. Experimental Concept for PGD Effects on Buried Pipelines with Elbows

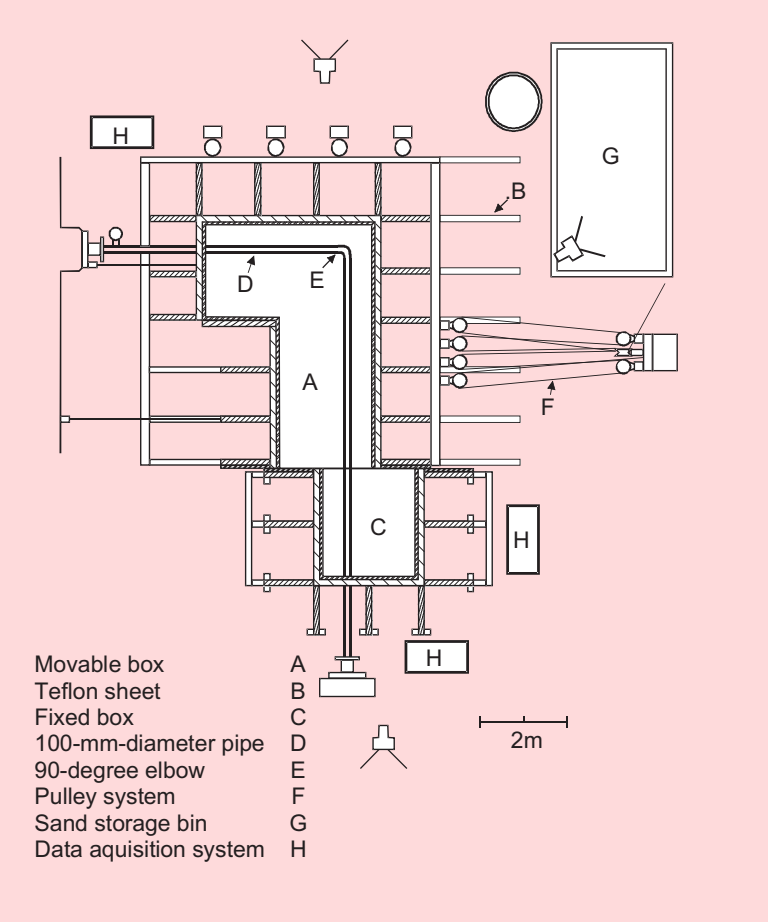

Figure 2. Plan View of Experimental Setup

distance. Soil-pipeline interaction under PGD is characterized by p-y and t-z curves, linking soil stresses on the pipe to the relative displacement between them. Lateral soil-pipeline interaction is characterized on the basis of laboratory experiments originally performed at Cornell (Trautmann and O'Rourke, 1985) and duplicated at Tokyo Gas experimental facilities.

In-plane bending experiments were conducted by Tokyo Gas (Yoshizaki et al., 1999 and 2001) on full-scale specimens of steel elbows in both the closing and opening modes. No leakage was observed in the closing mode, even when the opposing ends of the elbow were deformed into contact with each other and strains as high as 70% were measured. In contrast, leakage was observed in the opening mode for all cases except those in which the deformation was restricted because of the experimental loading device. The HYBRID MODEL was used to simulate the deformation behavior of the elbows using linear shell elements. Very good agreement was achieved between the analytical and experimental results for all levels of plastic deformation.

Large Scale Experiments

Figure 2 shows a plan view of the experimental setup that consisted of five main components, including a test compartment (A and C in the figure), pulley loading system (F), sand storage bin (G), sand container hoisted from storage bin to test compartment (not shown), and data acquisition system (H). The test compartment was composed of a movable box (A) and fixed box (C) within which the instrumented pipeline was installed and backfilled. The L-shaped movable box had inside dimensions of 4.2 m by 6m by 1.5 m deep. It was constructed on a base of steel I-beams positioned over Teflon sheets that were fixed to the floor. The Teflon sheets provided a low-friction surface on which the movable box was displaced by a pulley loading system. The fixed box, which was anchored to the floor, was designed to simulate stable ground adja-

cent to a zone of PGD similar to that illustrated in Figure 1.

A 100-mm-diameter pipeline with 4.1-mm wall thickness was used in the tests. It was composed of two straight pipes welded to a 90-degree elbow (E). The short section of straight pipe (D) was 5.4 m long, whereas the longest section was 9.3 m. Both ends of the pipeline were bolted to reaction walls. The elbows were composed of STPT 370 steel (Japanese Industrial Standard, JIS-G3456) with a specified minimum yield stress of 215 MPa and a minimum ultimate tensile strength of 370 MPa. The straight pipe was composed of SGP steel (JIS-G3452) with a minimum ultimate tensile strength of 294 MPa. About 150 strain gauges were installed on the pipe to measure strain during the tests. Extensometers, load cells, and soil pressure meters were also deployed throughout the test setup.

The pipeline was installed at a 0.9-m depth to top of pipe in each of four experiments. In each experiment, soil was placed at a different water content and in situ density. All experiments were conducted to induce opening-mode deformation of the elbow.

The experimental facility was designed with the assistance of the HYBRID MODEL that was used to simulate various testing configurations and compartment dimensions. Significant characteristics of the experimental facility are its size and volume. The storage bin for the sand was over three stories tall, with a capacity for 75 tons. Approximately 60 tons of sand were moved from the storage bin into the test compartment for each experiment with a container that was hoisted with the overhead conveyor. The sand was placed and compacted in 150-mm lifts with strict controls on water content and in situ density. One of the most significant challenges during the testing was the movement and controlled placement of such large volumes of sand with water content that was intentionally changed for each experiment.

The movable box was pulled by an overhead crane with an 8 to 1 mechanical advantage obtained through the pulley system shown in the figure. The maximum capacity of the loading system was

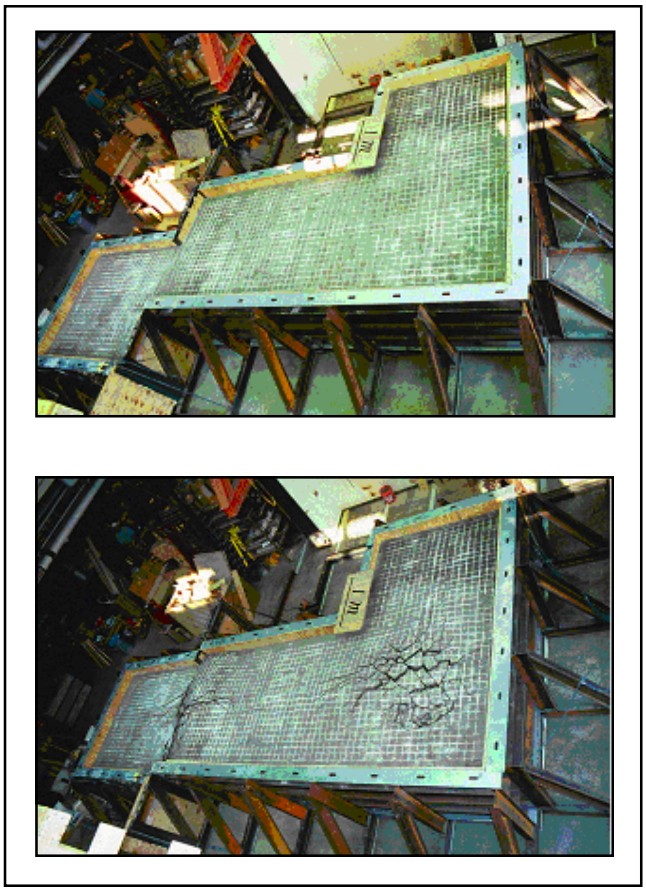

■ Figure 3. Overhead View of Test Compartment Before (top) and After (bottom) an Experiment

Figure 4. Overhead View of Deformed Experimental Pipeline

1 m of lateral displacement and 784 kN. The rate of displacement of the movable box was approximately 16mm/s.

Figure 3 shows the ground surface of the test compartment before and after an experiment. Surficial cracks can be seen in the area near the pipeline elbow and the abrupt displacement plane between the movable and fixed boxes after the test. In all cases, planes of soil slip and cracking reached the ground surface, but did not intersect the walls of the test compartment to any appreciable degree.

Figure 4 shows an overhead view of the test compartment after soil excavation to the pipeline following one of the experiments. Because each experiment was run until a total displacement of about 1m, the analytical models can be tested and calibrated through a broad range of deformation and strain in the elbow. The deformed shape of the pipeline can be seen clearly in the figure. Its shape is remarkably consistent with the shape shown by the finite element simulations discussed in the next section.

Analytical and Experimental Results

Finite element analyses were conducted with the HYBRD MODEL to check the ability of the analytical simulations to capture key aspects of the pipeline and elbow response to abrupt lateral displacement. Figure 5a compares the deformed pipeline shape of the analytical model with measured deformation of the experimental pipeline. There is excellent agreement between the two, and there is obvious agreement between the analytical deformation and the overhead view of the deformed pipeline in Figure 4. Figure 5b shows the measured and predicted strains under maximum ground deformation on both the tensile (extrados) and compressive (intrados) surfaces of flexure along the pipeline. Figures 5c and d show the measured and analytical strains around the pipe circumference in which the angular distance is measured from extrados to intrados of pipe, corresponding to 0 and 180°, respectively. In Figure 5d, the data point with an upward arrow indicates the maximum strain measured when the gauge was disconnected during the experiment. Because the disconnection occurred before maximum deformation of the elbow, it is likely that the actual strain was larger than the value plotted. Overall, there is good agreement for both the magnitude and distribution of measured and analytical strains.

The large-scale experiments have provided a rich and comprehensive database for understanding pipeline response to large PGD, particularly under conditions where local constraint at an elbow leads to complex three-dimensional response and high strain concentrations. Although the interpretation of the experimental results is still in progress, the data have already shown that, with appropriate modifications, the current generation of analytical models is able to simulate real performance in a reliable way.

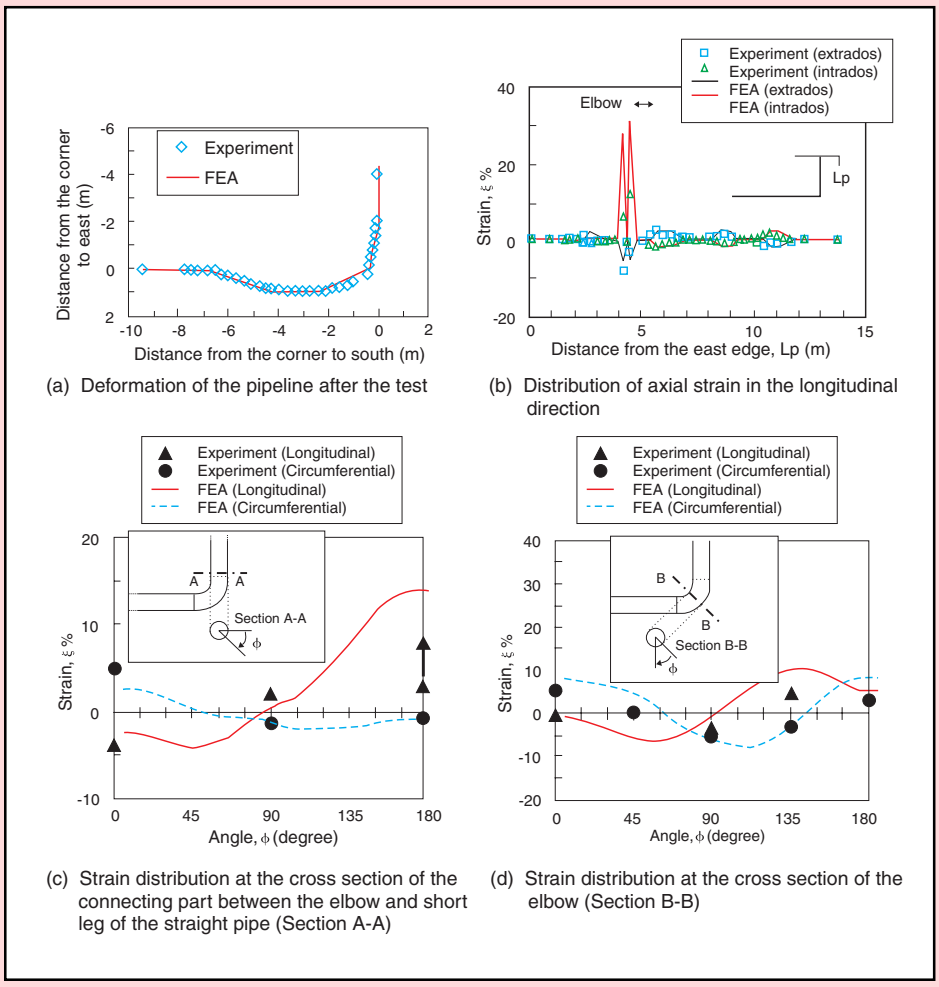

■ Figure 5. Comparison Between Analytical and Experimental Results

One of the most important aspects of the research has been to clarify the effects of moisture content on the pressures generated by soil-pipeline interaction during PGD. Current analytical models use p-y curves derived from laboratory test results with dry sand. Virtually all sand in the field is placed with measurable water contents that affect its in situ density and shear deformation characteristics. The large-scale experiments have shown that the failure surfaces and deformation patterns in soil adjacent to the pipeline during PGD are significantly different for dry and partially saturated sand.

Summary

Large-scale experiments sponsored by Tokyo Gas were successfully completed to evaluate the effects of earthquake-induced ground rupture on welded steel pipelines with elbows. The experimental set-up involved the largest full-scale replication of

ground deformation effects on pipelines ever simulated in the lab. The tests allow for calibration of a sophisticated soil-pipeline interaction analytical program developed in conjunction with the experimental work. The experimental data and analytical modeling products are of direct relevance for underground gas, water, petroleum, and electrical conduits.

Additional work at Cornell sponsored by Tokyo Gas is planned in the forthcoming year to investigate further the p-y characterization for partially saturated sand as a function a water content and compaction effort. Work also is planned with collaborating universities for developing the next generation of analytical model that will represent the soil as a continuum with specific constitutive relationships capable of simulating large ground deformation and its interaction with buried pipelines.

References

Hamada, M. and O'Rourke, T.D., Eds., (1992), *Case Studies of Liquefaction and Lifeline Performance During Past Earthquakes,* Vol. 1, NCEER-92-0001, National Center for Earthquake Engineering Research, University at Buffalo, April.

Oka, S. (1996), "Damage of Gas Facilities by Great Hanshin Earthquake and Restoration Process," *Proceedings*, *6th Japan-U.S. Workshop on Earthquake Resistant Design of Lifeline Facilities and Countermeasures Against Soil Liquefaction*, NCEER-96-0012, MCEER, University at Buffalo, pp.111-124.

O'Rourke, T. D. and Palmer, M. C. (1996), "Earthquake Performance of Gas Transmission Pipelines," *Earthquake Spectra*, Vol. 20, No. 3, pp.493-527.

O'Rourke, T.D., Bardet, J.P., and Hamada, M., (1999), Proceedings, *7th US-Japan Workshop on Earthquake Resistant Design of Lifeline Facilities and Countermeasures Against Soil Liquefaction*, MCEER-99-0019, MCEER, University at Buffalo, Nov.

Trautmann, C.H. and O'Rourke, T.D, (1985), "Lateral Force-Displacement Response of Buried Pipe," *Journal of Geotechnical Engineering*, ASCE, Vol.111, No.9, pp.1077-1092.

Yoshizaki, K., Hosokawa, N., Ando, H., Oguchi, N., Sogabe, K. and Hamada, M., (1999), "Deformation Behavior of Buried Pipelines with Elbows Subjected to Large Ground Displacement," *Journal of Structural Mechanics and Earthquake Engineering*, No.626/I-48, pp.173-184 (in Japanese).

Yoshizaki, K., O'Rourke, T. D. and Hamada, M., (2001), "Large Deformation Behavior of Buried Pipelines with Low-angle Elbows Subjected to Permanent Ground Deformation," *Journal of Structural Mechanics and Earthquake Engineering*, I-2130, pp. 41-52.

Experimental and Analytical Study of Base-Isolation for Electric Power Equipments

by M. Ala Saadeghvaziri and Maria Q. Feng

Research Objectives

The goals of this project are to develop rehabilitation strategies and enhance seismic design guidelines for key equipments in power substations, which are one of the most critical facilities in a power system. Furthermore, it will provide the knowledge base to be integrated into the overall loss estimation model for the entire power network.To achieve these goals, key substation equipments are identified and effectiveness of base-isolation to increase their seismic resilience are assessed using a comprehensive experimental and analytical study.

Sponsors

National Science Foundation, Earthquake Engineering Research Centers Program

Research Team

M. Ala Saadeghvaziri, *Associate Professor and* ***Selahattin Ersoy,*** *Graduate Student, Department of Civil and Environmental Engineering, New Jersey Institute of Technology*

Maria Q. Feng, *Associate Professor, Civil and Environmental Engineering Department, University of California, Irvine*

Nobuo Murota, *Bridgestone Company, Japan*

Critical power system facilities, such as substations, sustained significant damage in California and Japan earthquakes and more recently during the 1999 Chi-Chi,Taiwan, and the Izmit,Turkey earthquakes. Functionality of electric power systems, especially in the age of information technology, is vital to maintaining the welfare of the general public, sustaining economic activities and assisting recovery, restoration, and reconstruction of the seismically damaged built environment. Furthermore, enhanced seismic design and rehabilitation will ensure long-term reliability and longevity of critical equipments. In order to be able to assess the reliability of power systems and to develop seismic resistant mitigation strategies, critical components must be identified and their seismic performance evaluated.Transformers and their bushings are among the most critical components in a complex power system and their seismic performance during past earthquakes has not been satisfactory. Figure 1 shows damage to a transformer in Izmit-2 substation during the Izmit, Turkey earthquake of August 17, 1999 (EERI Newsletter, 1999).

Generally, there are several modes of substation transformer failure during an earthquake, namely movement and turn over of unanchored transformers, anchorage failure that can cause ripping of the transformer case and oil leakage, foundation failure causing rocking and tilting, and failure of the gasket and oil leakage due to the interaction between the transformer and the bushing. Some transformers are supported on rails for ease of installation and because such a set up allows for air circulation to provide additional cooling, thus enhancing corrosion resistance.Another

Collaborative Partners

- *National Center for Research in Earthquake Engineering (NCREE), Taipei, Taiwan*
- *Earthquake Protection System, Inc., Richmond, California*
- *Bridgestone Corporation, Kanagawa-ken, Japan*

form of damage in an unanchored transformer is large movement that can cause damage to other components connected to the unit, such as control cables and bushings. Damage due to the latter factor (i.e., interaction between transformer-bushing and other equipments) can be critical and can cause significant damage and delays in service.

■ Figure 1. Transformer Failure During the August 17, 1999, Izmit, Turkey Earthquake (EERI, Oct. 99)

It is more common to anchor transformers where considerations are given to seismic loads.This can be done by either bolting the transformer to its footing slab or by welding it to steel embedded in the slab (ASCE, 1999). Designing the anchorage at the supports requires consideration to large forces not only due to gravity and horizontal seismic forces but also from overturning moments in both directions. Furthermore, other appendages such as radiators and reservoirs are attached to a typical transformer.These appendages can cause significant torsional forces that must also be considered in the design of the supports. In addition to strength, the anchorage system must have adequate stiffness and tight tolerances to prevent initiation of impact forces that can damage internal elements or excite higher modes that can damage brittle porcelain members.

There are many cases of bolt or weld failure during past earthquakes (ASCE, 1999). However, with better attention to the details in the design of supports, their performance during an earthquake can be improved. Implementing well-designed anchorage for retrofit of existing transformers, nevertheless, can be difficult and costly. Furthermore, in many situations, for both new and existing transformers, a well-designed anchorage may only change the mode of failure to the foundation (i.e., the next weak link in the system). The failure shown in Figure 1 appears to be due to foundation settlement.

Boundary gaps due to back and forth motion of transformers and rocking of transformers and their footings due to soil-structure interaction have been observed during past earthquakes (ASCE, 1999). Therefore, in many cases, the use of base-isolation for transformers

Primary users of this research include utility companies and owners of electrical substation equipments, manufacturers of electrical equipments, and manufacturers of base-isolation devices. The research results can further be used by structural and electrical engineers for design and retrofit of electrical power equipments.

may be the only suitable remedy to alleviate these problems, especially for existing transformers in high seismic regions. Base-isolation will also reduce the input acceleration into the bushing and will lessen the interaction between the transformer and the bushing, which has been the cause of many bushing damages during past earthquakes. Furthermore, by reducing the inertia forces, base-isolation can also prevent the possibility of internal damage.

The after effect of an earthquake on reliability and longevity of a transformer is directly related to the level of shaking of internal elements. High levels of uncontrolled shaking may very well reduce the life expectancy and reliability of internal elements. Internal damage is normally difficult to observe and document because of limitations with post-earthquake inspections of the transformer internal system. However, there are reports of cases of internal damage to transformers (ASCE, 1999).

Satisfying the mobility requirement for maintenance purposes is another advantage of base-isolation over a tightly designed anchorage system. An issue with the use of base-isolation that demands careful consideration is the possible adverse effect of relatively large displacements on the response of inter-connecting equipments, especially bushings. Among possible remedies to be considered are a balanced approach to the design of the isolation system (displacement vs. inertia reduction), appropriate design of conductor slacks, and use of flexible conductor connections. Therefore, a successful application of this technology requires in-depth understanding of the responses of the individual systems involved as well as their interactions.

Within this study, two base-isolation systems are being investigated under a collaborative effort among several institutions and industrial partners. The following sections discuss the experimental program along with some of the findings. The two systems considered are a friction pendulum system and a hybrid system consisting of sliding and rubber bearings. It represents the first effort in testing base-isolated large-scale transformer-bushing systems using an earthquake simulator.

"This study represents the first effort in testing base-isolated large-scale transformer-bushing systems using an earthquake simulator."

Experimental Study

An extensive series of tests were conducted on a transformer model supporting a bushing. The primary objective was to compare the response of a fixed based transformer-bushing system to that of the system when isolated. The testing was conducted on the earthquake simulator at the National Center for Research on Earthquake Engineering (NCREE) in Taiwan in collaboration with the manufacturers. Uniaxial, biaxial, and triaxial excitations were conducted employing several earthquake records with PGAs in the range of 0.125g to 0.5g. The testing schedule also included white noise tests to identify dynamic characteristics of the bushings and the transformer model, resulting in more than 200 tests.

Considering the payload capacity of the earthquake simulator, the transformer model was designed to weigh 235.5 kN. The model is a four-layer steel frame structure

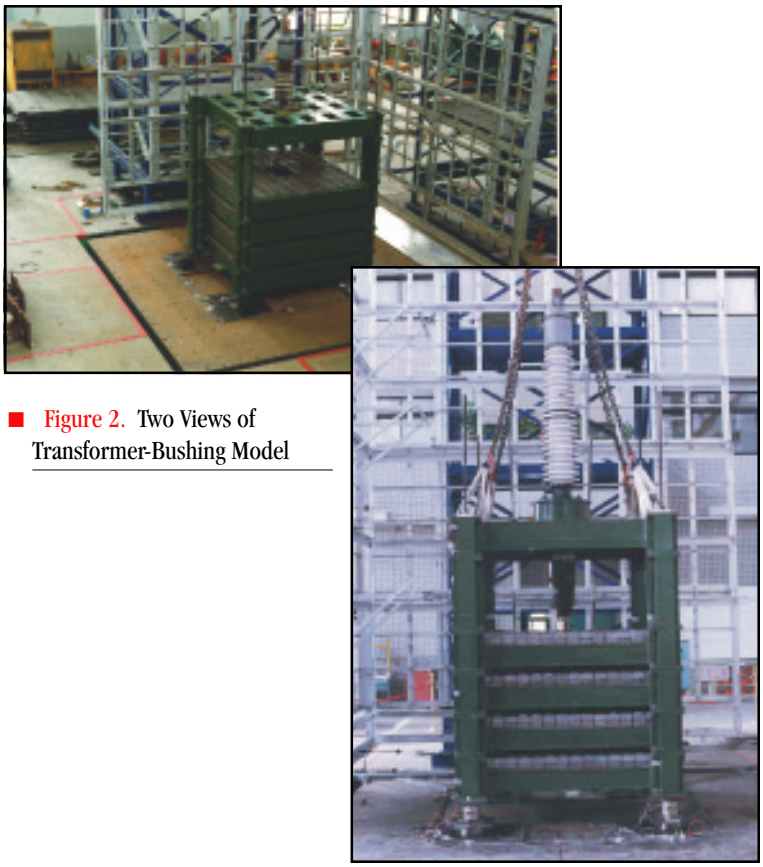

■ Figure 2. Two Views of Transformer-Bushing Model

with lead blocks loaded to represent the internal core and coil of a transformer.

Consistent with the practice employed by TaiPower, the bushing was attached to the transformer model top plate at a right angle. The connection represents some of the important structural aspects of the support of the bushing, which has been shown to be very important in quantifying the important interaction between the two components.

Figure 2 shows isometric and elevation views of the entire model. As can be seen from this figure, the bushing projects inside the transformer model as is the case in an actual situation. Two types of bushings, 69 kV and 161 kV, were used in the experiment. Several earthquake records were used for the testing, among them were the 1940 El-Centro, 1994 Sylmar (Northridge), and 1995 Takatori (Kobe) records. Transformer frequency was measured to be 12.5 Hz in both x and y directions. The frequencies for the 69 kV and 161 kV bushings were 27.0 Hz and 12.5 Hz in both x and y directions, respectively. The equivalent damping ratio for each component was around 2%.

Friction Pendulum System Results

One of the most recent base isolation systems to improve the earthquake resistance of structures is Friction Pendulum System (FPS), shown in Figure 3. Detailed description of the system along with in depth discussion of experimental and analytical results can be found elsewhere (Ersoy, et. al 2001; Saadeghvaziri and Ersoy, 2001). For structures isolated by this system, the period of vibration (similar to a pendulum) only depends on geometry (in this case radius of curvature) and the gravitational constant, and it does not depend on the mass. Therefore, FPS bearings are one of the most suitable isolation devices for a system with relatively small weight compared to a high-rise building (such as substation equipments). Furthermore, through friction,

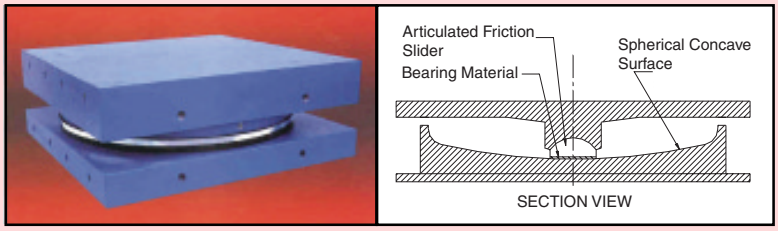

■ Figure 3. Photograph and Cross-Section View of an FPS Isolator

■ Table 1. Fixed and FPS Isolated Results for Several Cases Using the Sylmar (Northridge) Record

Case No.	Input and Response	Fixed Base			Base Isolated		
		x	y	z	x	y	z
1	PGA_{Target}	0.1250	-	-	0.1250	-	-
	PGA_{Real}	0.1468	-	-	0.1376	-	-
	A_2	0.1602	-	-	0.0778	-	-
	A_3	0.2457	-	-	0.1173	-	-
	A_{B1}	0.2715	-	-	0.1664	-	-
	A_{B2}	0.2507	-	-	0.1280	-	-
	A_{B3}	0.5127	-	-	0.1418	-	-
	A_{B4}	0.9188	-	-	0.2323	-	-
	D_2	0.8638	-	-	7.7837	-	-
	D_3	1.2757	-	-	7.8814	-	-
2	PGA_{Target}	0.2500	-	-	0.2500	-	-
	PGA_{Real}	0.2377	-	-	0.2817	-	-
	A_2	0.2586	-	-	0.1186	-	-
	A_3	0.4555	-	-	0.2044	-	-
	A_{B1}	0.4888	-	-	0.3748	-	-
	A_{B2}	0.4374	-	-	0.2824	-	-
	A_{B3}	1.0256	-	-	0.2111	-	-
	A_{B4}	1.8672	-	-	-	-	-
	D_2	1.6892	-	-	26.2215	-	-
	D_3	2.4049	-	-	26.6045	-	-
3	PGA_{Target}	0.3750	-	-	0.3750	-	-
	PGA_{Real}	0.3781	-	-	0.3793	-	-
	A_2	0.4191	-	-	0.1661	-	-
	A_3	0.6664	-	-	0.3323	-	-
	A_{B1}	0.8257	-	-	0.5718	-	-
	A_{B2}	0.6020	-	-	0.4200	-	-
	A_{B3}	1.4243	-	-	0.2564	-	-
	A_{B4}	2.7489	-	-	0.6234	-	-
	D_2	2.2553	-	-	46.3317	-	-
	D_3	3.0519	-	-	46.7391	-	-
4	PGA_{Target}	0.2500	0.1250	-	0.2500	0.1250	-
	PGA_{Real}	0.2313	0.1093	-	0.2637	0.1462	-
	A_2	0.2513	0.1082	-	0.1227	0.1158	-
	A_3	0.4282	0.1155	-	0.1883	0.2008	-
	A_{B1}	0.4819	0.4807	-	0.3981	0.4484	-
	A_{B2}	0.4267	0.2835	-	0.2722	0.3728	-
	A_{B3}	0.9657	0.6177	-	0.2255	0.2739	-
	A_{B4}	1.7932	1.3097	-	0.4328	0.6308	-
	D_2	1.5519	1.6678	-	21.1447	21.5628	-
	D_3	2.8855	3.3082	-	22.5074	21.7414	-
5*	PGA_{Target}	0.3750	0.2500	-	0.3750	0.2500	-
	PGA_{Real}	0.3699	0.2094	-	0.3809	0.2454	-
	A_2	0.4213	0.2167	-	0.3642	0.5833	-
	A_3	0.6257	0.4479	-	0.7031	1.0592	-
	A_{B1}	0.9549	1.1157	-	1.4774	4.6122	-
	A_{B2}	0.6118	0.5967	-	0.9029	2.7761	-
	A_{B3}	1.3414	1.1542	-	0.7015	1.2588	-
	A_{B4}	2.6399	2.5825	-	1.4507	3.0900	-
	D_2	2.6765	3.3448	-	65.0059	79.1818	-
	D_3	4.8021	5.5605	-	71.0776	80.1011	-
6	PGA_{Target}	0.2500	0.1250	0.1250	0.2500	0.1250	0.1250
	PGA_{Real}	0.2362	0.1160	0.1193	0.2676	0.1526	0.1239
	A_2	0.2570	0.1280	-	0.1367	0.1273	-
	A_3	0.4323	0.2539	0.1537	0.2017	0.2005	0.1728
	A_{B1}	0.5214	0.4160	0.1606	0.4075	0.4234	0.1745
	A_{B2}	0.4129	0.2671	0.1784	0.3052	0.3440	0.1727
	A_{B3}	1.0605	0.5432	0.1880	0.2478	0.2714	0.1633
	A_{B4}	2.0097	1.1053	0.1611	0.4534	0.6593	0.1762
	D_2	1.4588	1.8311	-	20.8579	22.5745	-
	D_3	2.9084	3.3387	-	22.2175	22.3609	-
7	PGA_{Target}	0.3750	0.2500	0.2500	0.3750	0.2500	0.2500
	PGA_{Real}	0.3833	0.2161	0.2362	0.4031	0.2414	0.2316
	A_2	0.4150	0.2123	-	0.2205	0.2330	-
	A_3	0.6180	0.4404	0.2844	0.4769	0.2743	0.3494
	A_{B1}	1.1053	1.0184	0.4418	1.0202	0.7539	0.3314
	A_{B2}	0.6412	0.5460	0.3679	0.7059	0.4971	0.3358
	A_{B3}	1.2734	1.0664	0.3858	0.5316	0.3782	0.3358
	A_{B4}	2.6668	2.3398	0.3550	1.0828	0.7979	0.3340
	D_2	2.5987	3.7217	-	60.4434	75.6554	-
	D_3	4.8967	5.9023	-	96.8357	65.5843	-

Note:

* For the base isolated case, the displacement limit of the FPS bearing is reached, causing impact.

the system can provide a high level of damping. Four 18.64" radius FPS bearings at the four corners were used to support the model for the isolated case.

The test results for Sylmar record are tabulated in Table 1 for isolated and non-isolated cases. In these tables, A_2 and A_3 show the acceleration values (in g) at the bottom and the top of the transformer model, respectively. A_{B1},A_{B2},A_{B3},A_{B4} represent the accelerations at different locations along the bushing. A_{B1} is the bottom of the bushing and A_{B4} is the top. Note that the bushing projects inside the transformer model. That is, it is connected to the transformer model somewhere between points A_{B2}, and A_{B3}. Thus, the bottom of the bushing (i.e., point A_{B1}) can have a response as large as the top of the bushing (A_{B4}). D_2, and D_3 (in mm) are the relative displacement values of the transformer model at the bottom and top, respectively.

In comparing these numbers a point should be noted with regard to the base-isolated results for Case

5. Inspection of the displacement results for this case indicates that the displacement capacity of the bearing has been reached causing impact. Thus, the results are not useful for comparison to the fixed base situation. However, they do highlight the fact that vertical motion has a noticeable effect on the response of FPS isolated structures. In this case, vertical motion has caused reduction in the horizontal displacements. Thus, for the 3-D case (Case 7 in Table 6), unlike the 2-D case, the displacements are within the bearing capacity.

The response acceleration maps for one case is shown in Figure 4. In this figure, x-axis shows the acceleration values normalized with respect to PGA. The y-axis shows different locations along the height of the test specimen ranging from the top of the shake table to the top of the bushing. As one can see from this figure, acceleration response of the transformer model is reduced significantly at different levels throughout its height. The level of acceleration reduction depends on the type of earthquake record used. That is, in addition to acceleration level and nature of the input (e.g., 1-D vs. 2-D), the ground motion characteristics affect the level of acceleration reductions.

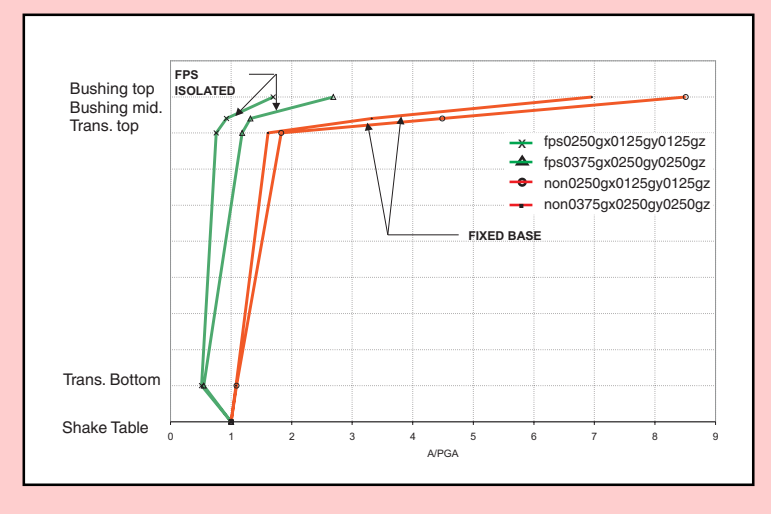

■ Figure 4. Acceleration Maps: Triaxial Simulation, FPS Bearings, Sylmar (Northridge) Record

The experimental results can be summarized as follow:

- Inertia reductions depend on peak ground acceleration (PGA) and bearing radius. The FPS system is more effective in reducing inertia forces for higher PGAs. Furthermore, both inertia reductions and maximum displacements are affected by the earthquake record used. Records with dominant period in the vicinity of the isolator period reduce the isolator effectiveness.
- FPS bearings can provide, on the average, 60% acceleration reductions within their displacement limits. This number is with respect to the isolation level. For a flexible system (as seen from the acceleration maps) accelerations are different at various levels, and the effectiveness of the base-isolation is more apparent when one considers the entire picture. For example, there is a significantly greater reduction in the bushing acceleration than that of the transformer.
- Coupling of responses in two horizontal directions does exist, which is due to dependency of frictional characteristics on total velocity. However, the effect tends to diminish for higher PGAs, since at higher velocities, frictional constants are less sensitive to the magnitude of velocity.
- The vertical component of ground motion has an effect on the response of the FPS bear-

ings. This effect is expected to be more pronounced for near field earthquakes (higher PGAs) and for sites where filtering of the motion due to local soil conditions is possible.

Hybrid Base-Isolation Results

It is difficult to use normal rubber bearings for seismic isolation of lightweight structures, such as transformers, due to their limited ability to elongate the natural period of the entire isolated system without buckling. This difficulty was alleviated in this study by combining sliding bearings (to support the entire weight) with rubber bearings (to provide restoring forces). The hybrid system was tested under a transformer-bushing model, as discussed, and the results were compared to the fixed base situation to investigate its effectiveness.

Four sliding bearings were installed at the corners of the transformer model and two rubber bearings were placed at the middle on two opposite sides, as shown in Figures 5. The sliding bearings carry the entire weight of the transformer model and the bushing, while the rubber bearings provide a horizontal restoring force without sustaining any vertical load. Detailed information on the design of the hybrid-isolation system and experimental results can be found in (Murota and Feng, 2001).

Peak response accelerations along with acceleration maps over the height of the transformer model and bushing, with and without the base isolation, are shown as a function of PGA in Figures 6 and 7 for the El Centro ground motion. Under other ground motion records, the peak responses show a similar trend. Like the FPS bearings, the hybrid system is very effective in reducing the accelerations, especially in terms of the response of the bushing top. Without base isolation, the peak acceleration at the top of the bushing reached 3.66 g, resulting in an amplification factor of 10.80.

On the other hand, for the base-isolated case, the peak response acceleration at the top of bushing was 0.354(g) with an amplification factor equal to 1.05. Note that in these discussions, including those on the FPS bearings, the PGA referred to and shown on the corresponding figures is the target PGA. The actual

"Research efforts over the past several years have revealed that understanding the seismic interaction among key equipments of a substation is critical to properly assessing their seismic performance."

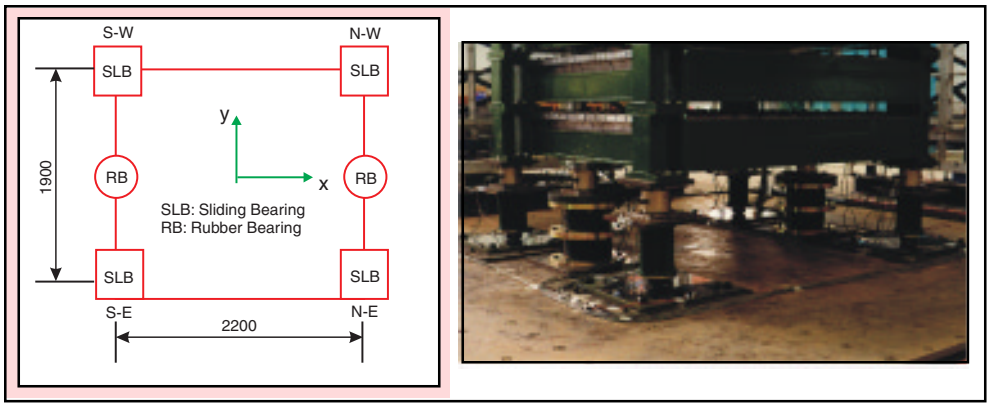

Figure 5. Layout and Experimental Set-up of the Hybrid Sliding-Rubber Bearings

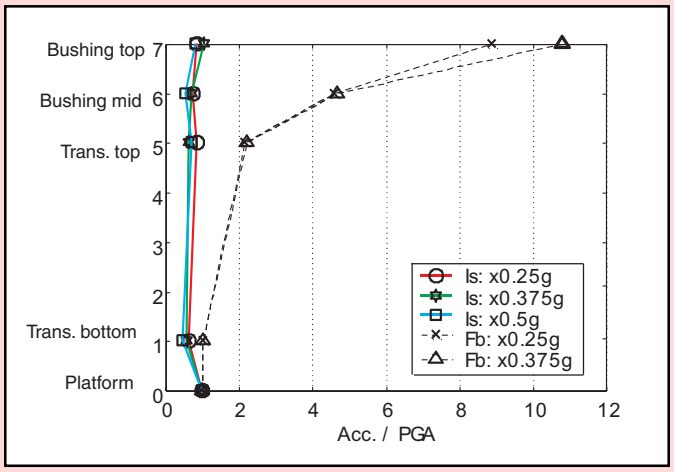

Figure 6. Acceleration Maps: Uniaxial Simulation, Hybrid Bearings, El-Centro Record.

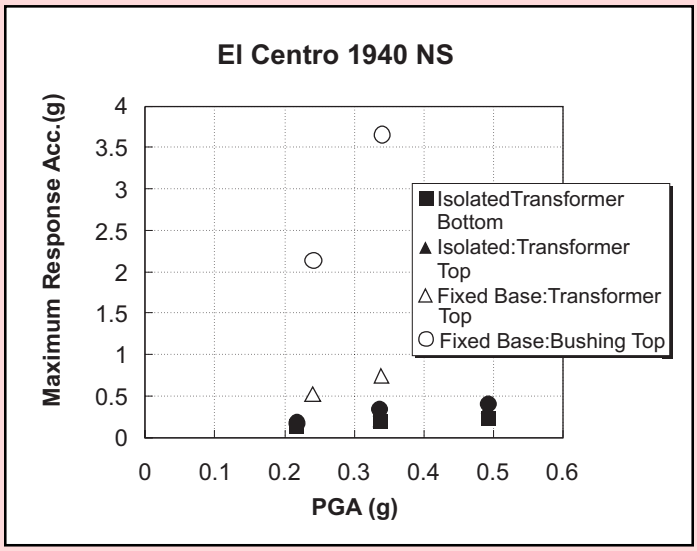

Figure 7. Peak Response Accelerations Under Uniaxial Shaking

or real input acceleration may have been different due to difficulty in exactly matching the intended PGA. Of course, response parameters (such inertia reduction) are calculated with respect to actual acceleration, not the target acceleration.

The hybrid base isolation becomes more effective as the PGA becomes larger (Figure 7), which is typical of a sliding isolation system. It is observed that for the base isolated system, the transformer response is not sensitive to the ground motion. For the fixed-based case, the interaction between the transformer (12.5 Hz) and the bushing was observed. As a result, the response of the 161kV bushing, with 12.5 Hz frequency, became larger than that of the 69kV bushing, which has a dynamic frequency of 27 Hz.

Under triaxial shaking, the transformer-bushing system showed significant difference in response from those under uniaxial and biaxial shaking. The response accelerations at the tops of both 161kV and 69kV bushings for the isolated cases were amplified, and in some cases (especially for the 69kV bushing), the response exceeded that of the fixed-based system. Figure 8 shows the acceleration response maps (amplification factors) for the worst case.

Detailed inspection of the results indicates that this is due to the effect of vertical motion on the friction force acting on the sliding bearings. Vertical records are generally rich in frequency content, resulting in high frequency fluctuations in the frictional force (20-30 Hz), which in turn causes excitation of high frequency modes.Thus, the reason for the 69 kV bushing, which has a fundamental frequency around 27 Hz, to be more affected by triaxial excitation.This is valuable information that has not be observed and/or investigated before. It also has significant implications for other structures (e.g., response of secondary systems in a building within the framework of performance-based design) and it will be investigated further.

In summary, the proposed hybrid sliding-rubber bearing isolation system is quite effective in reducing the response acceleration of a transformer-bushing system under uniaxial and biaxial earthquake simulator tests. It should be noted that the seismic performance of an actual transformer-bushing system equipped with the proposed isolation system will be even better, because the isolation period of an actual transformer will be much longer than that of the transformer-bushing model used in the test due to a much heavier weight of the actual transformer.Among ongoing objectives of the project are numerical studies and modifications to the design of the hybrid system to improve its effectiveness under triaxial motion.

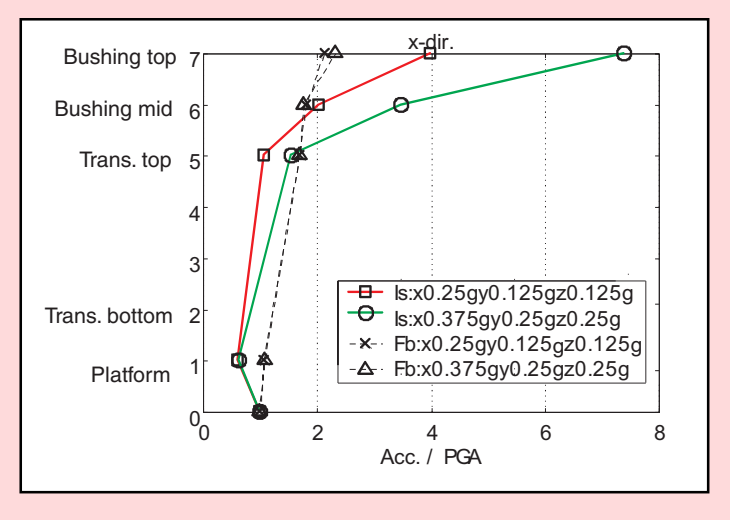

Figure 8. Acceleration Maps: Triaxial Simulation, Hybrid Bearings, El-Centro Record

Analytical Study

SDOF Model

Over the past decade or so, there have been several analytical and experimental studies on the seismic performance of FPS isolators. These works proved the effectiveness of FPS in reducing inertia forces within the displacement limit of the device. Practical applications of the system in the design of new structures and the rehabilitation of existing ones, including the historic Ninth Circuit U.S. Court of Appeals in San Francisco (Mokha, et al., 1996), have taken place. A more recent work by Almazan, et al., (1998) addresses several other important aspects of modeling and response such as constitutive relationships (small vs. large displacement), and refinement of the structural model.

During the initial phase of this study and parallel with the shake table tests, an extensive analytical work was conducted. Using SDOF idealization and equilibrium of the forces involved, the differential equations of motion were established and solved using IMSL routine IVPAG (Ersoy et al., 2001). Although the focus of this study is on application of FPS devices to transformers, it also addresses additional parameters and aspects of response that either have not been investigated before or have only been considered on a limited basis.Therefore, some of the findings are general and could have applications in the design of FPS bearings for other structures as well. Among the parameters considered are ground motion characteristics, bi-directional motions, the effect of vertical motion, and isolation radius.

Inertia reduction and the maximum displacement of the system were the criteria used in evaluating the seismic response and the effectiveness of FPS bearings. Based on the results of the parametric

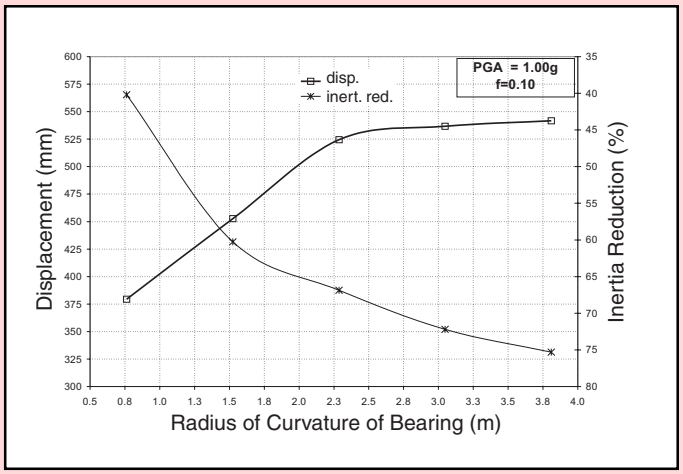

■ Figure 9. Analytical Displacement-Inertia Reduction Chart for FPS System (input PGA = 1.0 g)

study, charts for inertia reduction and the maximum displacement were developed. Shown in Figure 9 is a chart corresponding to ground motion with peak acceleration of 1.0g. The challenge in design will be the selection of radius of curvature of the bearing such that there is a balance between the desired inertia reduction and the displacement limits vis-à-vis bushing interaction with interconnecting equipments.

As can be seen from figure 9, the bearings can provide large inertia reductions. For example, for a system with radius of curvature equal to 1.5 m (60" inches) the inertia reduction is about 60%. That is, the transformer acceleration will be 0.4g when the peak ground acceleration is 1.g.

For this radius, the system period is 2.5 sec (i.e., frequency of 0.4 Hz) regardless of the weight of the transformer. However, the associated large displacement needs to be accommodated. To this end, there is a need for a simplified 3-D model to investigate the interaction between the transformer-bushing and interconnecting elements. To develop the knowledge base to achieve this goal, finite element models of typical transformers and bushings were developed, as discussed below, for time history analysis.

Finite Element Model

A power transformer is composed of six parts: transformer tank, radiators, reservoir, core and coil, oil, and bushings. The transformer tank is the main structural component of power transformers. It has core and coil centrally placed within it and the tank is completely filled by mineral oil. Radiators and reservoir are appendages and they are externally attached to the transformer tank.

A finite element model of a power transformer (55 MVA, 230/135 kV) from a substation in New Jersey is shown in Figure 10. The transformer weighs 1,335 kN (300 kips), and the radiators (on the side) and reservoir (on the top) weigh 120 kN and 40 kN, respectively. Thus, one can see the possibility of torsional response and higher demands on the supports in light of the relative weights of the appendages compared to the weight of the transformer itself.

The finite element package ANSYS was used to develop the finite element models. The transformer tank was modeled by shell elements. Braces around the transformer were modeled by offset beam elements. Currently, the core and coil inside the transformer were modeled as mass elements. Radiators and reservoir were modeled by 3-D solid elements. The contained oil inside the transformer

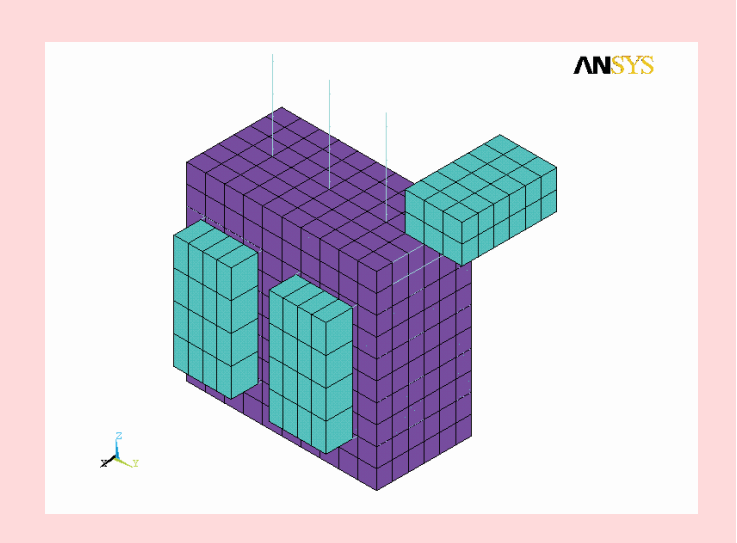

Figure 10. Finite Element Model of a Transformer-Bushing System

was modeled as solid with modulus of elasticity equal to the bulk modulus of the fluid.

The seismic response of bushings was dominated by the behavior of the gaskets between the porcelain units. The common failure mode involved movement of the upper porcelain unit relative to its support flange, causing oil leakage Therefore, the analytical model for the bushings uses simple beam elements with equivalent density and stiffness to represent porcelain units, dome, and aluminum support.

Gaskets between these elements were modeled using nonlinear axial and shear springs. For a fixed transformer, the translational degrees of freedom were removed at the location of the supports. The soil-structure interaction may be investigated using Winkler foundation elements to evaluate the level of stresses in the subgrade. Currently, time history analyses using various earthquake records are being conducted.

Conclusions

Research efforts over the past several years have revealed that understanding the seismic interactions among key equipments of a substation (transformers, bushings, foundation, and interconnecting elements) is critical to conducting a proper assessment of their seismic performance. Thus, the thrust of future efforts will be to evaluate seismic response, and propose design and rehabilitation guidelines, based on system performance. This will be achieved through further experimental tests and by developing a simplified model that can accurately represent critical elements of a substation in order to investigate their interactions in detail through a parametric study. The model will be developed based on the results of ongoing 3-D finite element analyses and the experimental results conducted over the past several years.

References

Almazan, J. L., De La Llera, J. C., and Inaudi, J., (1998), "Modeling Aspects of Structures Isolated with the Frictional Pendulum System," *Earthquake Engineering and Structural Dynamics*, 27, 845-867.

ASCE Manuals and Reports on Engineering Practice No. 96, (1999), *Guide to Improved Earthquake Performance of Electric Power Systems*, Edited by A. J. Schiff, ASCE, Virginia.

EERI Newsletter, (1999), "The Izmit (Kocaeli), Turkey Earthquake of August 17, 1999," Vol. 33, Number 10, October.

Ersoy, S., Saadeghvaziri,M. Ala, Liu, G. Y., and Mau, S.T., (2001), "Analytical and Experimental Evaluation of Friction Pendulum System for Seismic Isolation of Transformers," *Earthquake Spectra*, Journal of Earthquake Engineering Research Institute, (tentatively accepted).

IEEE, (1998), IEEE Std. 693-1997, *Recommended Practices for Seismic Design of Substations*, Piscataway, NJ, IEEE Standards Department.

Mokha, A., Amin, N., Constantinou, M., and Zayas, V., (1996), "Seismic Isolation Retrofit of Large Historic Buildings," *J. Structural Engineering*, ASCE, Vol. 122, pp. 298-308.

Murota, N., and Feng, M.Q., (2001), "Hybrid Base-Isolation of Bushing-Transformer Systems," *Proceedings, 2001 Structures Congress*, ASCE, Washington, DC, May 21-23.

Saadeghvaziri, M. Ala, and Ersoy, S., (2001), "Evaluation of Seismic Response of Transformers and Effectiveness of FPS Bearings for Base-Isolation," *Proceedings, 2001 Structures Congress*, ASCE, Washington, DC, May 21-23.

Recommended Changes to the AASHTO Specifications for the Seismic Design of Highway Bridges (NCHRP Project 12-49)

by Ian M. Friedland, Ronald L. Mayes and Michel Bruneau

Research Objectives

The ATC/MCEER Joint Venture is developing new specifications for the seismic design of highway bridges that can be recommended for incorporation into the *AASHTO LRFD Bridge Design Specifications*. The recommended specifications will be performance-based and address state-of-the-art aspects of highway bridge seismic design, including the latest approaches for representation of seismic hazard, design and performance criteria, improved analysis methods, steel and concrete superstructure and substructure design and detailing, and foundation design.

Sponsors

National Cooperative Highway Research Program of the National Research Council's Transportation Research Board
Applied Technology Council (ATC)/MCEER Joint Venture

Research Team

***Ian M. Friedland**, Applied Technology Council (P.I)*
***Christopher Rojah**, Applied Technology Council (Administrative Officer)*
***Ronald Mayes**, consultant (Technical Director)*
***Donald Anderson**, CH2M Hill, Inc.*
***Michel Bruneau**, University at Buffalo*
***Gregory Fenves**, University of California at Berkeley*
***John Kulicki**, Modjeski and Masters, Inc.*
***John Mander**, University of Canterbury*
***Lee Marsh**, BERGER/ABAM Consultants*
***Geoffrey Martin**, University of Southern California*
***Andrzej Nowak**, University of Michigan*
***Richard V. Nutt**, consultant*
***Maurice Power**, Geomatrix Consultants*
***Andrei Reinhorn**, University at Buffalo*

In August 1998, a joint venture of the Applied Technology Council (ATC) and MCEER initiated work on a project to develop the next generation of seismic design specifications for highway bridges in the United States. The project is sponsored by the American Association of State Highway and Transportation Officials (AASHTO) and is being conducted by the National Cooperative Highway Research Program (NCHRP) of the Transportation Research Board. NCHRP Project 12-49, "Comprehensive Specifications for the Seismic Design of Bridges," will result in the development of specifications and commentary which are expected to be incorporated into the *AASHTO LRFD Bridge Design Specifications*. These will be supplemented by a series of design examples demonstrating the application of key features of the new specifications.

The recommended specifications and commentary are currently being assessed by the AASHTO Highway Subcommittee on Bridges and Structures. The AASHTO Subcommittee is expected to make a decision regarding their adoption in May 2001. During the course of the project, three drafts of specifications and commentary will have been produced and reviewed, prior to completion and submission of the final draft to AASHTO.

The new specifications are expected to incorporate all current and state-of-the-art practices in highway bridge seismic design, and will be performance-based. They will address the latest approaches for representation of seismic hazard, design and performance criteria, analysis methods, steel and concrete superstructure and substructure design and detailing, foundation design, and soil behavior and properties. The specifications are also intended to address the differences in seismic hazard, soils, and bridge construction types found throughout the United States, and therefore are

Collaborative Partners

Project Engineering Panel
***Ian G. Buckle**, University of Nevada at Reno (chair)*
***Serafim Arzoumanidis**, Steinman Boynton Gronquist & Birdsall*
***Mark Capron**, Sverdrup Civil, Inc.*
***I. Po. Lam**, Earth Mechanics, Inc.*
***Paul Liles**, Georgia Department of Transportation*
***Brian Maroney**, California Department of Transportation*
***Joseph Nicoletti**, URS Greiner Woodward Clyde*
***Charles Roeder**, University of Washington*
***Frieder Seible**, University of California at San Diego*
***Theodore Zoli**, HNTB Corporation*

to be national in scope. These new specifications will be a marked departure from the design philosophy, approach, and requirements currently in use in the United States.

Technical Summary

A number of important changes in philosophy and approach will be included in these new specifications, when compared to the current AASHTO highway bridge seismic design provisions. Included in these are the following:

Design Criteria

A performance-based design criteria has been included in the new specifications and commentary (see Figure 1). Specifically, the project recommends adoption of a dual-level performance criteria, and two levels of seismic performance objectives, as shown in Table 1.

The recommended seismic performance objectives are performance-based and each State determines the desired performance objective for any particular bridge. This is a change from current AASHTO definitions of "other," "critical," and "essential" bridges for defining performance levels.

The upper level earthquake considered in these provisions is designated the Maximum Considered Earthquake (MCE). In general, the MCE ground motions have a probability of exceedance of 3% in 75 years, which is an approximate return period of 2,500 years. However, MCE ground motions are bounded deterministically to values lower than 2,500-year ground motions adjacent to highly active faults. It should be noted that the 75 year basis is equivalent to the theoretical design life of a highway bridge, as specified in the AASHTO provisions.

The definitions of service levels as shown in Table 1 are as follows:

Immediate–Full access to normal traffic shall be available following an inspection of the bridge.

Significant Disruption – Limited access (reduced lanes, light emergency traffic) may be possible after shoring; however the bridge may need to be replaced.

The damage level definitions shown in Table 1 are as follows:

None – Evidence of movement may be present but there is no notable damage.

If the seismic design provisions being developed under the NCHRP 12-49 project are adopted by AASHTO in whole or in part, they will become the national standard under which all highway bridges throughout the United States are designed. In addition, AASHTO specifications also often become the basis for the specifications adopted and used in many foreign countries. As a result, the users of this research will be the practicing bridge engineering community nationwide.

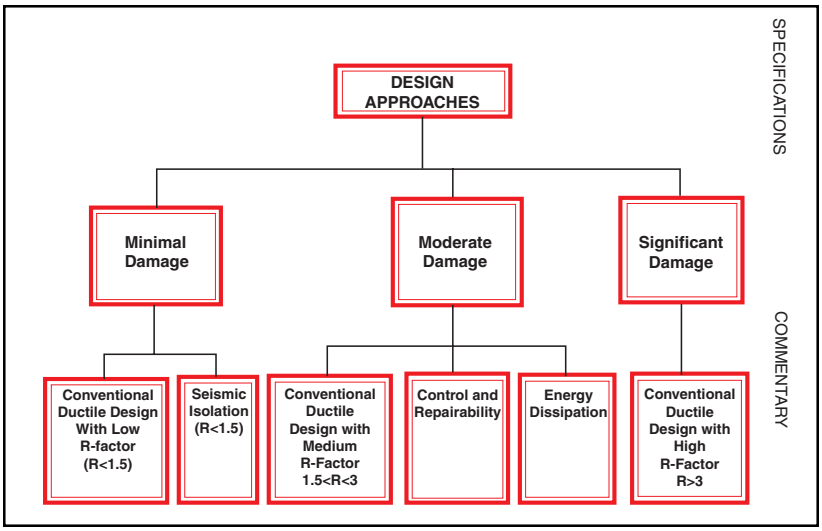

Figure 1. Design Approaches

Minimal – Some visible signs of damage. Minor inelastic response may occur, but post-earthquake damage is limited to narrow flexural cracking in concrete and the onset of yielding in steel. Permanent deformations are not apparent, and any repairs could be made under non-emergency conditions with the exception of superstructure joints.

Significant – Although there is no collapse, permanent offsets may occur and damage consisting of cracking, reinforcement yield, and major spalling of concrete and steel yielding and local buckling of steel columns, global and local buckling of steel braces, and cracking in the bridge deck slab at shear studs on the seismic load path is possible. These conditions may require closure to repair the damage. Partial or complete replacement may be required in some cases.

Geometric and Structural Constraints

In the initial phases of this project, an attempt was made to develop a set of geotechnical performance objectives that would be similar to those being developed for concrete columns. A two-day workshop was held to review initial draft proposals and to refine recommended criteria and approaches. The consensus of the workshop was that the amount of acceptable foundation and abutment movement should be related to geometric and structural constraints by bridge type, rather than explicit values on foundation movements (see Figure 2). As a result, the recommended specifications propose constraints that would implicitly provide foundation design limits for seismic loads to meet the various performance objectives. Since this is the first time an attempt has been made at developing these constraints, the specified values may

Table 1. Performance Objectives

		Performance Objective	
Probability of Exceedance for Design Earthquake Ground Motions		**Life Safety**	**Operational**
Rare Earthquake 3% in 75 years	Service	Significant Disruption	Immediate
	Damage	Significant	Minimal
Expected Earthquake 50% in 75 Years	Service	Immediate	Immediate
	Damage	Minimal	Minimal to None

Links to Current Research

- *The specifications being developed under this project draw heavily on the results of many research studies conducted within the MCEER Highway Project, and on related NSF-sponsored research, especially in the areas of seismic hazard representation and geotechnical/soils performance and response.*

Permanent Displacement Type	Possible Causes	Mitigation Measures	Immediate	Significant Disruption
Vertical Offset 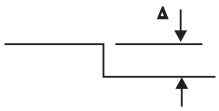	■ Approach fill settlement ■ Bearing failure	■ Approach slabs ■ Approach fill stabilization ■ Bearing type selection	0.083 feet (0.03 meters)	0.83 feet (0.2 meters) To avoid vehicle impact
Vertical Grade Break (2) 	■ Interior support settlement ■ Bearing failure ■ Approach slab settlement	■ Strengthen foundation ■ Bearing type selection ■ Longer approach slab	Use AASHTO "Green Book" requirements to estimate allowable grade break	None
Horizontal Alignment Offset 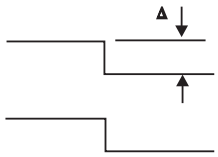	■ Bearing failure ■ Shear key failure ■ Abutment foundation failure	■ Bearing type selection ■ Strengthen shear key ■ Strengthen foundation	0.33 feet (0.1 meters) Joint seal may fail	Shoulder Width (To avoid vehicle impact)

■ Figure 2. Geometric Constraints on Service Level (partial listing, taken from Table C3.10.1.2, Revised LRFD Design Specifications, Third Draft of Specifications and Commentary)

require additional work in the future to refine them.

Geometric constraints generally relate to the usability of the bridge by traffic passing on or under it. Therefore, such constraints will usually apply to permanent displacements that occur as a result of the earthquake. The ability to repair (or the desire not to be required to repair) such displacements should be considered when establishing displacement capacities. When immediate service is desired, permanent displacements should be small or non-existent, and should be at levels that are within accepted tolerances for normal highway operations. When limited service is acceptable, the geometric constraints may be relaxed. These may be governed by the geometry or types of vehicles that will be using the bridge after an earthquake, and by the ability of these vehicles to pass through the geometric obstruction. Alternately, a jurisdiction may simply wish to limit displacements to a multiple of those allowed for immediate service. In the case of a significant disruption, post-earthquake use of the bridge is not guaranteed and therefore no geometric constraints would be required to achieve these goals. However, because life safety is at the heart of this performance level, jurisdictions applying the provisions should consider establishing some geometric displacement limits.

Structural constraints on displacements can be based on the requirements of a number of structural elements and can result from either transient displacements due to ground shaking or permanent displacements resulting from ground movement due to faulting, seismically induced settlements, lateral spreading, and so forth. Structural damage to foundation elements is limited primarily to piles since footings and pile caps are usually capacity protected. Although pile damage can often be avoided at a reasonable cost when piles are capacity protected, requiring this for all piles could lead to

overly conservative, and thus expensive, foundation designs. Therefore, it may be desirable to establish some lateral displacement limits for piles based on a limited amount of structural damage that is unlikely to compromise the structural integrity of the bridge. These limits will be based on the type and size of the piling, and the nature of the soil near the head of the pile. Caltrans has attempted to establish such limits for its standard piling based on physical testing. Other jurisdictions may attempt to do the same, or they may perform more complex analytical studies to establish similar displacement, capacity, and stiffness limits.

Earthquake Return Periods

Current AASHTO specifications consider a single-level earthquake hazard design event, based on a 500-year return period. At the time this event was incorporated into the AASHTO specifications, it was the only event readily available as a design value for seismic hazard representation in the United States.

The new provisions recommend a 2,500-year return period, which provides an equivalent 3% probability of exceedance in 75 years, be used as the upper level design event. A lower level event with an approximate 100-year return period, which would be based on a 50% probability of exceedence in 75 years, has also been recommended. In brief, the reasons for these recommended return periods include:

- For a frequent or expected earthquake (50% probability of exceedance in 75 years), this is the design level under which the bridge should remain essentially elastic (R = 1.0). This will result in a performance that is equivalent to an elastic (no damage) design for a 100 year flood, however, is less conservative but similar to an elastic design for a 100 mph base wind design.
- For a rare earthquake (3% probability of exceedance in 75 years), this design level is recommended in order to assure that a "no collapse" performance criteria for the MCE is satisfied. Since seismic loads increase much more significantly compared to wind and flood loads as the return period increases, earthquake design needs to consider longer return period design events.

A critical earthquake design issue in preventing collapse of a bridge is to ensure that deck displacements, and hence seat widths for the girders, can accommodate displacements from events that have occurred and can be realistically expected to reoccur. A return period of 500 years does not come close to capturing the force and displacement levels that may have occurred during earthquakes in the New Madrid region (1811-1812) and Charleston, South Carolina (1886). A return period of the order of 2,500 years is therefore required to obtain realistic displacement levels that may have occurred during these earthquakes.

It is noted that the MCE ground motion maps incorporate deterministic bounds on the ground motions adjacent to highly active faults. These bounds are currently applicable in California, along a portion of the California-Nevada border, in coastal Oregon and Washington, and in parts of Alaska and Hawaii. These deterministic bounds are

applied so that the ground motions do not become unreasonably large in comparison to the ground motions that could be produced by maximum magnitude earthquake on the faults. Deterministic bounds are defined as 150% of the median estimates of ground motions calculated using appropriate attenuation relationships, and assuming the occurrence of a maximum magnitude earthquake on the fault. However, they are limited to not less than 1.5 g for the short-period spectral acceleration plateau and 0.6 g for 1.0-second spectral accelerations.

Design Spectra Shape

The long period portion of the current AASHTO acceleration response spectra is governed by the spectrum shape and the soil factor, and it decays as $1/T^{2/3}$. There was considerable "massaging" of the factors that affect the long period portion of the current AASHTO spectra in order to produce a level of approximately 50% conservatism in the design spectra when compared to the ground motion response spectra beyond 1 second period.

Analysis of ground motion data indicates that the acceleration spectra generally decreases with period in the long period range as 1/T or more rapidly. The shape of the long period portion of the recommended response spectra is less conservative than the current spectral shape and it is recommended that the shape of the spectra decay as 1/T.

For periods longer than about 3 seconds, depending on the seismic environment, use of the 1/T relationship for spectral acceleration may be conservative because the ground motions may be approaching the constant spectral displacement region for which spectral accelerations decay as $1/T^2$. Either the 1/T relationship may be conservatively used or a site-specific study conducted to determine an appropriate long-period spectral decay.

Construction of the design response spectra requires the spectral acceleration value at 0.2 seconds and 1.0 second. The base curve constructed with these values is then modified according to the 1994 NEHRP short- (F_a) and long-period (F_v) soil site factors, as shown in Figure 3.

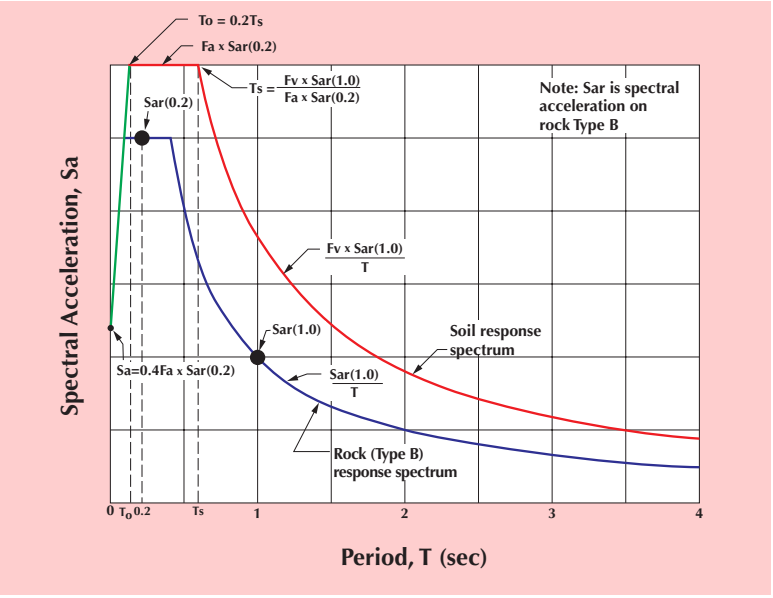

Figure 3. Response Spectrum Construction

Design Procedures and Response Modification Factors

The recommended specifications provide for three levels of design and analysis procedures in the moderate-to-high seismic zones. This is in addition to the current "no seismic" or low-level minimum requirements, which are defined as Level 0:

Level 0 – These are the current AASHTO Zone 1 provisions, which require minimum seat widths and specified design forces for fixed bearings of 10% dead load for Zone 1A and 25% dead load for Zone 1B.

Level 1 – This requires no formal seismic analysis but requires the use of capacity design principles and minimum design details.

Level 2A – This is a one-step design procedure based on an analysis method referred to as the "capacity spectrum method" and is applicable to very "regular" bridges. This method has been incorporated in some of the retrofit guidelines for buildings and provides the designer with the ability to assess whether or not a bridge designed for all non-seismic loads has sufficient strength and displacement capacity to resist the seismic loads.

Level 2B – This is a one-step design procedure based on an elastic (cracked section properties) analysis using either the Uniform Load or Multimode method of analysis. The analysis is performed for the governing design spectra (either 50%/75-year or 3%/75- year event) and the use of a conservative R-factor. The analysis will determine the moment demand at all plastic hinge locations in the column. Capacity design principles govern foundation and column shear design. If sacrificial elements are part of the design (i.e., shear keys) they must be sized to resist the 50%/75-year forces, and the bridge must be capable of resisting the 3%/75-year forces without the sacrificial elements (i.e., two analyses are required if sacrificial elements exist in a bridge).

Level 3 – This is a two-step design procedure using an elastic (cracked section properties) analysis with the multimode method of analysis for the governing design spectra to perform preliminary sizing of the moment capacity of the columns. Capacity design principles govern foundation and column shear design. A pushover analysis is then performed. The designer can change the design forces in the columns provided they are not lowered below those required by the 50%/75-year event and that they satisfy the displacement demand.

These provisions attempt to make the Level 1 approach applicable to as wide a range of bridges as possible. Level 2A will be applicable to very "regular" bridges that can be idealized as Single-Degree-of-Freedom systems, until more development work is done to extend the method.

Table 2. Typical Response Modification Factors

Substructure Element	Performance Objective			
	Life Safety		Operational	
	SDAP D	SDAP E	SDAP D	SDAP E
Wall Piers-larger dimension	2	3	1	1.5
Columns – Single and Multiple	4	6	1.5	2.5
Pile Bents and Drilled Shafts – Vertical Piles – above ground	4	6	1.5	1.5
Pile Bents and Drilled Shafts – Vertical Piles – 2 diameters below ground	1	1.5	1	1
Pile Bents and Drilled Shafts – Vertical Piles – in ground	n/a	2.5	n/a	1.5
Pile Bents with Batter Piles	n/a	2	n/a	1.5
Seismically Isolated Structures	1.5	1.5	1	1.5
Steel Braced Frame – Ductile Components	3	4.5	1	1.5
Steel Brace Frame – Nominally Ductile Components	1.5	2	1	1
All Elements for Expected Earthquake	1.3	1.3	0.9	0.9
Connections (superstructure to abutment; joints within superstructure; column to cap beam; column to foundation)	0.8	0.8	0.8	0.8

"If the seismic design provisions being developed under this project are adopted by AASHTO, in whole or in part, they will become the national standard under which all highway bridges in the U.S. are designed."

Base response modification (R-factors) are significantly more liberal and comprehensive in the new provisions than in current AASHTO. These values, as shown in Table 2, reflect the higher levels of seismic demand and analyses required by the recommended provisions. They also require equivalently elastic analysis for the 50%/75-year event. R-factors for all connections require essentially elastic behavior, but should not be used where capacity design principles are used to design the connections.

Level 1, No Seismic Demand Analysis

The "no seismic demand analysis" design procedures are an extremely important part of the recommendations because they are expected to apply as widely as possible in Zone 2. The purpose of the provisions is to provide the bridge designer the ability to design structures without the need to undertake dynamic analyses. The bridge elements are designed in accordance with the usual provisions, but the primary seismic resisting elements are specifically detailed for seismic resistance.

Capacity design requirements exist for shear reinforcement and confining reinforcement at plastic hinge locations in columns. There are also capacity design requirements for detailing the connection to pile and column caps. There are no additional design requirements for abutments or foundations with one exception – integral abutments must be designed for passive pressure. The premise for this is based on a parameter study that was conducted under the project which demonstrated that a foundation designed using a factor of safety of 3 will perform well in these lower seismic zones, assuming that the column connection to the pile cap is based on capacity design principles. These procedures will be permitted for use in sites with liquefaction potential, but will require some additional considerations if the predominant moment magnitude, MB, for the site exceeds 6.

The limitations on the applicability of the "no seismic demand analysis" provisions started with the definition of a "regular bridge" as contained in the current AASHTO seismic design provisions. Additional limits were added based on engineering judgment, and these should be reevaluated in the future. The limits as they currently exist consider (a) regularity, (b) axial load limits, (c) load path and force sharing, and (d) continuity. Table 3 provides the definition of a "regular" bridge for these provisions.

Span-to-span continuity must be provided by one or more of the following means:

- A superstructure that is monolithic with the substructure
- A superstructure seated on bearings that has transverse restraint
- Simply supported girders seated on bearings must be fixed at one support end, and transversely restrained at the other

Table 3. Parameter Definitions for "Regular" Bridges

Parameter	Value				
Number of Spans	2	3	4	5	6
Maximum subtended angle for curved bridge	20	20	30	30	30
Maximum span length ratio, from span to span	3	2	2	1.5	1.5
Maximum bent/pier stiffness ratio from span to span, excluding abutments	–	4	4	3	2

- A superstructure supported on isolation bearings that act in all directions that accommodate displacements

Foundations

Provisions for spread footings, driven piles, drilled shafts (or cast-in-drilled-hole piles), and abutments have been significantly improved over similar provisions in the current AASHTO specifications. These are, in large part, based on a number of advances made through research programs sponsored recently by the Federal Highway Administration, Caltrans, and others. For abutments, explicit recognition of sacrificial elements has been provided, including knock-off back walls and other similar fuse elements.

Steel Bridges

The current AASHTO Specifications do not have seismic requirements for steel bridges, except for the provision of a continuous load path to be identified and designed (for strength) by the engineer. Consequently, within the scope of this project subtask, a comprehensive set of special detailing requirements for steel components expected to yield and dissipate energy in a stable and ductile manner during earthquakes were developed (including provisions for ductile moment-resisting frame substructures, concentrically-braced frame substructures, and end-diaphragms for steel girder and truss superstructures).

In July 2000, MCEER hosted a workshop to review a draft of the proposed steel seismic provisions developed as part of this project. The workshop's participants consisted of representatives from academia, professional practice, State DOT's, FHWA, and the steel industry, with experience in seismic design and steel bridges. The objective of the workshop was to identify whether the proposed provisions were sufficiently comprehensive and answered needs identified in past projects with workable solutions.

The proposed seismic provisions for steel bridges were generally well received. It was also the consensus opinion that seismic provisions for steel structures were desirable, and that there may even be instances where steel substructures may be the preferred choice for seismic energy dissipation (particularly when combined with other advantages such as rapid construction). The final draft of the proposed

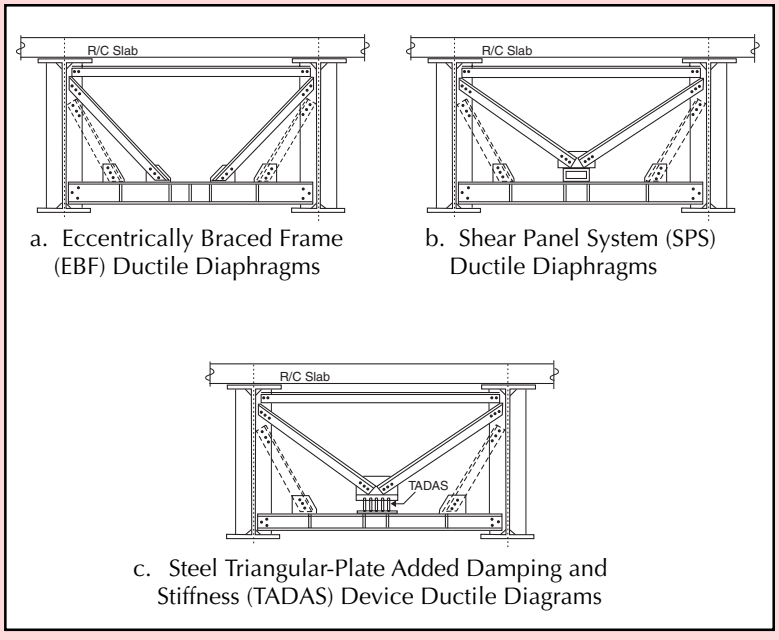

a. Eccentrically Braced Frame (EBF) Ductile Diaphragms

b. Shear Panel System (SPS) Ductile Diaphragms

c. Steel Triangular-Plate Added Damping and Stiffness (TADAS) Device Ductile Diagrams

Figure 4. Structural Model - Steel Structures

Specifications reflects much of the expert opinions expressed during this workshop. It is also structured to allow the use of innovative steel-based energy dissipation strategies (as shown in figure 4), provided seismic performance can be experimentally substantiated.

Special Considerations Regarding Seismic and Geotechnical Hazards

A number of special provisions have been included to address important considerations in seismic hazard. Included in these are specifications related to vertical accelerations and their impacts on bridge performance, and near fault (and so-called "fling") effects. A significant amount of work is also being done to address the issues of soil liquefaction and lateral spreading, especially as this relates to the infrequent but potentially large upper-level 2,500-year event.

Summary

The new specifications for the seismic design of highway bridges that have been developed under NCHRP Project 12-49 are a significant departure from the procedures and requirements found in current AASHTO specifications. Work on NCHRP Project 12-49 was completed in the spring of 2001, and the AASHTO Highway Subcommittee on Bridges and Structures will review the provisions resulting from the project, with possible adoption and publication by AASHTO in late 2001.

Literature Review of the Observed Performance of Seismically Isolated Bridges

by George C. Lee, Yasuo Kitane and Ian G. Buckle

Research Objectives

Despite the use of seismic isolation for the protection of bridges for more than 20 years, the performance of these bridges during strong ground shaking remains to be verified in the field. Numerous analytical and experimental studies have been completed in many countries to date demonstrating the validity of the concept, but full-scale field verification under strong shaking has yet to be obtained. This is partly due to the fact that the world population of these bridges is relatively small, but in addition, only a small fraction of this population is instrumented with strong motion instruments. However, recent earthquakes (even though small-to-moderate in size) have given some insight into the actual performance of seismically isolated bridges, and the experience-database for these bridges is growing. This research focuses on assembling currently available information on observed performance of isolated bridges and identifying areas where further research may be necessary to improve the state-of-the-art. This paper is a summary of a comprehensive literature review recently undertaken on observed performance in recent earthquakes. Based on collected information, possible future research needs are indicated.

The fundamental concept of seismic isolation is straightforward: to reduce earthquake-induced forces in a structure by lengthening its natural period, or by adding damping to the structure, or both. Most isolation systems fall into this last category, i.e., they both lengthen the period and add damping.

Although the concept of protecting structures from an earthquake, by introducing seismic isolators, was first proposed almost 100 years ago, it is only recently that seismic isolation has become a practical strategy for earthquake-resistant design (Chopra, 1995). In general, seismic isolators have the following four major functions (Skinner, 1993; Kelly, 1997):

- To transmit vertical load (e.g., dead load) from one part of a bridge to another, usually from the superstructure to the substructure, while allowing thermal and other movement effects to occur (i.e., to perform the same role as a conventional bearing).

Sponsors

Federal Highway Administration

Research Team

***Ian G. Buckle**, Professor, Department of Civil Engineering, University of Nevada, Reno*

***Yasuo Kitane**, Graduate Student, Department of Civil, Structural and Environmental Engineering, University at Buffalo*

***George C. Lee**, Director, Multidisciplinary Center for Earthquake Engineering Research, and Samuel P. Capen Professor of Engineering, University at Buffalo*

Web Sites

List of Seismically Isolated Bridges in the United States: http://www.eerc.berkeley.edu/prosys/usbridges.html

- To isolate the part of the bridge above the isolators by introducing flexibility in the horizontal plane, or by limiting the horizontal shear force that may be transmitted to the isolated part.
- To provide sufficient rigidity under low level loads such as wind and traffic loads, and minor earthquakes.
- To introduce additional damping into the bridge system, so that relative displacements across the isolators can be controlled. In some cases, damping is provided directly by the isolators; in others, additional devices are installed alongside the isolators to provide this additional damping, such as viscous fluid dampers.

The most common isolators in use today in the United States fall into one of two categories: elastomeric-based (e.g., lead-rubber bearings and high-damping rubber bearings), and friction-based (e.g., Eradiquake bearings and friction-pendulum bearings).

In the 1970s, seismic isolation systems began to be implemented in bridges as aseismic devices. The technology spread quickly for the next 30 years, and many applications can now be found around the world and particular in Canada, Italy, Iceland, Japan, New Zealand, Taiwan, and the U.S. (See, for example, list of Seismically Isolated Bridges in the United States at *http://www.eerc.berkeley.edu/prosys/usbridges.html*.) Extensive research and development efforts have made this rapid technology transfer possible. Numerous experiments in the laboratory and computer analyses have been performed to investigate the effectiveness of the isolation technique, and have demonstrated (in theory) the advantages of isolation design over conventional earthquake resistant design.

However, the number of seismically isolated bridges that have experienced actual earthquakes is very low, and the number of instrumented isolated bridges, that have seen earthquakes, is even smaller. As a consequence, there is very little recorded data on the response of these bridges and the effectiveness of isolation remains to be conclusively proven in the field, particularly for large earthquakes.

Nevertheless, collecting and synthesizing the performance data that is available is a worthy exercise because it gives insight on field experience as well as indicating where future research efforts might be directed. This paper is the result of such an exercise. A comprehen-

Engineers who design bridges in seismically active areas throughout the world will find information on the response of isolated bridges during earthquakes very valuable. Bridges that have both experienced actual earthquakes and have been instrumented are rare, however, this type of information is necessary to demonstrate the effectiveness of the isolation system. This survey is the first step in developing a database of performance characteristics of a variety of isolation devices, which will eventually affect design and manufacturing criteria for these devices, and impact guidelines for their use.

sive literature review has been conducted on the observed performance of seismically isolated bridges in recent earthquakes, and the results are presented below. Observations are also made and summarized.

Observed Seismic Performance

A database, summarizing the actual performance of seismically isolated bridges in real earthquakes, is growing gradually. This section summarizes some of this material for bridges located in Japan, New Zealand, Taiwan, Turkey and the U.S. Information is presented country-by-country, in alphabetical order.

Japan

The **Miyagawa** bridge, as shown in Figure 1, was built in 1991 and is a 3-span continuous steel plate girder bridge with a total length of 108.5 m and effective width of 10.5 m. This bridge was the first in Japan to be seismically-isolated. It uses lead-rubber bearings (LRBs) for the isolators, which are designed to yield at a lateral force of 12% of the weight of superstructure. In Japan, it is common to restrain the transverse displacement of bridge isolators, and therefore many bridges in Japan are isolated in the longitudinal direction only. This 'partial' isolation is called 'menshin' design, and the Miyagawa bridge is an example of this technique. In 1991, the bridge was subjected to ground motions from an earthquake with a magnitude of 4.9 and an epicenter 30 km northeast of the bridge site. The seismic response of the bridge was recorded by three accelerometers in the bridge superstructure. As shown in Table 1, the peak ground acceleration was small, the LRBs did not reach yield and the nonlinear behavior of LRBs was not significant. The maximum acceleration in the deck was about 50% of that recorded 10 m below the ground surface, which illustrates the effectiveness of the isolation. Spectral analysis showed that vibrations with frequencies in the 3.0 to 5.0 Hz range, were successfully filtered out by the isolators. However, it was also found that vibrations with frequencies of 1.2 Hz were amplified by a factor of 2.0 (by the isolators) when compared to the ground motion. Nonlinear behavior of the isolators may suppress this amplification in larger earthquakes but the importance of considering the predominant ground motion period, when selecting the isolated period, is illustrated (Kawashima et al., 1992).

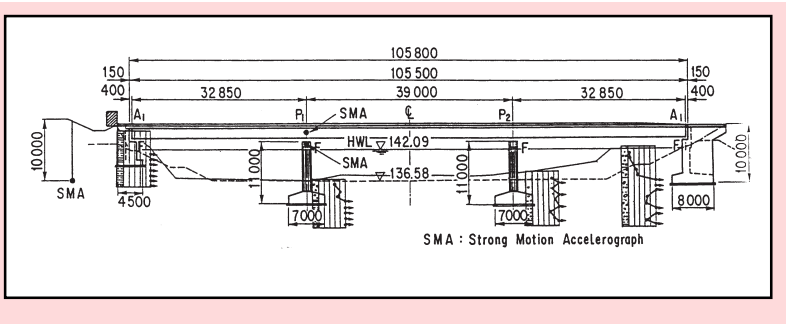

Figure 1. Miyagawa Bridge (Kawashima et al., 1992)

The **Yama-age** bridge was built in 1993 and is a 6-span continuous pre-stressed concrete box girder bridge with a total length of 246.3 m and an effective width of 10.5 m to 13.5 m. The bridge is seismically isolated with high damping rubber bearings, and is again isolated in the longitudinal direction only (menshin design). Seismic responses of this bridge were recorded during the 1994 Hokkaido-toho-oki earthquake

■ Table 1. Peak Accelerations and Amplification Factors for Bridges in Japan

			Longitudinal	Transverse	Vertical
Miyagawa Bridge[1]	Peak Acc.	Deck	0.0051 g	0.0043 g	0.0027 g
		Pier Crest	0.011 g	0.0067 g	0.0025 g
		Underground[2]	0.012 g	0.0091 g	0.0030 g
	Amplification Factor	Deck/Underground	0.431	0.483	0.897
		Pier Crest/Underground	0.897	0.742	0.862
		Deck/Pier Crest	0.481	0.652	1.04
Yama-age Bridge[1]	Peak Acc.	Deck	0.012 g	0.019 g	---
		Pier Crest	0.038 g	0.014 g	---
		Underground[3]	0.0093 g	0.0085 g	0.047 g
	Amplification Factor	Deck/Underground	1.30	2.28	---
		Pier Crest/Underground	4.05	1.71	---
		Deck/Pier Crest	0.320	0.133	---
Maruki-bashi Bridge	Peak Acc.	Deck	0.098 g	0.12 g	0.058 g
		Pier Crest	0.11 g	0.13 g	0.038 g
		Underground[4]	0.065 g	0.059 g	0.038 g
	Amplification Factor	Deck/Underground	1.51	2.07	1.52
		Pier Crest/Underground	1.69	2.19	0.997
		Deck/Pier Crest	0.890	0.947	1.52
Matsunohama Bridge[1]	Peak Acc.	Deck	0.19 g	---	---
		Pier Crest	0.20 g	0.36 g	0.077 g
		Footing	0.11 g	0.13 g	0.070 g
		Underground[5]	0.15 g	0.14 g	0.12 g
	Amplification Factor	Deck/Underground	1.30	---	---
		Pier Crest/Underground	1.39	2.64	0.655
		Footing/Underground	0.717	0.933	0.595
		Deck/Pier Crest	0.940	---	---

NOTES 1. Transverse movement is restrained in these bridges
2. 10 m below the ground surface
3. 5 m below the ground surface
4. 6 m below the ground surface
5. 1 m below the ground surface

with magnitude 8.1, whose epicenter was about 1,000 km away from the bridge. Recorded peak accelerations are shown in Table 1. Judging from obtained acceleration response records, none of the seismic isolators were exercised in their nonlinear range. Peak deck acceleration decreased to one-third of that at the pier top, in the longitudinal direction, while it increased by 30% in the transverse direction (restrained direction). Spectral analysis of the recorded responses showed that the vibration component, with a frequency equal to the fundamental frequency of the pier, was not transmitted to the deck through the seismic isolators (PWRI, 1995; Unjoh, 1996).

The **Maruki-bashi** bridge was built in 1992 as a seismically isolated bridge with lead-rubber bearings of a circular shape. It is isolated in the longitudinal and transverse directions. It is a 3-span continuous prestressed concrete box girder bridge with a total length of 92.8 m and an effective width of 11.0 m. The bridge was excited by ground motions and its seismic response was recorded during the 1994 Sanriku-haruka-oki earthquake with magnitude of 7.5. The epicenter was about 190 km from the bridge site. Recorded peak accelerations are shown in Table 1. The peak deck acceleration in the longitudinal direction decreased by 11% from that at the pier top, due to the seismic isolators, and by 5% in the transverse direction. The peak deck accelerations were 1.7 times and 2.2 times of the peak ground accelerations in the longitudinal and transverse directions, respectively. Judging from the recorded acceleration response, it can be concluded that seismic isolators remained elastic and did not yield. Therefore, the effectiveness of seis-

mic isolation is not very apparent from the recorded data. Spectral analysis of the recorded data shows amplification factors (ground to deck) with two peaks at 2.5 Hz and 16.7 Hz in the longitudinal direction (2.5 Hz is the fundamental frequency of the entire bridge, and 16.7 Hz is the frequency of the bridge pier itself). Moreover, it was also observed that the vibration component with the frequency equal to the fundamental frequency of the pier, was filtered out between the pier top and the deck by the seismic isolators, in the longitudinal direction (PWRI, 1995).

The **Matsunohama** bridge was subject to the 1995 Hyogoken-nanbu (Kobe) earthquake of magnitude 7.2 and epicentral distance 35 km from the bridge site. The bridge was built in 1991, and is a curved 4-span continuous steel box girder bridge with a total length of 211.5 m, a maximum width of 21.94 m, and a radius of curvature of 560 m. It is a seismically isolated bridge but only in the longitudinal direction (menshin design). Both ends of the bridge are supported by pivot roller bearings, and two lead-rubber bearings are installed on each of the three middle piers. Recorded peak accelerations are shown in Table 1. The peak acceleration of the deck was a little smaller than that of the pier top in the longitudinal direction, in which seismic isolation was effective. Judging from the displacement response obtained by integrating the acceleration records, the isolators reached yield. The maximum displacement was about twice the yield displacement, and about 8% of the design displacement for the isolators. Spectral analysis showed that the vibration component, corresponding to the frequency of the pier (1.0 Hz), was not transmitted from the pier to the deck by the isolators. These observations infer that the isolation system functioned as expected (PWRI, 1995; Naganuma et al., 1996; Fujino et al., 1997; Kouno et al., 1997).

New Zealand

The **Te Teko (Rangitaiki River)** bridge was built in 1983 and is a 5-span pre-stressed concrete U-beam bridge with a total length of 103 m. The bridge is seismically isolated by lead-rubber bearings at each pier and plain rubber bearings at each abutment. It was subject to the 1987 Edgecumbe (Bay of Plenty) earthquake with magnitude of 6.3 at a distance of 15 km from the bridge. The bridge was not instrumented but the peak ground acceleration, recorded about 11 km south of the bridge, was 0.33g. One of two bearings on the abutment was dislocated due to a construction deficiency (inadequate fastening detail for the isolator) and as a consequence, the bridge sustained minor damage. The superstructure suffered a small permanent displacement, a plastic hinge began to form in one pier that spalled a small amount of cover concrete, and a sacrificial knock-off device was pushed about 80 to 100 mm from its original position. Based on the fact that the bridge suffered only minor damage despite the severe ground shaking, it can be said that the bridge performed well, and that it may not have been damaged at all if the construction deficiencies had been avoided by better detailing (Mckay, 1990; Robinson, 1992; DIS, 1996).

"Testing of isolated bridge models at full scale is now possible due to multiple shake table facilities with biaxial motions under the NSF-NEES initiative."

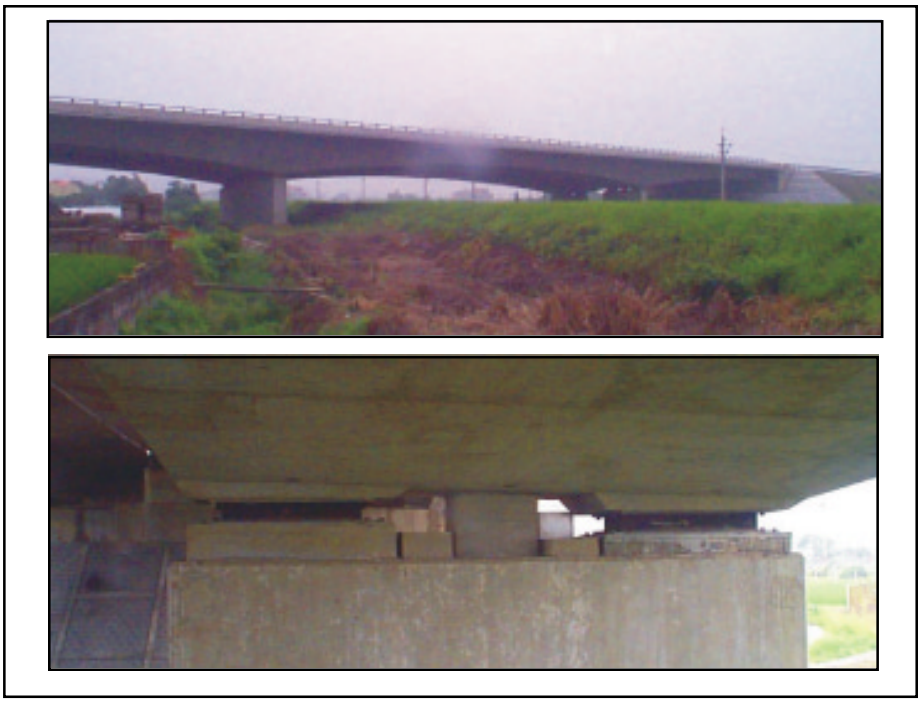

Figures 2 and 3. Bai-Ho Bridge (top) and Isolation System of the Bai-Ho Bridge (bottom)

Taiwan

The **Bai-Ho** bridge, as shown in figure 2, is a 3-span continuous non-prismatic prestressed concrete girder bridge with a total length of 145 m and a maximum width of 16.1 m. The bridge is seismically isolated with two lead-rubber bearings installed on each pier (see figure 3) and two PTFE coated rubber bearings at each abutment. Shear keys and specially designed steel rods are installed on both abutments to restrict the transverse movement of the superstructure. The bridge is therefore partially isolated in the transverse direction. Construction of the bridge was nearly completed but it was not in service at the time of the 1021 (1999) Gia-I earthquake of magnitude of 6.0. Eleven accelerometers had been mounted in the bridge prior to the earthquake and recorded peak accelerations and amplification factors are shown in Table 2. No damage was suffered. The peak acceleration in the deck in the longitudinal direction was slightly higher than that in the foundation, while the peak acceleration in the transverse direction was 2.5 times that of the foundation. Significant elongation of the structure period was observed in the longitudinal direction due to the nonlinear behavior of the LRBs. The bridge performed very well in this direction. On the other hand, two dominant vibration modes were observed in the transverse direction and the peak transverse response was governed by its second

Table 2. Peak Accelerations and Amplification Factors in the Bai-Ho Bridge

	Long.	Trans.	Vert.
Deck	0.18 g	0.26 g	0.11 g
Pier Top	0.15 g	0.12 g	---
Foundation	0.15 g	0.10 g	0.036 g
Free Field	0.17 g	0.18 g	0.053 g
Deck/Foundation	1.20	2.49	3.20
Pier Top/Foundation	0.991	1.10	---
Deck/Pier Top	1.19	2.26	---

mode. It is clear that the transverse restraint provided at the abutments adversely affected the response in this direction (compared to that in the longitudinal direction). This bridge also experienced the Chi-Chi earthquake on September 21, 1999, but no records were obtained at the time (Chang et al., 1999).

Turkey

The **Bolu** viaduct on the Trans European Motorway (see figure 4) in the Kaynasli valley was still under construction when the Duzce earthquake (M=7.2) occurred in November 1999. Many of the structural elements were complete at the time, but guardrails and paving remained to be installed. The bridge is composed of two parallel viaduct structures with pre-stressed concrete hollow T-girders and 58 monolithic column footings. It has a total length of 2,313 m and a width of 17.5 m. A typical module of the bridge (as shown in figure 5) is a 10-span viaduct with a maximum span length of 39.6 m and a maximum pier height of 49 m. The PTFE bearing and the crescent moon-type steel energy dissipation device are shown in Figures 6 and 7, respectively. The bridge is equipped with flat stainless steel-PTFE sliding bearings, a multidirectional crescent moon-type steel energy dissipation device at the central support of the 10-span unit, viscous connecting devices at other supports, steel strands restrainers at the expansion joints between the 10-span units, and bi-directional steel energy dissipation devices at the two abutments. The bridge was not instrumented at the time of the earthquake, but peak ground accelerations at the site have been estimated as over 1g (the strong motion station in Duzce, near the epicenter and about 5 km to the west of the viaduct, recorded accelerations in excess 1.0g.)

Figure 4. Bolu Viaduct on the Trans European Motorway (Xiao et al., 1999)

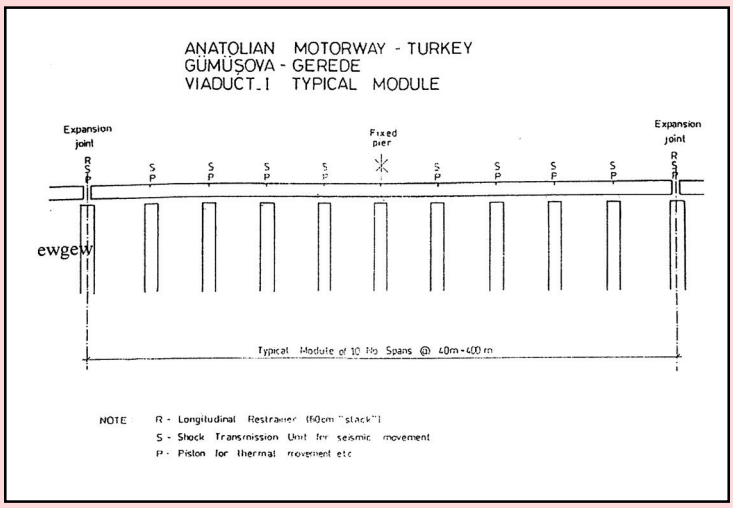

Figure 5. Typical Module of the Bolu Viaduct (Xiao et al., 1999)

The following observations were made by Xiao and Yaprak (1999). Ground rupture was observed near the south side of the bridge, and the fault crossed under the bridge near Pier 46. Soil around the footing of the pier was disturbed significantly and the pier appeared to have rotated about 12 degrees about its vertical axis. Damage to

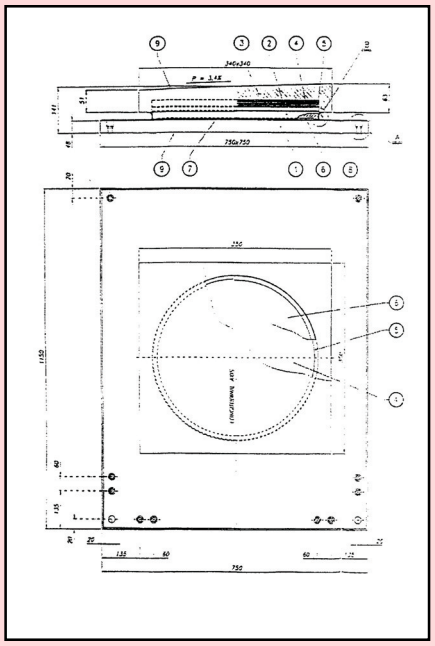

■ Figure 6. PTFE Bearing (Xiao et al., 1999)

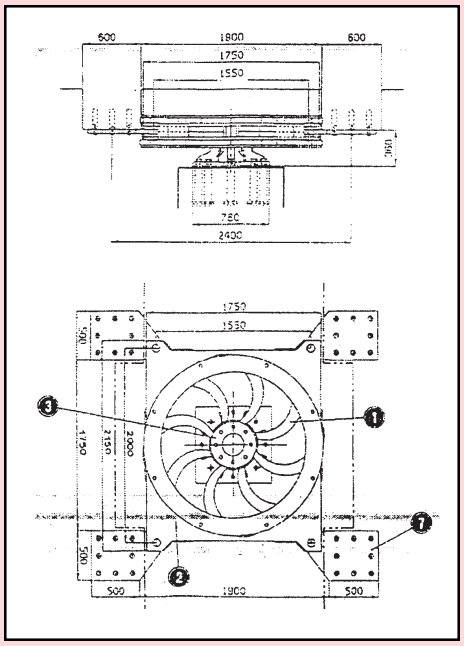

■ Figure 7. Energy Dissipation Device(Xiao et al., 1999)

the columns of the viaduct was limited to fine horizontal flexural cracks in the lower portion of several piers. Most of the structural damage was sustained by the superstructure and the abutments. Both superstructures (of the two bridges) had a westward permanent displacement relative to the piers with offsets at all girder ends. Some of the outer-most prestressed concrete girders slid off their concrete pedestals. Cracks occurred at the ends of many girders. Severe concrete spalling and crushing was observed for at least one pre-stressed concrete girder. The south side wing walls of the east abutments of the two bridges sustained severe damage due to pounding by the girder ends.A permanent southward transverse offset of about 250 mm was observed at the ends of both the south and north bridges. Concrete crushing and inclination of the abutments was observed at the west end of the viaduct, caused by pounding between the girders and abutments (Xiao et al, 1999).

■ Figure 8. Bearing Failure of the Bolu Viaduct (Xiao et al., 1999)

Stainless steel plates, bearing masonry and anchor plates, and PTFE bearings fell from their supports at almost all piers. Judging from the scratch signs on the stainless steel plates, these bearings were probably dislodged at a very early stage in the earthquake (see figure 8). This is consistent with the expec-

tation that the bridge encountered a near-fault or on-fault pulse-type motion during the earthquake, and that it experienced excessive displacement. Energy dissipation devices at the east abutment sustained distortion of the steel yielding elements and rupture of the anchor bolts of the devices. No span collapsed despite experiencing a level of ground shaking beyond the original design level during this earthquake. In addition, this viaduct survived the previous earthquake (August 17) without damage. The magnitude of the August earthquake was 7.4, and the peak ground accelerations were estimated as 0.39 g (longitudinal), 0.31 g (transverse), and 0.50 g (vertical) (Xiao et al, 1999).

United States

The **Sierra Point** overpass, U.S. 101, is a 10-span simply supported composite girder bridge with a skew angle of 59 degrees at the north abutment and 72 degrees at the south abutment. Its total length and width are 184.8 m and 35.1 m, respectively. The bridge was constructed in 1956, and retrofitted with lead-rubber bearings in 1985. It was the first bridge to be retrofitted in the U.S. using isolation and avoided the need to jacket the nonductile columns and strengthen the footings. However, the abutments were not modified for the larger clearances required for an isolation retrofit. They are therefore expected to engage during low-to-moderate shaking, and to be damaged in strong shaking.

The seismic response of this bridge was recorded by five accelerometers during the 1989 Loma Prieta earthquake. The peak ground acceleration at the base of the bridge columns was 0.090 g in the longitudinal direction and 0.050 g in the transverse direction. Significant amplification occurred at these low level accelerations in the steel superstructure of the bridge, due to the lock-up action of the abutments, which prevented the isolators from acting. No damage, however, was sustained (DIS, 1996).

The **Eel River** bridge was retrofitted with lead-rubber bearings in 1987. Two truss spans of the bridge were seismically isolated, and each span has a span length of 90.0 m (Buckle et al., 1987). The bridge was subjected to earthquake ground motions during the 1992 Cape Mendocino (Petrolia) earthquake, whose magnitude was 7.0 and epicenter was located 22 km from the bridge. The bridge was not instrumented but peak ground accelerations obtained at the Painter Street Overpass, a similar distance from the epicenter, were 0.55 g in the longitudinal direction, and 0.39 g in the transverse direction. As a consequence, it is believed that this is the strongest ground motion to have been felt by a seismically isolated structure in the United States. Judging from the displacement of the guardrail attached to the truss span, the maximum relative displacement between the isolated trusses and the abutment appear to have been of the order of 200 mm (longitudinally) and 100 mm (transversely). The bridge came to rest in its original position and structural damage was light and limited to concrete spalling at joints (DIS, 1992; DIS, 1996).

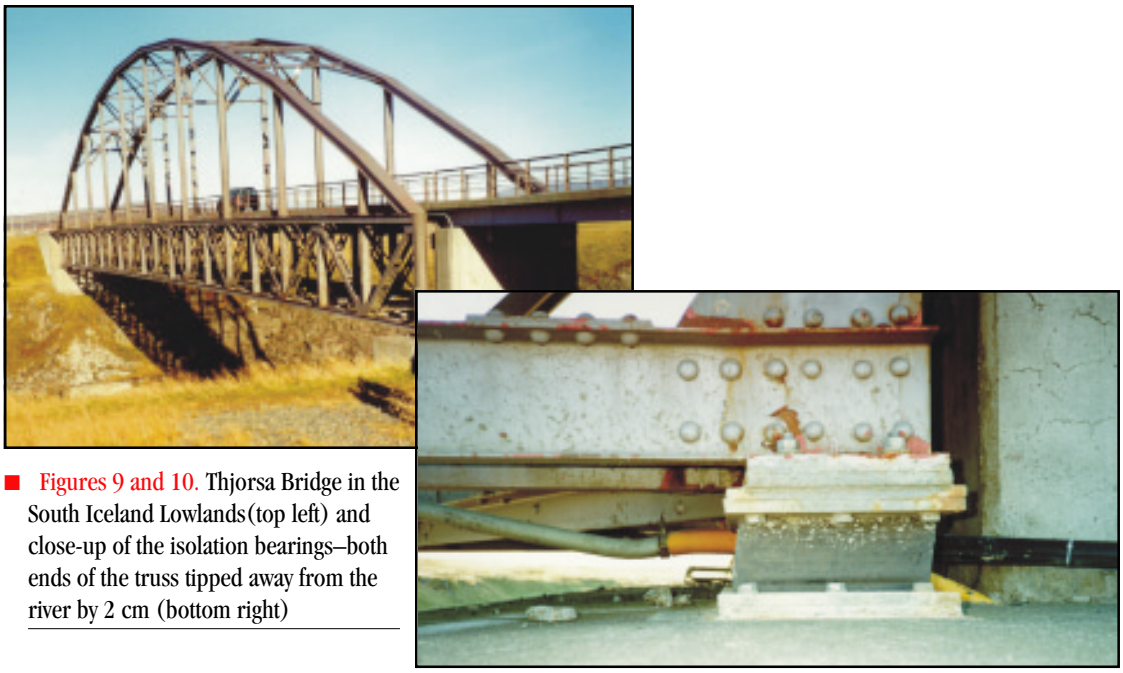

■ Figures 9 and 10. Thjorsa Bridge in the South Iceland Lowlands (top left) and close-up of the isolation bearings–both ends of the truss tipped away from the river by 2 cm (bottom right)

Observations

- Seismically isolated bridges have been researched and investigated by academia and engineers for many years. Due to this extensive effort, seismic isolation design has become a practical option for earthquake-resistant design.
- Results from numerous computer simulations and shake table experiments have shown the advantages of seismically isolated bridges compared to non-isolated bridges. However, few isolated bridges have experienced actual earthquakes and been able to demonstrate their effectiveness, especially under strong ground shaking. Furthermore, the majority of bridges that have been subject to earthquakes, have not been instrumented and performance must be inferred or extrapolated from nearby sites. Also, in the majority of cases, the earthquakes that have been captured are relatively small and the isolators have either not engaged or have remained in their elastic (and stiff) range. Recorded performance of an isolated bridge during strong ground motion is not yet available and thus the effectiveness of seismic isolation, especially during a large earthquake, remains to be proven in the field.
- An exception to the previous item might be the performance of several isolated bridges during the June 17 and 21, 2000, earthquakes in Iceland, which measured 6.6 and 6.5 on the Richter scale, respectively. These bridges include the Thjórsá bridge (see Figures 9 and 10), the Sog River bridge, the Stóra Laxá River bridge, and the Óseyrar River bridge (Higgins, 2000). Lead-rubber bearings are installed in all four bridges, which were subjected to large ground motions during these earthquakes. The peak ground acceleration was 0.84g at one of the

bridge sites, but no significant damage was found. Recorded responses are currently being analyzed at the Earthquake Engineering Research Center, University of Iceland (EERCUI). Results are expected later this year (2001).

- Our experience-database of isolated bridges is very sparse. Many more seismically isolated bridges need to be instrumented with strong motion arrays, in order to address this urgent need and increase the likelihood that field verification will be available in the near future.
- In the absence of field data, testing of isolated bridge models at full scale, in structural testing laboratories, could be undertaken. Such work has not been previously possible on a meaningful scale, but the current development of multiple shake table facilities with biaxial motions, under the NSF-NEES initiative, makes this option a practical reality.
- The performance of isolated bridges in the near field of active faults has been a concern since the Northridge earthquake in 1994. The damage sustained by the Bolu Viaduct in Turkey, described above, gives substance to this concern. An urgent need is a rigorous investigation of the Bolu Viaduct to determine the cause for the damage, and identify changes, if any, that should be made to U.S. design and manufacturing criteria for isolators.
- It is clear from several of the above case studies that small earthquakes rarely yield the isolators, which then perform in their elastic and stiff range. Accordingly, the observed amplification factors are higher than would be expected for an isolated bridge and this highlights the need for a class of isolators that have the 'intelligence' to optimize their properties according to demand.
- Various types of seismic isolators have been proposed, developed, and tested to date. However, only a few of these have been implemented in the field due to concerns about performance under extreme events and their durability and maintenance. Comparative performance of new devices, using either elastomeric isolators or friction pendulum devices as benchmarks, should be undertaken to continue to advance the state-of-the-art.

References

Buckle, I.G. and Mayes, R.L., (1987), "Seismic Isolation of Bridge Structures in the United States of America," *Proceedings of the Third U.S. Japan Workshop on Bridge Engineering*, Public Works Research Institute, Ministry of Construction, Tsukuba, Japan, pp. 379-401.

Chang, K. C., Wei, S. S., Chen, H. W., and Tsai, M. H., (1999), *Field Testing and Analysis of a Seismically Isolated Bridge*, Report No. CEER R88-07, Center for Earthquake Engineering Research, National Taiwan University, Taipei, ROC (in Chinese).

References (Con't)

Chopra, Anil K., (1995), *Dynamics of Structures: Theory and Applications to Earthquake Engineering*, Prentice Hall, NJ.

Dynamic Isolation Systems, (1992), *Performance of the Eel River Bridge in the Petrolia Earthquakes of April 25-26, 1992*, Dynamic Isolation Systems, Inc., CA.

Dynamic Isolation Systems, (1996), *Earthquake Performance of Structures on Lead-Rubber Isolation Systems*, Dynamic Isolation Systems, Inc., CA.

Fujino, Y., Yoshida, J., and Abe, M., (1997), "Investigation on Seismic Response of Menshin Bridge Based on Measured Records," *Proceedings of the 24th Symposium on Earthquake Engineering Research*, pp. 325-328 (in Japanese).

Kawashima, K., Nagashima, H., Masumoto, S., and Hara, K., (1992), "Response Analysis Buckle, I. G. and Mayes, R. L., (1987), "Seismic Isolation of Bridge Structures in the United States of America," *Proceedings of the Third U.S.–Japan Workshop on Bridge Engineering*, Public Works Research Institute, Ministry of Construction, Tsukuba, Japan, pp. 379-401.

Kelly, James M., (1997), *Earthquake-Resistant Design With Rubber*, Second Edition, Springer-Verlag, UK.

Kouno, T. and Kawashima, K., (1997), "Vibration Characteristics of Menshin Bridge Based on Measured Records," *Proceedings of the 24th Symposium on Earthquake Engineering Research*, pp. 329-332 (in Japanese).

Mckay, G.R., Chapman, H.E., and Kirkcaldie, D.K., (1990), "Seismic Isolation: New Zealand Applications," *Earthquake Spectra*, Vol. 6, No. 2, pp. 203-222.

Naganuma, T., Horie, Y., Kobayashi, H., and Sasaki, N., (1996), "The Analysis of Seismic Response of the Bridge with Menshin Bearings During the Hyogo-ken Nanbu Earthquake," *Proceedings of the Fourth U.S.-Japan Workshop on Earthquake Protective Systems for Bridges*, Japan, December 9 and 10, 1996, Technical Memorandum of PWRI, No. 3480, Public Works Research Institute, Japan, pp. 259-265.

Public Works Research Institute (1995), *Study on Seismic Response Characteristics of Menshin Bridges Based on Measured Records*, Technical Memorandum of PWRI, No. 3383, Public Works Research Institute, Japan.

Robinson, W.H., (1992), "Seismic Isolation of Bridges in New Zealand," *Proceedings of the Second U.S.-Japan Workshop on Earthquake Protective Systems for Bridges*, Japan, December 7 and 8, 1992, Technical Memorandum of PWRI, No. 3196, Public Works Research Institute, Japan.

Skinner, Robert Ivan, Robinson, William H., and McVerry, Graeme H. (1993), *An Introduction to Seismic Isolation*, John Wiley & Sons Ltd, England.

Unjoh, S., (1996), "Analysis of the Seismic Response of Yama-age Bridge," *Proceedings of the Fourth U.S.-Japan Workshop on Earthquake Protective Systems for Bridges*, Japan, December 9 and 10, 1996, Technical Memorandum of PWRI, No. 3480, Public Works Research Institute, Japan, pp. 149-163.

Xiao, Yan and Yaprak, Tolga Taskin, (1999), *Performance of a 2.3 km Long Modern Viaduct Bridge During the November 12, 1999 Duzce, Turkey, Earthquake*, U.S.C Structural Engineering Research Report, Report No. U.S.C-SERP 99/01, Department of Civil Engineering, University of Southern California, Los Angeles, California.

A Risk-Based Methodology for Assessing the Seismic Performance of Highway Systems

by Stuart D. Werner

Research Objectives

The objective of this research is to develop, apply, program, and disseminate a practical and technically sound methodology for seismic risk analysis (SRA) of highway-roadway systems. The methodology's risk-based framework uses models for seismology and geology, engineering (structural, geotechnical, and transportation), repair and reconstruction, system analysis, and economics to estimate system-wide direct losses and indirect losses due to reduced traffic flows and increased travel times caused by earthquake damage to the highway system. Results from this methodology also show how this damage can affect access to facilities critical to emergency response and recovery.

Past experience has shown that effects of earthquake damage to highway components (e.g., bridges, roadways, tunnels, etc.) may not only include life safety risks and post-earthquake costs for repair of the components. Rather, such damage can also disrupt traffic flows and this, in turn, can impact the economic recovery of the region as well as post-earthquake emergency response and reconstruction operations. Furthermore, the extent of these impacts will depend not only on the seismic response characteristics of the individual components, but also on the characteristics of the highway system that contains these components. System characteristics that will affect post-earthquake traffic flows include: (a) the highway network configuration; (b) locations, redundancies, and traffic capacities and volumes of the system's links between key origins and destinations; and (c) component locations within these links.

From this, it is evident that earthquake damage to certain components (e.g., those along important and non-redundant links within the system) will have a greater impact on the system performance (e.g., post-earthquake traffic flows) than will other components. Unfortunately, such system issues are typically ignored when specifying seismic performance requirements and design/strengthening criteria for new and existing components; i.e., each component is usually treated as an individual entity only, without regard to how its damage may impact highway system per-

Sponsors

Federal Highway Administration

Research Team

***Craig E. Taylor**, President, Natural Hazards Management Inc.*

***James E. Moore III**, Associate Professor, Departments of Civil Engineering and Public Policy and Management, University of Southern California*

***Sungbin Cho**, Research Associate, School of Policy, Planning, and Development, University of Southern California*

***Jon S. Walton**, Vice President, MacFarland Walton Enterprises*

***Stuart D. Werner**, Principal, Seismic Systems and Engineering Consultants*

Collaborative Partners

- ***Ian G. Buckle**, University of Nevada, Reno*
- ***Ian Friedland**, Applied Technology Council*
- ***John Mander**, University of Canterbury, New Zealand (formerly of the University at Buffalo)*
- ***Masanobu Shinozuka**, University of Southern California*

Other Contributors

- ***Howard Hwang**, Center for Earthquake Research and Information, University of Memphis*
- ***John Jernigan**, Ellers, Oakley, Chester and Rike, Inc., Memphis, Tennessee*
- ***Arch Johnson**, University of Memphis*
- ***W.D. Liu**, Parsons Brinckerhoff, Inc., formerly with Imbsen & Associates, Inc., Sacramento, California*
- ***David Perkins**, **Arthur Frankel** and **Eugene (Buddy) Schweig**, U.S. Geological Survey*
- ***Maurice Power,** Geomatrix Consultants, Inc., San Francisco*
- ***Sarah H. Sun**, Shelby County Office of Planning and Development*
- ***Edward Wasserman**, Tennessee Department of Transportation*
- ***T. Leslie Youd**, Brigham Young University*

formance. Furthermore, current criteria for prioritizing bridges for seismic retrofit represent the importance of the bridge as a traffic carrying entity only by using average daily traffic count, detour length, and route type as parameters in the prioritization process. No attempt is made to account for the systemic effects associated with the loss of a given bridge, or for the combination of effects associated with the loss of other bridges in the highway system.

To address these issues, current and recent highway research projects conducted by MCEER and funded by the Federal Highway Administration (FHWA) have included tasks to develop a SRA methodology for highway systems. This paper describes this methodology, presents results from a demonstration application of the methodology to the highway system in Shelby County, Tennessee, and summarizes plans for the further development, application, programming, and dissemination of the methodology. Further details on this methodology and its application are contained in the report by Werner et al. (2000).

Methodology Description

The SRA methodology (Figure 1) can be carried out for any number of scenario earthquakes and simulations, in which a "simulation" is defined as a complete set of system SRA results for one particular set of input parameters and model uncertainty parameters. The model and input parameters for one simulation may differ from those for other simulations because of random and systematic uncertainties.

For each earthquake and simulation, this multidisciplinary process uses geoseismic, engineering (geotechnical, structural, and transportation), network, and economic models to estimate: (a) earthquake effects on system-wide traffic flows and corresponding travel times, paths, and distances; (b) economic impacts of highway system damage (e.g., repair costs and costs of travel time delays); and (c) post-earth-

This SRA methodology will provide cost and risk information that will facilitate more rational evaluation of alternative seismic risk reduction strategies by decision makers from government and transportation agencies involved with improvement and upgrade of the highway-roadway infrastructure, emergency response planning, and transportation planning. Such strategies can include prioritization and seismic strengthening measures for existing bridges and other components, establishment of design criteria for new bridges and other components, construction of additional roadways to expand system redundancy, and post-earthquake traffic management planning.

quake traffic flows to and from important locations in the region. Key to this process is a GIS data base that contains four modules with data and models that characterize the system, seismic hazards, component vulnerabilities, and economic impacts of highway system damage (Figure 1b). These are incorporated into the four-step SRA procedure shown in Figure 1a.

This SRA methodology has several desirable features. First, it has a GIS database, to enhance data management, analysis efficiency, and display of analysis results. Second, the GIS database is modular, to facilitate the incorporation of improved data and models from future research efforts. Third, the procedure can develop aggregate SRA results that are either deterministic (consisting of a single simulation for one or a few scenario earthquakes) or probabilistic (consisting of many simulations and scenario earthquakes). This range of results facilitates the usefulness of SRA for a variety of applications (e.g., seismic retrofit prioritization and criteria, emergency response planning, planning of system expansions or enhancements, etc.). Finally, the procedure uses rapid engineering and network analysis procedures, to enhance its possible future use as a real-time predictor of component damage states, system states and traffic impacts after an actual earthquake.

Recent Developments

Improved procedures for characterizing scenario earthquakes, seismic hazards, bridge vulnerabilities, and transportation network analysis have been developed. These developments, which are summarized below, are now incorporated into a new pre-beta software package named REDARS 1.0 (Risks due to Earthquake DAmage to Roadway Systems).

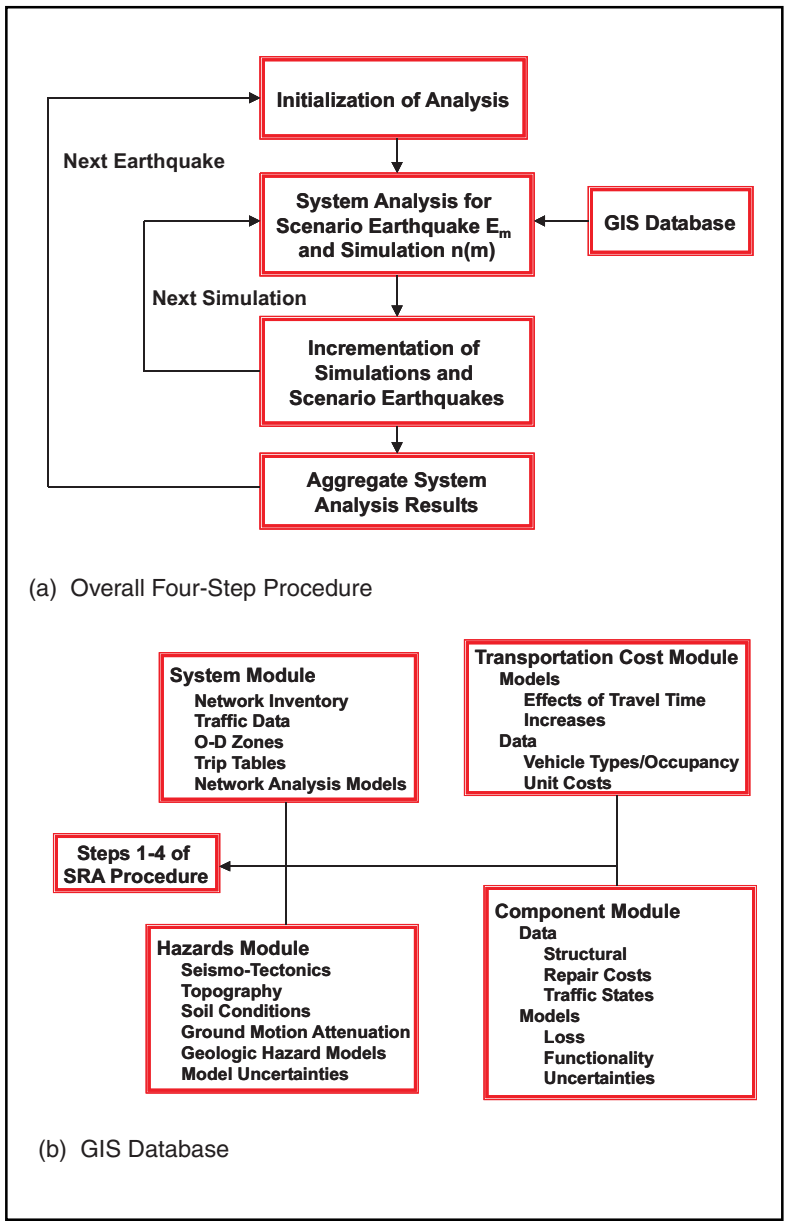

■ Figure 1. Risk-Based Methodology for Assessing Seismic Performance of Highway Systems

Links to Current Research

- *Seismic Vulnerability of Existing Highway Construction (Project 106)*
- *Seismic Vulnerability of the National Highway System (TEA-21 Project)*

Scenario Earthquakes

SRA of a highway system with spatially dispersed components requires use of scenario earthquakes to evaluate the simultaneous effects of individual earthquakes on components at diverse locations (including systemic consequences of damages). Earthquake models now being incorporated into REDARS are adaptations of work by Frankel et al. (1996) which was developed under the United States Geological Survey (USGS) National Hazard Mapping Program. Frankel et al. models for the Central (CUS) are summarized later in this paper. Adaptation of models for California (which also builds on work by the California Division of Mines & Geology) is now underway. All adaptations feature a "walk-through" analysis, which is a natural way to assess system loss distributions and their variability over time.

Seismic Hazards

The ground motion models for the SRA procedure include rock motion attenuation characteristics representative of the region where the system is located, as well as amplification of rock motions due to local soil conditions. For the Central United States, the Hwang and Lin (1997) rock motion attenuation relationships and soil amplification factors for NEHRP site classifications meet these requirements. Models appropriate to other regions of the country are now being incorporated. Liquefaction hazard models are based on work by Youd (1998), and include: (a) geologic screening to eliminate sites with a low potential for liquefaction; (b) use of modified Seed-Idriss type methods to assess liquefaction potential during each earthquake and (c) for those sites with a potential for liquefaction during the given earthquake, estimation of lateral spread displacement and vertical settlement using methods by Youd and by Tokimatsu and Seed (1987) respectively.

Component Models

Component models for highway system SRA develop traffic state fragility curves, which estimate the probability of a given traffic state (i.e., open lanes at various times after the earthquake) as a function of the level of ground shaking or permanent ground displacement at the component site. Thus far, this research has focused on developing such models for bridges only. These models estimate the bridge's damage state (damage types, locations, and extents) under a given level of ground shaking or displacement, and then obtain corresponding traffic states by using expert-opinion damage-repair models. The SRA methodology now includes three options for modeling damage states of bridges due to ground shaking: (a) an elastic capacity-demand approach by Jernigan (1998); (b) a simplified but rational mechanics-based method by Dutta and Mander (1998) that develops rapid estimates of damage states based on bridge-specific input parameters inferred from the FHWA National Bridge Inventory database; and (c) user-specified fragility curves, which can be developed for any bridge in the system, but are most appropriate for complex or unusual bridges. In addition, the SRA methodology includes a first-order

model for estimating bridge damage states due to permanent ground displacement.

Transportation Network Analysis

The SRA procedure contains two transportation network analysis methods. For deterministic SRA for a limited number of scenario earthquakes and simulations, a User Equilibrium (UE) method is used. This is an exact mathematical solution to an idealized model of user behavior, which assumes that all users follow routes that minimize their travel times. For probabilistic SRA involving many earthquakes and simulations, a new Associative Memory (AM) transportation network analysis procedure is used. This method provides rapid estimation of network flows, represents the latest well-developed technology for estimating traffic flows, is GIS compatible, and uses transportation system input data that are typically available from Metropolitan Planning Organizations. It is derived from the artificial intelligence field, and provides rapid and dependable estimates of flows in congested networks for given changes in link configuration due to earthquake damage (Moore et al., 1997).

Demonstration Application

System Description

The SRA methodology was used in a demonstration application to the highway system in Shelby County, Tennessee. Shelby County

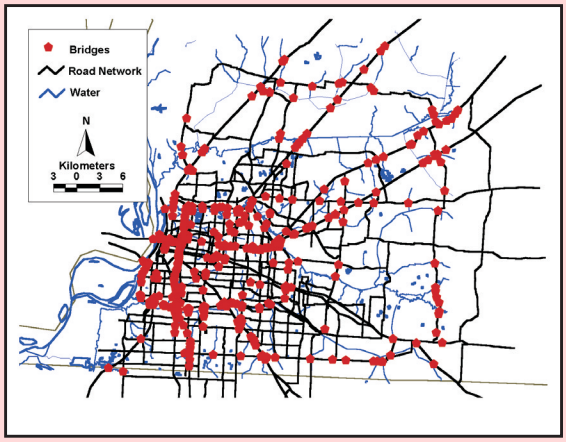

Figure 2. Shelby County Tennessee Highway System Model (7,807 Links and 15,604 Nodes)

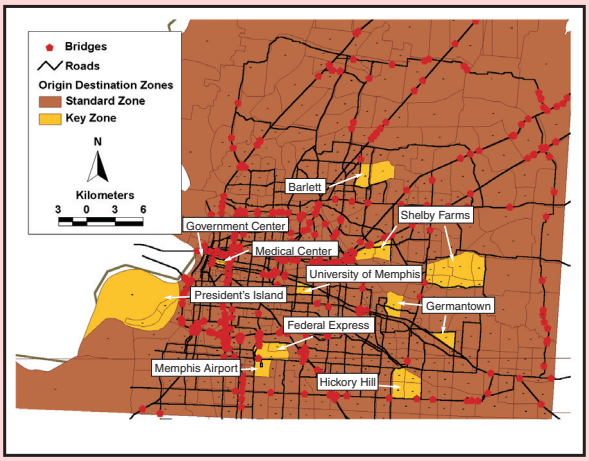

Figure 3. Origin-Destination Zones in Shelby County, Tennessee

is located in the southwestern corner of Tennessee, just east of the Mississippi River. Its highway-roadway system contains a beltway of highways that surrounds the city of Memphis, two major crossings of the Mississippi River, and major roadways that extend from the center of Memphis to the north, south, and east (Figure 2). Traffic demands on the system are modeled by trip tables that define the number of trips between all of the origin-des-

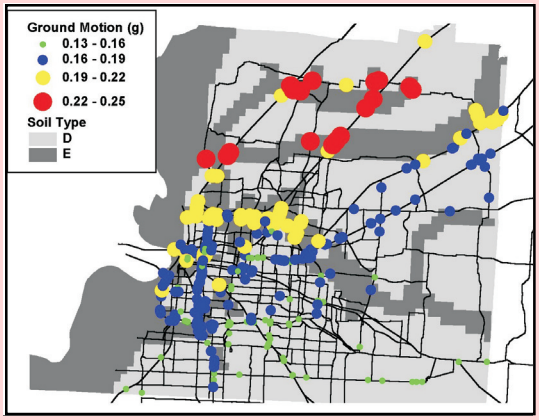

Figure 4. Ground Motion Hazard. Spectral Acceleration at Period of 1.0 Sec.

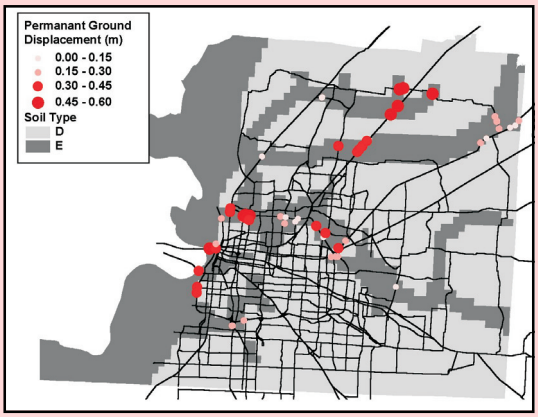

Figure 5. Liquefaction Hazard. Permanent Ground Displacement.

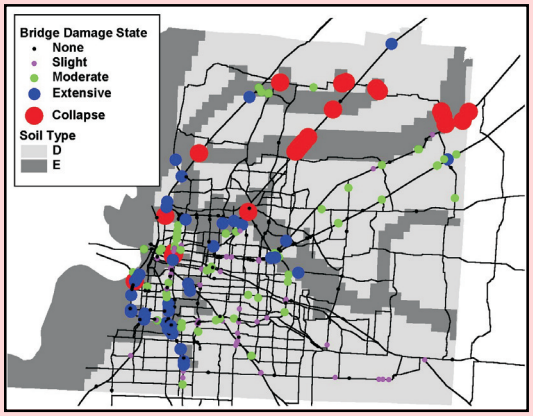

Figure 6. Bridge Damage States

tination (O-D) zones in the county. Figure 3 shows these O-D zones, as well as those zones for which post-earthquake travel times were monitored in this SRA.

Input Data

The input data for this SRA are as follows: (a) system input data describing the roadway network geometry, traffic capacities, O-D zones, and traffic demands were developed from a working file for the County's projected network for the year 2020 that was provided by the Shelby County Office of Planning and Development; (b) soils input data, in terms of NEHRP soil classifications and initial screening for liquefaction potential, were based on local geology mapping carried out by the Center of Earthquake Research and Development at the University of Memphis; and (c) attribute input data for each of the 384 bridges in the network were based on data compilation efforts by Jernigan (1998).

Scenario Earthquakes

This SRA was conducted as a walk-through analysis with a duration of 50,000 years. Earthquakes occurring during each year of this duration were estimated by adapting the Frankel et al. (1996) models of the region. This generated 2,321 earthquakes with moment magnitudes ranging from 5.0 to 8.0. Each earthquake was located into one of the 1,763 microzones (with lengths and widths of about 11.1

km) that encompassed the surrounding area.

Typical Results for One Scenario Earthquake and Simulation

To illustrate the form of the results for one earthquake and simulation, we consider a scenario earthquake with moment magnitude of 6.9 centered about 65 km northwest of downtown Memphis. For this event, ground shaking hazards and liquefaction hazards were estimated by the previously noted methods by Hwang and Lin (1997) and Youd (1998) respectively. (Figures 4 and 5). Next, the Dutta-Mander (1998) approach was used to estimate bridge damage states (Figure 6), and associated system states at various times after the earthquake were developed by applying the first-order repair model given in Werner et al. (2000) to these damage states (e.g., Figure 7). Network analysis procedures summarized earlier in this paper were then applied to each system state, to obtain corresponding system-wide traffic flows and travel time delays. Finally, simplified economic analysis methods adapted from California Department of Transportation models and summarized in Werner et al. (2000) were used to estimate corresponding economic losses (due to commute time increases only).

Economic Losses

After results of the type shown above are developed for each scenario earthquake and simulation during each year of the walkthrough, they can be aggre-

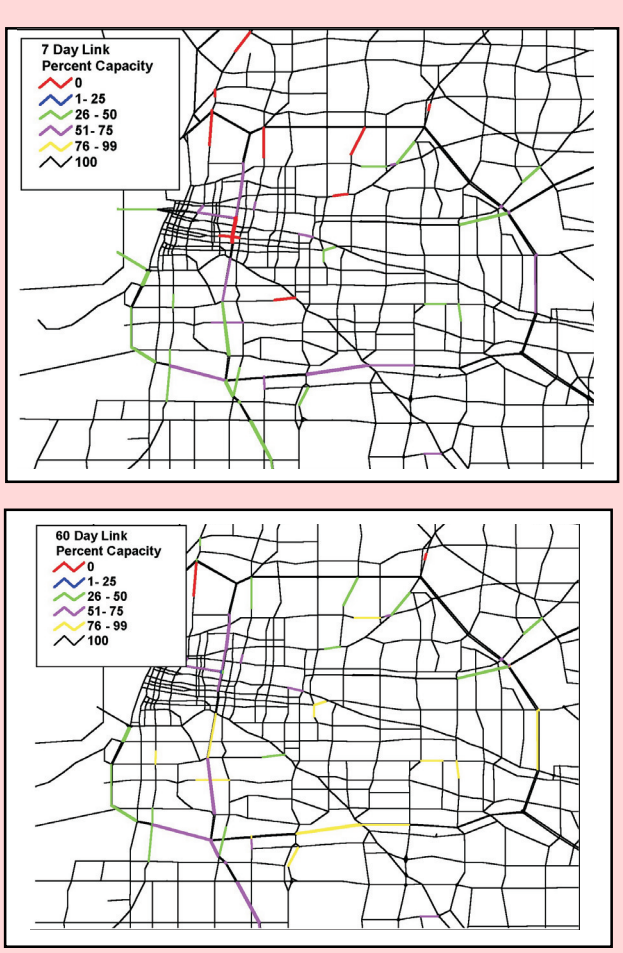

Figure 7. System States at 7 Days (top) and 60 days (bottom) after Earthquake

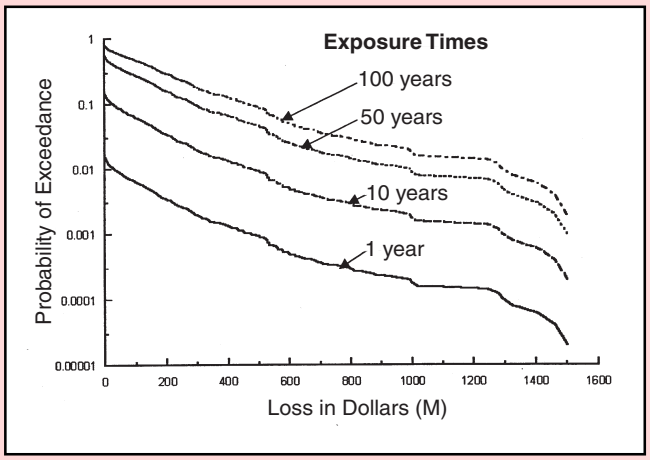

Figure 8. Economic Losses due to Earthquake-Induced Increases in Commute Times in Shelby County, Tennessee

■ Table 1. Increase in Access Times to Locations in Shelby County due to Damage to Highway System from Earthquake with Magnitude 6.8 centered 66 km Northwest of Downtown Memphis

Origin-Destination Zone (see Fig. 3)	Post-Earthquake Access Time		
	7 Days after EQ	60 Days after EQ	150 Days after EQ
9 (Government Center in downtown Memphis)	43.8%	5.8%	2.0%
28 (Major Hospital Center, just east of downtown Memphis)	44.6%	6.7%	2.0%
205 (Memphis Airport and Federal Express transportation center, south of beltway)	53.7%	4.0%	1.6%
73 (University of Memphis campus in central Memphis)	21.6%	4.3%	1.5%
310 (Germantown, residential area east of beltway)	2.9%	0.9%	0.4%
160 (President's Island, Port of Memphis at Mississippi River)	34.9%	6.1%	1.6%
246 (Hickory Hill, commercial area southeast of beltway)	3.9%	1.9%	1.1%
335 (Shelby Farms residential area northeast of beltway)	28.4%	4.8%	1.6%
412 (Bartlett, residential area north of beltway)	13.2%	3.0%	1.3%

gated to obtain probablistic estimates of economic losses. Figure 8 shows results of this type for exposure times of 1, 10, 50, and 100 years. Deterministic estimates of economic losses can also be obtained for selected individual earthquake events.

Travel Times for Selected Locations

For emergency planning purposes, it may be of interest to estimate how travel times to and/or from selected key locations in the region may be affected by earthquake damage to the highway system. Such results can be developed as aggregated probabilistic curves (similar in form to Figure 8) or as deterministic estimates for selected earthquake events (see Table 1).

Conclusions/Future Directions

The risk-based methodology described in this paper estimates how earthquake damage to highway systems can affect post-earthquake traffic flows and travel times. It is a technically sound and practical approach that will enable decision makers to consider system-wide traffic effects when evaluating various seismic risk reduction options for highway components and systems.

Although the basic SRA methodology is in place, further work remains before it can be disseminated and applied to highway systems nationwide. For example, the REDARS 1.0 pre-beta software package that is based on this methodology is now being independently validated and applied. This will help to identify future directions for further development of this software. Additional improvements now being planned include: (a) incorporation of models for estimating scenario earthquakes and ground motion hazards nationwide; (b) development of models for estimating system-wide landslide and surface fault rupture hazards; (c) de-

velopment of improved component repair models; (d) development of vulnerability/fragility models for retrofitted bridges as well as other highway components such as tunnels, slopes, pavements, walls, and culverts; and (e) development of the system module to accommodate post-earthquake traffic demands that differ from pre-earthquake demands.

References

Dutta, A. and Mander, J.B., (1998), "Seismic Fragility Analysis of Highway Bridges," *Proc. of INCEDE-MCEER Ctr-Ctr Workshop on Earthq. Engrg. Frontiers in Transp. Systems*, Tokyo Japan, June 22-23.

Frankel, A., Mueller, C., Barnhard, T., Perkins, D., Leyendecker, E.V., Dickman, N., Hanson, S., and Hopper, M., (1996), *National Seismic Hazard Maps*, June 1996 Documentation, Preliminary Report prepared at USGS, Denver CO, July 19.

Hwang, H.H.M. and Lin, H., (1997), *GIS-Based Evaluation of Seismic Performance of Water Delivery Systems*, University of Memphis, Memphis TN, Feb 10.

Jernigan, J.B., (1998), *Evaluation of Seismic Damage to Bridges and Highway Systems in Shelby County, Tennessee*, Ph.D. Dissertation, Univ. of Memphis, Memphis TN, Dec.

Moore, J.E. II, Kim, G., Xu, R., Cho, S., Hu, H-H, and Xu, R., (1997), *Evaluating System ATMIS Technologies via Rapid Estimation of Network Flows: Final Report*, California PATH Report UCB-ITS-PRR-97-54, Dec.

Tokimatsu, K. and Seed, H.B., (1987), "Evaluation of Settlements in Sand due to Earthquake Shaking," *J. of Geotech. Engrg.*, ASCE, Vol. 113, No. 8, pp. 861-878.

Werner, S.D., Taylor, C.E., Moore, J.E. II, and Walton, J.S., (2000), *A Risk-Based Methodology for Assessing the Seismic Performance of Highway Systems*, Report MCEER-00-0014, Multidisciplinary Center for Earthquake Engineering Research, University at Buffalo, (Dec. 31).

Youd, T.L., (1998), *Screening Guide for Rapid Assessment of Liquefaction Hazard at Highway Bridge Sites*, MCEER-98-0005, Multidisciplinary Center for Earthquake Engineering Research, University at Buffalo, May.

Analysis, Testing and Initial Recommendations on Collapse Limit States of Frames

by Darren Vian, Mettupalayam Sivaselvan, Michel Bruneau and Andrei Reinhorn

Research Objectives

The objective of this study is to develop a set of guidelines and analytical tools for use by practicing engineers to determine the collapse limit state of structures. A program of shake table testing of simple frames through collapse was carried out, and analytical strategies to capture this behavior have been developed and made available on the web via MCEER's users network. The research performed here helps to develop a better understanding of the collapse mechanism and provides tools for further investigation.

Sponsors

National Science Foundation, Earthquake Engineering Research Centers Program

Research Team

***Darren Vian**, Graduate Student, **Mettupalayam Sivaselvan**, Graduate Student, **Michel Bruneau**, Professor, and **Andrei Reinhorn**, Professor, Department of Civil, Structural and Environmental Engineering, University at Buffalo*

As inelastic behavior is more extensively relied upon in the dissipation of seismic input energy, the destabilizing effect of gravity becomes more significant in the structural evaluation of existing structures. However, practicing engineers have limited confidence in the adequacy of currently available analytical tools to accurately predict when collapse will occur (i.e., the collapse limit state). As a result, there is a need to investigate the seismic behavior of structures to enhance our understanding of the condition ultimately leading to their collapse, and to ensure public safety during extreme events. While many experimental studies and theoretical damage models support these calculated values, it remains that few experimental studies have pushed the shake table tests up to collapse.

This paper presents the results of research to provide some of that data through a program of shake-table testing of simple frames through collapse, developments of analytical strategies to capture this behavior, and recommendations for design. Note that every effort was made to ensure that the experimental data is fully documented (geometry, material properties, initial imperfections, detailed test results, etc.); it will be made broadly available on MCEER's Users Network such that these tests can be used at a later time by other researchers as a benchmark to which analytical models can be compared. An example of such use is the development made by the authors, described herein, using the benchmark test results.

Experimental Program

Fifteen specimens, each consisting of four columns, were tested to failure in the course of this research. These were subdivided into three groups of five with slenderness ratios of 100, 150, and 200. The dimen-

Web Sites

MCEER Users Network:
http://civil.eng.buffalo.edu/users_ntwk

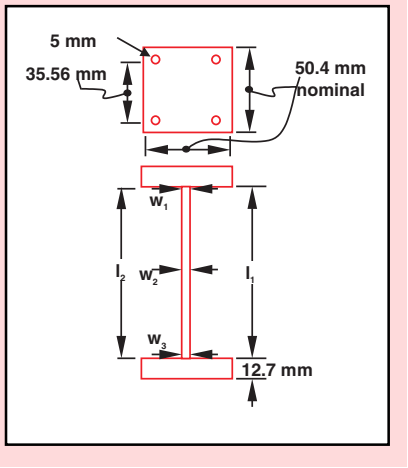

Figure 1. Typical Specimen

sions and mass used were varied within each group. Nominal specimen column widths ranged from 2.8 mm (1/8 in) to 9.8 mm (3/8 in). Column heights ranged from 91.7 mm (5.41 in) to 549.9 mm (21.65 in). Individual columns were cut from hot-rolled steel plate and then milled to size. Mass applied to each specimen column varied from approximately 150 kg to 385 kg. Predicted fundamental period of vibration for the specimens, using nominal dimensions, varied from 0.191 sec up to 1.098 sec considering the P-Δ effect. Note that the specimens were not intended to be scaled models of actual structures; therefore unscaled ground motions were used.

A sample column layout is shown in Figure 1. A range of values for axial capacity versus demand, P_u/P_n, was used for each slenderness ratio, where P_u is the weight of the mass plates used in the test, and P_n is the axial capacity of all columns in the specimen, calculated using the AISC-LRFD specifications (AISC 1993). This range of values is shown in Figure 2. A number of initial imperfections were carefully measured and documented, and movement in the transverse direction was prevented by flexible braces verified to have no impact on behavior in the principal direction, as reported in Vian and Bruneau (2001).

A schematic of the test setup and instrumentation is shown in Figure 3. Some special attachments and modifications to standard displacement transducers were developed (Vian and Bruneau, 2001) to ensure reliable measurements up to and

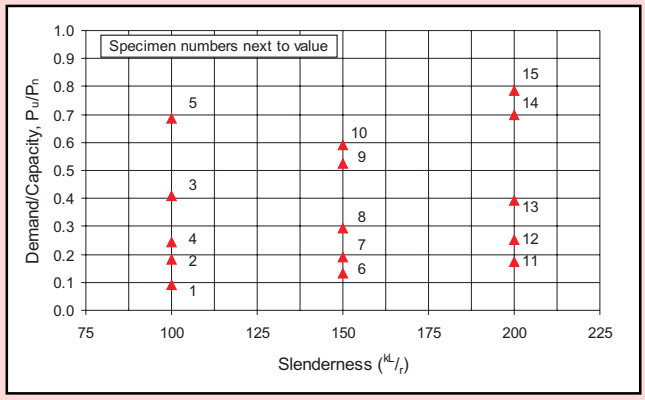

Figure 2. Specimen Axial Load-to-Strength Ratio versus Slenderness

The experimental data and analytical models from this research can be used by other researchers as a benchmark for comparison. Eventually, the research will enable structural engineers to adequately predict when collapse of a given structure will occur, thus ensuring public safety during strong earthquakes.

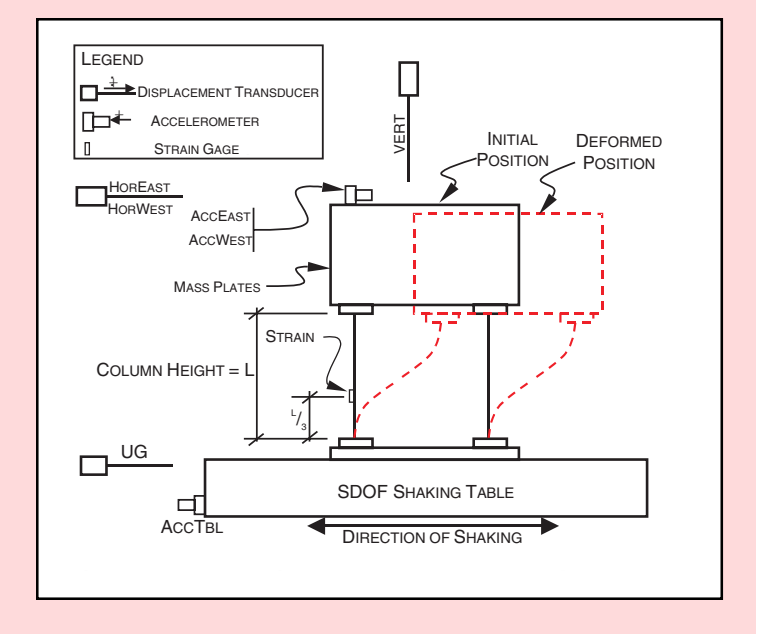

■ Figure 3. Schematic of Test Setup and Instrumentation (Looking West)

through collapse, but these details are beyond the scope of this paper.

A free vibration test was first performed on each specimen. Subsequently applied were a number of ground motions progressively increasing in magnitude from approximately two-thirds of the estimated peak elastic response to the estimated peak inelastic response. Among all the data recorded and stored, it is noteworthy that the actual total horizontal displacement of a specimen was calculated using the correction shown in Figure 4.

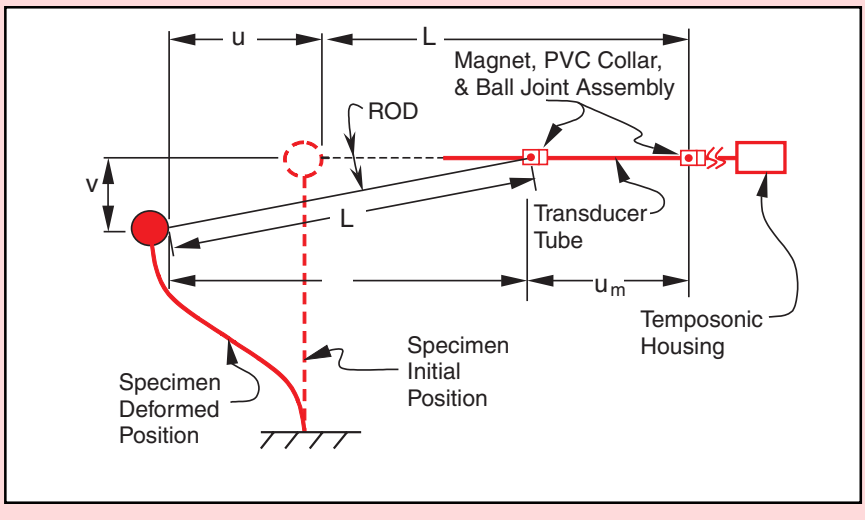

■ Figure 4. Definition of Variables used in Horizontal Displacement

Summary of Test Results

The fundamental period of vibration of each specimen is obtained experimentally via Fourier Spectrum Analysis of the time history data of free-vibration tests. Interestingly, the damping ratio was observed to vary as a function of the amplitude of linear elastic response. Results from the tests to collapse include:

- Seismic response of shake table tests including time history plots of target table acceleration, measured and filtered table acceleration, total mass acceleration, relative mass displacement, as well as a plot of estimated base shear including P-Δ, V_p^*, versus relative displacement.
- Time history plots of relative displacement for each test in the schedule for comparison of displacements throughout the range of progressive collapse.
- Plots of estimated base shear, V_p^*, normalized by the plastic base shear, V_{yo}, versus displacement ductility, μ, as well as similar plots of base shear versus percent drift, γ ($=u_{rel\text{-}max}/L_{avg}$).

Some typical results are shown in Figure 5.

Behavioral Trends

The value of the stability factor, indicated in the preceding discussion, has a significant effect on the response of the structure. In practical bridge and building structures, θ is unlikely to be greater than 0.10, and is generally less than 0.060 (MacRae et. al., 1993). Specimen 1 is the only one here that has a θ value near that suggested practical range for the stability factor, with a value of 0.065. Specimens 2, 6, and 11 have stability factors slightly larger than the likely upper limit, at 0.123, 0.101, and 0.138, respectively. All other specimens have a value of θ ≥ 0.155.

Three dimensionless acceleration parameters were compared with

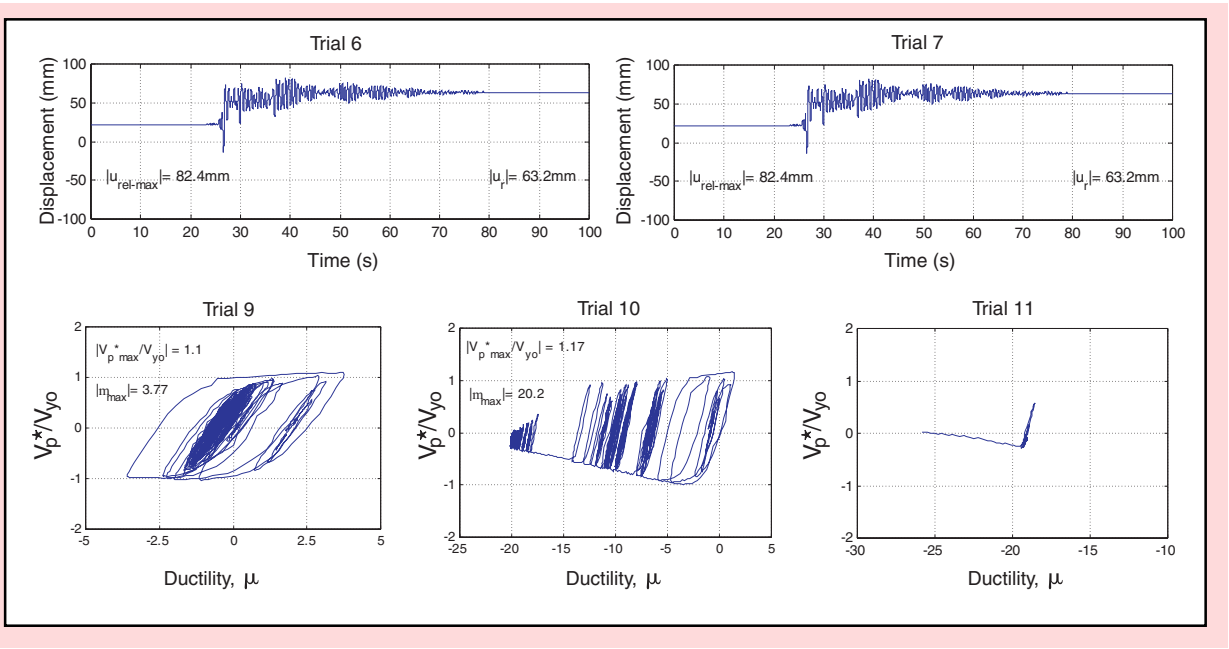

Figure 5. Typical Results from Tests to Collapse

five dimensionless displacement parameters. The following general observations can be made:

- The elastic spectral acceleration, S_a, ductility, μ, and percent drift, γ, were observed to have inverse relationships with θ. In support of this observation, these variables are plotted in Figures 6 and 7 versus the stability factor for the next to last test (given subscript "final"). This suggests that the structures may be less able to undergo large inelastic excursions before imminent instability as the stability factor increases.
- Specimen 1 was the only specimen that underwent both a ductility greater than five (20.35), and a drift larger than 20% of the specimen height (64%), prior to collapse, as shown in Figure 7. Recall that this is the only specimen that has a value of θ less than 0.1.

Overall, these Figures show a high dependence of ultimate inelastic behavior upon the stability factor for a P-Δ affected structure. For the specimens tested in this research, those that had a value of θ equal to or greater than 0.1, tended to have a relatively low level of inelastic behavior before collapse of the structure. Structures with $\theta < 0.1$ were able to withstand ground motions with higher spectral accelerations, experience larger values of ductility, and accumulate larger drifts, than those with $\theta > 0.1$. The more slender structures, characterized by a larger θ value, will undergo relatively small inelastic excursions prior to collapse.

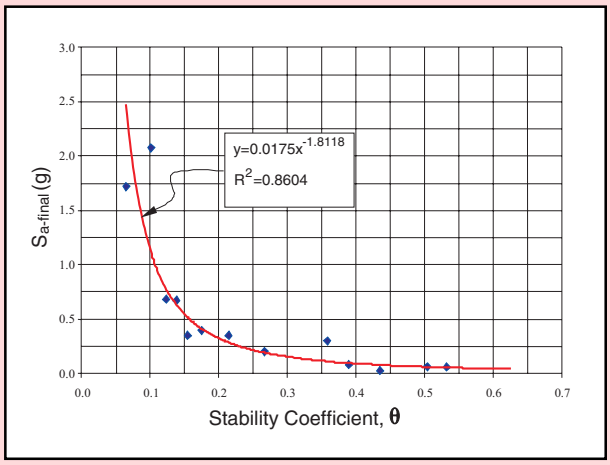

Figure 6. Spectral Acceleration versus Stability Coefficient

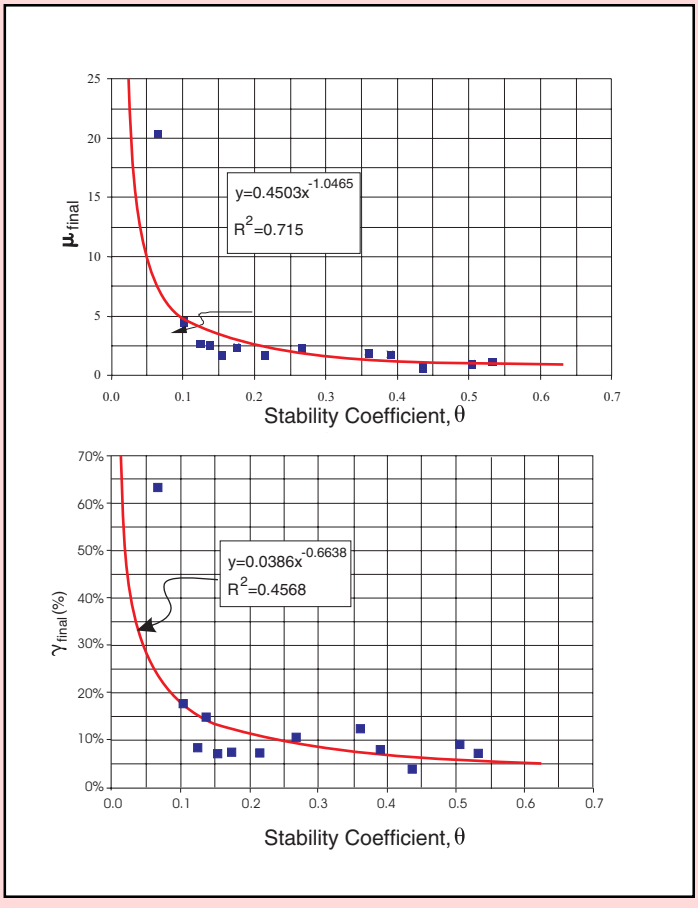

Figure 7. Plots of Displacement Ductility and Drift versus Stability Coefficient

Analytical Modeling and Verification using Data Generated From the Experiments

Data from the experiments performed in this research can be used in the verification of time history analysis programs in the modeling of inelastic structural behavior up to collapse. In these studies, an attempt was made to formulate a flexibility-based planar beam-column element, which can deform inelastically until it looses stability or deteriorates and cannot sustain gravity loads. The formulation has no restrictions on the size of rotations, using one co-rotational frame for the element to represent rigid-body motion, and a set of co-rotational frames attached to the integration points, as customarily used to represent the constitutive equations. The formulation shown in the next section provides an enhancement to the existing models by adding the inelastic behavior in an element, which is stable under static and reversible loads with large deformations using the flexibility approach. The solution procedure associated with the model allows verifying their performance up to complete collapse.

Element Equations

Figure 8 shows the deformed shape of an Euler-Bernoulli beam in co-rotational coordinates attached to the initially straight centerline of the beam. The nonlinear strain displacement relationships are given (Huddleston, 1979) by:

$$\frac{d\theta}{dx} = (1+\varepsilon)\phi \qquad (1)$$

$$\frac{d\xi}{dx} = (1+\varepsilon)\cos\theta \qquad (2)$$

$$\frac{d\eta}{dx} = (1+\varepsilon)\sin\theta \qquad (3)$$

where (ξ,η) is the coordinate of a point which was at $(x,0)$ before deformation, θ is the angle made by the tangent to the center-line with the horizontal, ε is the axial strain of the centerline and ϕ is the curvature.

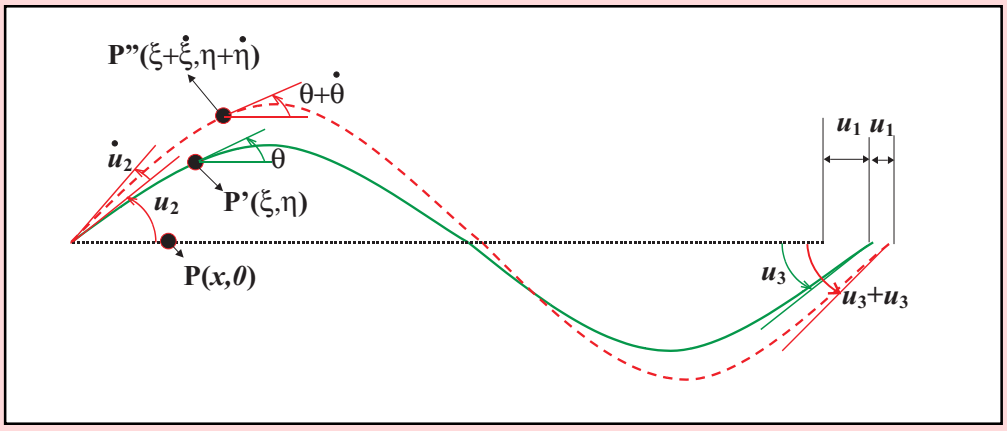

Figure 8. Euler Bernoulli Beam Subjected to Large Deformation

Considering a small perturbation about this deformed position, the incremental compatibility conditions are given by:

$$\frac{d\dot{\theta}}{dx} = \dot{\varepsilon}\phi + (1+\varepsilon)\dot{\phi} \quad (4)$$

$$\frac{d\dot{\xi}}{dx} = \dot{\varepsilon}\cos\theta - \left[(1+\varepsilon)\sin\theta\right]\dot{\theta} \quad (5)$$

$$\frac{d\dot{\eta}}{dx} = \dot{\varepsilon}\sin\theta + \left[(1+\varepsilon)\cos\theta\right]\dot{\theta} \quad (6)$$

Integrating these equations over the length of the element and performing a series of integrations by parts, the following variational equation is obtained:

$$\dot{\mathbf{u}} = \begin{Bmatrix} \dot{u}_1 \\ \dot{u}_2 \\ \dot{u}_3 \end{Bmatrix} = \int_0^L \mathbf{b}^T \begin{Bmatrix} \dot{\varepsilon} \\ \dot{\tilde{\phi}} \end{Bmatrix} dx = \int_0^L \mathbf{b}^T \dot{\varepsilon}\, dx \quad (7)$$

where u_1 = axial displacement, u_2 = rotation at left end and u_3 = rotation at right end as shown in Figure 8, $\tilde{\phi}$ = (1+ε) ϕ and is found to be the work conjugate of the co-rotational moment. This agrees with the result of Reissner (1972). **b** is a matrix given by:

$$\mathbf{b} = \begin{bmatrix} \cos\theta & -\dfrac{\sin\theta}{\xi(L)} & -\dfrac{\sin\theta}{\xi(L)} \\ \eta & \dfrac{\xi}{\xi(L)} - 1 & \dfrac{\xi}{\xi(L)} \end{bmatrix} \quad (8)$$

Constitutive Model

In this work, the inelastic behavior of the members is captured in a global sense.The relationships between stress resultants (axial force, bending moment, etc.) and generalized strains (centerline strain, curvature, etc.) are used directly instead of stress-strain relationships. Simeonov and Reinhorn (2001) derived a smooth three-dimensional plasticity model for arbitrarily shaped yield functions and used it to represent the constitutive behavior of beam-column cross-sections. This model is based on a parallel-spring plasticity model (Park and Reinhorn, 1986, and Nelson and Dorfmann, 1995) with an extension of Bouc-Wen hysteretic model (Wen, 1976, Sivaselvan and Reinhorn, 2000) and its generalization to multiple dimensions by Casciati (1989). The model determines the generalized force, **F**, vector (forces and moments) as:

$$\mathbf{F} = \mathbf{F}_e + \mathbf{F}_h \quad (9)$$

$$\mathbf{F}_e = \boldsymbol{a}\varepsilon \quad (10)$$

$$\dot{\mathbf{F}}_h = (\mathbf{I} - \mathbf{a})\mathbf{K}_0\left[\mathbf{I} - \mathbf{B}\boldsymbol{H}_1\boldsymbol{H}_2\right]\dot{\varepsilon} \quad (11)$$

where, F_e and F_h are the elastic and hysteretic components of **F**, **a** is the diagonal matrix of post-yield rigidity ratios, ε is the vector of strains and curvatures, $\boldsymbol{K}_0$ is the initial tangent rigidity matrix, **I** is the identity matrix and $\mathbf{H}_1$ and $\mathbf{H}_2$, the step functions for yielding and for loading reversals, respectively, are described below. **B** is the force-moment interaction matrix:

$$\boldsymbol{B} = \frac{\left(\frac{\partial\Phi}{\partial\mathbf{F}_h}\right)\left(\frac{\partial\Phi}{\partial\mathbf{F}_h}\right)^T(\mathbf{I}-\mathbf{a})\mathbf{K}_0}{\left(\frac{\partial\Phi}{\partial\mathbf{F}_h}\right)^T(\mathbf{I}-\mathbf{a})\mathbf{K}_0\left(\frac{\partial\Phi}{\partial\mathbf{F}_h}\right)} \quad (12)$$

where $\Phi(F_h)$ is the yield function. $H_1(F_h)$ is the step function the denoted yielding given by:

$$\boldsymbol{H}_1 = \left\|\Phi(\mathbf{F}_h)\right\|^N \quad (13)$$

where N is a parameter that governs the smoothness of the transition from the elastic to the plastic state. When N tends to infinity then the model collapses to a bilinear

model. $H_2(F_h, \dot{\varepsilon})$ is the step function denoting loading/unloading, given by:

$$H_2 = \eta_1 \operatorname{sgn}\left(\mathbf{F}_b^T \dot{\varepsilon}\right) + \eta_2 \qquad (14)$$

where η_1 and η_2 are parameters that govern the shape of the unloading curve. $\eta_1 + \eta_2 = 1$ to ensure compatibility with classical plasticity theory. It can be noticed that Eq. (7) is an implementation of the principle of virtual forces in rate form.

The compatibility equations (7) and the constitutive equations (9) to (14), are written as a set of differential-algebraic equations (DAE) along with the global equations of motion as proposed by Simeonov et al., (2000). The resulting system of equations is solved by the Backward Difference Method using the routine DASSL (Brenan et al., 1996).

Figure 9. Typical Specimen

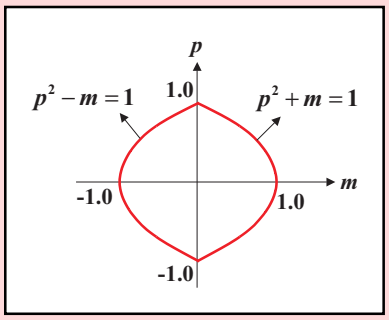

Figure 10. Yield Surface of a Square Cross-section

Verification Study

The results of the above developments are compared to those from other computational solutions as well as with the collapse experiments described above. The parameters of the example for verification were chosen to correspond to specimen 10a (Vian and Bruneau, 2001). This specimen consists of four columns each 137 mm tall and having a square cross-section of side 3.1 mm (see Figure 9). In the first step, the constitutive model of this cross-section is derived. The plastic interaction function of the square cross-section is shown in Figure 10. The yield function for positive and negative directions of the bending moment can be combined to obtain a single yield function as follows:

$$\Phi\left(P, M\right) = 2p^2 + m^2 - p^4 - 1 \quad (15)$$

where $p = P/P_P$, $m = M/M_p$, P_P= plastic axial force and M_p = plastic moment.

The formulation for this study is using the yield function and a smoothness parameter N=2 in Eq. (13) to represent the transition from initial yield to the plastic state. Equation (15) is substituted in equations (9) to (14) to obtain the necessary constitutive model.

The results obtained from the current formulation and those from the finite element analysis program ABAQUS for monotonic loadings, are shown in Figure 11 with good agreement. Figure 12 shows monotonic deflections of columns leading to complete loss of strength assuming actual elastic material behavior. The slight difference between the results stems from the representation of moment-curvature-behavior in the current approach vs. ABAQUS. The present formulation uses the smoothness parameter N=2 to represent the post-yield behavior. While this is sufficient for structural steel sections, a more accurate description is required for a square section. Efforts are underway to incorporate the exact moment-curvature equation presented by Stronge and Yu (1993).

In the dynamic analysis, the specimen was subjected to histories used in the experiment without considering the initial state of the model (previously subjected to series of base motions) and the result is shown in Figures 13 and 14.

The time history results differ from those obtained in the experiment (see Figure 14). However, when the initial deformation of the model is considered, the analysis model shows same pattern as the experiment as shown in Figure 15.

Comparison with NCHRP 12-49 Proposed P-Δ Limits

The National Cooperative Highway Research Program (NCHRP), Project 12-49, under the auspices of the Transportation Research Board, is investigating seismic design of bridges from all relevant aspects. At the conclusion of this

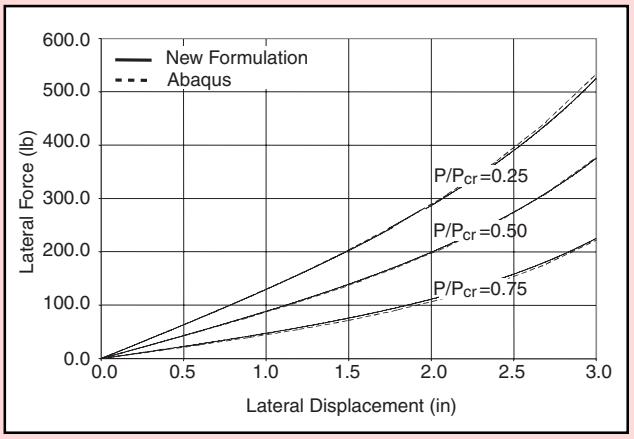

Figure 11. Analytical Results for Linear Elastic Material

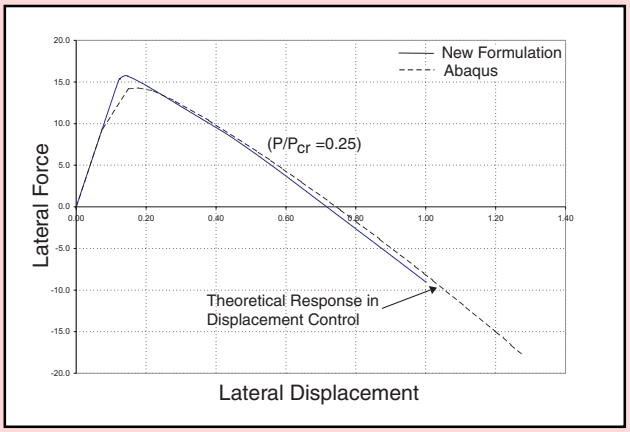

Figure 12. Static Analysis with Nonlinear Material

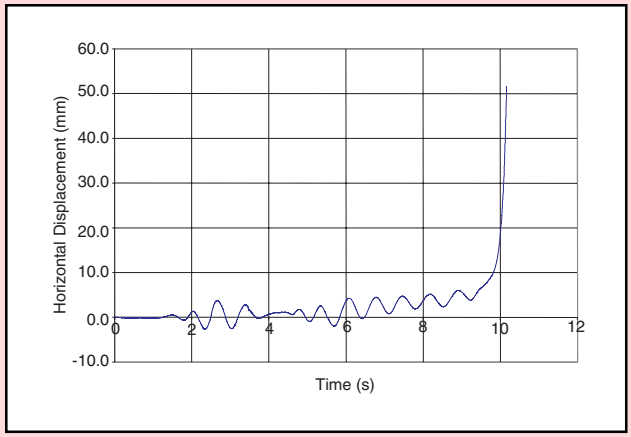

Figure 13. Horizontal Displacement from Dynamic Analysis

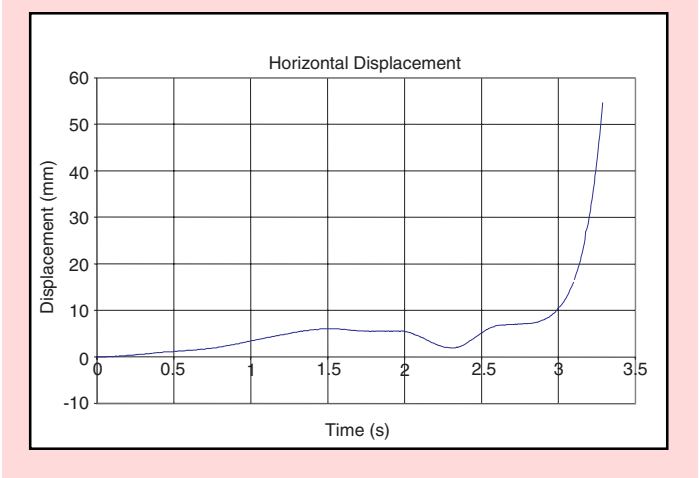

Figure 14. Displacement History from Experiment

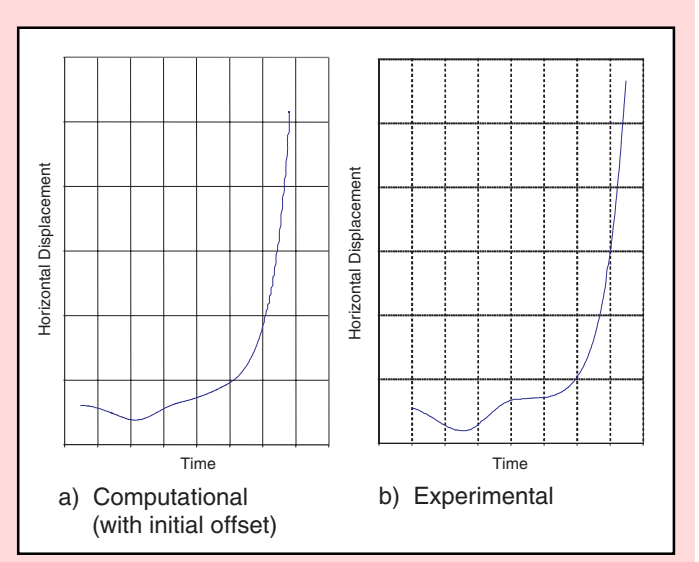

Figure 15. Displacement Response at the Verge of Collapse

project, proposed revisions to the current LRFD specifications for highway bridges will be presented to the American Association of State Highway Transportation Organizations (AASHTO) for review and possible implementation. Included in the proposed revisions are how additional demands from P-Δ affect structural performance. The most recent proposed provision, as of this writing, states:

The displacement of a pier or bent in the longitudinal and transverse direction must satisfy proposed AASHTO LRFD Equation 3.10.3.9.4-1:

$$\Delta m \le 0.25 \cdot C \cdot \left(\frac{W}{P}\right) \cdot H \qquad (16)$$

where:

$\Delta_m = R_d \Delta$; R_d is the factor related to response modification factor and fundamental period; Δ is the displacement demand from the seismic analysis; C is the seismic base shear coefficient based on lateral strength; W is the weight of the mass participating in the response of the pier; P is the vertical load on the pier from non-seismic loads; and H is the height of the pier.

For analysis of the specimens in this research, the W/P ratio is equal to unity, and the measured experimental displacements, u_{rel}, and estimated base shear coefficient, C_s*, can substitute for Δ_m and C, respectively.

Figure 16 compares the proposed limit with the peak experimental responses. The estimated base shear coefficient, C_s*, is plotted as a function of the maximum drift, γ. Results for specimens with $\theta < 0.25$ (1, 2, 4, 6, 7, 11, and 12) are shown. During the initial tests, when the proposed limit was satisfied, none of these specimens failed. Due to repeated inelastic action, the cumulative drifts of the structure increased, eventually causing progressive collapse and violating the proposed limit. Collapse always occurred only after the limit was exceeded in a prior test, thus validating the proposed criterion. As shown in Figure 16, the remaining specimens, for which $\theta \ge 0.25$, never satisfied the drift criteria, even for those tests that remained

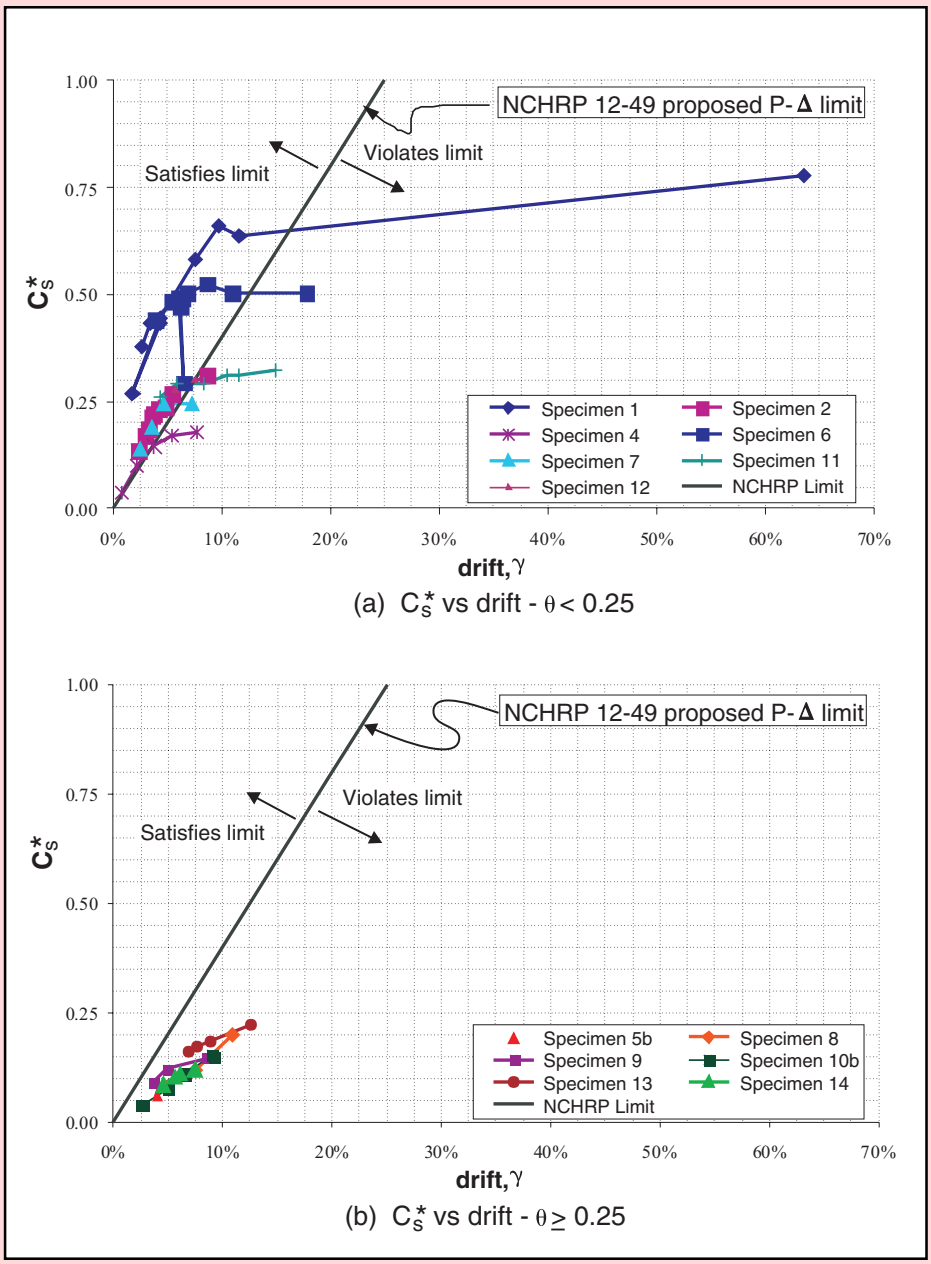

■ Figure 16. Test Results Comparison with NCHRP 12-49 Limits

in the elastic range. The stability factor for these specimens, however, is well above the practical range discussed previously; therefore, the limit violation is of no consequence.

Conclusions

The experimental data generated by this project provides a well-documented database of shake table tests of a SDOF system subjected to earthquakes of progres-

sively increasing intensity up to collapse due to instability. This data will be useful for, and shared with, other researchers who may wish to validate or develop algorithms capable of modeling inelastic behavior of steel frame structures up to and including collapse. The data presented here will also be located on the Internet (with all intermediate data files) for immediate access by other researchers.

An attempt was made to analytically model the collapse using an advanced flexibility based formulation with large deformation inelastic behavior. The verifications and the refinement of the model are done using the experimental data. Parametric studies can be performed with the model to support further codes and standards development efforts.

The research presented here demonstrated a number of important points that must be considered in the design of slender steel structures. The stability coefficient, θ, has the most significant effect on the behavior of the structure. As θ increases, the maximum attainable ductility, sustainable drift, and spectral acceleration, which can be resisted before collapse, all decrease. When this factor is larger than 0.1, the ultimate values of the maximum spectral acceleration, displacement ductility, and drift reached before collapse are all grouped below values of 0.75 g, 5, and 20%, respectively. Stability coefficient values less than 0.1 tend to increase each of those response values significantly. The research performed here helped develop a better understanding of the collapse mechanism and provides the tools for further work to modify or improve current design standards.

References

AISC, (1993), Load and Resistance Factor Design Specification for Structural Steel Buildings, American Institute of Steel Construction, Chicago, IL, December1.

Brenan, K. E., Campbell, S.L., and Petzold, L. R., (1996), *Numerical Solution of Initial-value Problems in Differential-Algebraic Equations*, Philadelphia, Society for Industrial and Applied Mathematics.

Casciati, F., (1989), "Stochastic Dynamics of Hysteretic Media," *Structural Safety,* Vol. 6, No. 2-4, pp. 259-269.

Huddleston, J. V., (1979), "Nonlinear Analysis of Elastically Constrained Tie-Rods under Transverse Loads," *International Journal of Mechanical Sciences,* Vol. 21, No. 10, pp. 623-630.

MacRae, G. A., Priestley, M.J.N., Tao, J., (1993), *P-Δ Effects in Seismic Design,* Report No. SSRP-93/05, Department of Applied Mechanics and Engineering Sciences, University of California, San Diego.

Nelson, R. B. and A. Dorfmann, (1995), "Parallel Elastoplastic Models of Inelastic Material Behavior," *Journal of Engineering Mechanics,* Vol. 121, No.10, pp. 1089-1097.

Park, Y.J. and Reinhorn, A.M., (1986), "Earthquake Responses on Multistory Buildings Under Stochastic Biaxial Ground Motions," *Proceedings of the Third U.S. Conference on Earthquake Engineering*, Charleston, South Carolina, Vol. 2, pp. 991-1001, August 1986.

References (Cont'd)

Reissner, E., (1972). "On One-Dimensional Finite-Strain Beam Theory: the Plane Problem," *Journal of Applied Mathematics and Physics* (ZAMP), Vol. 23, No. 5, pp. 795-804.

Simeonov, V. K., (1999). *Three-Dimensional Inelastic Dynamic Structural Analysis of Frame Systems*, Ph.D. Dissertation, Civil, Structural and Environmental Engineering, University at Buffalo.

Simeonov, V. K., Sivaselvan and A. M. Reinhorn, (2000), "Nonlinear Analysis of Structural Frame Systems by the State-Space Approach," *Computer-Aided Civil & Infrastructure Engineering*, Vol. 15, No. 2, pp. 76-89.

Simeonov, V. K. and Reinhorn, A.M., (2001), *Three-Dimensional Inelastic Dynamic Structural Analysis of Frame Systems*, Technical Report MCEER-01-xx, Multidisciplinary Center for Earthquake Engineering Research, University at Buffalo (in review).

Sivaselvan, M. V. and Reinhorn, A.M., (2000), "Hysteretic Models for Deteriorating Inelastic Structures," *Journal of Engineering Mechanics,* Vol. 126, No. 6, pp. 633-640.

Stronge, W. J. and Yu, T.X., (1993), *Dynamic Models for Structural Plasticity,* London, New York, Springer-Verlag.

Vian, D. and Bruneau, M., (2001), *Experimental Investigation Of P-Delta Effects To Collapse During Earthquakes*, Technical Report MCEER-01-0001, Multidisciplinary Center for Earthquake Engineering Research, University at Buffalo.

Wen, Y. K., (1976), "Methods of Random Vibration of Hysteretic Systems," *Journal of the Engineering Mechanics Division*, Vol. 102, No. 2, pp. 249-263.

Centrifuge-Based Evaluation of Pile Foundation Response to Lateral Spreading and Mitigation Strategies

by Ricardo Dobry, Tarek H. Abdoun and Thomas D. O'Rourke

Research Objectives

A first objective of the research is to identify and quantify the mechanisms and parameters determining the hazard to deep foundations and superstructure caused by the lateral spreading. Two main situations have been identified, depending on pile foundation bending response controlled by the pressure of the liquefied soil or by that of a shallow nonliquefied layer. Field evidence, centrifuge results, and analyses have shown the shallow nonliquefiable layer to be more critical and more amenable to retrofitting. A second objective of the research is to develop and evaluate strategies to retrofit deep foundations by decreasing the pressure exerted by this nonliquefied shallow layer, with emphasis in cost-effective and advanced materials. A third objective is to develop fragility curves for nonretrofitted and retrofitted foundations.

The effects of liquefaction on deep foundations are very damaging and costly. Permanent lateral ground deformation or lateral spreading is a main source of distress to piles, either alone or in combination with inertial superstructural forces and moments arising during shaking and acting on a soil already weakened by rising water pore pressures. Cracking and rupture of piles at shallow and deep elevations, rupture of pile connections, and permanent lateral and vertical movements and rotations of pile heads and pile caps with corresponding effects on the superstructure have been observed (Figure 1). This has affected buildings, bridges, port facilities and other structures in Japan, the U.S. and other countries including the 1989 Loma Prieta, California and the 1995 Kobe, Japan, earthquakes (Hamada and O'Rourke, 1992; O'Rourke and Hamada, 1992; Tokimatsu et al., 1996; Dobry and Abdoun, 2001).

Examination and analysis of case histories have revealed important aspects of the phenomenon and highlighted its complexity. It is essentially a kinematic soil-structure interaction process involving large ground and foundation permanent deformations, with the deep foundation and superstructure responding pseudostatically to the lateral permanent displacement of the ground.

While in some cases the top of the foundation displaces laterally a distance similar to that in the free field, like in Figure 1 where both the

Sponsors

National Science Foundation, Earthquake Engineering Research Centers Program
National Science Foundation: U.S.–Japan Cooperative Research for Mitigation of Urban Earthquake Disasters
Federal Highway Administration

Research Team

***Ricardo Dobry**, Professor,* ***Tarek H. Abdoun**, Research Assistant Professor,* ***Yinjuang Wang**, Graduate Student,* ***Ricardo Ramos**, Graduate Student, Civil and Environmental Engineering Department, Rensselaer Polytechnic Institute*
***Thomas D. O'Rourke**, Thomas R. Briggs Professor of Engineering and* ***Siang-Huat Goh,** Research Assistant, Department of Civl and Environmental Engineering, Cornell University*

Collaborative Partners

- ***Mourad Zeghal**, Assistant Professor and **Vivian Kallou**, Graduate Student, Civil and Environmental Engineering Department, Rensselaer Polytechnic Institute*
- ***Masanori Hamada**, Professor, Waseda University, Japan*

ground and foundation moved horizontally about 1 m, in others it moves much less due to the constraining effect of the superstructure, or of the deep foundation's lateral stiffness including pile groups and batter piles. The foundation may be exposed to large lateral soil pressures, including especially passive pressures from the nonliquefied shallow soil layer riding on top of the liquefied soil. In some cases, this soil has failed before the foundation with negligible bending distress and very small deformation of the foundation head and superstructure (Berrill et al., 1997); while in others the foundation has failed first in bending (Figure 1) and/or has experienced excessive permanent deformation and rotation at the pile heads. The observed damage and cracking to piles is often concentrated at the upper and lower boundaries of the liquefied soil layer where there is a sudden change in soil properties, or at the connection with the pile cap (Figure 1). More damage tends to occur to piles when the lateral movement is forced by a strong nonliquefied shallow soil layer (end-bearing pile No. 2 in Figure 1), than when the foundation is freer to move laterally and the forces acting on them are limited by the strength of the liquefied soil (floating Pile No. 1 in Figure 1).

Lateral spreading has been identified as a major hazard to pile foundations of hospital buildings, and centrifuge modeling as a key tool to identify and quantify mechanisms, calibrate analyses and evaluate retrofitting strategies for pile foundations. Figure 2 shows the 100 g-ton RPI geotechnical centrifuge used for this research, which is located at the RPI campus in Troy, New York. This centrifuge, originally commissioned in 1989 with support from MCEER (then NCEER), has in-flight earthquake simulation capability allowing base shaking to be applied to the base of the model. It was recently selected by NSF together with other earthquake en-

Engineering design firms, foundation and consulting engineers, hospital authorities, state transportation departments, and port and harbor authorities will all be interested in the results obtained through this research. The work is part of a broader geotechnical task focusing on ways to remediate potentially dangerous sites and/or rehabilitate deep foundations of hospitals and other structures vulnerable to earthquakes, by reducing or eliminating the effects of soil liquefaction, including those due to permanent lateral and vertical ground deformations. Lateral spreading has been identified as a major hazard to deep foundations, and centrifuge modeling is a key tool to identify and quantify mechanisms, calibrate analyses and evaluate retrofitting strategies for pile foundations. This centrifuge-based research provides the foundation component to the effort to mitigate the seismic hazard to hospitals with the help of cost-effective and advanced materials and technologies.

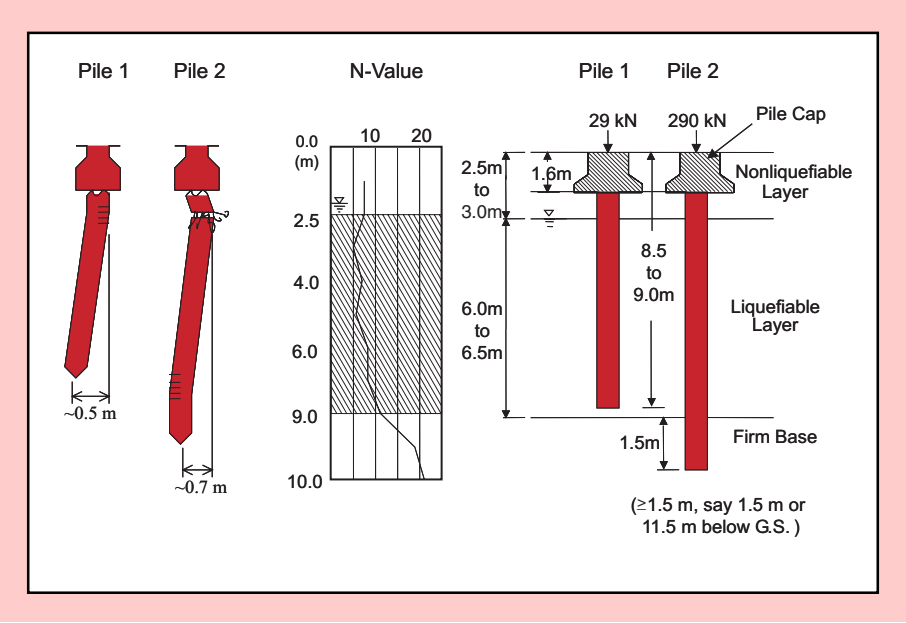

■ Figure 1. Damage to pile foundations due to lateral spreading under NFCH building, 1964 Niigata earthquake, Japan (Hamada, 1992, 2001)

gineering experimental sites throughout the U.S. to form the George E. Brown, Jr. Network for Earthquake Engineering Simulation (NEES, *www.eng.nsf.gov/nees*). Additional information on the centrifuge equipment used in this research, results from other projects and the basic principles of centrifuge modeling, can be found at the RPI web site (*www.ce.rpi.edu/centrifuge*), which also has useful links to other relevant web sites; see also summary articles by Dobry et al. (1995) and Dobry and Abdoun (1998, 2001). In addition to the centrifuge experiments themselves done at RPI, this centrifuge-based research has included other analytical, laboratory, case history review and retrofitting strategy components, conducted either at Cornell University or in close cooperation between the RPI and Cornell teams. The RPI-Cornell joint centrifuge-based research on lateral spreading effects on piles started in 1995 with support from NCEER and NSF and has continued since then with current support from both MCEER and NSF. The technical discussion below is divided in three parts: case of pile bending response to lateral spreading controlled by the pressure of the liquefied soil, case of response controlled by shallow nonliquefied soil layer, and pile retrofitting strategies and results.

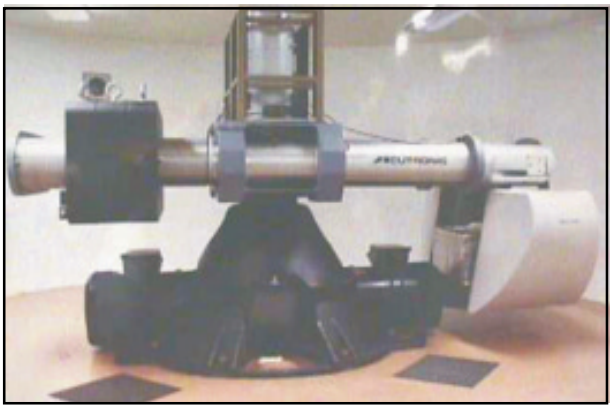

■ Figure 2. 100 g-ton geotechnical centrifuge with in-flight shaking capability at RPI

Web Sites

RPI 100 g-ton geotechnical centrifuge facility:
http://www.ce.rpi.edu/centrifuge
The complete visualization or "movie" produced from the data recorded in the centrifuge test illustrated by the single frame of Figure 5 can be viewed in this web site. To see this movie, after entering the web site, go to Research and then to Visualization.

NEES Initiative:
http://www.eng.nsf.gov/nees

Pile Bending Response Controlled by the Liquefied Soil

Figure 3 shows centrifuge pile Model 3, simulating the bending response of a pile foundation subjected to the lateral pressure of a liquefied soil due to lateral spreading. These and other experiments were conducted using the rectangular, flexible-wall laminar box container sketched in Figure 3. This laminar box is comprised of a stack of up to 39 rectangular aluminum rings separated by linear roller bearings, arranged to permit relative movement between rings with minimal friction. In Model 3 as well as in all other lateral spreading spreading experiments, the laminar box and the shaker under it are inclined a few degrees to the prototype horizontal direction to simulate an infinite mild slope and provide the shear stress bias needed for a lateral spread. The flexibility of this box container is demonstrated by the large permanent deformations and strains attained in the experiments (Figure 5).

In the test of Figure 3, the soil profile consists of two layers of fine Nevada sand saturated with water: a top liquefiable layer of relative density, D_r = 40% and 6 m protoype thickness, and a bottom slightly cemented nonliquefiable sand layer having a thickness of 2 m. The prototype single pile is 0.6 m in diameter, 8 m in length, has a bending stiffness, EI = 8000 kN-m^2, and is free at the top. The pile model is instrumented with strain gages to measure bending moments along its length, and a lateral LVDT at the top to measure the pile head displacement. The soil is instrumented with pore pressure transducers (piezometers) and accelerometers, as well as with lateral LVDTs mounted on the rings of the flexible wall to measure soil deformations in the free field. A prototype input accelerogram consisting of 40 sinusoidal cycles of a peak acceleration of 0.3 g was applied to the base, which liquefied the whole top layer in a couple of cycles and induced a permanent lateral ground surface displacement in the free field of about 0.8 m.

Results of this experiment are shown in Figures 4 and 5. As soon as the top sand layer liquefied at the beginning of shaking, it started moving laterally downslope throughout the shaking, with the maximum displacement at all times measured at the ground surface, and with this surface ground displacement increasing monotonically with time to its final value D_H = 0.8 m at the end of shaking. The maximum bending moment along the pile at any given time occurred at the interface between the two soil layers, that is at a depth of about

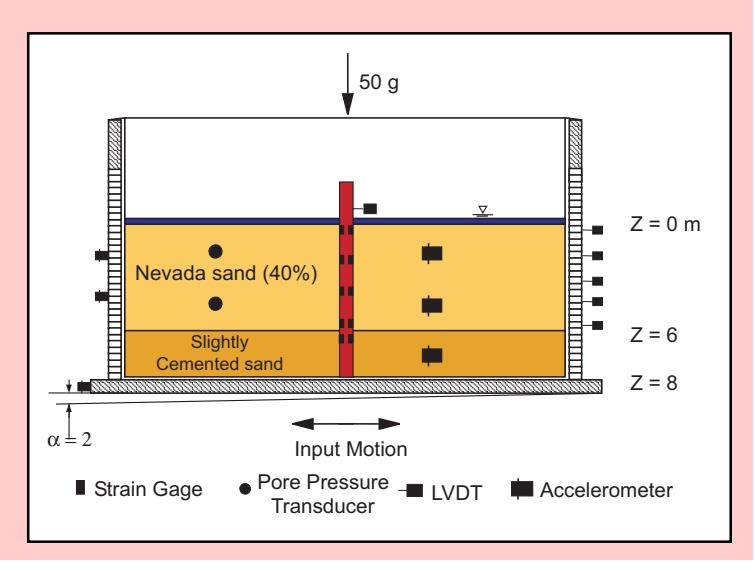

Figure 3. Lateral spreading pile centrifuge model in two-layer soil profile (Abdoun, 1997)

6 m. Figure 4 shows the time history of this prototype bending moment for Model 3, measured at z = 5.75 m; the plot reveals that the moment increased to a maximum M_{max} = 110 kN-m at a time, $t^a \approx 17$ sec, with the moment decreasing afterwards despite the continuation of shaking and the continuous increase of the soil deformation in the free field. The pile head displacement in the same figure also reached a maximum at about 17 sec and decreased afterwards. Clearly at this time the liquefied soil reached its maximum strength and applied a maximum lateral pressure to the pile, with the soil flowing around the pile, exhibiting a smaller strength and applying a smaller pressure afterwards; as a result, the model pile bounced back and the bending moments decreased. The two photos in Figure 6 - taken after the centrifuge tests - illustrate this flow of liquefied soil around the pile in other two models where colored sand had been placed around the pile.

Figure 5 summarizes the state of the system during a repeat of Model 3, at the time when the pile head displacement and the bending moment at a depth of about 6 m attained their maximum values. This is a frame taken from the visualization of the experiment produced from the measurements (the whole visualization may be viewed at the RPI centrifuge web site). The displaced shape of the box container indicates the lateral spreading in progress, with concentration of permanent shear straining in the lower part of the liquefied soil; this box shape was obtained from the lateral LVDTs placed on the side walls. This distorted shape is also copied as a white mesh to the right side of the pile for direct comparison between ground and pile displacements as well as to visualize the larger movement of the liquefied

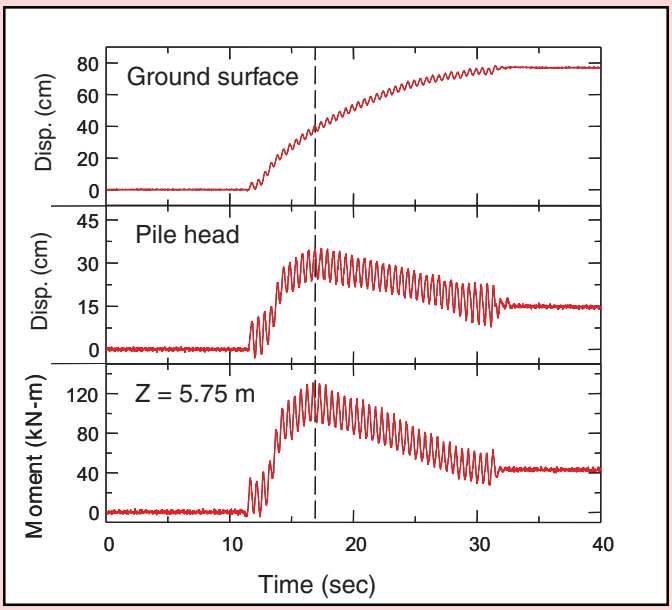

Figure 4. Prototype lateral displacement of soil and pile and ground surface, and pile bending moment at a depth of 5.75 m in model of Figure 3 (Abdoun, 1997)

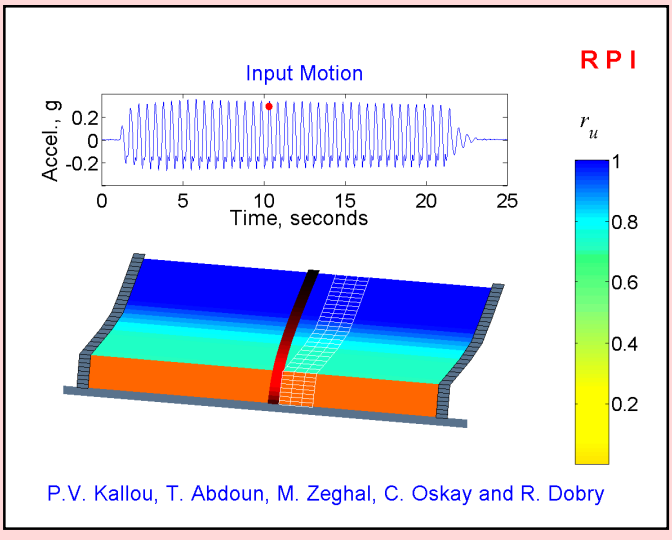

Figure 5. Frame taken out of visualization of two-layer centrifuge model of Figure 3, produced from the recorded data (Kallou et al., 2001; to see whole visualization, visit *http://www.ce.rpi.edu/centrifuge*)

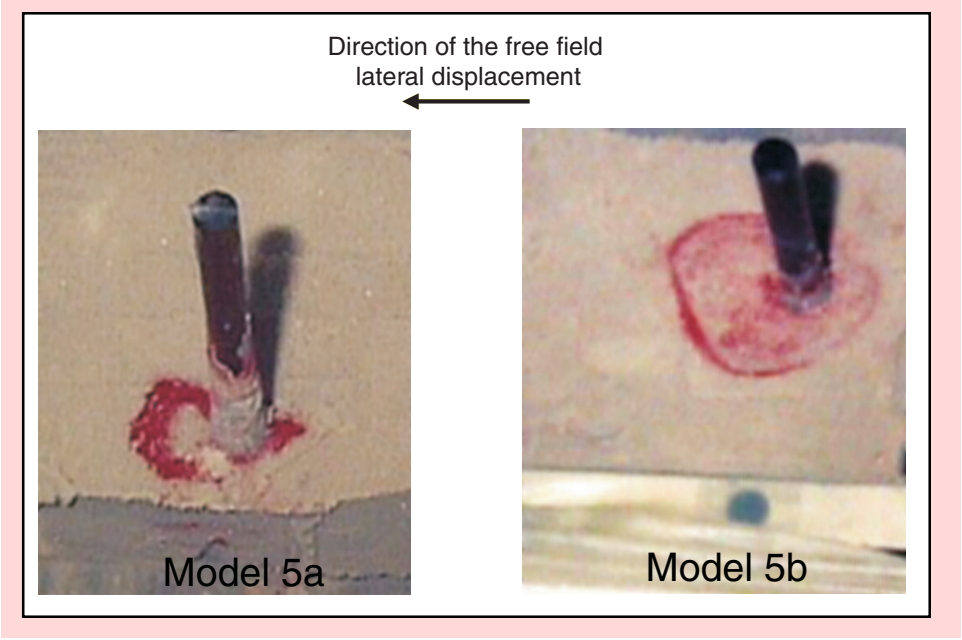

Figure 6. Photos showing flow of liquefied sand around the pile in the downslope direction in two-layer centrifuge models (Abdoun, 1997). The photos were taken after the test in models where colored sand had been placed in a circular ring around the pile

soil flowing around the pile, compared with the displacement of the pile itself. The blue color in the upper part of the loose sand layer indicates complete liquefaction as measured by the piezometers, while the green color in the lower part of the layer indicates lower excess pore pressure due to dilative cyclic stress-strain response of the liquefied sand in that part of the shaking cycle. At other times corresponding to different parts of the shaking cycle, the whole layer is blue and hence completely liquefied.

In addition to Model 3 summarized in Figures 3 to 5, similar centrifuge tests of a single pile with a pile cap, with densification around the pile to simulate pile driving, and with 2x2 pile groups indicated that, while M_{max} still occurs at a depth of about 6 m sometime during the shaking, the value of M_{max} increases with the area of pile foundation exposed to the soil lateral pressure and decreases in the pile groups due to the contribution to moment of the axial forces in the piles (frame effect). Simple limit equilibrium calculations with a constant assumed maximum pressure of the liquefied soil along the pile, p_l, indicate that values of p_l of the order of 10 kPa explain well all measured trends and values of M_{max} in this series of centrifuge tests.

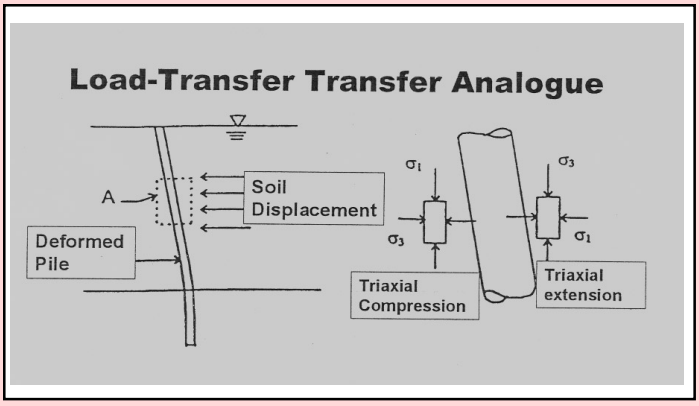

Figure 7. Concept used to develop undrained triaxial extension model for the lateral loading of liquefied soil on the pile (Goh and O'Rourke, 1999; Goh, 2001)

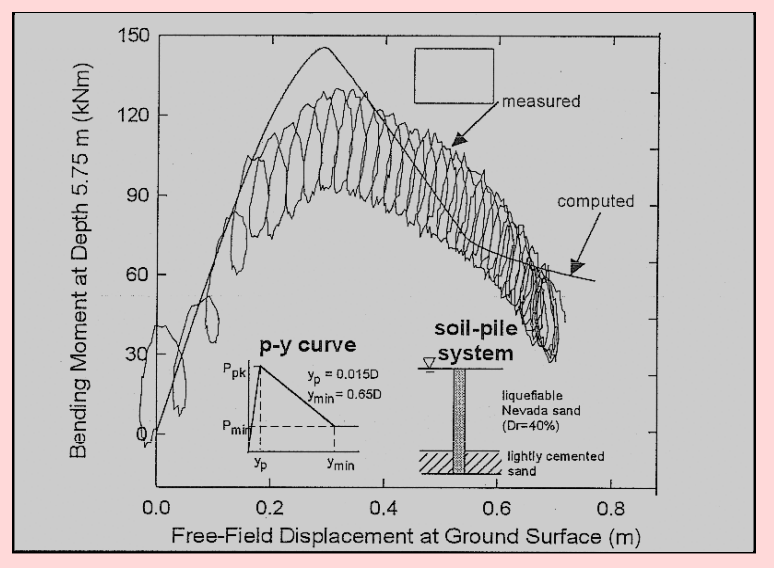

■ Figure 8. Comparison between predicted and measured pile bending moment in centrifuge model of Fig. 3 at the lower boundary of liquefied soil using triaxial extension undrained loading approach (Goh and O'Rourke, 1999; Goh, 2001)

The physical origin and basic mechanisms determining the behavior of the liquefied soil, including the lateral pressure on pile foundations and values such as p_l and M_{max} measured in these centrifuge tests, are not yet well understood and are the subject of intense research. The Cornell team has proposed the explanation sketched in Figure 7, with p_l and M_{max} controlled by the peak undrained shear strength of the saturated sand loaded in the extension mode (Goh and O'Rourke 1999; Goh, 2001). Based on p-y curves generated analytically from triaxial extension tests conducted at Cornell using the same Nevada sand and relative density of the centrifuge tests, nonlinear Beam-on-Winkler-Foundation (BWF) analyses of centrifuge Model 3 were able to predict closely the measured bending response (Figure 8).

Pile Bending Response Controlled by Shallow Nonliquefied Layer

Figure 9 shows centrifuge Model 2, where a strong shallow nonliquefied soil layer increases significantly the bending response of the pile foundation to lateral spreading. The shallow top layer

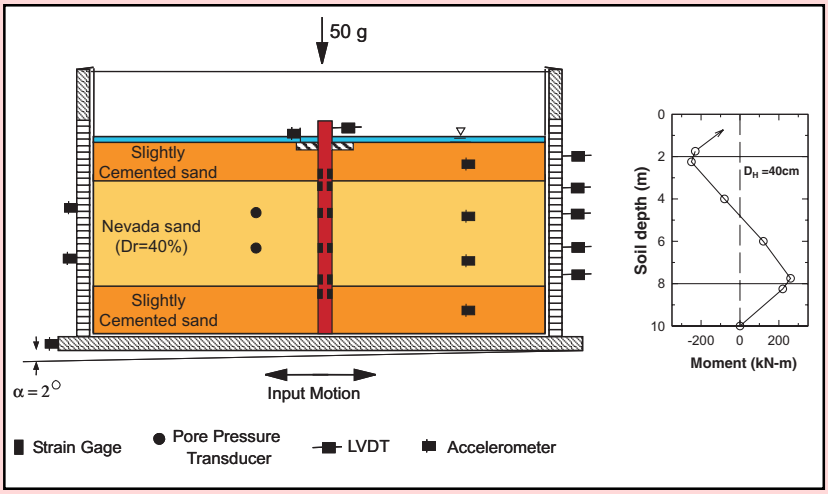

■ Figure 9. Lateral spreading pile centrifuge model in three-layer soil profile (Abdoun, 1997)

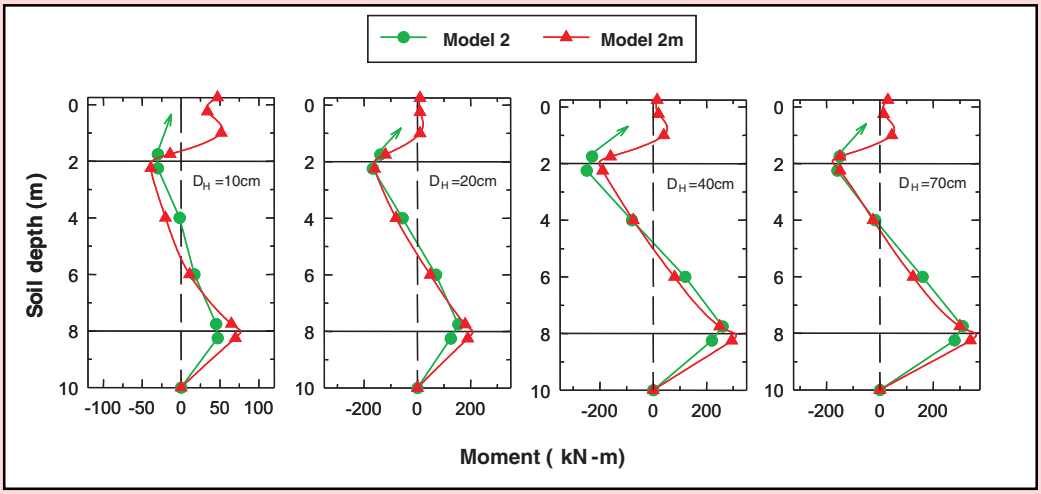

■ Figure 10. Measured bending moment response along pile in lateral spreading centrifuge models without (Model 2) and with (Model 2m) inertial loading (Wang, 2001)

consists of a 2-m thick (in prototype units), free draining, slightly cemented sand. Model 2m, not shown here, is similar to Figure 9 but with a mass added above ground to evaluate the combined effects of lateral spreading and inertial loading.

Figures 10-11 summarize the main characteristics of the bending response of Model 2 (only lateral spreading), which is also typical of other pile models tested in this 3-layer soil profile. The same as in Model 3 discussed before, the 6-m thick noncemented sand layer liquefied early in the shaking after which the lateral spreading increased monotonically, reaching a value D_H = 0.7 m at the end of shaking (Figure 11). The pile bending moments in the top 2 m first increased with time of shaking and then decreased after passive failure of the top nonliquefiable layer against the pile (Figure 10); while the bending moments near the bottom increased monotonically and never decreased, as the bottom nonliquefiable layer did not fail. The values of maximum bending moments at 2 m and 8 m are close to 300 kN-m, much greater than those measured in 2-layer tests such as shown in Figure 3, which did not exceed 170 kN-m even when a pile cap was added.

The shapes of the bending moment profiles at various times presented in Figure 10 indicate that the deformed shape of the pile had a double curvature caused by the top and bottom soil layers loading the pile in opposite directions. This double curvature was confirmed by the fact that when the top soil layer failed, the pile head and cap "snapped" in the downslope direction (Figure 11), showing that at very shallow depths, the pile was pushing the soil rather than the other way around. Both the passive failure of the top layer and the moment concentrations at the top and bottom boundaries of the liquefied layer indicated by the figures are consistent with the experience from earthquake case histories.

These moment concentrations are also predicted by theory (e.g., Meyersohn, 1994; Meyersohn et al., 1992; Debanik, 1997). Another interesting aspect of Figures 10 and 11 is that the bending moments vary linearly within the liquefied layer, suggesting that they are essentially controlled by the loading of the top and bottom layers, with the pressure of the liquefied soil being negligible. The values of M_{max} at z = 2 m and z = 8 m are higher than the corresponding values of M_{max} at z = 6 m for the 2-layer soil profiles, such as in Figure 4, which were controlled by the strength of the weaker liquefied soil. The authors have successfully calibrated a limit equilibrium method to predict M_{max} in some of these 3-layer pile centrifuge models, after incorporating basic kinematic considerations to allow for the change in pile curvature (and hence of the sign of the passive soil pressure on the pile) within the top nonliquefied soil layer.

The comparisons in Figures 10 and 11 between Models 2 and 2m reveal interesting aspects of the role played by superstructural inertia in the lateral spreading process. For depths greater than 2 or 3 m, the effect of lateral spreading predominates and the inertial loading due to the mass can be ignored. However, at shallow depths of less than 2 m, that is in the top nonliquefiable layer, the bending moments of the two centrifuge models are very different, with those of Model 2m changing rapidly with time due to the combined effect of inertia and lateral spreading. However, even in Model 2m the maximum moments still tend to concentrate at the upper and lower boundaries of the liquefied layer. Despite the rapid change in shallow bending moments due to the mass, when the top soil layer failed in passive in Model 2m, the pile head and cap "snapped" in the downslope direction, exactly the same as in Model 2 (Figure 11), showing that the soil failure mechanism was still controlled by lateral spreading.

Another factor which has been studied in the centrifuge for the 3-layer soil model is the influence of the superstructural stiffness that field case histories has shown to be important. This has been done by the addition of lateral and rotational springs above ground connected to the pile head, such as spring k in Figure 12 (Ramos, 1999). As expected, the analysis of these centrifuge results has required significant kinematic considerations and parameters, even when simple limit equilibrium calculations are conducted. On the other

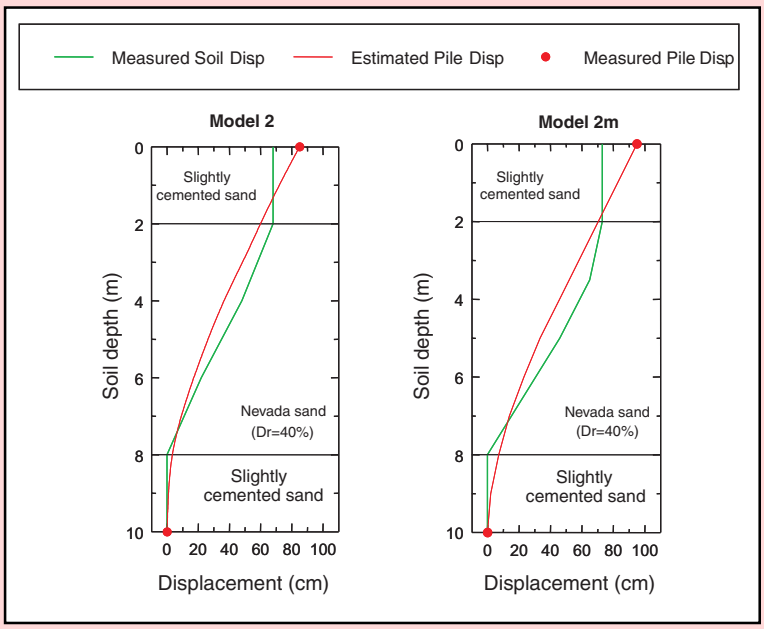

Figure 11. Snapping of pile in downslope direction in centrifuge models without (Model 2) and with (Model 2m) inertial loading (Wang, 2001)

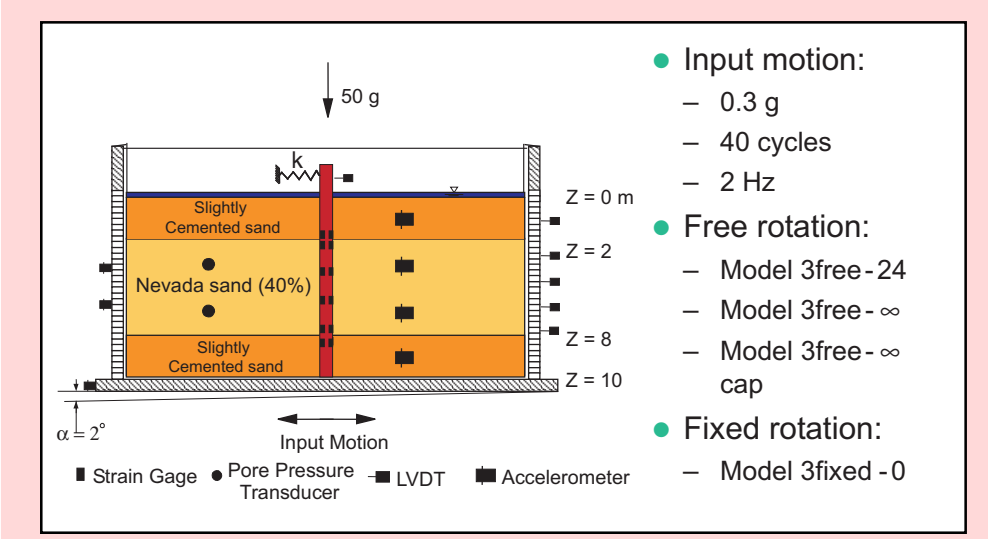

Figure 12. Lateral spreading pile centrifuge model incorporating effect of superstructural stiffness (Ramos, 1999)

hand, some aspects of the analysis become simpler compared with the case of k = 0 (Figure 3), in that if the value of k is large enough, there is no double curvature of the pile at very shallow depths, and no "snapping" of the pile in the downslope direction as in Figure 11. That is, the constraining effect of spring k forces the lateral pressure of the nonliquefied layer on the pile to act in the same downslope direction at all depths between 0 and 2 m.

Pile Retrofitting Strategies and Results

Both case histories and centrifuge models have shown the great importance of the shallow nonliquefiable soil in increasing the bending response of the pile foundation. Therefore, a promising rehabilitation approach of existing foundations is to replace the shallow soil in a trench around piles and pile cap by a frangible material that will yield under constant lateral soil forces (Figure 13a). This would decrease both bending moments and foundation deformations while allowing the ground lateral spreading to take place without interference from the foundation. As this retrofitting scheme also decreases the lateral resistance of the foundation to inertial loading, the desired frangible material selected, while yielding to static force should remain resilient under the transient inertial loading. Alternatively, the trench surrounding the foundation with frangible material may be located at some distance from the foundation so as to increase the resistance to inertial loading (Figure 13b).

A series of centrifuge models of a single pile with pile cap in the 3-layer soil profile were conducted using the retrofitting setups of Figure 13, labeled respectively Strategy 1 and Strategy 2. These experiments are listed in Table 1, which include also the benchmark nonretrofitted Models 2 and 2m,

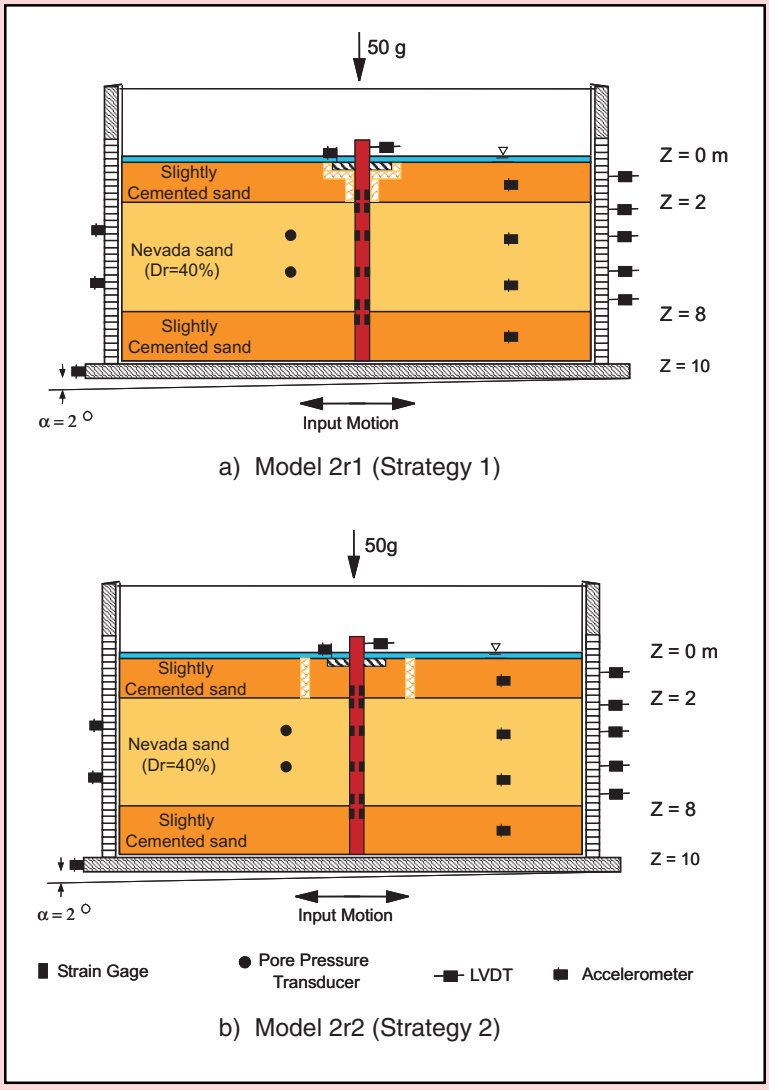

■ Figure 13. Lateral spreading pile centrifuge models to evaluate retrofitting strategies (Wang, 2001)

already discussed. Models 2r1, 2mr1a and 2mr1b were done with Strategy 1, without and with a mass above ground, and Models 2r2 and 2mr2 were conducted with Strategy 2. In both cases, a soft clay was placed in a trench either directly around or at some distance from the foundation. In future tests the use of an artificial frangible material with higher resistance to transient loading is planned (Wang, 2001).

Figures 14 and 15 illustrate measurements and observations obtained from Models 2r1 and 2r2. The free field lateral ground displacements during shaking in centrifuge tests without and with pile foundation retrofitting were essentially the same (Figure 11), consistent with the assumption that they represent truly free field response. Figure 14 compares the bending moment response without and with retrofitting. As expected, there

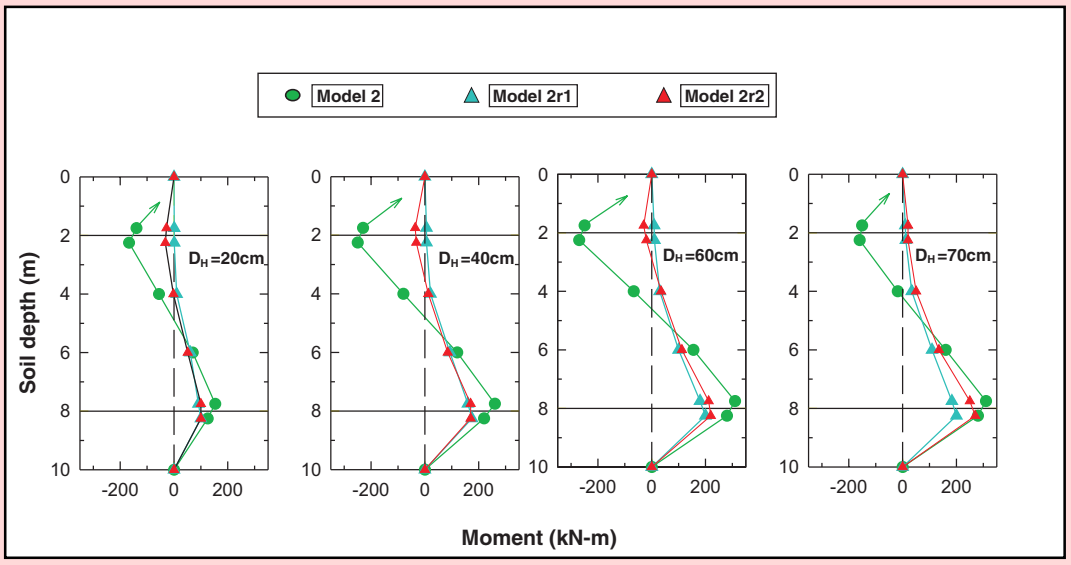

■ Figure 14. Measured bending moment response along pile in lateral spreading centrifuge models without (Model 2) and with (Models 2r1 and 2r2) foundation retrofitting (Wang, 2001)

is a dramatic reduction in the moments in the top 2 m of pile in contact with the nonliquefiable soil. The maximum moment there was close to 300 kN-m in Model 2 and becomes about 10 kN-m after retrofitting.A smaller reduction is also observed for the maximum bending moment at the lower boundary of the liquefied layer, at about 8 m depth. Similarly, the pile head displacements at the end of the tests were reduced by a factor of two by retrofitting (from 85 to 40-50 cm, with D_H = 70 to 80 cm for the soil in the free field). The photo of Model 2r1 in Figure 15, taken after the test, illustrates the corresponding "crunching" of the soft clay against the pile cap in the upslope side, and opening of a gap downslope between soil and foundation. However, the counterpart to this reduction in permanent bending response to lateral spreading of the pile foundation was an increase of transient pile accelerations and displacements, especially in the tests incorporating inertial loading (Models 2mr1a,b and 2mr2, not shown), due to the reduced lateral ground support in the top 2 m of the foundation; future tests will address this problem.

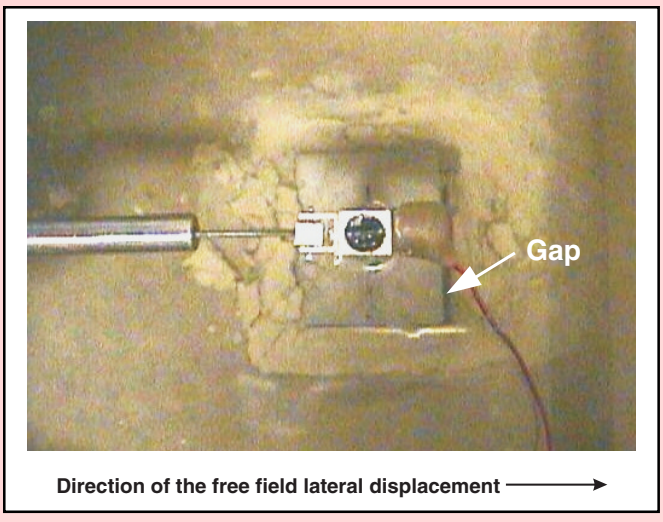

■ Figure 15. Plan view of retrofitted pile cap and ground after the test, Model 2r1 (Wang, 2001)

■ Table 1. Program of Centrifuge Tests to Evaluate Retrofit Strategies 1 and 2 (Wang, 2001)

Test No.	Cap	Mass	Retrofitting	Comments
2	Yes	No	No	
2r1	Yes	No	Yes	
2r2	Yes	No	Yes	
2m	Yes	Yes	No	
2mr1a	Yes	Yes	Yes	
2mr1b	Yes	Yes	Yes	Repeat of 2mr1a
2mr2	Yes	Yes	Yes	

Conclusions and Future Research

Case histories during earthquakes have shown the significance of lateral spreading in causing damage to deep foundations and supported structures during earthquakes.The complexity of the problem requires use of centrifuge physical modeling to clarify mechanisms, quantify relations and calibrate analysis and design procedures. Centrifuge results so far have clarified the deep foundation response, have shown significant agreement with field experience, and are being used to calibrate limit equilibrium and Beam-on-Winkler-Springs (p-y) analytical methods. Specifically, the importance of the shallow nonliquefiable soil layer riding on top of the liquefied soil in increasing foundation bending response has been clarified. Retrofitting strategies are being evaluated in the centrifuge, aimed at mitigating the effect of lateral spreading associated with the pressure of this shallow layer while preserving needed lateral resistance to inertial loading. Additional work is needed to understand and quantify the response of nonretrofitted and retrofitted pile foundations, with centrifuge model experiments combined with case studies and theory, toward improving the state-of-practice of seismic design and retrofitting of deep foundations against liquefaction.

References

Abdoun, T. H., (1997), *Modeling of Seismically Induced Lateral Spreading of Multi-Layer Soil Deposit and Its Effect on Pile Foundations*, Ph.D. Thesis, Dept. of Civil Engineering, Rensselaer Polytechnic Institute, Troy, NY.

Berrill, J. B., Christensen, S. A., Keenan, R. J., Okada, W. and Pettinga, J. K., (1997), *Lateral-spreading Loads on a Piled Bridge Foundation*, Seismic Behavior of Ground and Geotechnical Structures, (Seco E Pinto, ed.), pp. 173-183, Balkema, Rotterdam.

Debanik, C., (1997), *Pile Response to Liquefaction-Induced Lateral Spread*, Ph.D. Thesis, Cornell University, Ithaca, NY.

Dobry, R., Taboada, V. and Liu, L., (1995), "Centrifuge Modeling of Liquefaction Effects During Earthquakes," Keynote lecture, *Proc. 1st Intl. Conf on Earthquake Geotechnical Engineering* (K. Ishihara, ed.), Tokyo, Japan, Nov. 14-16, Vol. 3, pp. 1291-1324.

References (Cont'd)

Dobry, R. and Abdoun, T. H., (1998), "Post-Triggering Response of Liquefied Soil in The Free Field and Near Foundations," State-of-the-art paper, *Proc. ASCE 1998 Specialty Conference on Geotechnical Earthquake Engineering and Soil Dynamics* (P. Dakoulas, M. Yegian and R. D. Holtz, eds.), University of Washington, Seattle, Washington, August 3-6, Vol. 1, pp. 270 – 300.

Dobry, R. and Abdoun, T. H., (2001), "Recent Studies on Seismic Centrifuge Modeling of Liquefaction and its Effect on Deep Foundations," State-of-the-Art Paper, *Proc. 4th Intl. Conf. on Recent Advances in Geotechnical Earthquake Engineering and Soil Dynamics and Symposium to Honor Prof. W.D.L. Finn* (S. Prakash, ed.), San Diego, CA, March 26-31, SOAP-3, Vol. 2.

Goh, S. H., (2001), *Soil-pile Interaction During Liquefaction-Induced Lateral Spreading*, PhD Thesis, Cornell University, Ithaca, NY.

Goh, S.-H. and O' Rourke, T. D., (1999), "Limit State Model for Soil-Pile Interaction During Lateral Spread," *Proc. Seventh U.S.-Japan Workshop on Earthquake Resistant Design of Lifeline Facilities and Countermeasures Against Soil Liquefaction*, Seattle, WA, August 15-17, Technical Report MCEER-99-0019, Multidisciplinary Center for Earthquake Engineering Research, University at Buffalo, (O'Rourke, Bardet and Hamada, eds.), pp. 237-260.

Hamada, M., (1992), "Large Ground Deformations and their Effects on Lifelines: 1964 Niigata Earthquake," Ch. 3 of *Case Studies of Liquefaction and Lifeline Performance During Past Earthquakes, Vol. 1: Japanese Case Studies*, (Hamada and O'Rourke, eds.), 3-1 to 3-123.

Hamada, M., (2001), Personal Communication.

Hamada, M. and O'Rourke, T. D., (eds.) (1992), "Case Studies of Liquefaction and Lifeline Performance During Past Earthquakes," *Vol. 1: Japanese Case Studies*, Technical Report NCEER-92-0001, National Center for Earthquake Engineering Research, University at Buffalo, February.

Kallou, V., Abdoun, T. H., Zeghal, M., Oskay, C. and Dobry, R., (2001), *Visualization of Centrifuge Models of Lateral Spreading and Pile Bending Response* (in preparation).

Meyersohn, W. D., (1994), *Pile Response to Liquefaction Induced Lateral Spread*, Ph.D. Thesis, Dept. of Civil and Environmental Engineering, Cornell University, Ithaca, New York.

Meyersohn, W. D., O'Rourke, T. D. and Miura, F., (1992), "Lateral Spread Effects on Reinforced Concrete Pile Foundations," *Proc. 5th US-Japan Workshop on Earthquake Disaster Prevention for Lifeline Systems*, Tsukuba, pp. 173-196.

O'Rourke, T. D. and Hamada, M., (eds.), (1992), "Case Studies of Liquefaction and Lifeline Performance During Past Earthquakes," *Vol. 2: United States Case Studies*, Technical Report NCEER-92-0002, National Center for Earthquake Engineering Research, University at Buffalo, February.

Ramos, R., (1999), *Centrifuge Study of Bending Response of Pile Foundation to a Lateral Spread Including Restraining Effect of Superstructure*, Ph.D. Thesis, Dept. of Civil Engineering, Rensselaer Polytechnic Institute, Troy, NY

Tokimatsu, K., Mizuno, H. and Kakurai, M., (1996), "Building Damage Associated with Geotechnical Problems," *Soils and Foundations,* pp. 219-234, January.

Wang, Y., (2001), *Evaluation of Pile Foundation Retrofitting Against Lateral Spreading and Inertial Effects During Liquefaction Using Centrifuge Models*, MS Thesis, Dept. of Civil Engineering, Rensselaer Polytechnic Institute, Troy, NY.

Other Publications

Abdoun, T.H., Dobry, R., O'Rourke, T.D. and Chaudhuri, D., (1996), "Centrifuge Modeling of Seismically-induced Lateral deformation During Liquefaction and its Effect on a Pile Foundation," *Proc. Sixth Japan-U.S. Workshop on Earthquake Resistant Design of Lifeline Facilities and Countermeasures Against Soil Liquefaction*, Technical Report NCEER-96-0012, Multidisciplinary Center for Earthquake Engineering Research, University at Buffalo, pp. 525-539.

Abdoun, T.H. and Dobry, R., (1998), "Seismically Induced Lateral Spreading of Two-layer Sand Deposit and its Effect on Pile Foundations," *Proc. Intl. Conf. Centrifuge'98* (T. Kimura, O. Kosakabe and J. Takemura, eds.), Tokyo, Japan, Sept. 23-25, Vol. 1, pp. 321-326.

Dobry, R., (1994), "Foundation Deformation Due to Earthquakes," *Proc. ASCE Specialty Conference on Settlement '94*, College Station, TX, June 16-18, pp. 1846-1863.

Dobry, R., (1995), "Liquefaction and Deformation of Soils and Foundations under Seismic Conditions," State-of-the-art paper, *Proc. Third Intl. Conf on Recent Advances in Geotechnical Earthquake Engineering and Soil Dynamics* (S. Prakash, ed.), St. Louis, MO, April 2-7, Vol. III, pp. 1465-1490.

Dobry, R., Abdoun, T.H. and O'Rourke, T. D., (1996), "Evaluation of Pile Response Due to Liquefaction-Induced Lateral Spreading of the Ground," *Proc. 4th Caltrans Seismic Research Workshop*, Sacramento, CA, July, 10 pages.

Dobry, R., Van Laak, P., Elgamal, A.-W., Zimmie, T. F. and Adalier, K, (1997), "The RPI Geotechnical Centrifuge Facility," *NCEER Bulletin*, April, pp. 12-17.

Elgamal, A.-W., Dobry, R., Van Laak, P. and Nicolas-Font, J., (1991), "Design, Construction and Operation of 100 g-ton Centrifuge at RPI," *Proc. Intl. Conf. Centrifuge'91* (H.-Y. Ko and F. G. McLean, eds.), pp. 27-34.

O' Rourke, T., Meyersohn, W. D., Shiba, Y. and Chaudhuri, D., (1994), *Evaluation of Pile Response to Liquefaction-Induced Lateral Spread*, Tech. Rept. NCEER-94-0026, Multidisciplinary Center for Earthquake Engineering Research, University at Buffalo, pp. 445-455.

Ramos, R., Abdoun, T. H. and Dobry, R., (1999), "Centrifuge Modeling of Effect of Superstructure Stiffness on Pile Bending Moments Due to Lateral Spreading," *Proc. Seventh U. S.-Workshop Workshop on Earthquake Resistant Design of Lifeline Facilities and Countermeasures Against Soil Liquefaction*, Seattle, WA, August 15-17, 10 pages.

Ramos, R., Abdoun, T. H. and Dobry, R., (2000), "Effect of Lateral Stiffness of Superstructure on Bending Moments of Pile Foundation Due to Liquefaction-induced Lateral Spreading," *Proc. 12th World Conf. on Earthquake Engineering*, Auckland, New Zealand, Jan. 30 - Feb. 4, 8 pages.

Taboada, V.M. and Dobry, R., (1998), "Centrifuge Modeling of Earthquake-Induced Lateral Spreading in Sand," *J. Geotechnical and Geoenvironmental Engineering,* ASCE, Vol. 124, No.12, pp. 1195-1206.

Van Laak, P., Elgamal, A.-W. and Dobry, R., (1994a), "Design and Performance of an Electrohydraulic Shaker for the RPI Centrifuge," *Proc. Intl. Conference Centrifuge'94*, Singapore, August 31-Sept. 2, (C.F. Leung, F.H. Lee and T.S. Tan, eds.), A.A. Balkema, Rotterdam, pp. 139-144.

Van Laak, P., Taboada, V., Dobry, R. and Elgamal, A.-W., (1994b), "Earthquake Centrifuge Modeling Using a Laminar Box," *Dynamic Geotechnical Testing II* (R. J. Ebelhar, V. P. Drnevich and B. L. Kutter, eds.), ASTM STP 1231, pp. 370-384.

Van Laak, P., Adalier, K., Dobry, R. and Elgamal, A.-W., (1998), "Design of RPI's Large Servohydraulic Shaker," *Proc. Intl. Conf. Centrifuge'98* (T. Kimura, O. Kosakabe and J. Takemura, eds.), Tokyo, Japan, Sept. 23-25, Vol. 1, pp. 105-110.

Analysis and Design of Buildings with Added Energy Dissipation Systems

by Michael C. Constantinou, Gary F. Dargush, George C. Lee (Coordinating Author), Andrei M. Reinhorn and Andrew S. Whittaker

Research Objectives

This article is a summary of the progress made during 2000-2001 by MCEER researchers working in the subtask of facilitating technologies. These research progresses should be viewed from the context that the long term (3-4 year) objective is to complete an MCEER monograph on *Analysis and Design of Buildings with Added Energy Dissipation Systems*. Although each individual researcher is advancing the state-of-the-art knowledge with his respective graduate students and research collaborators, it is the total systems integrated effort directed toward the practicing professional that underpins the projects within this group. This undertaking is possible by using the "Center Approach" in earthquake engineering research.

MCEER's research program 2 on the seismic retrofit of hospitals concentrates on developing cost-effective retrofit strategies for critical facilities using new and emerging materials and enabling technologies. Current emphasis is given to hospitals that should remain functional during and immediately after damaging and/or destructive earthquakes.

The major disciplinary components of this program are geotechnical, structural, nonstructural, advanced technologies and high performance materials, socio-economic issues and systems integration. One important research task concerning the methods of analysis and design of buildings with added emerging materials (e.g., composite infill walls) and/or enabling technologies (e.g., damping devices) is carried out by a group of research investigators under the title "Facilitating Technologies." This task is the heart of the systems integrated approach concerning the performance of a system (i.e., the performance of hospital buildings and contents with added earthquake protective systems so that the medical functions can be carried out). To develop retrofit strategies for buildings by using added materials and/or enabling devices, practicing engineers need to know how to choose appropriate technologies to satisfy building performance indices and/or objectives cost-effectively for given earthquake risk. In view of FEMA 273/274 and NEHRP 2000, which encourage the

Sponsors

National Science Foundation, Earthquake Engineering Research Centers Program

Research Teams

***Michael C. Constantinou**, Professor and Chair, Department of Civil, Structural and Environmental Engineering, University at Buffalo, **Panos Tsopelas**, Assistant Professor, Catholic University of America, **Wilhelm Hammel**, Senior Consultant, KPMG, Germany, and **Ani N. Sigaher**, Ph.D. candidate, Department of Civil, Structural and Environmental Engineering, University at Buffalo*

***Gary F. Dargush**, Associate Professor. **Ramesh Sant**, Ph.D. Candidate, and **Rajesh Radhakrishnan**, Graduate Student, Department of Civil, Structural and Environmental Engineering, University at Buffalo*

Research Team continued on page 2

Research Team (cont.)

***George C. Lee**, Director, MCEER, and Samuel P. Capen Professor of Engineering, Department of Civil, Structural and Environmental Engineering, University at Buffalo, **Mai Tong**, Senior Research Scientist, MCEER **Yihui Wu**, Research Scientist, MCEER,and **Wei Liu**, Ph.D. candidate, Department of Civil, Structural and Environmental Engineering, University at Buffalo*

***Andrei Reinhorn**, Professor, Department of Civil, Structural and Environmental Engineering, University at Buffalo, **Katrin Winkelmann**,Visiting Research Associate, Department of Civil, Structural and Environmental Engineering, University at Buffalo from the University of Darmstadt and **Mettupalayam Sivaselvan**, Ph.D. candidate, Department of Civil, Structural and Environmental Engineering, University at Buffalo*

***Andrew S. Whittaker**, Associate Professor, **Oscar Ramirez,** Graduate Student, and **Juan Gomez**, Graduate Student, Department of Civil, Structural and Environmental Engineering, University at Buffalo*

use of emerging technologies to achieve building performance objectives, there is a need to develop principles and design guidelines for these engineers. This is the fundamental rationale of the research task on facilitating technologies.

MCEER investigators have made many key contributions to the two most advanced codes and guidelines related to the implementation of passive energy dissipation systems: *FEMA 273/274 Guidelines for the Seismic Rehabilitation of Buildings*, published in 1998, and the *NEHRP 2000 Guidelines for Seismic Regulations for New Buildings and Other Structures*, that will be published in the next few months.

The *FEMA 273 Guidelines* and *274 Commentary* represented the culmination of more than a decade of work funded by the Federal Emergency Management Agency, the National Science Foundation and other agencies. These documents provide structural engineers with new information on procedures for the analysis, evaluation, and design of existing and retrofit construction. Information is also presented on performance-based earthquake engineering, modeling and analysis, steel, concrete, and timber structures, foundations, and nonstructural components. MCEER researchers have contributed to FEMA 273/274 in two areas: modeling and analysis, and seismic isolation and damping systems (see Constantinou et al., 1998 and Tsopelas et al., 1997).

The *2000 NEHRP Recommended Provisions for Seismic Regulations for New Buildings and Other Structures* includes robust procedures for the analysis and design of passive energy dissipation systems (Appendix to Chapter 13) using force-based methods of analysis that are consistent with those methods used for the analysis and design of conventional construction. The development of force-based analysis and component-checking methods for highly nonlinear or velocity-dependent energy dissipation devices proved to be a most demanding task. MCEER researchers have developed the technical underpinnings of the methods presented in NEHRP 2000 (see Ramirez et al., 2000).

Since the publication of FEMA 273/274 in 1998, many practicing engineers have been interested in using these guidelines to retrofit existing buildings with base isolation and/or energy dissipation devices. As a result, several major retrofit projects have been completed and their results publicized,

Structural engineers who develop cost-effective retrofit designs for existing buildings will find information regarding how to select the best passive energy dissipation device system for a given type of building (e.g., high rise, low-medium height, steel, reinforced concrete, masonry, timber, relatively symmetrical, irregularly-shaped, etc.) and for given earthquake risk very useful. Other procedures, such as how to optimally distribute damping devices throughout a structure and how to consider multi-performance indices are also of critical importance.

particularly in the area of base isolation systems, in which MCEER researchers (most notably, M. Constantinou and A. Whittaker) have acted as consultants. Because base isolation technology has a longer history of practical implementation for buildings and bridges, more projects have been successfully completed. However, only limited reports are available in the open literature on passive energy dissipation devices applied to buildings. This is primarily due to the relatively short history in experience of practical applications and the fact that many available devices/approaches are reported in research publications, many developed and/or improved by MCEER researchers.

During the past two decades, many advances have been reported on the performance and vibration reduction properties of passive energy devices. As noted earlier, MCEER researchers have played a significant role in the development of a variety of devices. This "device-based" line of pursuit will be continued as new ideas, materials and/or devices become available.

A new systems-based approach is now being undertaken to provide answers to the many questions on choosing appropriate devices. Regarded as the "building-device system based" consideration, these studies emphasize the performance of the building with added passive energy dissipation devices. This new systems-based approach is the central theme of the research task on facilitating technologies, and this paper focuses on these new approaches.

To develop analytical models or to carry out experimental observations for the systems-based study is considerably more complicated than to model or to test the behavior of a single device.

First, existing buildings themselves have different dynamic characteristics and are complicated to model. The performance of the devices cannot be generalized based on one simple structure. Many multiple degree of freedom (MDOF) systems cannot be treated as single DOF systems (decoupling assumption) with sufficient accuracy. To develop simplified finite element (FE) analysis models for complicated MDOF systems is itself a challenge.

When energy dissipation devices are implemented in these MDOF structures, the total building-device systems are generally nonlinear systems. Much creativity and fundamental research in structural dynamics principles have to be pursued to develop a reasonably simple and accurate analysis and design procedure. The current, MCEER studies may be grouped into three separate categories.

Type I Projects: New Devices and Systems —continued development of new ideas in passive energy dissipation devices and semi-active systems. The semi-active systems can extend the range of traditional passive energy dissipation systems and can be combined to provide an added fail-safe feature to these systems.

Type II Projects: MDOF Modeling of Building-Device Systems—This category of studies is concerned with the behavior and design of the building-device system that must be studied by using multiple DOF models, including when the systems are nonproportionally damped. These studies provide quantitative information on the er-

Collaborative Partners

- ***Martin Johnson**, Group Manager, EQE International*
- ***Ali Karakaplan**, President, LARSA, Inc.*
- ***Charles Kircher**, Principal, Charles Kircher and Associates*
- ***Douglas Taylor**, President, Taylor Devices, Inc.*
- *U.S. Department of Commerce*

rors when such buildings are approximated by decoupled single DOF systems.

Type III Projects: Analysis and Design Software—MCEER will continue its development of analysis and design software for buildings with added energy dissipation systems. Some projects are fundamental in nature to establish new approaches while others emphasize the development of user-friendly simplified procedures for design professionals with acceptable accuracy.

The findings from research in these three categories will culminate in a monograph on *Analysis and Design of Buildings with Added Energy Dissipation System* for the design professional. The following sections provide brief descriptions of the progress made in current projects.

Scissor-Jack Seismic Energy Dissipation System (Type I Project)

Energy dissipation systems are being employed in the United States to provide enhanced protection for new and retrofit building and bridge construction. The hardware utilized includes yielding steel devices, friction devices, viscoelastic solid devices and mostly, so far, viscous fluid devices.

Engineers are familiar with and have extensively used diagonal and chevron brace configurations for the delivery of forces from energy dissipation devices to the structural frame (Soong and Dargush, 1997; Constantinou et al., 1998). New configurations have been developed which offer certain advantages, either in terms of cost of the energy dissipation devices, or in terms of architectural considerations such as open space requirements. Particularly, stiff structural systems under seismic load or structural systems under wind load undergo small drift and the required damping forces are large. This typically results in larger damping devices and accordingly, greater cost. In other cases, energy dissipation devices cannot be used in certain areas due to open space requirements and the ineffectiveness of damping systems when installed at near-vertical configurations.

Two recently developed configurations, the toggle-brace and the scissor-jack energy dissipation system configurations, offer advantages that overcome these limitations. Both utilize innovative mechanisms to amplify displacement and accordingly lower force demand in the energy dissipation devices. However, they are more complex in their application since they require more care in their analysis and detailing. The theory and development of these systems has been described in Constantinou et al. (2001) and Constantinou and Sigaher (2000). This section briefly presents these new configurations and compares them with the familiar chevron brace and diagonal configurations.

The toggle-brace and scissor-jack systems are configurations for magnifying the damper displacement so that sufficient energy is dissipated with a reduced requirement for damper force. Conversely, they may be viewed as systems for magnifying the damper force through shallow truss configurations and

then delivery of the magnified force to the structural frame.

Figure 1 illustrates various damper configurations in a framing system. Let the interstory drift be u, the damper relative displacement be u_D, the force along the axis of the damper be F_D and the damping force exerted on the frame be F. It may be shown that

$$u_D = f\,u \tag{1}$$

$$F = f\,F_D \tag{2}$$

where f = magnification factor. Expressions for the magnification factor of various configurations are shown in Figure 1. The significance of the magnification factor may be best demonstrated in the case of linear viscous dampers, for which

$$F_D = C_o \dot{u}_D \tag{3}$$

where $\dot{u}_D$ = relative velocity between the ends of the damper along the axis of the damper. The damping ratio under elastic conditions for a single-story frame (as shown in Figure 1) with weight, W, and fundamental period, T, is:

$$\beta = \frac{C_o f^2 g T}{4\pi W} \tag{4}$$

That is, the damping ratio is proportional to the square of the magnification factor. The toggle-brace and scissor-jack systems can achieve magnification factors larger than unity. The systems can be typically configured to have values f = 2 to 3 without any significant sensitivity to changes in the geometry of the system. By contrast, the familiar chevron-brace and diagonal configurations have f less than or equal to unity.

For the purpose of comparison, consider the case of the use of a linear viscous damper with C_o=160 kN-s/m (= 0.9 kip-s/in) in the framing systems of Figure 1 with weight W = 1370 kN (= 308 kip) and T = 0.3 second. The resulting damping ratios are shown in Figure 1. The effectiveness of the toggle-brace and scissor-jack systems is clearly

Web Sites

MCEER Users Network:
http://civil.eng.buffalo.edu/users_ntwk

IDARC Users Group:
http://civil.eng.buffalo.edu

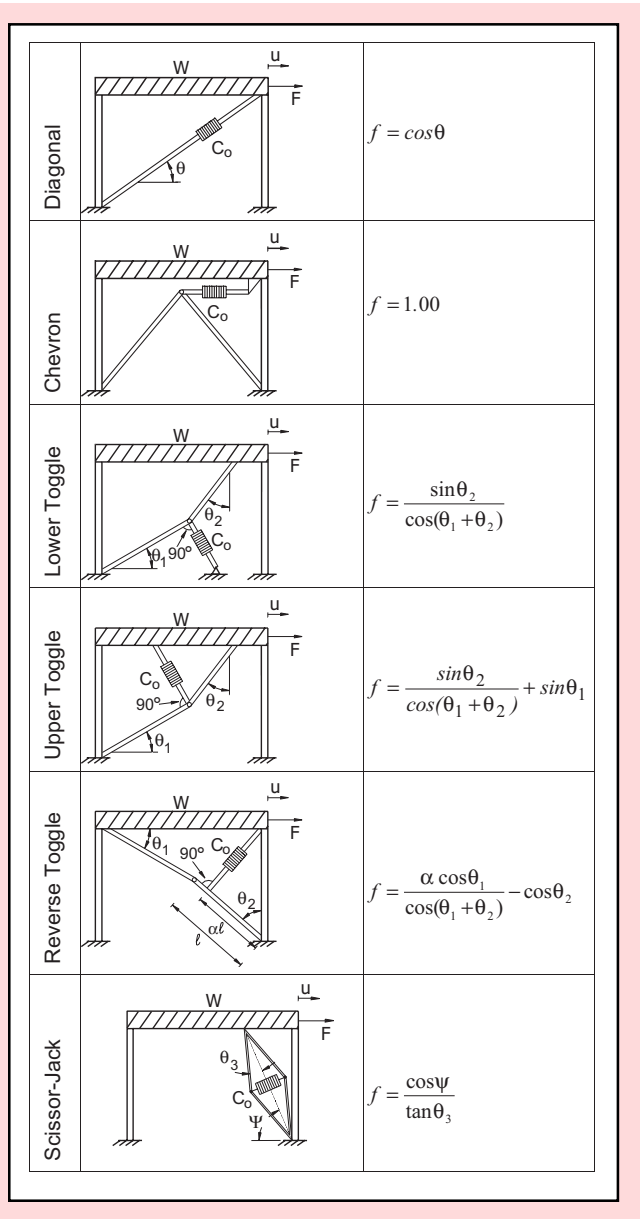

Figure 1. Effectiveness of Damper Configurations in Framing Systems

■ Figure 2. Tested Scissor-Jack Damper Configuration

demonstrated. It should be noted that the configurations for these two systems are identical to those tested at the University at Buffalo.

It is clear in the results of Figure 1 and in equations (1), (2) and (4) that the toggle-brace and scissor-jack configurations may provide substantial energy dissipation capability with the use of low output force devices. This may result in an important cost advantage in systems that undergo small drifts such as stiff structural systems under seismic load and most structural systems under wind load. Such cases of small drift lead to a requirement for increased volume of fluid viscous devices and accordingly increased cost. The use of the new configurations eliminates the necessity for large volume damping devices and may result in reduced cost.

Moreover, the scissor-jack system may be configured to allow for open space, minimal obstruction of view and slender configuration, which are often desired by architects. As an example, Figure 2 illustrates the scissor-jack system tested at the University at Buffalo. The open bay configuration, the slenderness of the system and the small size of the damper are apparent.

Damping Ratio as a Seismic Response Reduction Measure of Non-Proportionally Damped Structures (Type II Project)

In FEMA 273/274 (1997), an important design parameter for added devices is the effective damping ratio. As suggested in FEMA 273/274, displacements are reduced as the effective damping ratio is increased. Some believe that placing more dampers at the level of maximum inter-story drift will achieve optimized damping effects. This is true for proportionally damped or single degree of freedom (SDOF) systems. It has been shown by Lee et al., (2001) that for multiple degree of freedom (MDOF) systems, higher damping ratios could, in some cases, increase the seismic response. For structures with added passive energy dissipation or seismic isolation devices, the damping is no longer proportional nor negligibly small. To study the damping effects on MDOF building structures, the analysis method should consider the effects of non-proportional damping.

For non-proportionally damped MDOF systems, the damped mode shape is not orthogonal to the damping matrix in the n-dimensional physical domain. The complex mode shapes are orthogonal in the state-space domain, where real valued

modal superposition methods cannot be directly applied. The "double modal superposition" approach developed by Gupta and Law (1986) is used in this analysis, where the response is the superposition of "modal displacement" and "modal velocity." These modes are not the un-damped system modes, nor the complex system modes. The conventional modal analysis routine of fast calculation can be used in this approach and the damping effects can be more readily explained by using structural dynamic parameters.

Theoretical Background

In a proportionally damped system, the damping ratio is used to describe damping effects. However, damping can affect the response of an MDOF non-proportionally damped system in many ways, including modal response, modal shape and natural frequencies, and damping ratio.

For an MDOF system subjected to earthquake excitation, the equation of motion can be written as:

$$\mathbf{M}\ddot{\mathbf{U}} + \mathbf{C}\dot{\mathbf{U}} + \mathbf{K}\mathbf{U} = -\mathbf{M}\mathbf{U}_b\ddot{u}_g \qquad (5)$$

where **M**, **C** and **K** denote mass, damping and stiffness matrices, respectively; **U** is the relative displacement vector; $\mathbf{U}_b$ is a displacement vector obtained by statistically displacing the support by unity in the direction of the input motion; and u_g is the ground displacement.

The double modal superposition method obtains the response by equation (6):

$$\mathbf{U} = \sum_{i}^{N} \mathbf{U}_i, \quad \mathbf{U}_i = \mathbf{U}_i^d - \mathbf{U}_i^v \qquad (6)$$

$$\mathbf{U}_i^d = \psi_i^d X_i, \quad \mathbf{U}_i^v = \psi_i^v \dot{X}_i \qquad (7)$$

where $\mathbf{U}_i^d$ and $\mathbf{U}_i^v$ are real value response associated with the modal shape, as defined by equation (8), and ψ_i^d and ψ_i^v are displacement and velocity mode shapes, respectively. They are real value mode shapes and are calculated by the state vector eigen-equation. These mode shapes are determined not only by the system mass and stiffness but also by the added damping matrix. In some cases, the added damping will dominate the mode shapes (as when the fundamental modal shape collapse due to added damping.). X_i is the modal response of the following "modal" equation.

In equation (8), ζ_i and ω_i are the "modal damping ratio and circular frequency of mode i", and u_g is the ground motion.

$$\ddot{X}_i + 2\zeta_i\omega_i\dot{X}_i + \omega_i^2 X_i = -\ddot{u}_g \qquad (8)$$

The damping ratio and natural circular frequency ζ_i, ω_i in the above equation are determined by the complex state vector eigenvalue solution, like the mode shape. Because the state vector will vary for different damping devices added, the modal shape, circular frequency and damping ratio will not be constant. Thus, the system response defined by equation (6) cannot be always reduced by increasing the damping ratio.

Case Studies

To illustrate how system characteristics change and their impact on seismic response due to added damping, a four DOF frame structure was analyzed. The first two vi-

"The results from modeling and analysis of a California hospital building will provide the engineering community with a three-dimensional nonlinear analysis platform that currently does not exist."

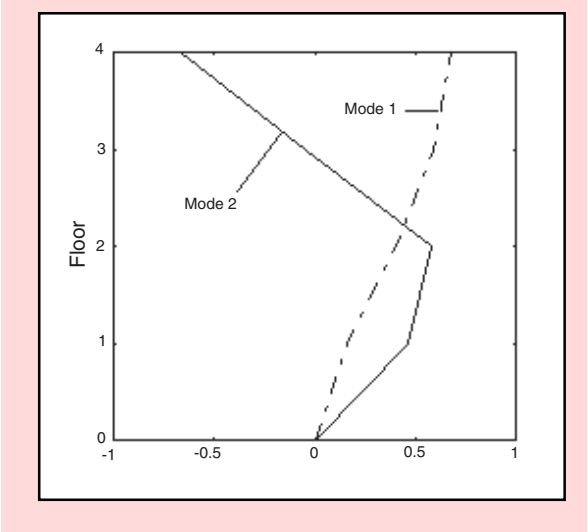

Figure 3. First Two Modal Shapes

bration modes of the frame are shown in Figure 3.

The added damping was limited to a maximum of 30% of the effective damping ratio (defined in FEMA 273 as a proportional ratio). Fifty-two linear viscous damper configurations were examined.The 52 configurations were arranged by considering all possible damper locations and their combinations, then changing the damping parameters to make the first modal effective damping ratio 5%, 10%, 20% and 30% (damping ratio by the added device plus 2%). As listed in Table 1, dampers were installed on every floor independently, every two floors, every three floors or on all four floors. There were 13 different damper configurations, with four damping ratios.

As noted above, the first mode of the complex damping ratio may be different from the first mode of the controlling effective damping ratio. The first complex modal damping ratio for all 52 cases is listed in Table 2. For small damping ratios (5%), the complex damping ratio is almost the same, however, when the damping ratio is increased to 10%, case 4 shows a dramatic change, while the other cases stay the same. Cases 3, 4, 7, 10, and 12 have very different values when the controlling ratio increases to 20%. Finally, the first complex damping ratio for cases 1, 3, 4, 7 and 12 becomes 99% when the ratio is increased to 30%.

The change in natural frequency in the first mode is given in Table 3. Both damping ratio and frequency changes are related to the modal change for different damper configurations.

To illustrate the non-proportional mode shape change, the first dis-

Table 1. Damper Location

Case	1	2	3	4	5	6	7	8	9	10	11	12	13
1st story	X				X			X		X		X	X
2nd story		X			X	X		X	X		X		X
3rd story			X			X	X	X	X	X			X
4th story				X			X		X		X	X	X

Table 2. Damping Ratio Comparison (First mode)

Case	1	2	3	4	5	6	7	8	9	10	11	12	13
5%	0.05	0.05	0.05	0.04	0.05	0.05	0.05	0.05	0.05	0.05	0.05	0.05	0.05
10%	0.10	0.10	0.10	0.99	0.10	0.10	0.09	0.10	0.10	0.10	0.10	0.10	0.10
20%	0.16	0.20	0.13	0.99	0.20	0.20	0.13	0.20	0.20	0.20	0.20	0.99	0.20
30%	0.99	0.28	0.99	0.99	0.31	0.31	0.99	0.30.	0.30	0.30	0.30	0.99	0.30

Table 3. Natural Frequency Comparison (First mode) (in Hz)

Case	1	2	3	4	5	6	7	8	9	10	11	12	13
5%	2.03	2.02	2.03	2.05	2.02	2.02	2.03	2.02	2.02	2.02	2.02	2.03	2.02
10%	2.06	2.04	2.07	1.17	2.03	2.07	2.02	2.03	2.03	2.03	2.03	2.05	2.02
20%	2.22	2.12	2.24	0.50	2.06	2.07	2.23	2.03	2.07	2.08	2.09	2.14	2.03
30%	1.96	2.29	1.50	0.32	2.12	2.15	1.41	2.04	2.14	2.17	2.20	1.30	2.04

placement mode shape at the controlling effective damping ratios of 5%, 10%, 20% and 30% are shown in Figure 4. The figure shows that, as the damping ratio becomes higher, dramatic changes can result in cases 1, 3, 4, 7 and 12 (the fundamental mode collapsed). When the fundamental mode shape collapses, the second mode shape becomes dominant in the system response, as shown in Figure 5.

The relationship between the maximum displacement response and the controlling effective damping is shown in Figure 6. Except for case 4, the response decreases as the damping ratio increases. When the controlling damping ratio is higher than 15%, different damper configurations will result in different response reductions even though they may achieve the same effective damping ratio value. It may also be seen from the figure that the maximum responses with a 30% effective controlling damping ratio for some cases are higher than those with 20%. Table 4 lists the maximum displacement re-

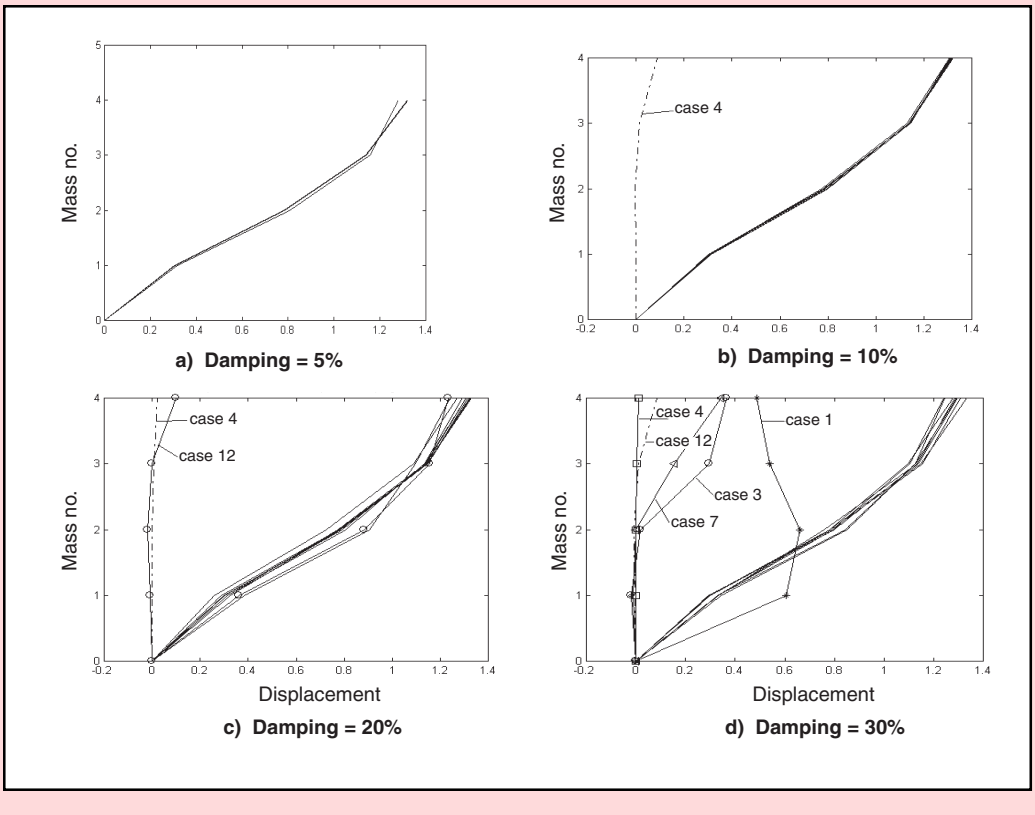

Figure 4. Displacement Modal Shapes

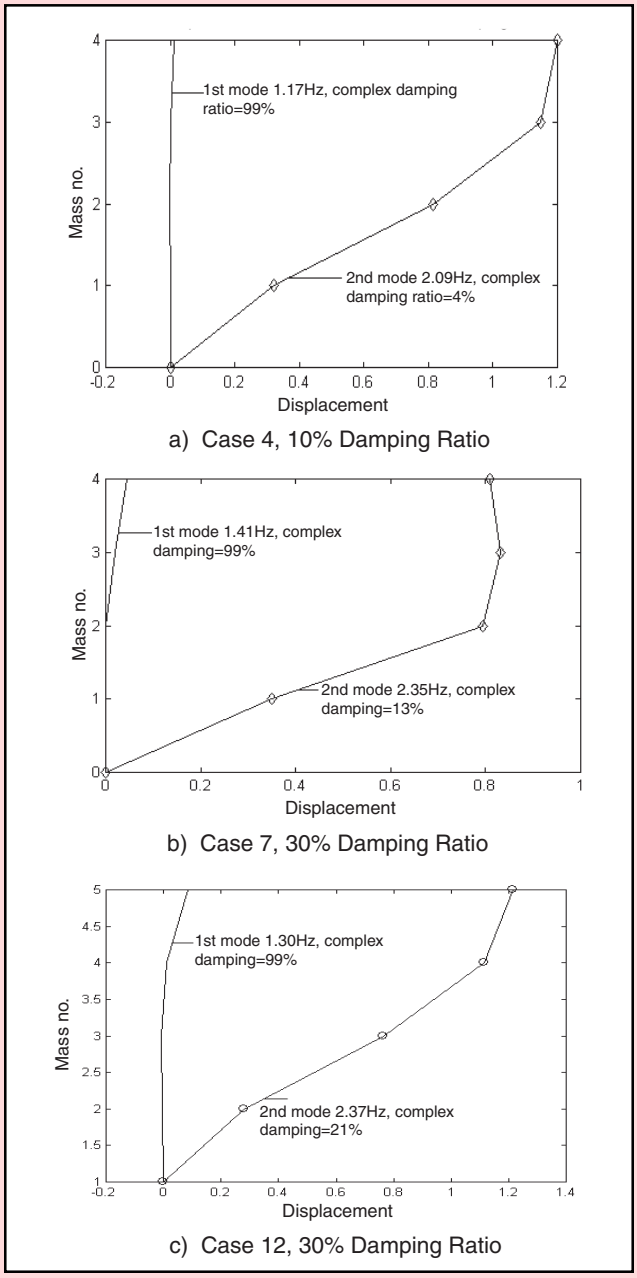

■ Figure 5. Mode Collapse

sponses for these two damping ratio values, calculated for the El Centro earthquake. As seen in the table, the damping increases in two ways: the first is where the response increased after more dampers were added and the configuration was unchanged (cases 3 and 4). The second case is when more dampers are added in different locations and configurations, as shown in case 1 at 20%, case 3 at 30%, case 4 at 30% and the rest of the cases are at 20%. This conclusion has also been obtained using other earthquake records, such as from the Northridge earthquake.

Continuing Effort

It is important to understand the limitations of using the damping ratio as the key seismic response reduction measurement. For many non-proportionally damped structures, the evaluation of performance should be based on response history analysis. In this regard, a simple method to cope with the various non-proportional damping effects will be valuable for engineering applications. This team is currently attempting to develop such a method.

■ Table 4. Maximum Displacement Response at the Top Level of the Frame Using Standard El Centro Earthquake Record

Case	1	2	3	4	5	6	7	8	9	10	11	12	13
20%	0.357	0.398	0.381	0.738	0.403	0.392	0.397	0.409	0.399	0.392	0.383	0.365	0.414
30%	0.343	0.287	0.384	0.765	0.324	0.315	0.374	0.339	0.309	0.313	0.289	0.280	0.350

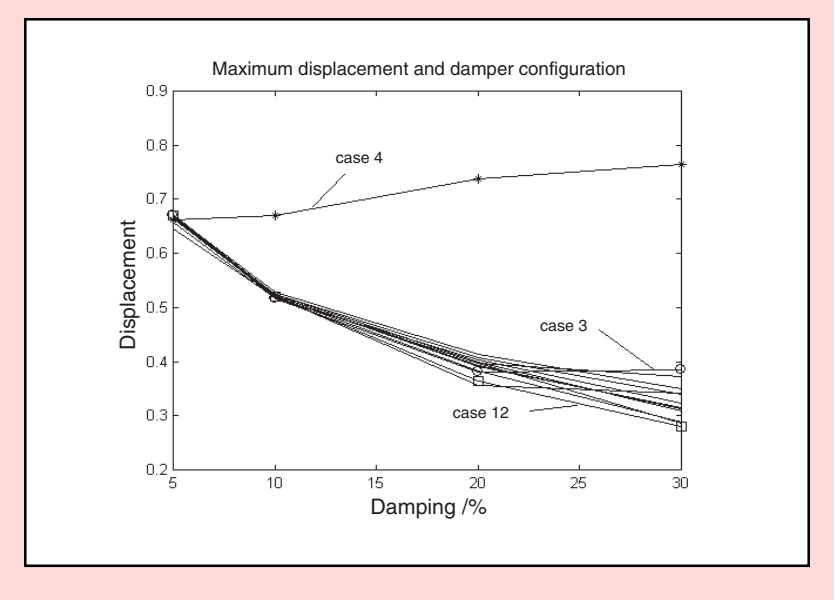

Figure 6. Maximum Displacement Response

Optimal Design of Damping Devices for Multi-story Steel Frames Based on Multi-performance Indices (Type III Project)

FEMA 273, NEHRP 2000 and the Blue Book 1999 provide primary design guidelines for buildings with supplemental damping devices. These procedures can address building design for different performance objectives using linear or nonlinear methods after the damping device configuration has been determined. However, the rule or procedure of how to optimally distribute these damping devices throughout the building and how to consider multi-performance indexes is still not available. These procedures are very critical for practicing engineers. Since adding damping devices causes the structure to be non-proportionally damped, a "systems approach" considering the change in characteristics is necessary.

The earthquake ground acceleration can be approximated as a finite Fourier series expansion, and the seismic response as the linear combination of all responses to the single frequency excitation. Thus, to find the effective configuration, it is necessary to know the dominant frequency response (or dominant mode), the modal composition, and its mass participating factors. The selection of the response will follow the performance index. With this knowledge, an optimization scheme for damping devices can be developed.

Analysis and Design Procedure

The design procedure is outlined as follows:

1. Calculate the characteristics of each potential configuration

2. Compare these with the original structural system's characteristics, and identify for each configuration:
   a. Natural frequencies (Some modes may collapse into each other due to added damping. This is particularly critical when damping becomes non-proportional. It follows that the natural frequencies may change significantly.)
   b. Modal damping ratio (100% critical damping usually implies a mode collapsed, which may be a problem for modal response reduction)
   c. Mode shapes
   d. Modal loading factors (variation in this characteristics may strongly influence the absolute acceleration response)
   e. Phase differences between the modes.
3. For a mass point of interest, check which natural frequencies will contribute most in the response, by using sinusoidal excitations of different amplitudes. Examine each corresponding steady state response vector to identify the largest contribution vector. A general excitation can be simplified as a sum of this sinusoidal excitation of various amplitudes, multiplied by certain envelopes. Thus, the response will be dominated by the combination of n basic vectors.
4. The vectors computed above can be further split into modal contributions. In this regard, comparisons can be made among modal shapes, loading factors, natural frequencies (which provides information on relative phase lags) and damping ratios (which provide information on dynamic amplification factors). This information illustrates the modes that are important in the response of a given mass point.
5. The damping distribution may be very different if the optimization target is selected as the story drift or acceleration. The drift response is dominated by the major modes. Thus, with a higher modal participation factor and a higher damping ratio, the drift responses will be further reduced. This is not the case for acceleration response, which includes more higher mode contributions.
6. For acceleration response, if a damper is placed between the i^{th} and $i+1^{th}$ floors, then the $i+1^{th}$ floor acceleration is usually lower than the i^{th} floor. In addition, $i-1^{th}$ floor acceleration will be lower than that of i^{th} floor.

Case Study

An 11-story steel frame building structure was used as an optimal design example. The building's typical plan and north-south elevation are shown in Figures 7 and 8. This building had been designed with supplemental damping devices. The typical device configuration in the frame is shown in Figure 9. A total of 120 dampers were added to the building, with 24 dampers on the first story, and gradually decreasing as the story height increases.

If the performance index is selected as optimal story drift, the first story mass contributes less to the dominant mode of the system response. Better results may be obtained if the dampers in this story are redistributed. The optimized distribution removes most of the devices from the first story, and

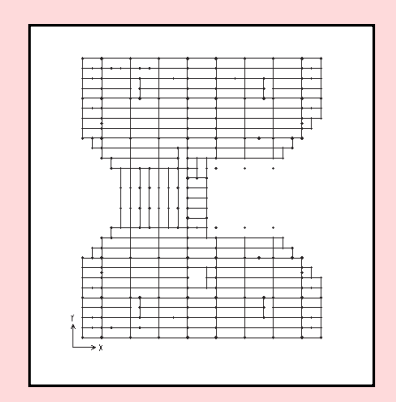

Figure 7. Floor Frame Plan

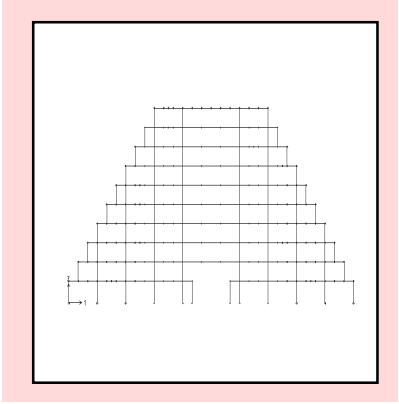

Figure 8. Elevation Frame Plan

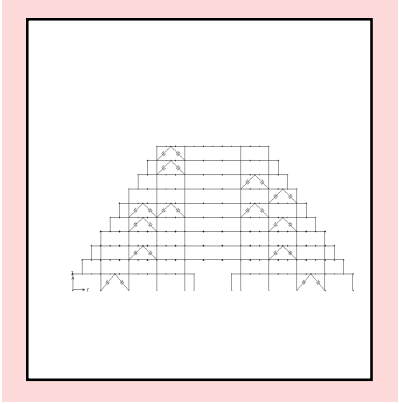

Figure 9. Damper Distribution

adds them to the 6th to 11th stories. The same total number of dampers is used as in the original damper distribution. With this optimized distribution, the total system damping is increased by 4%. More importantly, the damping ratio of the dominant mode is increased by 19%, and the largest story drift, which occurred in the 6th floor, is reduced by an average of 11% for a series of spectra-compatible earthquake. If the performance index is selected as acceleration, the optimal distribution will be different.

Current Efforts

The design and analysis procedure proposed here is based on frequency domain analysis and time domain verification. Since response spectrum or time history analysis are preferred in structural design, the method is currently being improved and optimized using response spectrum-based objective functions.

Computational Aseismic Design and Retrofit for Passively Damped Structures (Type III Project)

Over the past two decades, considerable effort has been directed toward the development and enhancement of protective systems for the control of structures under seismic excitation. In the area of passive energy dissipation systems, applications typically involve metallic yielding dampers, friction dampers, viscous fluid dampers or viscoelastic dampers (e.g., Soong and Dargush, 1997; Constantinou et. al., 1998). Although the introduction of these new concepts and systems presents the structural engineer with additional freedom in the design process, many questions also naturally arise. In the case of passive energy dissipation systems, these questions range from performance and durability issues to concerns related to the sizing and placement of damping elements.

One promising direction for future research involves the further development of the FEMA 273/274

and NEHRP 2000 design guidelines based upon additional numerical simulations and practical experience. Alternatively, one may envision a dramatically different design process for passively damped structures by adopting a computational approach. Such an approach should incorporate the dynamics of the problem, the uncertainty of the seismic environment, the reliability of the passive elements and perhaps also some key socioeconomic factors. With these requirements in mind, one can conceptualize aseismic design as a complex adaptive system and begin to develop a general computational framework that promotes the evolution of robust, and possibly innovative, designs.

Complex Adaptive Systems

There is a broad class of systems in nature and in human affairs that involve the complicated interaction of many components or agents. These may be classified as complex systems, particularly when the interactions are predominantly nonlinear. Within this class are systems whose agents tend to aggregate in a hierarchical manner in response to an uncertain or changing environment. These systems have the ability to evolve over time and to self-organize. In some cases, the system may acquire collective properties through adaptation that cannot be exhibited by individual agents acting alone. Key characteristics of these complex adaptive systems are nonlinearity, aggregation, flows and diversity (Holland, 1995). Examples include the human central nervous system, the local economy, a rain forest or a multidisciplinary research center.

Holland (1962, 1992) also developed a unified theory of adaptation in both natural and artificial systems. In particular, Holland brought ideas from biological evolution to bear on the problem. Besides providing a general formalism for studying adaptive systems, this led to the development of *genetic algorithms.*

Computational Framework for Aseismic Design

With these ideas, one can now envision a new aseismic design approach based upon the creation of an artificial complex adaptive system. The primary research objective is to develop an automated system that can evolve robust designs under uncertain seismic environments. With continued development, the system may also be able to provide some novel solutions to a range of complex aseismic design problems.

Figure 10 depicts the overall approach for computational aseismic design and retrofit (CADR), borrowing terminology from biological evolution. Design involves a sequence of generations within a sequence of eras. In each generation, a population of individual structures is defined and evaluated in response to ground motion realizations. Cost and performance are used to evaluate the fitness, which in turn determines the makeup of the next generation of structures. Performance is judged by performing nonlinear transient dynamic analysis. Presently, this analysis utilizes either ABAQUS (2000) or an explicit state-space transient dynamics code (tda). The implementation of the genetic algorithm

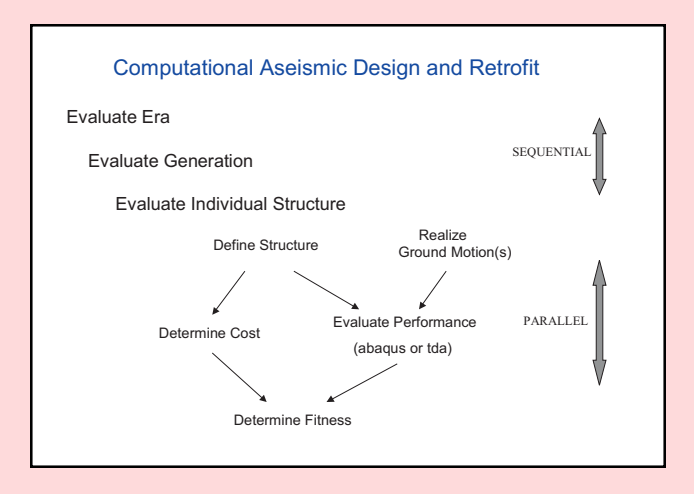

■ Figure 10. Overall Framework for Computational Aseismic Design and Retrofit

controlling the design evolution is accomplished within the public-domain code Sugal (Hunter, 1995).

Model Problem: Five-Story Steel Moment Frame

Consider an example of a five-story steel moment frame retrofit with passive energy dissipators as shown in Figure 11. Three different types of dampers are available: metallic plate dampers, linear viscous dampers, and viscoelastic dampers. For each type, five different sizes are possible. Consequently, a 20-bit genetic code is employed to completely specify the dampers used in each story of any particular structure $A \in \alpha$. Thus, for this problem, the set α contains 2^{20} (i.e., more than one million) possible structures. Figure 11 also defines a hierarchical approach in which different structural models with varying levels of complexity are utilized in each era. The idea is to first use simple models to widely explore the design space and then to employ more complicated and computationally expensive models later in the design process. Currently, a two-surface cyclic plasticity model is applied for the primary structural system and metallic plate dampers, while a coupled thermoviscoelastic model with inelastic heat generation is used for the viscoelastic dampers. Both interstory drift and story acceleration limits are set in order to establish acceptable performance.

As a specific example, consider the application of the CADR strategy to a typical five-story steel moment frame based upon Era 1 (i.e.,

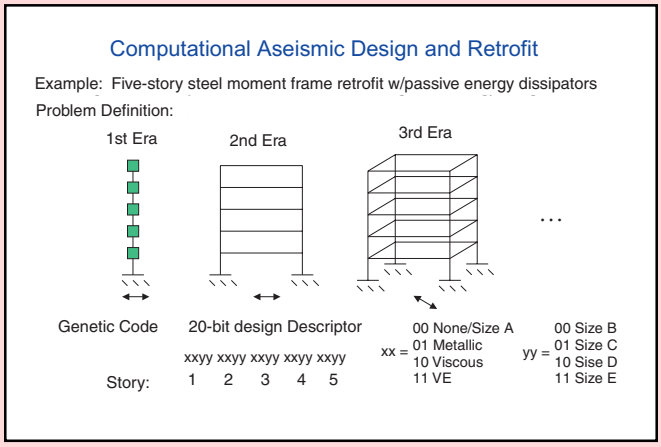

■ Figure 11. Problem Definition for Five-story Steel Moment Frame

lumped parameter) simulations. Let k_i and W_i represent the i^{th} story elastic stiffness and story weight, respectively. The baseline frame model has uniform story weights $W_i = W = 125$ kips for i =1,2,...5 and story stiffness $k_1 = k_2 = k_3 = 193$ kip/in, $k_4 = 147$kip/in, $k_5 = 87$ kip/in. The first two natural frequencies are 1.07 Hz and 2.72 Hz. A two-surface cyclic plasticity model is employed to represent the hysteretic behavior of the primary structure.

A retrofit strategy is now developed to protect this structure situated on firm soil in a simplified hypothetical seismic environment that can be represented by a uniform distribution of earthquakes with magnitude $7.2 \leq M_w \leq 7.8$ and epicentral distance 20 km $\leq r \leq$ 30km. Each ground motion realization is generated according to the model of Papageorgiou (2000) for eastern U.S. earthquakes. For the retrofit, it is assumed that linear viscous (visc) dampers, metallic yielding (tpea) dampers and viscoelastic (ve) dampers are available and the 20-bit genetic code defined in Figure 11 is applied. Hypothetical device cost data for various size dampers were set as indicated in Table 5. Each increment in damper size corresponds roughly to a doubling of the damping capacity.

For the automated design, a population of $N_p = 40$ individual structures was evolved for a total of $N_g = 40$ generations. Within each generation, each structure was subjected to a total of $N_s = 10$ seismic events. Crossover and mutation operators were used to evolve new structures from an initially random pool. At the end of each generation, one-half of the structures were replaced with potentially new individuals. As generations pass, generally speaking, the average fitness increases, indicating that the population becomes enriched with more robust structures. However, the evolution of average fitness is not monotonic, because the genetic algorithm continues to explore the design space for better structures. Table 5 also presents the five structures that have appeared most frequently in the population. These are high fitness designs that have survived over many generations. The table data includes the total number of earthquakes that each of the five structures has experienced and the success (or survival) rate. Notice, according to Table 5, that the high fitness designs most often utilize viscous dampers and that the largest dampers are placed on the first story. In four of the high fitness designs, size C dampers appear in the fourth story, suggesting perhaps that the second mode response also requires damping.

■ Table 5. Five-Story Steel Moment Frame –Baseline (Case 1)

Allowable Drift =1.500 in. Allowable Acceleration =193.200 in/s^2					
Device Cost:					
	A	B	C	D	E
visc	2.00	4.00	6.00	8.00	10.00
tpea	2.00	4.00	6.00	8.00	10.00
ve	2.00	4.00	6.00	8.00	10.00
High Fitness Designs:					
No. Trials:	2350	1900	570	410	320
Damper Cost:	26.00	26.00	26.00	28.00	26.00
Success Rate:	0.9655	0.9611	0.9614	0.9561	0.9625
Story 5	visc A	visc A	visc A	visc A	visc A
Story 4	ve C	ve C	visc C	ve C	tpea B
Story 3	visc B	ve B	ve B	ve C	tpea C
Story 2	visc C	visc C	visc C	visc C	visc C
Story 1	visc D	visc D	visc D	visc D	visc D

Concluding Remarks

In this research, a new computational aseismic design and retrofit (CADR) approach is advocated. This approach centers on the development of an artificial complex adaptive system within which robust aseismic designs may evolve. As a first phase of this research program, a genetic algorithm is applied for the discrete optimization of a passively damped structural system, subjected to an uncertain seismic environment. The results of preliminary applications, involving the seismic retrofit of multi-story steel moment frames, suggest that continued development of the approach may prove beneficial to the engineering community. Current efforts are underway to work with several MCEER Industry Partners to enhance the CADR software and to develop applications associated with critical facilities.

Development of Analysis Tools for Engineering Community (Type III Project)

Any implementation of protective systems in design of new buildings or bridges, or in their retrofit, requires modeling and analysis of integral systems including the structures and the devices. When these multiple-DOF systems are implemented with energy dissipation devices, the total building-device system in general is nonlinear. Much creativity and fundamental research in structural dynamics principles have to be pursued in order to develop a reasonably simple and accurate analysis and design procedure for use by the practicing professionals. Two ongoing MCEER projects are described in the following sections. One is fundamental in nature to establish new approaches while the other emphasizes the development of user-friendly simplified procedures for the design professionals.

Nonlinear Structural Analysis by the State Space Approach

The State Space Approach (SSA) is an alternative approach to the formulation and solution of initial-boundary-value problems involving nonlinear distributed-parameter structural systems.The response of the structure, which is spatially discretized following a weak formulation, is completely characterized by a set of state variables.These include global quantities such as nodal displacements and velocities and element (or local) quantities such as nodal forces and strains at the integration points.The nonlinear evolution of the global state variables during the response of structures is governed by physical principles, such as momentum balance, and the nonlinear inelastic evolution of the local variables is governed by constitutive behavior. The essence of the SSA is to solve the two sets of evolution equations simultaneously in time using direct numerical methods, in general as a system of differential-algebraic equations. The proposed methodology results in a more consistent formulation with a clear distinction between spatial and temporal discretization.

"Much creativity and fundamental research in structural dynamics principles have to be pursued to develop a simple and accurate analysis and design procedure for practicing professionals."

Objectives and results

A material nonlinear three-dimensional beam column element and a fully geometric (equilibrium and nonlinear strain-deformation relations) and material nonlinear two-dimensional beam-column element have been developed in this framework based on a flexibility formulation. A general three-dimensional interactive constitutive macro-model has been developed. In this model, hysteretic degradation can also be modeled using suitable constitutive equations (Sivaselvan and Reinhorn, 2000). The resulting platform can study structures near collapse. The basic approach has been used to model a structure, which collapsed in shake table under severe lateral buckling (see Vian et al., in this volume).

The above models and solution procedure have been implemented in an object-oriented computer program that uses the graphical user interface (GUI) of the commercial structural analysis program, LARSA. Figure 12 shows the response of a three-dimensional frame with hysteretic behavior to bi-axial non-proportional loading. Figure 13 shows results of analysis of extremely large deformations, which allows an elastic beam to be bent into a circle. Figure 14 shows the collapse pattern of a simple structure while Figure 15 shows that all the models are developed using the macro model approach in which structures are represented by beam-column elements with hysteretic degradation.

Three Dimensional Inelastic Dynamic Analysis of Structures with Protective Systems: IDARC3D Version 2.0

The nonlinear analysis of inelastic structures with energy dissipation systems and base isolations was the subject of research and development throughout the existence of the Center's activities. The research work, both analytical and experimental, resulted in a series computer platforms, IDARC and 3DBASIS, now available nationally and internationally to the public at large through a dedicated Users Group (*http://civil.eng.buffalo.edu*). (See also Park et. al., 1987, Reinhorn et. al., 1988, Kunnath et. al., 1989, Nagarajaiah et. al., 1989, Nagarajaiah et. al., 1991, Tsopelas et. al., 1991, Kunnath et. al., 1992, Nagarajaiah et. al., 1993, Tsopelas et. al., 1994,

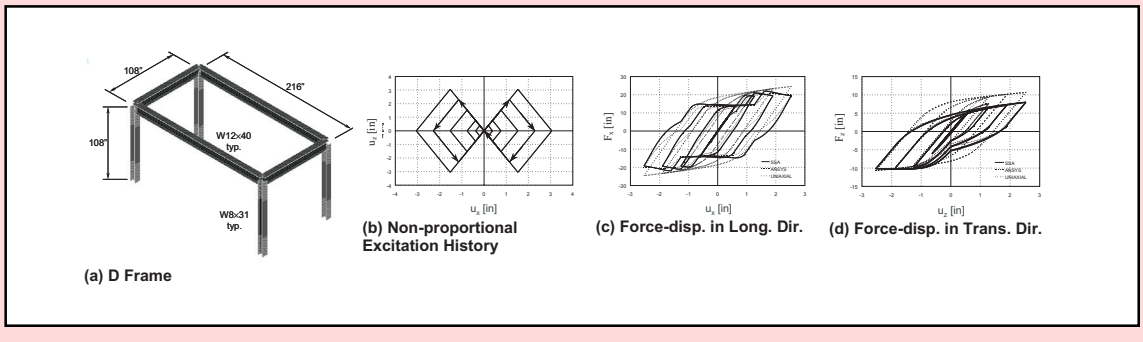

■ Figure 12. Inelastic Response of Frame Using 3D Interaction Elements

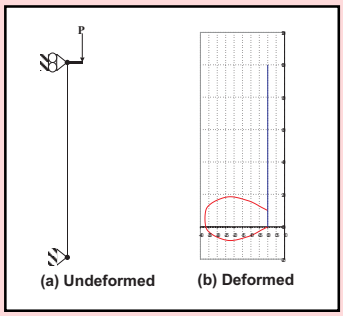

■ Figure 13. Eccentric Axially Loaded Elements

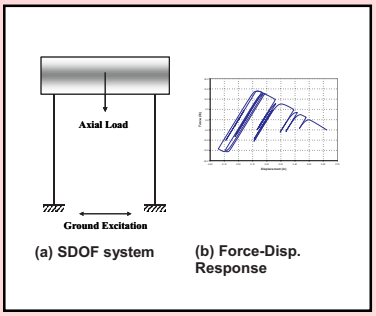

■ Figure 14. Dynamic Collapse using Geometric Nonlinear Beam

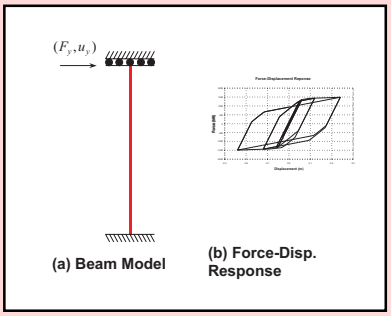

■ Figure 15. Hysteretic Degradation

Reinhorn et. al., 1994, Valles et. al., 1996, and Reinhorn et. al., 1998.)

The authors undertook an expansion to the three-dimensional systems of the code of IDARC in a redevelopment effort using an object-oriented approach. The resulting software architecture will enable progressive growth by easy addition of new models from other research tasks and provides the outcome to the engineering community at large. The current focus of work is to provide the tools for modeling damping and other advanced systems using a unified approach to nonlinear systems. The work done in cooperation with LARSA, Inc., a software developer, enables creation of a user friendly and acceptable analysis platform.

Objectives and results

The redevelopment includes three main steps. The first step is to create a flexible and extendable setup for the platform using an object-oriented finite element programming approach. This modular framework clearly separates the different elements of the program by encapsulating data in classes. Classes are black boxes, which provide easy to use interfaces throughout the program. Thus if a new class is added, the developer has to deal only with the data and routines of the new class itself. Also, changes to one class will not affect the rest of the program because of the encapsulation. This simplifies the integration of new parts.

In the second step, components are incorporated in the new platform IDARC3D Version 2.0: (i) energy dissipation systems / dampers and (ii) a computing core capable of nonlinear analysis. The new program structure provides possibilities to easily add new elements such as base isolators, adapted from the platform 3D-BASIS also developed by Reinhorn and Constantinou in multi-annual projects. To ensure convenience, IDARC3D Version 2.0 operates on a PC and has a graphical user interface for input and output (I/O). The I/O is decoupled from the core of the program so that it can be changed without interfering with the actual program.

The third step is to model and evaluate a structure with protective systems and to verify the results of the nonlinear analysis with IDARC3D 2.0 against results from other standard analysis programs or experiments.

The implementation of the new design is realized using FORTRAN 90 to be consistent with the previous and existing IDARC programs. Much of the existing code is reused in the new platform to minimize programming new code. Although FORTRAN 90 is not an object-oriented programming language, object-oriented features can be simulated with a reasonable effort. Also, source code written in FORTRAN 90 and C++ (as an example for an object-oriented programming language) can be used to form one platform together.

The documentation developed for the new platform includes guidelines to further develop the system, a users manual and installation examples. The developer's manual, which describes the modular setup and provides the reader with the necessary information to change or extend the program, will be published through the MCEER Networking activities.

A California hospital building is being modeled for research by other center investigators, and a benchmark physical model tested on the shake table at University at Buffalo is being analyzed to provide the first example cases. The result of this development will provide the engineering community with a three-dimensional nonlinear analysis platform that currently does not exist.

References

ABAQUS, (2000), *Theory Manual*, Version 6.1, Hibbitt, Karlsson and Sorensen, Pawtucket, RI.

Constantinou, M.C., Tsopelas, P., Hammel, W. and Sigaher, A.N., (2001), "Toggle-Brace-Damper Seismic Energy Dissipation Systems," *Journal of Structural Engineering*, ASCE, Vol. 127, No. 2, pp. 105-112.

Constantinou, M.C., and Sigaher, A.N., (2000), "Energy Dissipation System Configurations for Improved Performance," *Proceedings, 2000 Structures Congress*, ASCE, Philadelphia, PA, May.

Constantinou, M.C., Soong, T.T., and Dargush, G.F., (1998), *Passive Energy Dissipation Systems for Structural Design and Retrofit*, MCEER-98-MN01, Multidisciplinary Center for Earthquake Engineering Research, University at Buffalo.

Federal Emergency Management Agency, (1997), *NEHRP Guidelines for the Seismic Rehabilitation of Buildings*, FEMA 273, Federal Emergency Management Agency, October.

Federal Emergency Management Agency, (1997), *NEHRP Commentary on the Guidelines for the Seismic Rehabilitation of Buildings, FEMA 274*, Federal Emergency Management Agency, October.

Gupta A. K. and Law J. W., (1986), "Seismic Response of Non-classically Damped Systems," *Nuclear Engineering and Design 91*, pp. 153-159.

Holland, J.H., (1962), "Outline for a Logical Theory of Adaptive Systems," *J. Assoc. Comp. Mach.*, Vol. 3, pp. 297-314.

Holland, J.H., (1992), *Adaptation in Natural and Artificial Systems*, MIT Press, Cambridge, MA.

References, (Cont'd)

Holland, J.H., (1995), *Hidden Order*, Addison-Wesley, Reading, MA.

Hunter, A., (1995), *Sugal Programming Manual*, Version 2.1, University of Sunderland, England.

Kunnath, S.K., Reinhorn, A.M. and Lobo, R.F., (1992), *IDARC Version 3.0: Inelastic Damage Analysis of Reinforced Concrete Structures*, Technical Report NCEER 92-0022, Multidisciplinary Center for Earthquake Engineering Research, University at Buffalo.

Kunnath, S.K. and Reinhorn, A.M., (1989), *Inelastic Three-Dimensional Response Analysis of Reinforced Concrete Building Structures (IDARC-3D): Part 1 – Modeling*, Technical Report NCEER-89-0011, Multidisciplinary Center for Earthquake Engineering Research, University at Buffalo.

Lee, G. C., Tong, M. and Wu, Y.H., (2001), "Some Design Issues for Building Seismic Retrofit Using Energy Dissipation Devices," *Int'l. Journal of Structural Engineering and Mechanics*, (in press).

Nagarajaiah, S., Li, C., Reinhorn, A.M. and Constantinou, M.C., (1993), 3D-BASIS-TABS: Computer Program for Nonlinear Dynamic Analysis of Three Dimensional Base Isolated Structures, Technical Report NCEER-93-0011, Multidisciplinary Center for Earthquake Engineering Research, University at Buffalo.

Nagarajaiah, S., Reinhorn, A.M. and Constantinou, M.C., (1991), *3D-BASIS – Nonlinear Dynamic Analysis of Three-Dimensional Base Isolated Structures: Part II*, Technical Report NCEER-91-0005, Multidisciplinary Center for Earthquake Engineering Research, University at Buffalo.

Nagarajaiah, S., Reinhorn, A.M. and Constantinou, M.C., (1989), *Nonlinear Dynamic Analysis of Three-Dimensional Base Isolated Structures (3D-BASIS)*, Technical Report NCEER-89-0019, Multidisciplinary Center for Earthquake Engineering Research, University at Buffalo.

Papageorgiou, A.S., (2000), "Ground Motion Prediction Methodologies for Eastern North America," *Research Progress and Accomplishments, 1999-2000*, Multidisciplinary Center for Earthquake Engineering Research, University at Buffalo, pp. 63-67.

Park, Y.J., Reinhorn, A.M. and Kunnath, S.K., (1987), *IDARC: Inelastic Damage Analysis of Reinforced Concrete Frame – Shear-Wall Structures*, Technical Report NCEER-87-0008, Multidisciplinary Center for Earthquake Engineering Research, University at Buffalo.

Ramirez, O., Constantinou, M.C., Kircher, C.A., Whittaker, A.S., Johnson, M.W. and Gomez, J.D., (2000), *Development and Evaluation of Simplified Procedures for Analysis and Design of Buildings with Passive Energy Dissipation Devices*, MCEER-00-0010, Multidisciplinary Center for Earthquake Engineering Research, University at Buffalo.

Reinhorn, A.M., Simeonov, V., Mylonakis, G. and Reichman, Y., (1998), *IDARC Bridge: A Computational Platform for Seismic Damage Assessment of Bridge Structures*, Technical Report MCEER-98-0011, Multidisciplinary Center for Earthquake Engineering Research, University at Buffalo.

Reinhorn, A.M., Nagarajaiah, S., Constantinou, M.C., Tsopelas, P. and Li, R., (1994), *3D-BASIS-TABS Version 2.0: Computer Program for Nonlinear Dynamic Analysis of Three Dimensional Base Isolated Structures*, Technical Report NCEER-94-0018, Multidisciplinary Center for Earthquake Engineering Research, University at Buffalo.

Reinhorn, A.M., Kunnath, S.K. and Panahshahi, N., (1988), *Modeling of R/C Building Structures With Flexible Floor Diaphragms (IDARC2)*, Technical Report NCEER-88-0035, Multidisciplinary Center for Earthquake Engineering Research, University at Buffalo.

References, (Cont'd)

Simeonov, V.K., Sivaselvan M. and Reinhorn, A.M., (2000), "Nonlinear Analysis of Frame Structures by the State-Space Approach," *Computer-Aided Civil and Infrastructure Engineering*, (Special Volume in honor of Prof. Gear), Vol. 15, Jan 2000, pp. 76-89.

Sivaselvan, M., and Reinhorn, A.M., (2000), "Hysteretic Models for Deteriorating Inelastic Structures," *Journal of Engineering Mechanics*, Vol. 126, No. 6, Jun. 2000, pp.633-640.

Soong, T.T. and Dargush, G.F., (1997), *Passive Energy Dissipation Systems in Structural Engineering*, J. Wiley, England.

Tsopelas, P., Constantinou, M.C., Kircher, C.A. and Whittaker, A.S., (1997), *Evaluation of Simplified Methods of Analyses for Yielding Structures*, NCEER-97-0012, Multidisciplinary Center for Earthquake Engineering Research, University at Buffalo.

Tsopelas, P.C., Constantinou, M.C., and Reinhorn, A.M., (1994), *3D-BASIS-ME: Computer Program for Nonlinear Dynamic Analysis of Seismically Isolated Single and Multiple Structures and Liquid Storage Tanks*, Technical Report NCEER-94-0010, Multidisciplinary Center for Earthquake Engineering Research, University at Buffalo.

Tsopelas, P., Nagarajaiah, S., Constantinou, M.C. and Reinhorn, A.M., (1991), *3D-BASIS-M: Nonlinear Dynamic Analysis of Multiple Building Base Isolated Structures*, Multidisciplinary Center for Earthquake Engineering Research, University at Buffalo.

Valles, R.E., Reinhorn, A.M., Kunnath, S.K., Li, C. and Madan, A., (1996), *IDARC2D, Version 4.0: A Computer Program for the Inelastic Damage Analysis of Buildings*, Technical Report NCEER-96-0010, Multidisciplinary Center for Earthquake Engineering Research, University at Buffalo.

Winklemann, K., (2001), "IDARC3D VERSION 2.0: Three Dimensional Inelastic Dynamic Analysis of Structures with Protective Systems," MS Thesis, University of Darmstadt (completed while Visiting Research Associate at the University at Buffalo).

Using Cost-Benefit Analysis to Evaluate Mitigation for Lifeline Systems

by Howard Kunreuther (Coordinating Author), Chris Cyr, Patricia Grossi and Wendy Tao

Research Objectives

The purpose of this research is to examine how cost-benefit analysis (CBA) can be utilized to evaluate the attractiveness of mitigation for lifeline systems subject to earthquake ground motion. We propose a framework for the CBA that can be used in conjunction with work being completed by other researchers at MCEER (Shinozuka et al., 2000; Chang et al., 2000). With their development of fragility curves and insight into specific utility lifelines systems, our framework is useful for the next step in the analysis. In this paper, we use an example of a transportation system to show the CBA framework. Then, we consider two case studies to show the effects of the disruption of utility lifeline service on two stakeholders in the analysis. First, the indirect economic loss to business owners is studied, and then, the cost to public agencies to shelter displaced residents is considered.

The two lifelines serving as case studies for this work are the electric power system in Shelby County, Tennessee [building on previous work done at MCEER] and the water distribution system in Alameda and Contra Costa Counties, California [working with the East Bay Municipal Utility District (EBMUD)]. Our research provides a framework to link data from the physical and engineering sciences (i.e., seismology of the region and vulnerability of the lifeline) with the social sciences (i.e., costs of natural disasters and public policy implications of mitigation).

Sponsors

National Science Foundation, Earthquake Engineering Research Centers Program

Research Team

Howard Kunreuther, *Co-director,* ***Chris Cyr,*** *Undergraduate Student,* ***Patricia Grossi****, Post-Doctoral Researcher, and* ***Wendy Tao****, Undergraduate Student, Wharton Risk Management and Decision Processes Center, The Wharton School, University of Pennsylvania*

Cost-benefit analysis (CBA) is a systematic procedure for evaluating decisions that have an impact on society. There are different ways to conduct a valid CBA, depending on the information one has and the nature of the problem at hand. We chose a simplified five-step procedure to illustrate this approach (Figure 1). A more comprehensive approach, which incorporates several additional steps, is discussed in Boardman et al. (2001). The five-step procedure includes: defining the nature of the problem, including the alternative options and interested parties; determining the direct cost of the mitigation alternatives; determining the benefits of mitigation, via the difference between the loss to the system with and without mitigation; calculating the attractiveness of the mitigation alternatives; and, finally, choosing the best alternative.

Collaborative Partners

- ***David Lee*** *and* ***Tim Fuette****, East Bay Municipal Utility District*
- *Water distribution systems in Alameda and Contra Costa Counties, California (working with East Bay Municipal Utility District)*

These steps were chosen keeping in mind the complex process of estimating losses to lifeline systems and evaluating the benefits of mitigation to the system. Previous work performed at the Wharton School analyzed the cost-effectiveness of mitigation to residential structures (Kleindorfer and Kunreuther, 1999). In this analysis, the reduction in damage to the structure was accomplished through a shift in the fragility (i.e., vulnerability) curve in the analysis and a recalculation of the expected loss. If the expected reduction in loss exceeds the cost of undertaking mitigation (e.g., step 4 in Figure 1), then one can justify investing in it.

The analysis of the benefits of mitigating lifeline systems is a more complicated process than for a residential structure. Lifeline systems have unique characteristics, which make the calculation of damage to the system difficult (Chung et al., 1995). First, the loss of function of the lifeline is dependent on many parts of the system, often buried underground, spread across a large geographic region rather than at one location (e.g., as in the case of a residential structure). For example, in analyzing the functional

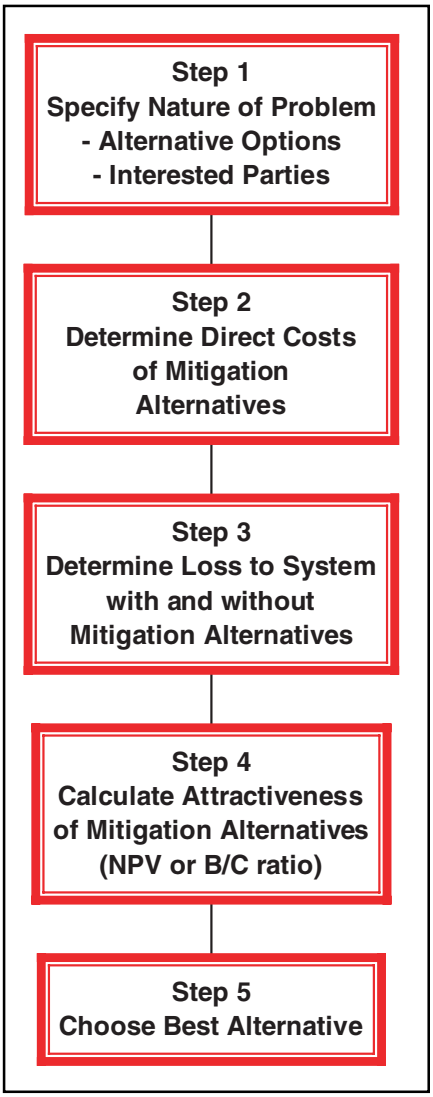

Figure 1. Simplified Cost-Benefit Analysis for Lifeline Systems

The cost to mitigate is primarily undertaken by owners, but everyone in a region benefits from uninterrupted or faster restoration of lifeline service after a disaster. Therefore, the primary users of this research are the operators of lifeline systems, which could be government agencies or private sector organizations who fund the cost of implementing mitigation measures. Cost benefit analyses can help determine if the expected reduction in loss exceeds the cost of undertaking mitigation. The thrust of the research is to encourage and justify implementation of retrofit schemes for a variety of lifeline systems.

reliability of an electric power transmission network, one needs to consider the loss of connectivity of different substations, as well as the vulnerability of the various components of each substation, to the system as a whole. This process can be even more complex when one must consider the collocation of different lifeline systems. For example, if the electric power system's cables are adjacent to the water distribution system's pipelines underground, damage to one can compound the damage to the other.

Second, the damage to the system, measured in outage or service disruption, needs to be translated into dollar loss to the interested parties in the cost-benefit analysis. The benefits of mitigation are the difference between the loss without mitigation and the loss with mitigation. The costs of mitigating the system must also be estimated. While these mitigation costs are generally borne by the owner and operator of the lifeline, everyone in the region benefits from the uninterrupted or faster restoration lifeline service after a disaster.[1] Therefore, the attractiveness of mitigation to a lifeline system should be viewed as beneficial to society as a whole, calculated via a societal benefit-cost ratio. The thrust of this research is to encourage and justify funding for earthquake hazard mitigation of lifeline systems.

The Five-Step Procedure

Step 1: Specify Nature of the Problem

To initiate a CBA, one needs to specify the options that are being considered and the interested parties in the process. Normally, one alternative is the status quo. In the case of the current analyses, the status quo refers to the current vulnerability of the lifeline system without a mitigation measure in place. The status quo is likely to be the reference point for evaluating how well other alternatives perform. In general, if there is sufficient political dissatisfaction with the proposed mitigation options and/or the perceived expected benefits (i.e., reduction in lifeline disruption) are considered to be less than the expected costs to mitigate the system, then the status quo will be maintained.

For the utility lifeline problem we are studying in Shelby County, Tennessee, the status quo is the vulnerability of the electric power system currently in place. An alternative option is to retrofit or replace some or all of the substation equipment components in the electric power system so they are still functional after a severe earthquake. For example, the transformers in the substations can be seismically retrofitted to withstand lateral loading. Alternatively, the high-voltage transformer bushings can be replaced before an earthquake occurs.

Each of the alternative options will impact a number of individuals, groups and organizations in our society. It is important to indicate who will benefit and who will pay the costs associated with different alternative options when undertaking a CBA analysis. In the case of a lifeline system, one needs to consider a broad set of interested parties. These include residents and business owners affected by the earthquake, public sector agencies that must respond and fund the re-

Links to Current Research

Program 1: Seismic Evaluation and Retrofit of Lifeline Networks

- *Task 1.3 Loss Estimation Methodologies*
- *Task 1.4 Memphis Lifeline Systems Analysis*
- *Task 1.10 Rehabilitation Strategies for Lifelines*

Program 2: Seismic Retrofit of Hospitals

"The attractiveness of mitigation to a lifeline system should be viewed as beneficial to society as a whole."

covery process, as well as the general taxpayer that will bear some of the repair costs of the damaged lifeline system(s).

Step 2: Determine Direct Costs of Mitigation Alternatives

For each mitigation alternative (i.e., all alternatives except the status quo), one needs to specify the direct cost to implement the mitigation measure. For a lifeline system, the owner and operator of the system incurs the costs of mitigation. In a large majority of the cases in the United States, it is a public sector agency. Furthermore, the costs are most likely direct monetary costs to structurally retrofit or replace some components of the lifeline system. In the case studies we will present, a government agency incurs the direct cost of mitigation.

Step 3: Determine the Benefits of Mitigation Alternatives

Once the costs are estimated for each mitigation alternative, one needs to specify the potential benefits that impact each of the interested parties. In the case of seismic risk, one considers either a scenario earthquake event or a set of scenario earthquakes of different magnitudes, location, duration, and attenuation that can affect the system. With the specification of the vulnerability of the lifeline system, the damage to the various components of the system is then estimated for each alternative option. Then, overall system reliability is estimated.

With the status quo, there will be no benefits because no retrofit or replacement scheme is characterized. In other words, the status quo is the damage to the system without mitigation. In the other alternatives, benefits will be estimated from the change in damage to the system with the status quo and damage to the system with mitigation in place. Once the system reliability with each mitigation alternative has been specified, it should be possible to quantify the effects of serviceability to the interested parties by attaching a dollar value to them. The calculation from damage to loss is a complicated process and will differ from one interested party to another (e.g., losses to industry from business interruption differs from residential loss due to relocation).

Step 4: Calculate Attractiveness of Mitigation Alternatives

In order to calculate the attractiveness of mitigation, the nature of the benefits to each of the interested parties is estimated and compared to the upfront costs of mitigation. With respect to lifelines, the alternatives involve a degree of outage or serviceability over a prescribed time horizon (T). One characterizes the impact on the key interested parties during the days or weeks that the system will not be fully functional. One then utilizes a societal discount rate to convert the benefits and costs of the alternative over time into a net present value (NPV). If the NPV is greater than zero, then the alternative is considered attractive. Alternatively, one could calculate the ratio of the discounted benefits to the upfront costs to determine the attractiveness of the alternative. Whenever this ratio exceeds 1 the alternative is viewed as desirable.

To illustrate, consider the case of damage to a water distribution system from a scenario earthquake

event. There could be a period of time where businesses may not be able to operate in a normal manner due to loss of service. If mitigation were implemented (e.g., underground pipelines were replaced or retrofitted), the time to restore water to businesses may be shortened. Suppose that the mitigation measure reduced the restoration time by 3 days following a severe earthquake. The resulting savings in business interruption costs during this three-day time interval following the earthquake are then discounted back to the present. These savings are multiplied by the annual probability of such an earthquake occurring to compute the expected benefits of mitigation. A similar calculation would be made for any earthquake that could occur in the area. These savings are then summed up to determine the total expected benefits which are then compared to the upfront costs of mitigation to determine the cost-effectiveness of the mitigation measure.

One must be careful, however, when considering the time that service is unavailable to the users of certain lifeline systems. Depending on the type of system (e.g., transportation, water distribution, electric power), days without service are, on average, less with electric power systems than other types of systems. This is primarily due to the redundancy in these systems and the critical nature of electric power systems in emergency response and coordination following an earthquake (Chung et al., 1995).

Step 5: Choose the Best Alternative

Finally, once the attractiveness of each alternative is calculated through a net present value calculation or a ratio of the benefits to the costs, one can choose the alternative with the highest NPV or benefit-cost ratio. This criterion is based on the principle of allocating resources to its best possible use so that one behaves in an economically efficient manner.

Applying the Five-Step Procedure to a Transportation System

We now illustrate how the above five-step procedure of CBA can be utilized to evaluate mitigation for a lifeline system through a simple example. In the next section, we will indicate the types of data that are required to undertake different levels of analyses of more realistic problems.

Step 1: Specify Nature of the Problem

The following question has been posed to a public agency that owns and operates a transportation network in an earthquake prone region in the United States: Should the transportation agency seismically upgrade their 2,200 highway bridges so that they perform adequately in a major earthquake?

There are only two alternatives for this problem:

A1. Seismically retrofit the bridges
A2. Do not retrofit the bridges (i.e., maintain status quo)

There are a number of interested parties who are affected by this problem. These include the residents who use the bridges to commute to work, the businesses that use the transportation network to move goods, the owner of the transportation network, police and fire teams that cannot move across the bridge, environmental groups concerned with the impact of a col-

"Developing a meaningful cost-benefit analysis methodology requires bringing scientists, engineers and social scientists together to analyze a problem."

lapsed bridge on residents of the sea. We will focus on just the owner of the network to keep the analysis simple.

Step 2: Determine Direct Costs of Mitigation Alternatives

The direct cost associated with seismically retrofitting the bridges is the material and labor cost to complete the retrofit scheme. In this case, we assume that, on average (i.e., over 2,200 bridges), this cost is approximately $30 per square foot.

Step 3: Determine the Benefits of Mitigation Alternatives

The benefits of retrofitting the bridges depend on whether or not an earthquake occurs and the length of time (T) that the bridges are impaired after the earthquake with and without the retrofit scheme in place. For simplicity, we consider only one scenario event, with two possible outcomes: (1) the earthquake occurs with probability, p, or (2) no earthquake occurs with probability, $1\text{-}p$.

For this event, the benefits consist of several different impact categories. We will consider one category for this analysis: the damage to the bridges. Damage and loss will be the same or lower if the bridges are retrofitted (A1) than if they are not (A2). In other words, the benefits from mitigation are the reduction in costs to repair the damaged bridges. In this case, we assume that the cost to repair the damaged bridges without a retrofit scheme (i.e., replace the bridges) is $140 per square foot. With the retrofit scheme, the cost is zero.

Step 4: Calculate Attractiveness of Mitigation Alternatives

To determine the impact of retrofitting the bridges through a net present value calculation, three additional pieces of data are required: (1) the probability of the scenario earthquake, p; (2) the life of the bridge, T, in years; and (3) the annual societal discount rate, d.

As each of these parameters is varied, one will obtain a different relationship between the net present value (NPV) of the expected benefits and costs of A1 and A2. To illustrate this point, suppose that one utilized the following parameters to determine whether or not retrofitting the bridges is beneficial to the transportation department. First, the probability of the earthquake occurring, p, is a 1 in a 100-year event (i.e., $p = 0.01$). The life of the bridge, T, is 50 years, and the discount rate, d, is 4%.

Suppose an earthquake occurred and the bridges were retrofitted. Then, the reduction in losses from this retrofit scheme is $140 per square foot, and the expected benefits from mitigation would be calculated (1/100)(140) = 1.4. With d = 4%, the expected discounted benefits of retrofitting over the 50 year life of the average bridge would be $30 per square foot. As we vary each of the parameters, the discounted expected benefits from mitigation will change. In general, higher values of d and/or smaller values of p and T will cause benefits to decrease. If the cost of retrofitting the bridges were set at $30 per square foot, then the net present value would be exactly 1. Any time that this cost was less than $30 it would be beneficial to retrofit the bridge. Of course, from a societal point of view, it would

be beneficial to retrofit the bridge if the cost per square foot exceeded $30. There would be additional benefits to residents who use the bridges to commute to work or for pleasure, businesses using the bridges to move goods, and avoidance of business interruption due to loss of the transportation network. These additional benefits of mitigation are due to the reduction in time to repair the damaged bridges.

Step 5: Choose the Best Alternative

The criterion used by CBA is to maximize net present value (NPV) of societal benefits or minimization of the total societal costs. In the above example, with the expected costs equal to the benefits of $30 per square foot, retrofitting the bridges (A2) would be preferable over maintaining the status quo (A1).

In addition to the maximization of social benefits, there may be equity considerations that play a role in the evaluation of different alternatives. For example, if there were concerns by taxpayers on how much extra they would have to pay for tolls over the bridges to reflect the extra expenditures of retrofitting the bridges, then this may impact on the implementation of A2 even if it was deemed cost-effective using maximization of NPV as a criterion.

In essence, the choice of an optimal alternative is based on a set of assumptions that need to be carefully examined. In particular, one will want to undertake a set of sensitivity analyses to determine how robust the proposed solution is. For example, if the expected cost of retrofitting the bridges were only $15 per square foot, then there would be little doubt that mitigation would be a cost effective one. The reasoning is simple. The benefit-cost ratio for this problem would be (30/15), which is 2. Even if the estimates of the benefits of mitigation were off by a factor of 2, one would still want to retrofit the bridges if the cost of this measure is $15 per square foot.

Mitigation of Lifelines in Tennessee and California

We now turn to the two case studies of lifeline systems to illustrate how one would compute the benefits and costs of mitigation: an electric power system in Shelby County, Tennessee and a water distribution system in Alameda and Contra Costa counties, California. The impacts of an earthquake on these lifeline systems include a wide range of direct and indirect losses. Our focus is on two types of losses to two different stakeholders: (1) the impact of interruption of service on business operations and the resulting losses in gross regional product (to Shelby County) and (2) loss of service to residential customers and the need to relocate individuals and entire families to temporary shelters (in Alameda and Contra Costa counties).

In these analyses, we consider only these two limited impacts of earthquake loss. Other impacts, such as the costs associated with fire following an earthquake, are not considered here. For the total loss to the water distribution system in Alameda and Contra Costa counties, we refer the reader to the study completed for the East Bay Municipal Utility District (Homer and Goettel, 1994).

Mitigation of an Electric Power System in Shelby County, Tennessee

As a continuation of an analysis done by researchers at MCEER (Shinozuka et al., 1998), we developed a framework to look at the cost-effectiveness of mitigation to the electric power system of the Memphis Light, Gas, and Water Division (MLGW) of the Memphis, Tennessee area. Loss to the gross regional product (GRP) of the different business sectors in the region due to loss of power is considered.

Figure 2 depicts a map of the Memphis/Shelby County area with indicated Modified Mercalli Intensity (MMI) impacts by census tract for a M = 7.5 earthquake. The Shelby County area is at risk from seismic activity in the New Madrid Seismic Zone (NMSZ) of the Central United States.This seismic zone lies within the central Mississippi Valley, extending from northeast Arkansas, through southeast Missouri, western Tennessee, western Kentucky to southern Illinois, and whose center is located to the northwest of Memphis.The NMSZ has a history of earthquake activity, with the largest earthquakes recorded in 1811-1812, and thus, it is an interesting case study for potential earthquake damage.

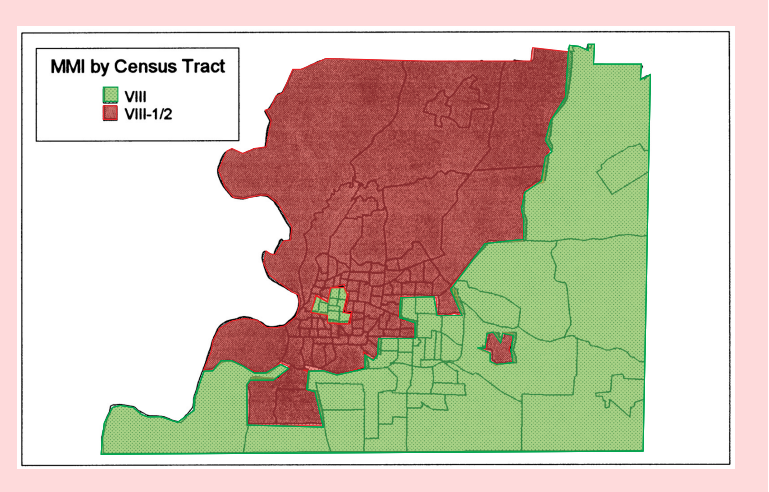

Figure 2. Shelby County, Tennessee (NCEER Bulletin 1996)[2]

For this analysis, we used a M = 7.5 earthquake with an epicenter in Marked Tree, Arkansas, situated fifty-five kilometers northwest of downtown Memphis. We looked specifically at mitigation that could be undertaken on electric power systems, basing this study on a network of electric power serviced by Memphis Light, Gas and Water (MLGW). We examine the loss of serviceability of the electric power system from the scenario M = 7.5 earthquake, based on data developed by Chang (See Shinozuka et. al, 1998).We should note that damage to the overall system reliability was estimated using Monte Carlo simulation techniques, and with this damage, loss of service to different service zones was estimated. The focus of this research is how to use this output from the simulation analysis to look at the cost-effectiveness of mitigation.

Electric power is absolutely crucial in maintaining the social systems of a city, directly affecting businesses that cannot operate without it.The study of mitigation for the gas, power and water distribution systems is not studied here. For an update on the damage and loss to the water distribution system, see Chang et al. (2000).

Mitigation in this case is a seismic retrofit of a component of the electric power substation. Specifically, the transformers, used within the substations of the network to convert power, are retrofitted to

withstand lateral loading. Tying down the wheels on the track can significantly improve the sliding movement and reduce the chances that these large, critical structures will overturn.[3]

The estimation of loss to the businesses in the area, due to service interruption, is calculated using the direct economic loss methodology from ATC-25 and modified by Chang to accommodate the importance factors specific to the Memphis area. The initial loss, L_j, to business sector j in the region directly following earthquake is estimated by equation (1).

$$L_j = (1 - a) \cdot g_j \cdot F_j \qquad (1)$$

In the above equation, a is the initial availability to the area. In other words, it is the percentage of customers receiving service immediately after the earthquake. gj is the gross regional product (GRP) in the region for the business sectors, j. In our case, j includes ten separate sectors. Examples include agriculture, construction, manufacturing, and services. The GRP was developed using data from the U.S. Census Bureau. Finally, Fj is the importance factor of the business sector, described as the percentage of production in sector j that would be lost if electric power service were completely disrupted (ATC-25, 1991).

For the scenario earthquake event, suppose restoration time is T days. So, the loss of production over T days, LT, is addressed by equation (2).

$$L_T = \sum_{t=0}^{T} L_j * \frac{(T - t)}{T} \qquad (2)$$

In this simplified analysis, if the transformers are seismically retrofitted, then we assume the loss of serviceability will be reduced, since some or all of the transformers would be functional after the earthquake. After knowing the difference in the number of functional transformers before seismic retrofit and after the retrofit scheme, one can then compute the savings to the business sector. In other words, the reduction in electric power outage characterizes the benefits of mitigation should the scenario earthquake occur in the service area. The *expected* benefits of mitigation are calculated by multiplying these benefits by the probability of the earthquake (p) and discounting over the relevant time horizon (T) that the transformer is expected to be in use (i.e., step 4 in the cost-benefit analysis).

To illustrate the type of CBA that could be undertaken, consider the following illustrative example. Assume that the cost of retrofitting each transformer is $10,000. If all 60 transformers in the electric power system are retrofitted, there is a one-time total cost of $600,000. Therefore, there are two alternatives: the status quo and retrofitting all the transformers for an upfront cost of $600,000. The stakeholders in the analysis are the businesses in the area needing electric power for production output. The benefits of mitigation are the reduction in restoration time due to more transformers functional following the earthquake event.

Additionally, we assume that the electricity system will last for 50 years and an 8% annual discount rate is used to compute the expected benefits over the 50-year horizon from retrofitting the trans-

formers. We consider an earthquake of M = 7.5 would occur in the region once every 500 years, estimated from a study done by the USGS (Atkinson et al., 2000).

Figure 3 depicts the sensitivity of the CBA to restoration times of the electric power system would be reduced by either 1, 3 or 5 days. The figure is designed to show how CBA can be utilized to evaluate whether or not mitigation of certain parts of the system is cost-effective to certain stakeholders in the analysis. In this example, retrofitting transformers can be seen to be beneficial (i.e., the benefit-cost ratio is greater than 1) for a time horizon T greater than 13 years when restoration of the power system is reduced by five days and for T greater than 23 years when restoration is reduced by three days. Retrofitting the transformer is not cost-effective for any T when restoration of the power system is only one day. This is important to note because after the Northridge earthquake in 1994, electric power (LAPWD) was restored to ninety-

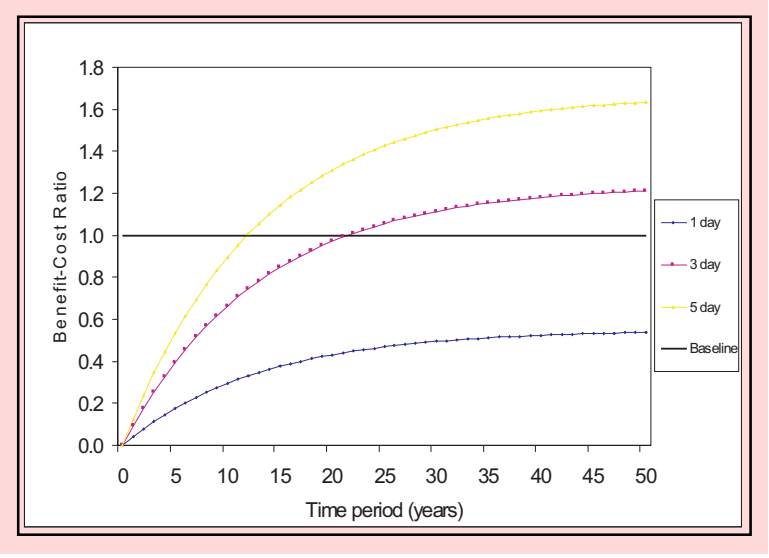

Figure 3. Illustrative Example of Effects of Electricity Lifeline Mitigation

percent of the users within one day. But, in the Chi-Chi, Taiwan earthquake in 1999, it took longer to restore power, with rolling blackouts to the northern part of the island for a week or more.

This analysis should be viewed as illustrative rather than definitive, since it is highly dependent on the assumptions made regarding the costs of retrofitting and the business interruption savings as well as the discount rate, d. For example, if d were four percent, then retrofitting the transformers would be even more attractive than under the current analysis.

Mitigation of a Water Distribution System in Alameda and Contra Costa Counties, California

The East Bay Municipal Utility District (EBMUD) is the public utility that provides potable water service to Alameda and Contra Costa Counties in northern California. We utilized information from the EBMUD Seismic Evaluation Program Final Report (Homer and Goettel, 1994), an intensive study of the East Bay water system that developed mitigation initiatives that will be completed during their Seismic Improvement Program. Our analysis focuses on the mitigation of 172 water storage tanks in 120 of the 122 EBMUD pressure zones.

To conduct this analysis, four scenario earthquake events were chosen for analysis, based on the completed EBMUD report (Table 1). These events represent the maximum plausible earthquake event that could occur on any given fault, with the exception of the Hayward

M = 6.0. For the Hayward fault, an earthquake of magnitude M = 6.0 is the most probable event and M =7.0 is the maximum plausible event.

In this analysis, there are two alternatives: the status quo and the mitigation of the water storage tanks.Those affected by the disruption of the water supply system are the residents in the service area that may be forced to relocate to temporary shelters for a period of days or even weeks.The direct cost of retrofitting the water tanks is based on data supplied by the EBMUD and given in Table 2.

Loss of Serviceability and Effects on Residential Displacement

The benefits of mitigation are the losses resulting from loss of water service to residential customers with and without the seismic upgrade of the tanks. When water service is disconnected from a place of residence, the individuals who live in these buildings will be forced to find alternative shelter until water service is restored. In the event of an earthquake, the potable water system can be damaged to an extent that water service may not be restored to an area until many weeks following the event. Figure 4 details our methodology for estimating the costs that are associated with these displaced individuals.

First, we determined the likelihood of tank failure in each pressure zone. EBMUD performed a detailed analysis of their system, us-

■ Table 1. Scenario Events

Fault Name	M	Description
Hayward	7.0	event ruptures 50 to 60 km long segment of fault
Hayward	6.0	event ruptures an 8 to 13 km long segment of the fault
Calaveras	6.75	event ruptures the northernmost part of the known active fault
Concord	6.5	event occurs along this fault east of the EBMUD service area

■ Table 2. Direct Cost to Retrofit Water Tanks

Tank Size	Seis. Upgrade Cost [1]	Partial Loss: Cost to make 'operational' after EQ. No upgrade prior to EQ" [2]	Partial Loss: Repair time for upgrade to make 'Operational' after EQ	Full Loss: Install Temp. Bolted Steel Tank for "Operational Restoration" [3]	New Tank Cost: Steel Replacement [4]	Full Loss: Replace Tank with Equivalent size tank
Concrete						
0.5	$ 500,000	$ 150,000	6 weeks	10 weeks	$ 1,000,000	1 year
1	$ 600,000	$ 150,000	7 weeks	10 weeks	$ 1,500,000	1 year
1.5	$ 750,000	$ 150,000	7 weeks	10 weeks	$ 1,750,000	1 year
2	$ 900,000	$ 200,000	8 weeks	10 weeks	$ 2,000,000	1 year
3	$ 1,200,000	$ 200,000	8 weeks	10 weeks	$ 2,500,000	1 year
5	$ 1,500,000	$ 200,000	9 weeks	10 weeks	$ 3,000,000	1 year
Steel						
0.25	$ 100,000.00	$ 50,000	1 week	10 weeks	$ 650,000	1 year
0.5	$ 200,000.00	$ 50,000	1 week	10 weeks	$ 1,000,000	1 year
1	$ 250,000.00	$ 50,000	1 week	10 weeks	$ 1,500,000	1 year
3	$ 300,000.00	$ 70,000	2 weeks	10 weeks	$ 2,500,000	1 year
5	$ 400,000.00	$ 70,000	2 weeks	10 weeks	$ 3,000,000	1 year

Footnotes:
1 Includes non-seismic upgrades, which are approximately 15% of seismic costs.
2 Partial loss for steel tank due to damaged valve pit piping. Time due to valve replacement. The tank structure assumes to either fully survive or fully fail.
3 The existing tanks may be out of service for this period of time; however, if there are multiple reservoirs in a pressure zone, the business interruption will likely be a much lesser time than indicated. Assume temporary replacement with either a .28 MG or 0.4 MG tank.
4 Cost includes: demolish existing tank, valve pit modification, metal appurtenances, miscellaneous site work, water quality piping, 15% construction contingencies.

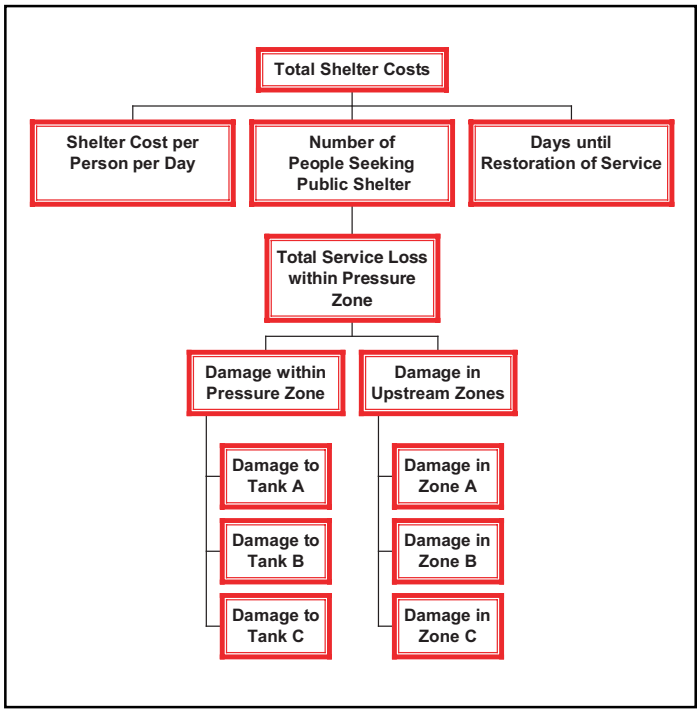

Figure 4. Cost to Shelter Displaced Residents from one Pressure Zone

ing their own system risk analysis software, SERA. Ten simulations of each of the four above earthquakes (i.e., forty simulations in all) were run to determine the extent of damage that their system is expected to face following an earthquake. For each simulation, tanks were said to fully fail, partially fail, or not fail. Our analysis of expected loss consists only of two of these three states – full failure and no failure – since we have no means by which to accurately analyze the complex network effects of partial loss. Therefore, if a tank was said to fully fail in 6 of 10 Hayward M 7.0 scenarios, then we say there is a 60% chance of full tank failure following a Hayward M 7.0.

Next, determination of likely water service within individual pressure zones was calculated. Some pressure zones are served by more than one tank, and therefore, the overall loss of service in a pressure zone is a combination of the effects of individual tanks in the pressure zone failing. The loss to pressure zone one, L_{PZ1}, therefore, can by defined by equation (3). In the equation, A_{N1} is the probability of full loss for a tank in pressure zone one and N1 is the number of tanks in zone one.

$$L_{PZ1} = \sum_{t=0}^{N} \frac{A_{N1}}{N1} \qquad (3)$$

Although a pressure zone may experience loss of service due to failure of its internal tanks, it may also experience service interruption if pressure zones that provide water to its tanks experience failure. To fully understand the total loss within a zone, we must take this into consideration as indicated by equation (4):

$$P_1 = (X_1 \cdot X_2 \cdots X_n) + [1 - X_1 \cdot X_2 \cdots X_n] \cdot L_{PZ1} \qquad (4)$$

In equation (4), P_1 is the percentage of customers in pressure zone one that will be without service following an earthquake, X_1 through X_N represent the probability of failure in pressure zones that feed into pressure zone one, and L_{PZ1} is the loss due to tank failure in pressure zone one. If every pressure zone that provides water to the tanks in pressure zone one fails, then no customers in pressure zone one will have service. The probability that this occurs is represented by the product of the probabilities that each individual precedent pressure zone will fail. If any or all of these precedent pressure zones has service, however, we will assume that the district will be able to provide enough water to its

tanks in pressure zone one so that customers have their minimum water demands met. Then, the only residents without water service will be those represented by L_{PZ1}, or those who do not have service due to tank failure within pressure zone one.

Once the overall service to each pressure zone is calculated, the number of people displaced and seeking temporary shelter can be determined. Since we are analyzing 120 pressure zones in the system, the number of people seeking temporary shelter following an earthquake is as follows:

$$R_S = \sum_{z=1}^{120} u_z \cdot P_z \cdot n_{bz} \cdot s_z \qquad (5)$$

In equation (5), R_s represents the number of residents seeking temporary public shelter following a disaster and u_z is the number of occupied housing units in pressure zone z. This is found by overlaying U.S. Census data on the service district. P_z is the percent of service loss in pressure zone z, or the percentage of housing units without water service, and n_{hz} is the number of people per housing unit in zone z. This is calculated by dividing the total population in zone z by the total number of occupied housing units. Finally, s_z is percentage of displaced residents in zone z who well seek shelter in a public facility. This is determined by inputting U.S. Census tract demographic information into a methodology developed for HAZUS (NIBS, 1997)[4]. This analysis is run for each of the districts 120 pressure zones considered, then aggregated to determine the total number of residents across the district who will seek shelter following a disaster.

To determine the total cost of sheltering residents displaced by loss of potable water service to their home following the earthquake, we multiply R_s by $11.50. This value is based on an American Red Cross estimate of between $10 and $13 to shelter a person for a single day (Red Cross, 2000).

Finally, to determine the total aggregate displacement costs following an earthquake, we must first consider whether the per-day costs will remain constant over time. We assume that if a tank is fully damaged it will not be able to supply water to any of its customers until it is fully repaired, or until a replacement tank can be acquired. Therefore, there will be no incremental increase in service over time and the per-day total costs of sheltering residents will remain constant over that period (since people are not able to return home). Based on this assumption, the total cost to shelter displaced residents following an earthquake is easily calculated by multiplying the total cost per day by the total time until restoration of service. In this case, we assume ten weeks or seventy days, based on information provided by EBMUD.

Note that the above analysis characterizes the impact on shelter costs under the assumption that the status quo was being maintained. The alternative option is to retrofit the water tanks in some of the pressure zones in Alameda and Contra Costa counties. By undertaking this protective measure, one reduces the chances that one or more of the tanks will fail and hence, disrupt water service for some period of time. The benefits of this mitigation measure will be determined by the reduction in res-

toration time for water to residences in the area affected by the earthquake.

One also needs to take into account whether individuals were forced to evacuate their homes because there was severe structural damage due to the earthquake. Suppose one is evaluating the benefits of retrofitting water tanks to residents in the area. Then one should eliminate any homes where evacuation would be required even if the was no disruption of water. Otherwise, one would be overstating the benefits from retrofitting the water tanks in the East Bay area.

This analysis of the residential sector in the East Bay area illustrates the type of calculations one would make to evaluate the expected benefits of mitigation. Turning to business interruption losses from an earthquake, a similar analysis to the one in Shelby County is being undertaken with EBMUD in northern California to evaluate the impact of mitigation on this sector. Combining both the residential displacement costs and business interruption, one could undertake a more comprehensive CBA, determining under what circumstances the proposed mitigation will be most cost-effective.

Making CBA Useful for Policy Analysis

The above examples are only illustrative as to how CBA can be used, rather than how it is actually applied to either Shelby County, Tennessee or Alameda and Contra Costa counties, California. For CBA to be a useful tool for policy analysis in a specific region, one must have the most accurate data available for the analysis and keep the interested parties' priorities in mind. For this reason, we have been working very closely with personnel at EBMUD to ensure that our analysis of their water supply is a meaningful one.

Our intention is to undertake a sufficiently rich analysis of how mitigation can be utilized for particular lifeline systems, such as the EBMUD water distribution system. Unless key decision makers can appreciate the role CBA can play in determining whether to implement specific mitigation measures, this methodology may have some theoretical interest but no practical importance.

The task of making CBA a useful methodology is a challenging one. It requires bringing together scientists and engineers with social scientists to analyze a problem. It requires one to articulate the nature of the uncertainties associated with the recurrence interval of earthquakes of different magnitudes, as well as the confidence intervals surrounding the expected benefits and costs of different alternative strategies. In a nutshell, it requires the integration of science with policy.

The data and techniques are now available to undertake this type of integration with respect to earthquake mitigation. The challenge is to present the analyses to decision makers so they are willing to defend the proposed recommendation because it makes economic sense to them while satisfying their political concerns. Cost-benefit analysis provides a framework for accomplishing this important task.

Endnotes

[1] Of course, the public utility or private sector organization operating the lifeline facility may raise its rates to reflect the additional cost of the mitigation measure. In this sense, all the users of the facility bear the costs of loss prevention.

[2] http://mceer.buffalo.edu/publications/bulletin/96/02/apr96nb.html.

[3] This type of mitigation was chosen, based on discussions with Masanobu Shinozuka and insight from the annual MCEER conference in November 1999.

[4] This methodology does consider that a proportion of displaced residents will stay with friends or family rather than seek publicly-funded shelters.

References

ATC-25, 1991, *Seismic Vulnerability and Impact of Disruption of Lifelines in the Conterminous United States*, Applied Technology Council, Redwood City, California.

Atkinson, G. et al., 2000, "Reassessing New Madrid." *2000 New Madrid Source Workshop*, http://www.ceri.memphis.edu/usgs/pubs.shtml.

Boardman, A., Greenberg, D., Vining, A., and Weimer, D., 2001. *Cost-Benefit Analysis: Concepts and Practice (2nd Edition),* Upper Saddle River, New Jersey: Prentice Hall.

Chang, S., Rose, A., Shinozuka, M., Svekla, W.D., and Tierney, K., 2000. *Modeling Earthquake Impact on Urban Lifelines Systems: Advances and Integration*. Research Report, Multidisciplinary Center for Earthquake Engineering Research, Buffalo, New York.

Chung, R.M., Jason, N.H., Mohraz, B., Mowrer, F.W, and Walton, W.D., (eds.), 1995. *Post-Earthquake Fire and Lifelines Workshop: Long Beach California, January 30-31, 1995 Proceedings*, NIST Special Publication 889, U.S. Department of Commerce.

Homer, G. and Goettel, K., 1994. *Economic Impacts of Scenario Earthquakes,* Final Report for East Bay Municipal Utility District.

Kleindorfer, P. and Kunreuther, H., 1999, "The Complementary Roles of Mitigation and Insurance in Managing Catastrophic Risks." *Risk Analysis,* 19:727-38.

NIBS, 1997. *HAZUS: Hazards U.S.: Earthquake Loss EstimationMethodology*, National Institute of Building Sciences, NIBS Document Number 5200.

Red Cross, 2000. Phone conversation with Garrett Nanninga, American Red Cross National Headquarters, 28 July 2000.

Shinozuka, M., Rose, A. and Eguchi, R. (eds.), 1998, *Engineering and Socioeconomic Impacts of Earthquakes: An Analysis of Electricity Lifeline Disruption in the New Madrid Area,* Monograph No. 2, Multidisciplinary Center for Earthquake Engineering Research, Buffalo, New York.

Shinozuka, M., Cheng, T.-C., Feng, M., and Mau, S.-T., 2000. *Seismic Performance Analysis of Electric Power Systems,* Research Report, Multidisciplinary Center for Earthquake Engineering Research, Buffalo, New York.

Shinozuka, M., Grigoriu, M., Ingraffea, A.R., Billington, S.L., Feenstra, P., Soong, T., Reinhorn, A., and Maragakis, E., 2000. *Development of Fragility Information for Structures and Nonstructural Components,* Research Report, Multidisciplinary Center for Earthquake Engineering Research, Buffalo, New York.

Retrofit Strategies For Hospitals in the Eastern United States

by George C. Lee, Mai Tong and Yasuhide Okuyama

Research Objectives

This paper describes an approach used to develop retrofit strategies for hospitals and other critical facilities in low to moderate seismic hazard zones, where strong earthquakes are infrequent, but if they should occur, the consequences would be high. Hospitals in New York State and other urban centers in the eastern U.S. fall into this category, where seismic retrofit requires information on the impact of losing medical services after a destructive earthquake. A team of MCEER researchers is currently developing an approach to address this task. It is a truly multidisciplinary effort, with team members from a variety of disciplines including engineering, seismology, structural dynamics, risk and reliability analysis, manufacturing process engineering, computer simulation, urban and regional planning, and economics. When this research task is completed, it will be united with MCEER's general hospital project to develop seismic retrofit strategies.

A major MCEER research thrust is the development of retrofit strategies for critical facilities. By fostering team efforts, the research is focused on comprehensive protection of emergency medical service function of hospitals in the event of a destructive earthquake. This research requires system integrated studies involving earthquake hazards, fragilities of all structural and nonstructural components and systems, as well as human services provided by medical and support staff, and impact and benefit-cost analyses. Experiences and approaches developed from the hospital projects will then be extended to seismic retrofit of other critical facilities such as communication centers or manufacturing complexes.

MCEER's hospital retrofit research program addresses two specific types of seismic hazard locations. The first is for hospitals located in regions with frequent and/or high seismic hazard levels such as many communities in California where retrofit is required by law. The second type of hospitals are those located in regions with low seismic hazard levels where earthquakes have a very long return period but the structures and contents are likely to be damaged when earthquakes do occur.

Sponsors

National Science Foundation, Earthquake Engineering Reseach Centers Program

Research Team

George C. Lee, *Director, Multidisciplinary Center for Earthquake Engineering Research, and Samuel P. Capen Professor of Engineering,* ***Apostolos Papageorgiou****, Professor, and* ***Mai Tong****, Senior Research Scientist, Department of Civil, Structural and Environmental Engineering, University at Buffalo*

Li Lin*, Associate Professor, Department of Industrial Engineering, University at Buffalo*

Yasuhide Okuyama, *Assistant Professor and* ***Ernest Sternberg****, Associate Professor, Department of Architecture and Planning, University at Buffalo*

Masanobu Shinozuka*, Fred Champion Chair in Civil Engineering, Department of Civil Engineering, University of Southern California*

Collaborative Partners

- *State of New York Department of Health, Bureau of Architectural and Engineering Facility Planning, Troy, New York*
- *Columbia Presbyterian Medical Center, New York, New York*
- *Erie County Medical Center, Buffalo, New York*

For the first type of hospitals (e.g., those in California) a considerable amount of engineering and social science studies are being carried out by MCEER and other researchers (for example, see Johnson et al., 1999). Relatively little information is available on how to approach hospitals located in low seismic hazard regions but having high risks (e.g., those located in eastern U.S. urban centers). This article briefly summarizes MCEER's approach in developing retrofit strategies for the latter, with an emphasis on establishing an evaluation system for retrofit strategies.

Different Questions Asked for California and New York Hospitals

Because of California Law SB1953 (Alquist Act), California hospital administrators and code writing authorities are required to consider the nature of functional design for critical care facilities. OSHPD (California Office of Statewide Health Planning and Development), which is directed by SB1953 to address and implement the legal requirements, now requires that by January 1, 2030, all hospital buildings will meet the seismic standards of the Hospital Act. Also, OSHPD is in the stage of writing the implementation procedures required by SB1953 for the nonstructural provisions. Under such legal requirements, the challenges for California are largely focused on engineering tasks.

In areas of the eastern U.S. such as New York City, hospital retrofit decisions are made based on different considerations. In particular, given that only limited financial resources are available for protection from various natural hazards of approximately the same level of probability of occurrence, retrofit decisions become an optimal risk management issue. For these two different conditions, we may thus begin by asking two different questions for the MCEER hospital project.

For California hospitals:

- How can the requirements to retrofit be met cost-effectively?

For New York hospitals:

- Should resources be allocated for the seismic retrofit of hospitals?

MCEER's hospital project is divided into two separate aspects in their initial phase. For the more general situation (represented by California hospitals), major efforts are devoted to engineering activities to establish fragility information for the physical components and systems, and identify critical problem areas in structures, nonstructural

Hospital administrators, building owners and other stakeholders in regions of minor to moderate seismicity can use the evaluation system for retrofit strategies to make optimal risk management decisions. Resources for hazard mitigation of all types are limited, and a decision-making method based on solid cost-benefit principles will be a valuable tool.

components, equipment, etc. that require seismic retrofit. For the second situation (represented by hospitals in the eastern U.S.), we concentrate on establishing a decision-making method which can provide information on the impact to the community if medical service function is lost after an earthquake due to different levels of damage scenarios to the various required service functions of the hospital. Once a decision is made to perform seismic retrofit, the process will be merged with that developed for the California hospitals. At that point, we consider impact to the community when there are multiple hospitals, followed by benefit-cost analyses for different possible retrofit options.

System Evaluation for Hospitals in New York

We envision a five-step decision-making process for the seismic retrofit of hospitals. These steps are:

1. Establish earthquake hazard
2. Develop fragility information and identify critical problem areas in the physical system
3. Establish an analysis tool (hospital operation model) to carry out evaluation of selected seismic scenarios to determine their impacts to medical services of a given hospital
4. Carry out community impact analyses (multiple hospitals/health care facilities)
5. Perform benefit-cost analysis and determine retrofit options.

For a free-will decision, the third step is crucial because the retrofit benefit has to be evaluated in comparison to those of other competing projects for limited resources.

Being aware of this important link, MCEER is concentrating on the third step by working with several hospitals in New York State. These hospitals are located in Seismic Zone C (Z = 0.15), where earthquakes with magnitude ≥4.5 or intensity ≥VI have been experienced historically.

For the purpose of evaluating various natural hazard reduction schemes, we start to develop a hospital operation model based on patient flow as shown in Figure 1.

If hospital services are considered as a process, the key element in this patient-flow model is the center block that describes the process of how patients receive their medical services. The services are supported by two types of resources: human

Links to Current Research

Program 2: Seismic Retrofit of Hospitals

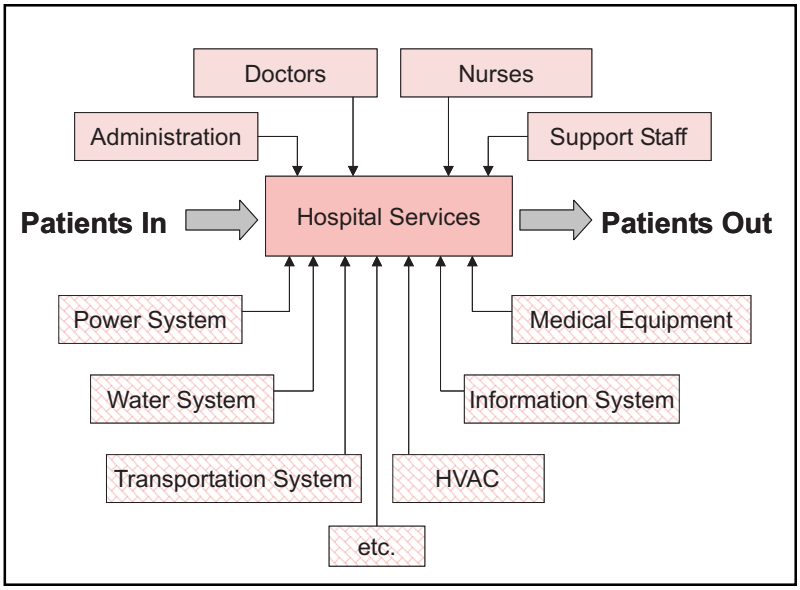

Figure 1. The Patient Flow Model of a Hospital

and material. Since our target is to evaluate the benefits of structural/nonstructural retrofit, the emphasis is given to material resources, which typically include power systems, water systems, information systems, medical systems, transportation systems, HVAC and others. Depending on the designated function of hospitals (trauma center, general hospitals, special medical care, etc.), the center block will involve different service units. Our current emphasis is on modeling the emergency medical service, which is illustrated in Figure 2.

Each of the service units has internal structures and are interconnected. Therefore, modeling of the hospital operation has to consider two layers of relationships.

With the emergency medical service unit of a hospital configuration described in Figure 2, a key step of modeling is the internal relationship between various service units (departments) and the delivery of emergency medical services. In particular, some factors such as seasonality, abnormality, and patient distribution, a critical disaster event may have a different impact to these relationships. Also, to evaluate different retrofit schemes, the level of detail of the model may vary. In Figure 2, only some typical service units are indicated for the purpose of illustration. The arrows only provide examples of possible one direction patient flow. The total system would be too complicated for illustration of the concept. In general, an all-purpose comprehensive model may not be a good approach, since too many factors introduce too many uncertainties, which would eventually lead to an unreliable model.

Similar to modeling the necessary components of providing emergency medicine, the utility system such as water supply, as expressed in Figure 3, can be modeled so that the relationship among the various units can be examined (e.g., effect of damaged water pumps on the water supply). This utility model can be linked to the emergency medical service model, where consumption of water is required. Here,

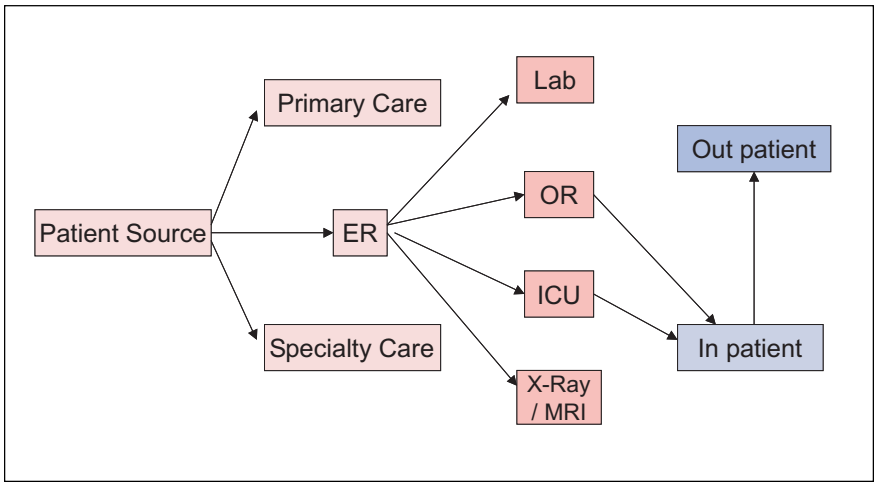

Figure 2. Hospital Medical Service Units

it is important to understand that the same utility system may be modeled differently for application to various physical problems and retrofit treatments.

Forrester Network Model

As mentioned earlier, the purpose of modeling hospital operation is to evaluate the benefit of seismic retrofit. For this reason, we need a quantitative model. This requirement can be satisfied by a Forrester type of network model. The essential steps of a Forrester model are to break down the physical units and their relations into standard input/output units and networked relations between these basic units. Then the relations are modeled by difference functions including differentiation, integration, and other elementary functions; or they could be represented by an empirical function or some logical relations.

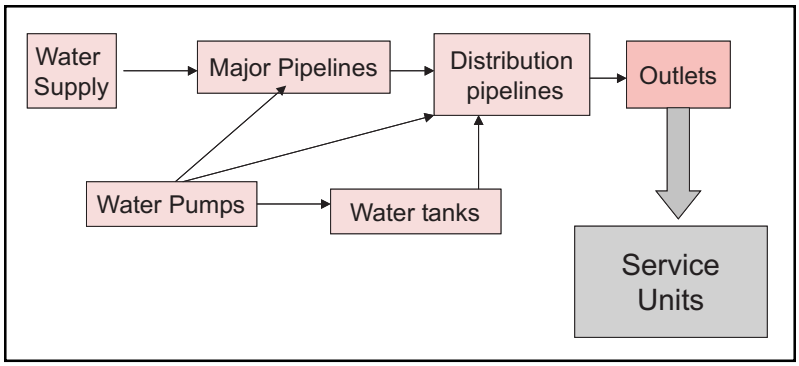

Figure 3. Water System Units

Figure 4 shows an example of Forrester-type systems model for the emergency room in a large hospital. Incoming patients are classified into three categories: minor, moderate and major injuries/illness. Patients classified as minor and moderate are attended to first, and complete an information sheet in

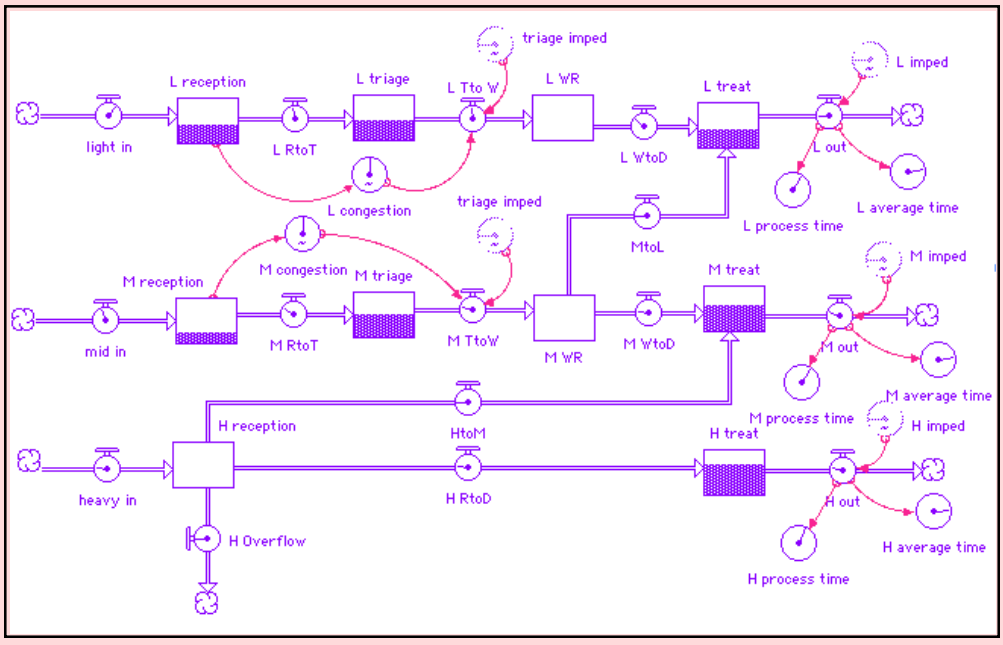

Figure 4. Forrester Type Systems Model for Emergency Room Operation

the reception area; they then proceed to the triage rooms for treatment.The time spent in this process (reception to triage) depends on the degree of injuries/illness (patients classified as "moderate" spend more time than those classified as "minor") and on the capacity of the triage rooms.Then, after the triage room, the patients proceed to the waiting room before receiving treatment. The time spent in this process (waiting room to treatment room) also depends on the degree of injuries/illness and the capacity of treatment rooms for minor and moderately injured patients. On the other hand, a severely injured patient skips the triage process, due to the urgency of their injuries/illness, and the information on their injuries is provided by paramedic staff.The time spent from reception to treatment for a patient classified as "major" depends on the capacity of the treatment rooms. Because this model represents only the operation of an emergency room, the patients are moved out of the model after the treatment rooms.

Once an internal disaster occurs (such as fire, water pipe broken, power outage, and so forth), the process times of the triage room and treatment room are affected and become longer depending on the damage. In order to simulate an internal disaster, the material resources of the hospital are modeled as shown in Figure 5. Internal disaster in this model can be damage to either water pipes, electric lines, medical gas pipes, emergency room structure, structure in the other areas, medical supplies in the emergency room, the inventory of medical supplies in the hospital, or any combination of these situations. The damage can be defined as a time variant function (either continuous or discrete). In general, lifeline facilities, medical gas, and medical supplies are modeled such that under normal circumstances, these resources are consumed on a per patient basis, and the inventory is filled either when consumed (water, electricity, medical gas) or when additional supplies are purchased (medical supplies). Once an internal disaster occurs, one or more of these resources sustain damage. For water, electricity, and medical gas, the piping may be damaged and they cannot be supplied as usual (reduced amount or total cut off). Then, emergency transfer from the reserve tanks (for water and medical gas) or from the hospital power generators (for electricity) compensates for the reduced supply. The capacity of these reserve emergency measures can be specified by resource. For medical supplies, when an internal disaster limits their capacity in the emergency room or damages them directly, reserve supplies can be transferred from the hospital's inventory. In conjunction with damage to lifelines and supplies, related laboratories (such as X-ray, blood test, and so on) and facilities (operating rooms, intensive care units, and so forth) in the hospital are also restricted by the internal disaster.

The impacts on these material resources are then fed back to the operation model discussed above. Due to the internal disaster and related damage, the process times of both triage and treatment rooms are affected, and become longer. Consequently, the number of patients treated in this emergency room may be reduced in a complex manner. The degree of impact to each patient (classified as minor,

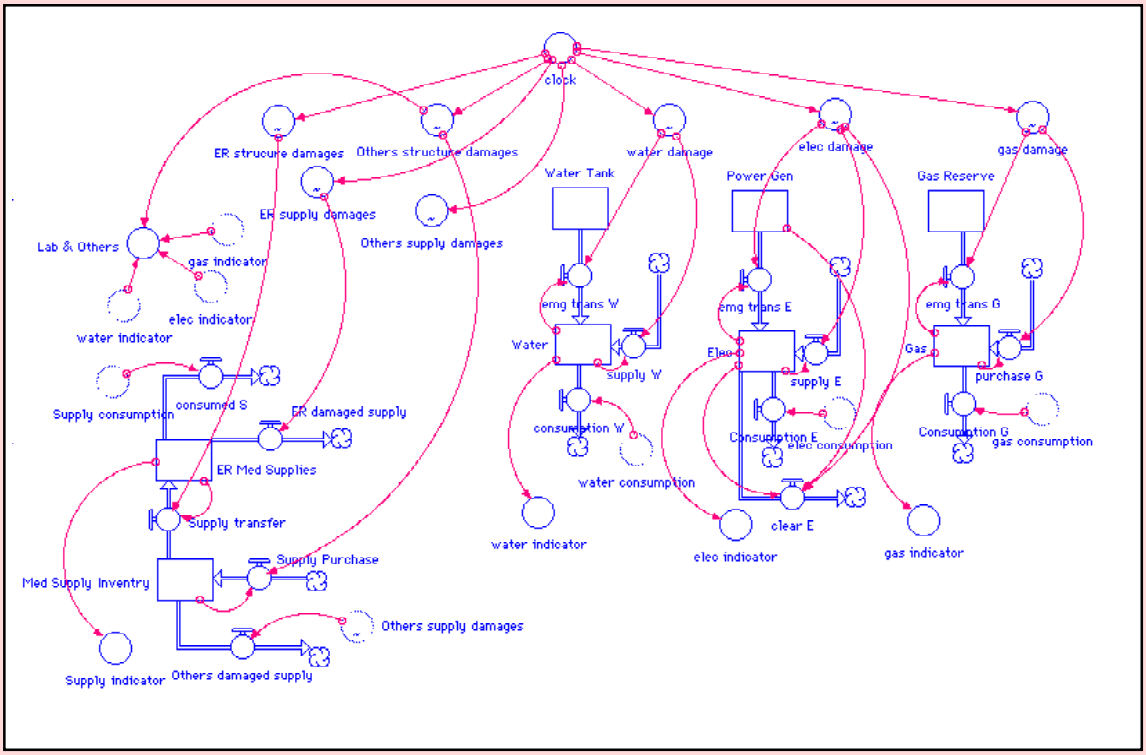

Figure 5. Sub-Model of Material Resources for Internal Disaster

moderate or major) may vary due to the different requirements for treatment (for example, a patient with major injuries requires more electricity, medical gas, and medical supplies than less seriously classified patients).

This model can be tailored for a specific hospital with information regarding the capacity of the emergency room and hospital, and the size of its emergency reserve of resources. The model can simulate patient flows through the emergency room under any scenario of internal disaster, external disaster, or a combination of both. The model can also provide statistics, such as average treatment time, average time spent in the waiting room, and so forth.

Transfer Function and State-Space Models

A Forrester type of network model is convenient for modelers, but it is not easy to carry out system analysis and evaluation. Fortunately, we have several other analytical models which are equivalent to the time domain network model. Two of the most useful equivalent models are the transfer function model and state-space model. For these models, many available control theoretical analyses can be applied. For instance, the zero-pole analysis for transfer function analysis may help us to understand the frequency domain characteristics of the modeled system. Several impact response pa-

rameters such as arising time, adjusting time, peak response time and PO% (percentage overshoot) may provide a quantitative measure of the hospital performance under a sudden hazard event.

For instance, consider an earthquake event which results in a sudden increase of in-flow patient rate and simultaneous damage to some utility systems. With the shortage of medical staff, water and power supply, the medical services of the hospital will be reduced while patients are arriving at a much higher rate. The rising time indicates how quickly the hospital capacity will be saturated. Adjusting time reveals how long the services delay problem will last. The peak response time indicates when the worst case will be and PO% describes how bad the situation could be. With these evaluations, we may be able to determine how much service loss will be from the event. Consequently, the value of a retrofit will be evaluated against the chance of the risk and the associated potential loss.

Conclusion

Based on information supplied to us from the hospitals in New York, we are in the process of establishing these models. It is our intention to examine the dynamic behavior of the emergency medicine unit of the hospitals under prescribed hazard conditions and damage scenarios, and eventually to develop a cost vs. risk evaluation procedure leading to decision-making support for seismic retrofit.

Some pertinent references concerning retrofit strategies for hospitals are provided.

References

Chong, W.H. and Soong, T.T., *Sliding Fragility of Unrestrained Equipment in Critical Facilities*, Technical Report MCEER-00-0005, University at Buffalo, July 2000.

Coyle, R.G., *Management System Dynamics*, John Wiley & Sons, 1977.

Forrester, J.W., *Industrial Dynamics*, The MIT Press, 1980.

Johnson, G.S., Sheppard, R., Quilici, M.D., Eder, S.J., and Scawthorn, C. R., *Seismic Reliability Assessment of Critical Facilities: A Handbook, Supporting Documentation, and Model Code Provisions*, Technical Report MCEER-99-0008, University at Buffalo, April 1999.

Roth, C., "Logic Tree Analysis of Secondary Nonstructural Systems with Independent Components," *Earthquake Spectra*, Vol. 15, No. 3, 1999.

Shinozuka, M., Grigoriu, M. (Coordinating Author), Ingraffea, A.R., Billington, S.L., Feenstra, P., Soong, T.T., Reinhorn, A.M. and Maragakis, E., "Development of Fragility Information for Structures and Nonstructural Components," *MCEER Research Progress and Accomplishments*, May 2000.

Soong, T.T. (Coordinating Author), Yao, G.C., and Lin, C.C., "Damage to Critical Facilities Following the 921 Chi-Chi, Taiwan Earthquake," *MCEER Research Progress and Accomplishments*, May 2000.

Zhu, Z. and Soong, T.T., "Toppling Fragility of Unrestrained Equipment," *Earthquake Spectra*, Vol. 14, No. 4, 1998.

Passive Site Remediation for Mitigation of Liquefaction Risk

by Patricia M. Gallagher and James K. Mitchell

Research Objectives

Passive site remediation is a new concept proposed for non-disruptive mitigation of liquefaction risk at developed sites susceptible to liquefaction. It is based on the concept of slow injection of stabilizing materials at the edge of a site and delivery of the stabilizer to the target location using the natural groundwater flow. Stabilizer candidates need to have long controllable gel times and low viscosities so they can flow into a liquefiable formation slowly over a fairly long period of time. Colloidal silica is a potential stabilizer for passive site remediation because at low concentrations it has a low viscosity and a wide range of controllable gel times of up to about 200 days. Loose sands treated with colloidal silica grout had significantly higher deformation resistance to cyclic loading than untreated sands. Groundwater and stabilizer transport modeling were done to determine the range of conditions where passive site remediation might be feasible. For a 200-foot by 200-foot treatment area with a single line of injection wells, it was found that passive site remediation could be feasible in formations with hydraulic conductivity values of 0.05 cm/s or more and hydraulic gradients of 0.005 and above.

At many sites susceptible to liquefaction, the simplest way to mitigate the liquefaction risk is to densify the soil. For large, open and undeveloped sites, the easiest and cheapest methods for densification are by "traditional" procedures such as deep dynamic compaction, explosive compaction, or vibrocompaction. However, at constrained or developed sites, ground improvement by densification may not be possible due to the presence of structures sensitive to deformation or vibration. Additionally, access to the site could be limited and normal site use activities could interfere with mitigation activities. At these sites, the most common methods for remediation are grouting or underpinning. Passive site remediation is a new concept proposed for non-disruptive improvement of developed sites susceptible to liquefaction. Passive site remediation is based on the concept of the slow injection of stabilizing materials at the up gradient edge of a site and delivery of the stabilizer to the target location using the

Sponsors

National Science Foundation, Earthquake Engineering Research Centers Program

Research Team

Patricia M. Gallagher,
Assistant Professor, Department of Civil and Architectural Engineering, Drexel University, Former Graduate Assistant, Department of Civil Engineering, Virginia Polytechnic Institute and State Universtity

James K. Mitchell,
University Distinguished Professor Emeritus, Department of Civil Engineering, Virginia Polytechnic Institute and State University

Collaborative Partners

- ***Mr. Chris Gause*** *of Master Builders contributed materials for laboratory testing of microfine cement grouts and expertise on grouting technology.*
- ***Dupont*** *provided some of the colloidal silica used in the experimental program.*
- ***Dr. Ernst Ahrens****, Sandia National Laboratory and* ***Mr. Henry Pringer****, Blue Circle, contributed cement for testing.*

natural or augmented groundwater flow. The concept is illustrated in Figure 1.

The set time of the stabilizer would be controlled so there would be adequate time for it to reach the desired location beneath the site prior to gelling or setting. If the natural groundwater flow were inadequate to deliver the stabilizer to the right place at the right time, it could be augmented by use of low-head injection wells or downgradient extraction wells. Once the stabilizer reached the desired location beneath the site, it would gel or set to stabilize the formation.

Passive site remediation techniques could have broad application for developed sites where more traditional methods of ground improvement are difficult or impossible to implement. It would be less disruptive to existing infrastructure and facilities than existing ground improvement methods. Additionally, access to the entire site would be unnecessary using this technology, and normal site use activities would probably not need to be disrupted. Finally, excessive deformation and disturbance of the ground around and beneath existing structures could be avoided.

The objective of this study was to establish the feasibility of passive site remediation. The work included identification of stabilizing materials, a study of how to adapt or design groundwater flow patterns to deliver the stabilizers to the right place at the right time, and an evaluation of potential time requirements and costs.

Performance Criteria and Identification of Potential Stabilizers

For a stabilizer to work in this application, it should have a low viscosity and a long induction period between mixing and the onset of gelation. Once gelation starts, it should proceed rapidly. The stabilizer should also be permanent, nontoxic and cost-effective. Materials evaluated as potential stabilizers included colloidal silica, microfine cement grouts, chemical grouts, zero-valent iron, and ultramicrobacteria. Colloidal silica was selected as a potentially suitable stabilizing material because it has a wide range of gel times and a low viscosity. Colloidal silica is an aqueous suspension of tiny silica particles that can be made to gel

Passive site remediation is a new technology for mitigation of liquefaction and ground failure risk at developed and inaccessible sites where more traditional methods for ground improvement are not suitable. Slow permeation of chemical soil stabilizer beneath and around foundations on and in potentially liquefiable soils should be especially attractive to owners, engineers, and planners who are charged with assuring seismic safety of existing infrastructure.

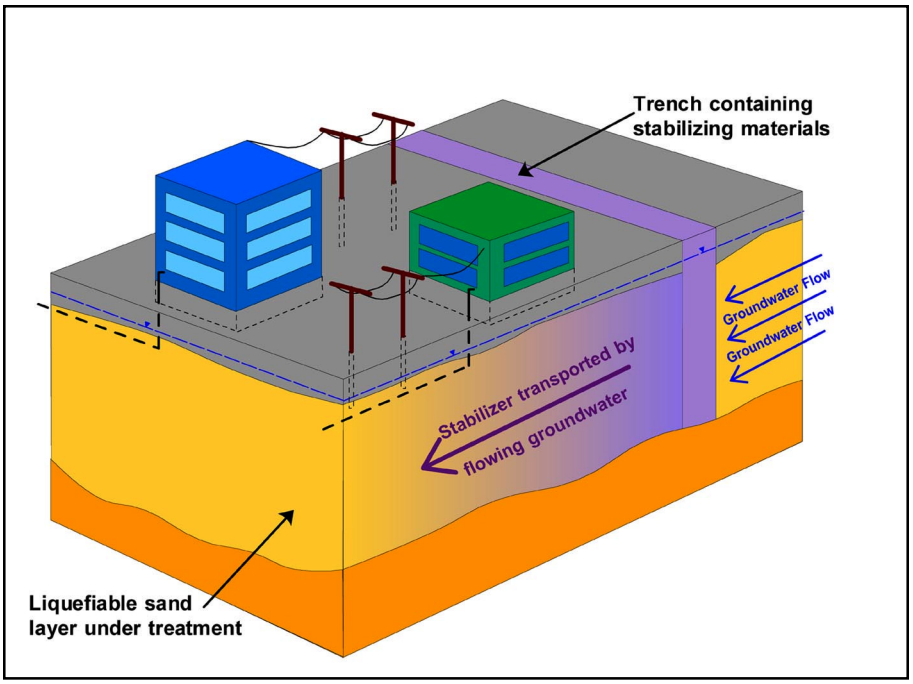

Figure 1. Passive treatment for mitigation of liquefaction risk.

by adjusting the pH or the salt concentration of the solution. Gel times of more than 200 days have been measured in laboratory tests. Additionally, the initial viscosities of dilute solutions of colloidal silica are about 2 centipoise (water=1 cP) and the viscosities remain very low for most of the induction period.

Microfine cement grout was eliminated because its viscosity is too high to meet the necessary requirements for passive site remediation. Additionally, since cement grouts are particulate suspensions, the particles tend to settle in the suspension and further increase the viscosity. Numerous chemical grouts were considered. All were eliminated as potentially suitable stabilizers, but for different reasons. Sodium silicate was eliminated because gel time is not well controlled at long gel times. Additionally, the chemical durability of sodium silicate formulations with long gel times is questionable. Acrylamide is a neurotoxin in powdered form, so it was eliminated due to environmental, safety, and handling concerns. Additionally, it is very expensive. Acrylate was eliminated due to durability concerns. Epoxy and polysiloxane were rejected because they are very expensive. Zero-valent iron is extremely sensitive to oxidation and reduction, so it would be difficult to treat a large area and the minerals precipitated would probably not be chemically durable. Ultramicrobacteria might be able to clog the pores of a formation with a biofilm, but biofilms can be dissolved by strong oxidants such as bleach, so there are durability concerns.

Feasibility

The feasibility of passive site remediation depends on the answers to the following questions:

Program 2: Seismic Retrofit of Hospitals

- *Task 2.3, Geotechnical Rehabilitation Site and Foundation Remediation*
- *Task 2.6, MEDAT-2 Workshop on Mitigation of Earthquake Disaster by Advanced Technologies*

1. Will the colloidal silica grout adequately stabilize the soil?
2. Can the stabilizer be delivered to the liquefiable formation and achieve adequate coverage within the induction period of the grout?
3. How much will it cost?

Strength testing of stabilized sands was done to address the first issue. Groundwater and stabilizer transport modeling were done to determine if the stabilizer could be delivered to the formation within the induction period of the grout. Finally, a preliminary cost analysis was done to address the final issue.

Strength Testing of Stabilized Sands

Cyclic triaxial tests were done on Monterey No. 0/30 sand samples treated with colloidal silica grout to investigate the influence of colloidal silica grout on the deformation properties of loose sand (relative density, Dr = 22%). The grain size distribution of Monterey No. 0/30 sand is shown in Figure 2. Distinctly different deformation properties were observed between grouted and ungrouted samples. Untreated samples developed very little axial strain after a few cycles of loading and prior to the onset of liquefaction. However, once liquefaction was triggered, large strains occurred rapidly and the samples collapsed within a few additional cycles. In contrast, grouted sand samples experienced very little strain during cyclic loading. What strain accumulated did so uniformly throughout loading and the samples remained intact after cyclic loading.

An example is shown in Figure 3 for two samples at a relative density of 22 percent that were tested at a cyclic stress ratio of 0.27. The cyclic stress ratio is defined as the ratio of the maximum cyclic shear stress to the initial effective confining stress. The untreated sample strained 1 percent in 11 cycles and collapsed in 13 cycles. The sample treated with 10 weight percent colloidal silica was tested for 400 cycles. It strained less than about half a percent in 11 cycles, about 8 percent in 400 cycles, and never collapsed. Only the first 40 loading cycles are shown in Figure 3. These results are typical for samples treated with 10 percent colloidal silica by weight. For comparison, a magnitude 7.5 earthquake would be expected to generate about 15 uniform stress cycles.

Samples stabilized with concentrations of 15 and 20 weight percent colloidal silica experienced very little (less than two percent) strain during cyclic loading. Sands stabilized with 10 weight percent colloidal silica resisted cyclic loading well, but experienced slightly more (up to eight percent) strain. Overall, treatment with colloidal silica grout significantly increased the deformation resistance of loose sand to cyclic loading.

Groundwater and Stabilizer Transport Modeling

Stabilizer delivery is the main feasibility issue with respect to passive site remediation. Preliminary groundwater and solute transport modeling were done using the codes MODFLOW, MODPATH, and

MT3DMS for a generic liquefiable formation. A "numerical experiment" was done to determine the ranges of hydraulic conductivity and hydraulic gradient where passive site remediation might be feasible. For a 200-foot by 200-foot treatment area, with single lines of injection and extraction wells, travel times through the treatment area will be about 100 days or less if a formation has a hydraulic conductivity greater than about 0.05 cm/s and a hydraulic gradient higher than about 0.005. Based on the possible gel times, this time frame is considered feasible. Extraction wells will increase the speed of delivery and help control the down gradient extent of stabilizer movement.

The results of solute transport modeling indicate that stabilizer delivery will vary throughout the treatment area. A typical stabilizer contour plot for a hypothetical formation with a uniform hydraulic conductivity of 0.05 cm/s and a hydraulic gradient of 0.005 is shown in Figure 4. A stabilizer concentration of 100 g/l would be delivered through an infiltration trench for 100 days. The best coverage would be achieved close to the source of the stabilizer. Concentrations would decrease laterally away from the source and down gradient of the source. If the minimum amount of stabilizer required for adequate stabilization could be delivered to the majority of the treatment area, it is likely that the formation would be stable enough to withstand seismic loading. However, there could be some differential or variable response across the site. It may be necessary to deliver a higher concentration at the up gradient edge of the treatment area

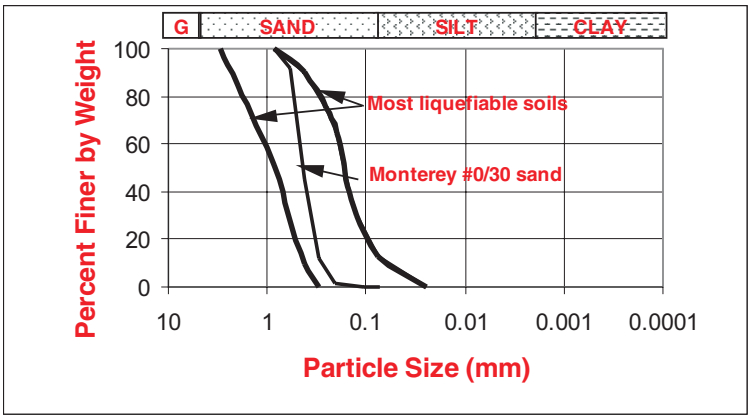

Figure 2. Gradation curve for Monterey No. 0/30 sand.

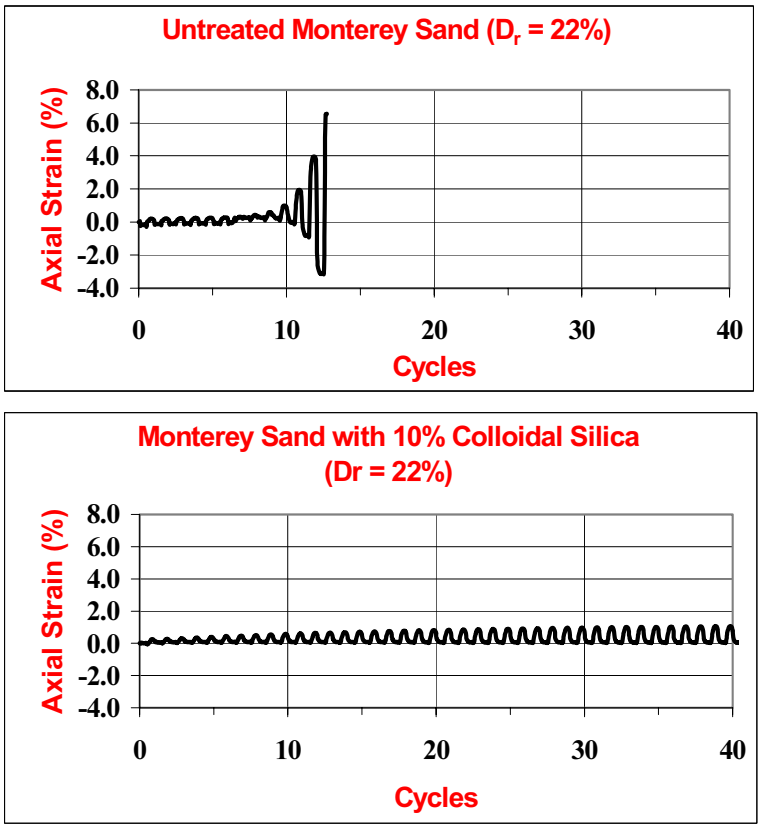

Figure 3. Axial deformation during cyclic loading (CSR=0.27) for treated and untreated sand.

in order to get an adequate concentration at the down gradient edge.

Heterogeneity in the formation will actually control how well the stabilizer can be delivered. If the formation is highly variable, then the stabilizer concentration will vary from point to point within the formation. An example stabilizer contour profile through a treatment area with a variable hydraulic conductivity is shown in Figure 5. In this case, the hydraulic conductivity was varied slightly in each layer as shown for a total variation throughout the layer of about one order of magnitude. The remainder of the simulation is the same as the previous case. The layers with higher hydraulic conductivity have a higher concentration at the down gradient edge. These layers would probably be more stable than layers with lower hydraulic conductivity that receive a lower concentration of grout during the treatment period. However, even if the regions of lower hydraulic conductivity liquefy, the presence of very stable seams will likely lessen the severity of the overall deformation. Accurate characterization of the hydraulic conductivity throughout the treatment area will be essential for successful treatment by passive site remediation.

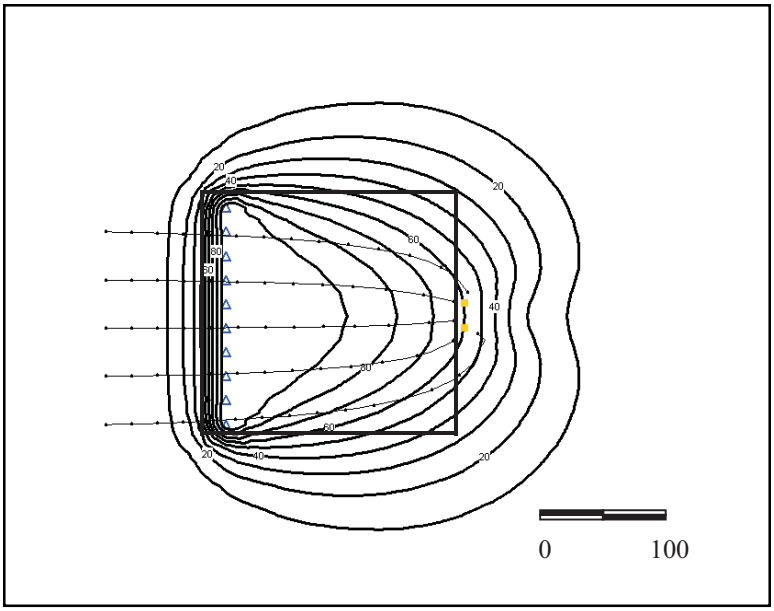

■ Figure 4. Stabilizer contours for 200 ft. by 200 ft. treatment area (outlined in black) after 100 days of treatment. Stabilizer delivered through infiltration trench at concentration of 100 g/l. Two extraction wells at the down gradient edge withdraw a total of 7500 cfd. Contour intervals are 10 g/l. Concentration at extraction wells is 60 g/l. Travel paths for individual water particles are superimposed over the treatment area in 10-day increments. Particle travel times are about 75 to 80 days.

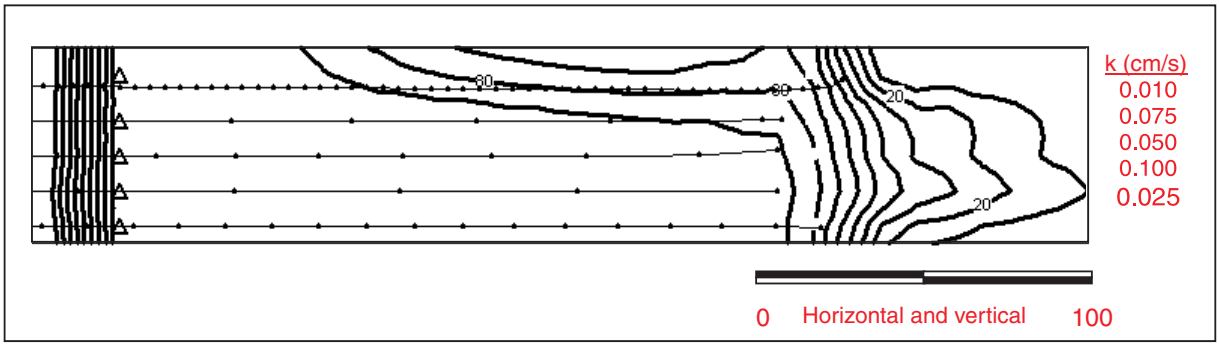

■ Figure 5. Stabilizer profile through centerline of 200 ft. by 200 ft. treatment area after 100 days of treatment. Stabilizer delivered through infiltration trench at concentration of 100 g/l. Extraction wells at the down gradient edge withdraw a total of 7500 cfd. Contour intervals are 10 g/l. Concentration at extraction wells is about 70 g/l in lower 30 ft. Travel paths for individual water particles are superimposed over the treatment area in 10-day increments. Particle travel times range from about 40 to 420 days.

Cost

The cost of passive site remediation is expected to be comparable to other methods of chemical grouting. It is likely that a 10 weight percent concentration of colloidal silica will be adequate to stabilize a liquefiable formation. It is possible that lower concentrations could be used. Based on a 10 percent concentration, it is expected that materials costs would be in the range of $120 to $180 per cubic meter of treated soil. These costs are competitive with other methods of chemical grouting.

Conclusion

Based on the feasibility analysis, passive site remediation appears to be a promising new concept for mitigation of liquefaction risk. At this time, a minimum concentration of 10 percent colloidal silica appears to be suitable for stabilizing liquefiable sands. Additional testing is being done with concentrations of 5 weight percent to determine if the level of strain during cyclic loading would be acceptable.

Delivery of the stabilizer is the central feasibility issue with respect to passive site remediation. For a 200-foot by 200-foot treatment area with a single line of injection wells, it was found that passive site remediation could be feasible in formations with hydraulic conductivity values of 0.05 cm/s or more and hydraulic gradients of 0.005 and above. However, the actual concentration profile across the site will depend on the variation in hydraulic conductivity throughout the formation.

The anticipated final outcome of this work is a new technology for mitigation of liquefaction and ground failure risk. Passive site remediation technology will be less disruptive to existing infrastructure and facilities than existing methods. It is expected that passive site remediation will be cost-competitive with other methods of chemical grouting. Model testing of both the injection method and the performance of grouted ground is planned as the next step in the evaluation of this new technology. It will be done using a geotechnical centrifuge equipped with a shake table.

Advanced GIS for Loss Estimation and Rapid Post-Earthquake Assessment of Building Damage

by Thomas D. O'Rourke, Sang-Soo Jeon, Ronald T. Eguchi and Charles K. Huyck

Research Objectives

The objectives of the research are to: 1) develop regressions between building damage and various seismic parameters to improve loss estimation, 2) identify the most reliable seismic parameter for estimating building losses, and 3) develop GIS-based pattern recognition algorithms for the identification of locations with the most intense post-earthquake building damage. This latter objective is coupled to the goal of improving emergency response as part of the MCEER vision of creating earthquake resilient communities. GIS-based technologies for visualizing damage patterns provide a framework for rapidly screening remote sensing data and dispatching emergency services to the locations of greatest need.

Lifeline Damage

MCEER researchers working on the seismic retrofit and rehabilitation of lifelines (Program 1) and on seismic response and recovery (Program 3) have collaborated on a project organized to apply advanced GIS techniques for the rapid identification of locations with most intense building damage. This collaboration has resulted in the development of regressions between building damage and various seismic parameters, as well as the application of GIS-based recognition algorithms with the potential for screening remote sensing data to identify areas of highest post-earthquake damage intensity.

Using GIS technology, Cornell researchers developed the largest U.S. database ever assembled for spatially distributed transient and permanent ground deformation in conjunction with earthquake damage to water supply lifelines (O'Rourke et al., 1999). This research has helped to delineate local geotechnical and seismological hazards in the Los Angeles region that are shown by zones of concentrated pipeline damage after the Northridge earthquake. The research has resulted in regressions between repair rates for different types of trunk and distribution pipelines and various seismic parameters. The regressions are statistically reliable and have improved predictive capabilities compared with the default relationships currently used in loss estimation programs. They will be referenced in the next version of HAZUS software that implements the National Loss

Sponsors

National Science Foundation, Earthquake Engineering Research Centers Program

Research Team

***Thomas D. O'Rourke**, Thomas R. Briggs Professor of Engineering and **Sang-Soo Jeon**, Graduate Research Assistant, Department of Civil and Environmental Engineering, Cornell University*

***Ronald T. Eguchi**, President and **Charles K. Huyck**, Vice President, ImageCat, Inc.*

Collaborative Partners

- *California Office of Emergency Services (OES)*
- *Los Angeles Department of Water and Power*
- *Federal Emergency Management Agency*

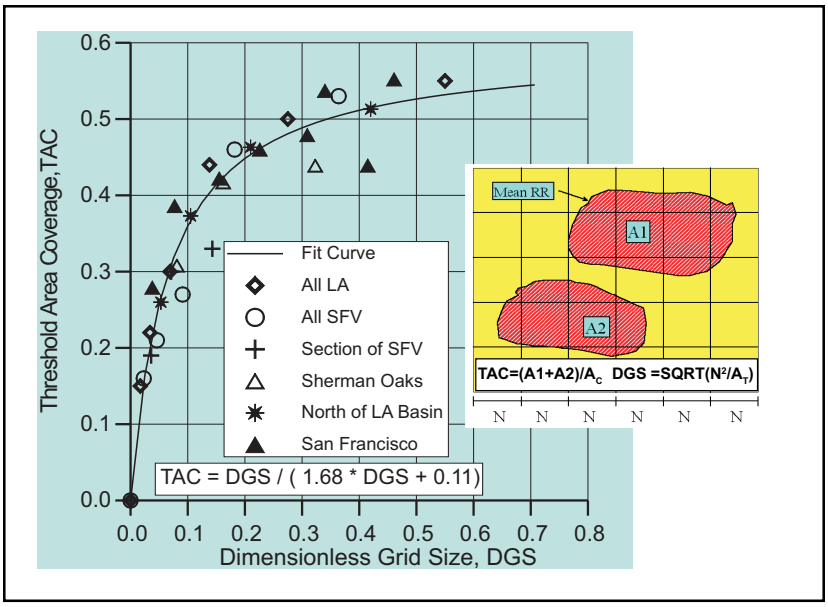

■ Figure 1. Hyperbolic Fit for Threshold Area Coverage and Dimensionless Grid Size for Pipeline Damage Patterns (Toprak, et al., 1999)

Estimation Methodology sponsored by FEMA. The regressions and statistical databases are being incorporated in pre-standards for estimating water supply losses developed by the American Lifeline Alliance through ASCE under contract with FEMA.

The research has led to the discovery of a relationship for visualizing damage patterns by linking the two dimensional representation of local damage with the grid size used in GIS to analyze the spatial distribution of data. This concept is illustrated in Figure 1, which shows the relationship developed for visualizing post-earthquake pipeline damage (O'Rourke et al., 1999).

With GIS, the spatial distribution of damage can be analyzed by dividing any map into squares, or cells, each of which is n by n in plan. A repair rate is defined as the number of repairs divided by the total distance of pipelines in each cell. Contours of equal repair rate, or damage rate, can then be drawn using the grid of equi-dimensional, n-sized cells. If the contour interval is chosen as the average repair rate for the entire system or portion of the system covered by the map, then the area in the contours represents the zones of highest (greater than average) earthquake intensity as reflected in pipeline damage.

The users of this research include two main groups: 1) water distribution companies, such as the Los Angeles Department of Water and Power (LADWP) and the East Bay Municipal Utility District (EBMUD) and 2) those who benefit from improved loss estimation, such as insurance companies, the Federal Emergency Management Agency, state and municipal planners, and emergency service providers.

A hyperbolic relationship was shown to exist between the threshold area coverage (TAC) [in this case, the fraction of the total map area with damage exceeding the overall average repair rate] and the dimensionless grid size, defined as the square root of n^2, the area of an individual cell, divided by the total map area, A_T. This relationship is illustrated in Figure 1, for which a schematic of the parameters is provided by the inset diagram. The relationship was found to be valid over a wide range of different map scales spanning 1200 km^2 for the entire Los Angeles water distribution system affected by the Northridge earthquake to 1 km^2 of the San Francisco water distribution system in the Marina affected by the Loma Prieta earthquake (Toprak et al., 1999)

As explained by O'Rourke et al. (1999), the hyperbolic relationship can be used for damage pattern recognition, and for computer "zooming" from the largest to smallest scales to identify zones of concentrated disruption. If such a relationship can be shown to be valid for building damage, then remote sensing data acquired to characterize building damage can be evaluated rapidly for the locations of highest loss intensity and thereupon targeted for emergency response.

Building Damage

Inspection records available through the California Office of Emergency Services (OES) were obtained for 62,020 buildings that were investigated after the Northridge earthquake. Of these, 48,702 buildings were associated with one and two-story timber frame structures, principally single and multiple family residences. The inspection records include location and estimate of damage as a percentage of replacement cost. Figure 2 shows the types of timber frame structures included in the database with examples of damage, as presented by the NAHB Research Center (1994). The database did not include specific information about the type of damage to each structure.

The number of one to two story timber frame structures affected by the Northridge earthquake was estimated from tax assessor records supplied through OES. The numbers of structures determined in this way was 278,662. As a check, an alternate number was estimated from 1990 census block data (Wessex, 1996) by evaluating the number of buildings associated with detached and attached single housing units in combination with the buildings needed to accommodate two and three to four housing units. The resulting number was 267,868, which is in excellent agreement with the 278,662 units estimated from tax assessor records.

Links to Current Research

Program 1: Seismic Evaluation and Retrofit of Lifeline Networks

Program 3: Earthquake Response and Recovery

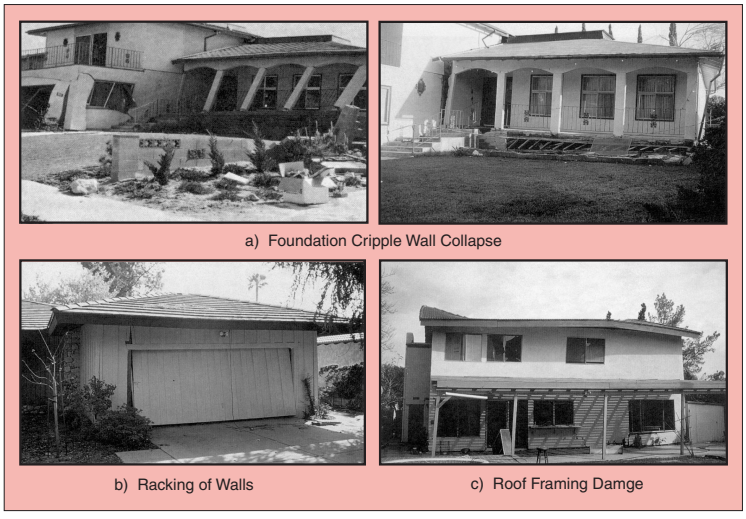

Figure 2. Typical Damage to 1-2 Story Timber Frame Buildings after the Northridge Earthquake (after NAHB, 1994)

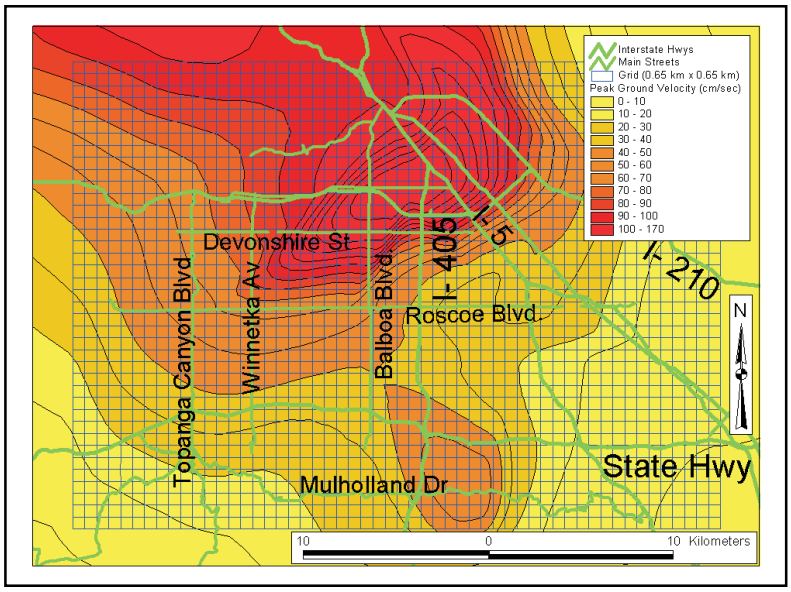

■ Figure 3. GIS Grid with Tax Assessor Data Superimposed on Peak Ground Velocities

Two damage parameters, referred to as damage ratio and damage factor, were calculated with the database. Damage ratio is the fraction or % of existing structures with damage equal to or exceeding a particular damage factor. Damage factor is damage expressed as a % of building replacement cost.

Loss Estimation Regressions

A GIS grid composed of 2,106 cells was created, and the number of relevant structures within each 0.42 km² cell was calculated and geocoded at the cell center. Figure 3 shows the GIS grid developed with tax assessor records superimposed on the spatial variation of peak ground velocity determined from more than 240 strong motion records geocoded as part of this study. By superimposing a grid in which each cell is characterized by various damage ratios linked with damage factors, linear regressions can be performed to quantify damage vs. seismic excitation for loss estimation purposes.

Figures 4a and b show the linear regression of damage ratio (DR) vs. peak ground velocity (PGV) and Spectrum Intensity (SI) for various damage factors (DF). Most regressions for PGV show excellent fits

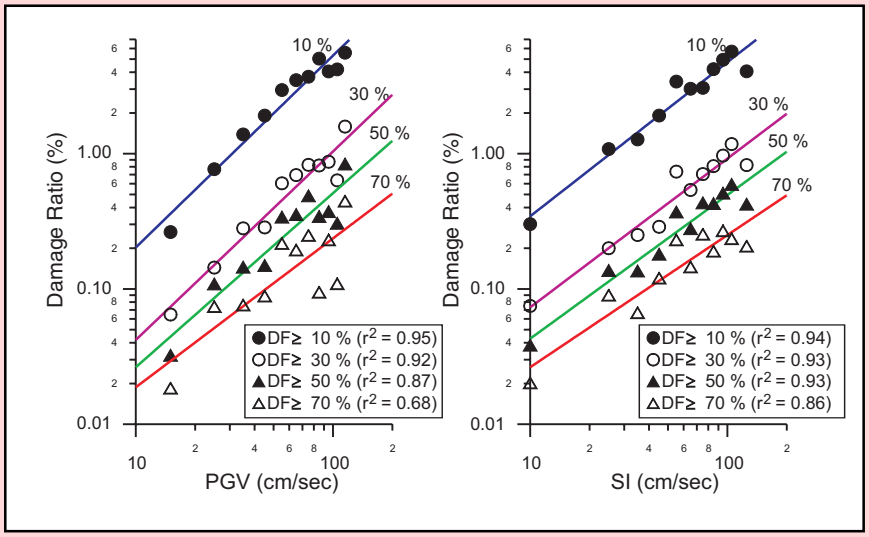

■ Figure 4. Damage Ratio Regression with Peak Ground Velocity (PGV) and Spectrum Intensity (SI) for 1-2 Story Timber Frame Buildings

as indicated by high r^2, although the "goodness" of fit is relatively low for DF ≥ 70%. In contrast, all regressions for SI have high r^2 and excellent characteristics with respect to residuals. The relationships between damage and various seismic parameters were probed in this way to determine which parameters were statistically most significant as damage predictors. The seismic parameters investigated include the measured peak ground acceleration, velocity, and displacement; spectral acceleration and velocity for periods of 0.3 and 1.0 s; Arias Intensity; and SI.

SI is defined as the area under the pseudo-velocity, SV, response spectra curve for a damping ratio, ξ of 20 % between periods, T, of 0.1 and 2.5 s:

$$SI = \int_{0.1}^{2.5} SV(T,\xi)\ DT \qquad (1)$$

SI was first proposed by Housner (1959) as a measure of the maximum stresses that would be induced in elastic structures by ground motion. Katayama et al. (1988) found that house damage correlated more strongly with SI than with peak acceleration, and recommended that SI calculations be performed for ξ = 20%.

An examination of Figure 4 reveals that DR, DF, and the seismic parameter, SP, are interrelated in a consistent way. Using multiple linear regression techniques, this interrelationship can be expressed as

$$\text{Log DR} = \text{Log K} + \alpha\,\text{Log SP} - \beta\,\text{Log DF} \qquad (2)$$

in which K, α, and β are constants. (2) can be rewritten as

$$DR = K(SP / DF^{\beta/\alpha})^{\alpha} \qquad (3)$$

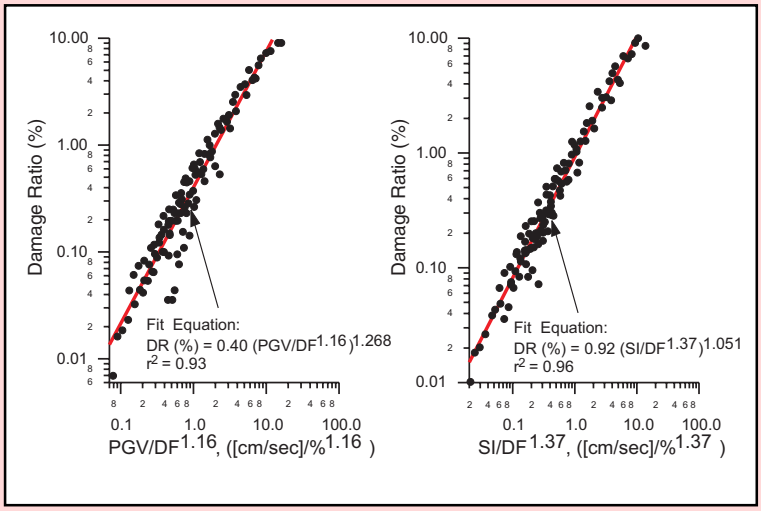

■ Figure 5. Damage Ratio Regression for Scaled PGV and SI for 1-2 Story Timber Frame Buildings

in which $(SP/DF^{\beta/\alpha})$ is the scaled seismic parameter.

Using (3), the data in Figure 4a and b are replotted in Figures 5a and b as linear regressions that account for DR, DF, and SP. As evinced by high r^2 and excellent characteristics with respect to residuals, the relationships in Figures 5a and b are statistically significant.

Seismic parameters normalized with respect to DF combine the effects of strong motion and damage level in a convenient way that facilitates loss estimation. For example, consider an area for which the predicted SI is 30 cm/sec. The % of timber structures in that area that would have damage equal to or exceeding 10% of the building replacement cost is calculated as $DR = 0.92(30/10^{1.37})^{1.051}$, or 1.19%. For damage equal to or exceeding 50% replacement cost, $DR = 0.92(30/50^{1.37})^{1.051}$, or 0.11%.

"By combining an advanced GIS with advanced remote sensing, MCEER is developing the enabling technologies for a new generation of emergency response and rapid decision support systems."

Damage Pattern Recognition

Using the same concepts that were applied to the spatial distribution of pipeline damage, investigations were undertaken to define a relationship between TAC (defined for buildings as the fraction of the total map area with DR exceeding the overall average DR) and the dimensionless grid size. The grid containing tax assessor data was sufficiently refined to evaluate the effects of progressively larger grid sizes by developing grids with cell sizes of n by n, 2n by 2n, 4n by 4n, and 8n by 8n. The data generated for these grids and various DFs are plotted in Figure 6. All relationships are well described by hyperbolic functions, similar to the one for pipeline damage in Figure 1. Because building damage is characterized by DF, it has an additional dimension when compared to the single hyperbolic curve for pipelines. In fact, Figure 6 is actually a hyperbolic surface for which the initial slopes and asymptotes vary as a function of DF.

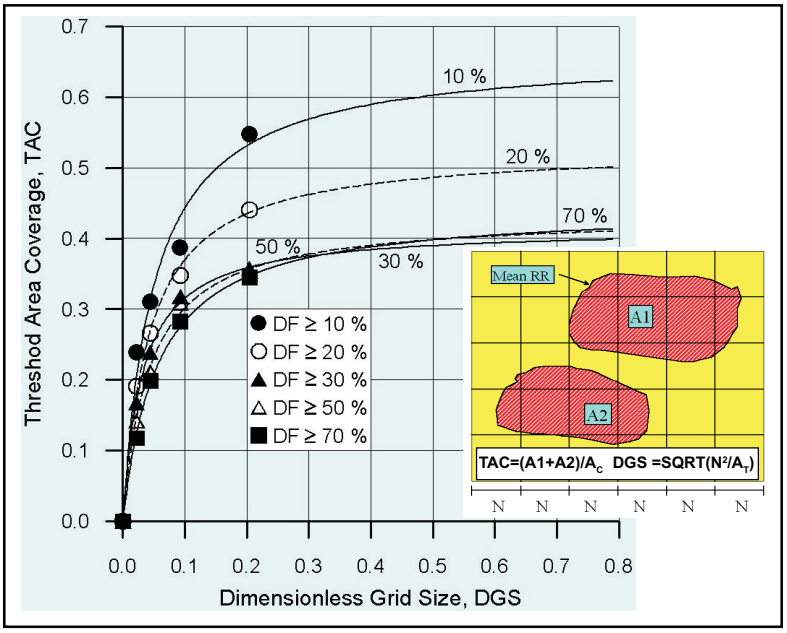

■ Figure 6 Hyperbolic Fit for Threshold Area Coverage and Dimensionless Grid Size for 1-2 Story Timber Frame Buildings

Experience has shown that the ideal TAC for visualization is about 0.33. Figure 6 indicates that the dimensionless grid size to achieve this TAC varies significantly, depending on DF.

Figure 7 illustrates the application of Figure 6 for damage intensity recognition and computer "zooming." The top map shows the entire San Fernando Valley and adjacent areas. The figure shows a cascade of different computer screens that "zoom" on increasingly smaller areas from top to bottom. Each screen shows as blue dots the actual locations of one to two story timber frame structures with DF ≥ 70% after the Northridge earthquake. The red contour lines indicate areas of highest damage intensity.

The contour lines in the top map were generated by analyzing the data with a GIS grid size chosen for TAC = 0.33 from Figure 6. The area outlined in red in the top map was identified for more detailed assessment. The grid size for this assessment was again determined for TAC = 0.33 from Figure 6. The map in the center of the figure shows an expanded view of the area outlined above after computer analysis. The zones of highest damage intensity for this new map are surrounded by red contour lines.

A similar procedure was followed for the center map in which an area for more detailed assessment was identified within the blue outline. The map at the bottom of the figure shows an expanded view of this new area in which the areas of greatest damage intensity are again surrounded by red contour lines.

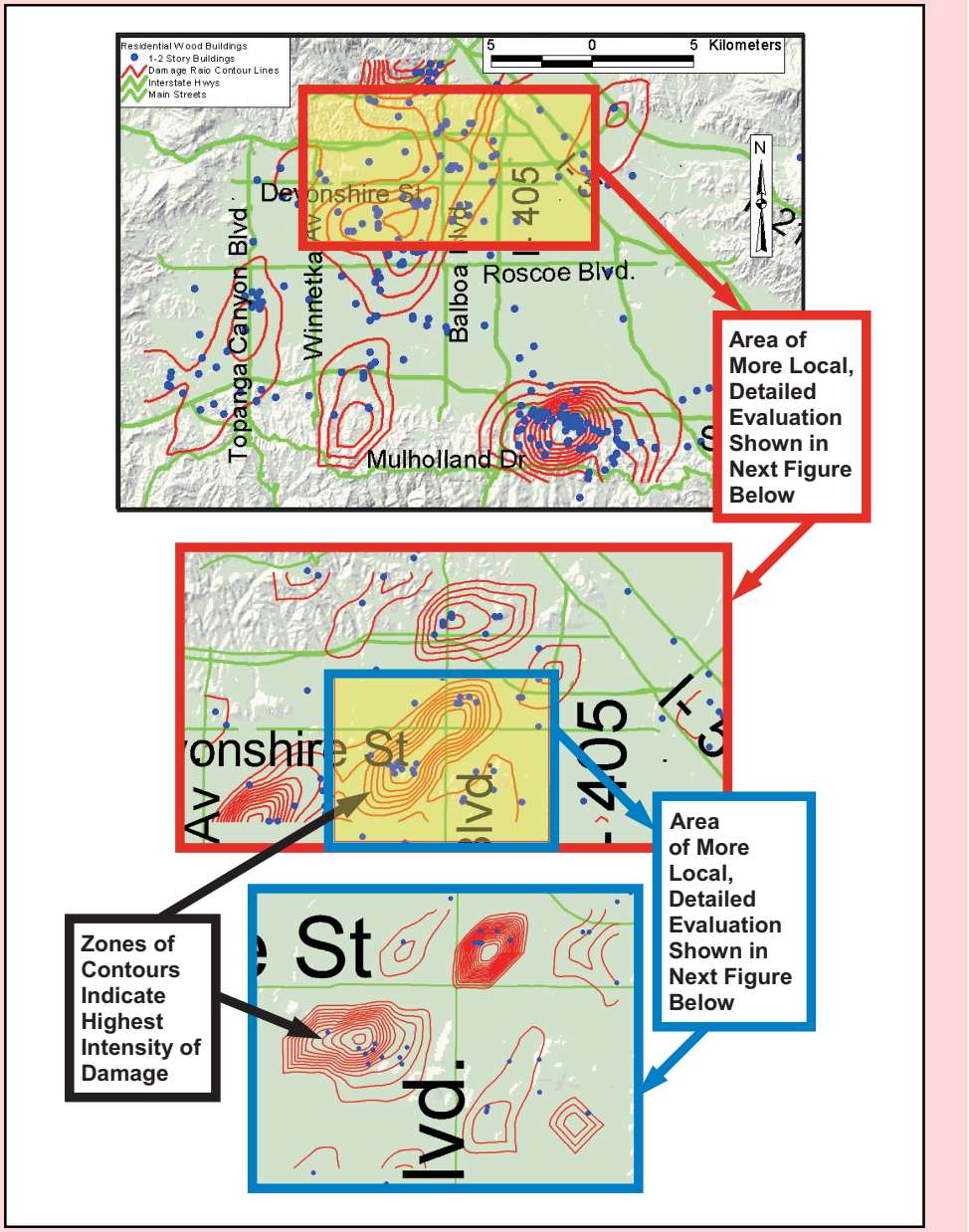

■ Figure 7. GIS Evaluation of Building Damage for DF ≥ 70 %

Increasing density of contour lines reflects increasing intensity of damage.The scale embodied in the bottom map allows the viewer to discriminate damage patterns on virtually a block-by-block basis.

Because the relationships in Figure 6 are independent of scale, the same algorithm for a specific DF can be used for increasingly smaller portions of the original map to "zoom" on areas of most intense damage.The visualization algorithm

allows personnel who are not specifically knowledgeable about structures or trained in pattern recognition to identify the locations of most severe damage for allocation of aid and emergency services. The entire process is easy to computerize, and personnel would be able to outline any part of a map with a "mouse" and click on the area so defined. In each instance of defining a smaller area for evaluation, the average DR is recalculated for the new, smaller-sized map. In this way, the average is calibrated to each new map area.

When the damage pattern recognition algorithms are combined with regional data rapidly acquired by advanced remote sensing technologies, the potential exists for accelerated management of data and quick deployment of life and property saving services. By combining an advanced GIS with advanced remote sensing, MCEER is developing the enabling technologies for a new generation of emergency response and rapid decision support systems.

Summary

GIS research on visualizing damage patterns in pipeline networks has been extended to buildings. Algorithms developed for pipelines have been modified and validated to chose optimal GIS mesh dimensions and contour intervals for visualizing post-earthquake damage patterns in buildings. This work has been performed by a collaboration with researchers working in Programs 1 and 3 on advanced technologies for loss estimation and real-time decision support systems. Robust and statistically significant regressions have been developed between the fraction of existing timber frame buildings at any damage state and the magnitudes of various seismic parameters. Such work improves loss estimation significantly and also creates advanced technology to visualize post-earthquake damage patterns in buildings for rapid decision support and deployment of emergency services.

References

Housner, G. W., (1959), "Behavior of Structures During Earthquakes," *Journal of Engineering Mechanics Division*, ASCE, Vol. 85, No. EM4, pp. 109-129.

Katayama, T., Sato, N., and Saito, K., (1988), "SI-Sensor for the Identification of Destructive Earthquake Ground Motion," *Proceedings, 9th World Conference on Earthquake Engineering*, Vol. VII, Tokyo-Kyoto, Japan, August, pp. 667-672.

NAHB Research Center, (1994), *Assessment of Damage to Residential Buildings Caused by the Northridge Earthquake*, Reported Prepared for U.S. Department of Housing and Urban Development by NAHB Research Center, Upper Marlboro, MD.

O'Rourke, Thomas D., Toprak, Selcuk, and Jeon, Sang-Soo, (1999), "GIS Characterization of the Los Angeles Water Supply, Earthquake Effects, and Pipeline Damage," *Research Progress and Accomplishments 1997-1999*, Multidisciplinary Center for Earthquake Engineering Research, University at Buffalo, July, pp. 45-54.

Toprak, S., O'Rourke, T.D., and Tutuncu, I., (1999), "GIS Characterization of Spatially Distributed Lifeline Damage," *Proceedings, 5th US Conference on Lifeline Earthquake Engineering*, Seattle, WA, ASCE, Reston, VA, August, pp. 110-119.

Wessex (1996), *U.S. Demographics*, Wessex, Inc., Winnetka, IL.

Seismic Evaluation and Retrofit of the Ataturk International Airport Terminal Building

by Michael C. Constantinou, Andrew S. Whittaker and Emmanuel Velivasakis

Research Objectives

MCEER was part of a team charged with the seismic upgrade of Istanbul's Ataturk International Airport Terminal Building. The project involved analysis of post-earthquake damage to the Terminal Building following the 1999 Marmara, Turkey earthquake, and development of a retrofit scheme. Nonlinear static and dynamic analyses were conducted using procedures set forth in FEMA 273 (including numerous contributions from MCEER researchers). Pushover analyses were conducted using IDARC (developed with MCEER support). Dynamic analyses of the roof-isolated structure considering inelastic frame behavior were conducted using computer software based on modifications of program 3D-BASIS (developed with MCEER support). Several retrofit schemes were investigated, including conventional methods and materials, and new technologies. The scheme selected included isolation of the roof trusses, addition of shock transmission units, and selected retrofit and strengthening of reinforced concrete construction.

The Turkish build-operate-transfer consortium, TEPE-AKFEN-VIE (TAV) and its advisor, New York-based Turner International, approved the evaluation and retrofit scheme. Members of the team were LZA Technology, a division of Thornton-Tomasetti Group (leader), Michael C. Constantinou and Andrew S. Whittaker (formerly of PEER), both of the University at Buffalo, and Tuncel Engineering and Fondsiyuon Muhendislik Insaatvetic Ltd., both of Istanbul. The project is an excellent example of bringing research results to implementation.

At the time of the August 19, 1999, Izmit earthquake, the new Ataturk International Airport Terminal building was nearing completion. The airport, which is located 25 km from the center of Istanbul, was shaken and damaged by the earthquake. (The airport is located approximately 70 km from the fault rupture plane.) The new Terminal building is a three-story reinforced concrete building with a space-frame roof. The plan footprint is approximately 240 m by 168 m. A view of the terminal building is presented in Figure 1.

Sponsors

LZA Technology, Thornton-Tomasetti Group

National Science Foundation, Earthquake Engineering Research Centers Program

Research Team

***Michael C. Constantinou**, Professor, **Andrew S. Whittaker**, Associate Professor, **Oscar Ramirez**, Graduate Research Assistant, **Ani Natali Sigaher**, Graduate Research Assistant, **Eric Wolff**, Graduate Research Assistant, and **Tony Yang**, Undergraduate Student, Department of Civil, Structural and Environmental Engineering, University at Buffalo*

***Emmanuel Velivasakis**, Senior Vice President, LZA Technology, New York, New York*

Collaborative Partners

- ***Eric Stovner*** *and* ***John Abbruzzo****, LZA Technology*
- ***Anoop Mokha****, Vice President, Earthquake Protection Systems*
- ***Douglas Taylor****, Taylor Devices*
- ***Faruk Tuncel****, Engineer of Record, Tuncel Engineering and Construction Co., Ltd., Turkey*
- ***Thomas J. McCool****, Project Engineer and Construction Consultant, Turner Steiner International, New York*
- ***Sani Sener,*** *CEO, and* ***Gokhan Ozber****, Deputy General Manager, Tepe Akfen Vie (TAV), Investment Construction and Operation Inc., Turkey (Airport Owner)*

■ Figure 1. New Ataturk International Airport Terminal Building

The lowest story of the building provided mechanical and baggage handling services. The second and third stories of the building housed the Arrivals and Departures Halls, respectively. A plan view of the building is shown in Figure 2a. As shown in Figure 2a, the 240 m by 168 m building is composed of 20 pods (or independent frames); the typical pod dimension is 48 m by 48 m. A typical pod is shown shaded in this figure. The pods were separated by 50 mm wide expansion joints (EJs). Figure 2b shows the framing in the third and second stories of a typical pod; the framing in the first story was similar to that in the second story. Figure 2c is a cross-section through the building showing typical framing. The building is framed in reinforced concrete. Above the third floor level, cantilever columns on 24 m centers supported a three-dimensional steel space-frame roof structure. The space-frame roof was equipped with sleeved movement joints to permit thermal expansion and contraction of the roof. These movement joints did not align with the expansion joints in the reinforced concrete framing. At the third floor and below, gravity loads were supported by reinforced concrete waffle slabs and columns at 12 m on center. Lateral loads were resisted by waffle-slab moment-frame construction in each direction. Solid beams of a depth equal to that of the waffle slab spanned between the columns. Around the perimeter of each pod, the column sizes were substantially reduced from those in the interior of the pod. At the corners of each pod, the four columns were approximately square but with dimensions one-half of those of the interior columns (and called

It is anticipated that this project will be of interest to building owners in seismic regions throughout the world. Three different retrofit approaches were taken, to strengthen various sections of the building. The performance of the seismic isolation and lock-up devices in future seismic events will provide additional data on their reliability and effectiveness for earthquake hazard mitigation. The entire evaluation and subsequent installation of the retrofit scheme was accomplished in less than four months.

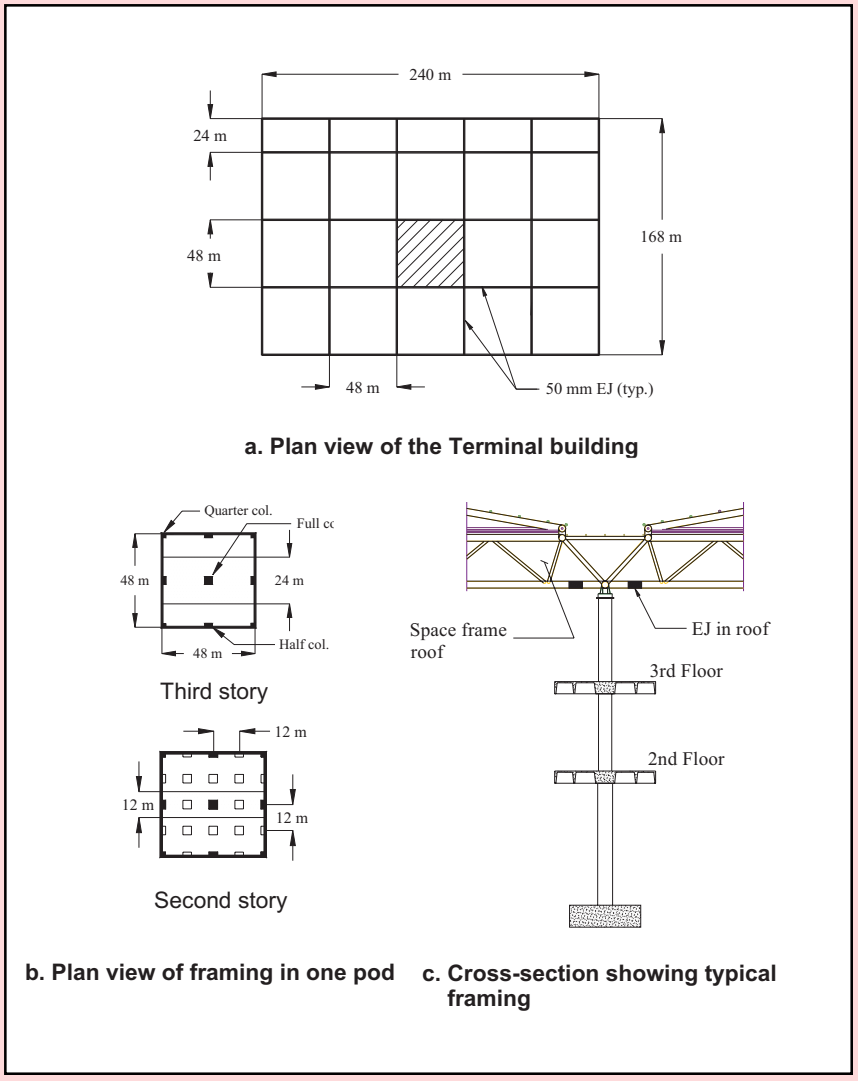

■ Figure 2. Construction of the Terminal Building

Links to Current Research

- *The seismic evaluation procedures used in this project were developed with full or partial MCEER support, including IDARC 4.0, 3D-BASIS, FEMA 273/274 and NEHRP 2000.*

quarter columns in this paper). Along each edge of each pod, and between the corner quarter columns, the columns were approximately rectangular and half the area of the typical interior columns (and called half columns in this paper.)

During the August 19, 1999 earthquake, the Terminal building was subjected to modest earthquake shaking. The maximum recorded horizontal ground acceleration recorded at the Airport was approximately 0.1 g; the maximum vertical acceleration was less than 0.05g. Investigations by LZA engineers immediately following the earthquake identified damage to parts of the building, including spalling of the cover concrete and buckling of the longitudinal rebar at the base of the third story columns (showing also lap splices and little transverse rebar in the hinge zones), loss of concrete at the underside of the roof truss-cantilever column connections and slippage of the roof-truss baseplates atop the columns,

Web Sites

Overall Project Information:
***LZA Technology**:*
http://www.lzagroup.com

Hardware Information:
Earthquake Protection Systems:
http://earthquakeprotection.com
Taylor Devices:
http://www.taylordevices.com

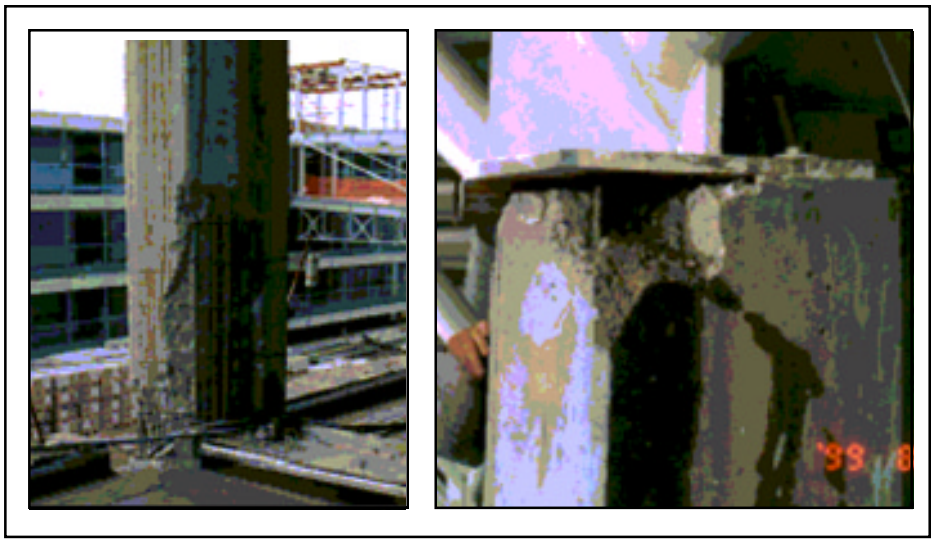

Figure 3. Observed Damage to the Terminal Building; base of third story column (left) and base of roof truss connection to column (right)

and splitting cracks and spalled concrete in the beam-column joints at the third floor level (indicating no transverse reinforcement in the joints). Photographs of damage to the building are shown in Figure 3.

Seismic Evaluation of Terminal Building

One frame in one of the typical 48 m by 48 m pods was selected for evaluation by nonlinear static analysis.The objectives of the analysis of the existing building were to (a) correlate the locations of the observed damage and that predicted by analysis, (b) to estimate the displacement capacity of the existing framing system, and (c) to provide guidance to the design team on plausible retrofit schemes. The lightly shaded zones in Figure 2b indicate the location and width of the sample frame.The central bay of framing was selected because it included the third story cantilever columns that were damaged during the earthquake.This frame was 24 m wide above the 3rd floor level and 12 m wide at that level and below.

The nonlinear static (or push-over) analysis was conducted using the procedures set forth in FEMA 273 (FEMA 1997).The existing framing was modeled using the as-built construction drawings. The tributary widths of the waffle-slab or beam framing for stiffness calculations was set equal to 12 m; the strength of the beam framing was based on the reinforcement in the solid segments of the waffle slabs between the column. The third-story columns were linked at the roof level by rigid axial elements to simulate the effect of the space-frame roof structure.The deformation capacities of the reinforced concrete components were set equal to the values listed in Chapter 6 of FEMA 273 for reinforced concrete columns, beams, and beam-column joints. Because little transverse reinforcement was provided in the critical or hinging regions, the deformation capacities of all components were established

assuming non-conforming transverse reinforcement. A sample calculation for the third-story column showed a maximum plastic rotation of 0.01 radian for the performance level of collapse prevention because the axial load ratio was less than 0.1, the transverse reinforcement was non-conforming, and the shear force ratio was less than 3. A target displacement for the pushover analysis was established based on revised criteria established by the owner after the August 19 earthquake, namely, a spectrum with ordinates equal to 150 percent of the elastic spectrum set forth in the 1997 Turkish seismic code for the site of the airport. The resulting target displacement at the roof level was 230 mm for an elastic period of 1.25 seconds.

The pushover analysis was accomplished using IDARC 4.0 (Valles et al., 1996). The existing building was analyzed using two lateral-load profiles; second-order effects were automatically included. For this frame, both a uniform pattern and a modal pattern were used. The collapse mechanism involved hinging of the third story cantilever columns for both loading profiles. Figure 4 presents the base shear-roof displacement relationships for the two lateral-load profiles. The significant difference between the two curves is due to the large differences between the weights at the roof and lower levels and the resulting differences between the loading profiles. Nearly all of the building deformation occurs in the third story of the building with the modal load pattern and the framing below the third story does not yield. Such a distribution of predicted damage is completely consistent with the observed damage

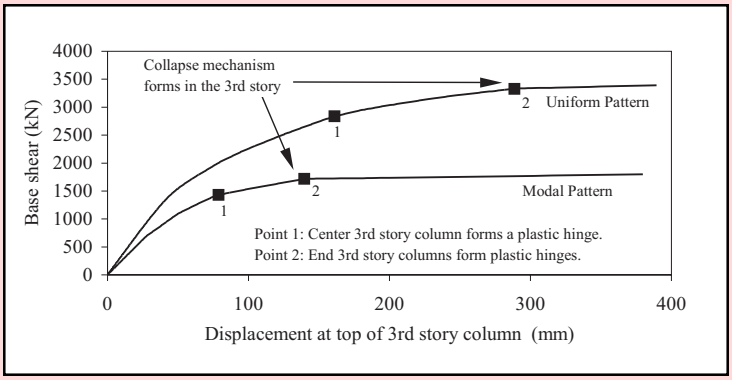

Figure 4. Pushover Analysis of a Frame in the Original Building

to the reinforced framing with one exception: the beam-column joint damage was not predicted because these joints were assumed to be rigid for the analysis. For information, the third-story drift corresponding to a plastic rotation of 0.01 radian in the third-story column was 80 mm. Clearly, the deformation capacity of the third-story columns would be exhausted well before the target displacement at the roof level was achieved. Further evaluation of the existing building showed that the moment-resisting frames were undesirable weak column-strong beam frames.

Conventional and Protective Systems Retrofit Concepts

Retrofit schemes for the Terminal building were developed using conventional methods and materials and new technologies. The conventional retrofit options considered by the design team all made use of a new ductile lateral-force-resisting system, including steel braced frames, special reinforced concrete shear walls, and special reinforced concrete moment frames. All of the conventional retrofit schemes in-

cluded new foundations under the new lateral-force-resisting components, repair and reconstruction of the third-story column to roof-truss framing, elimination of the expansion joints between the pods, joining and jacketing adjacent quarter and half columns, and jacketing of the interior third-story columns. The addition of a new lateral-force-resisting system was not considered feasible because substantial new vertical elements (walls or braced frames) could not be installed in or below the first story.

New technologies in the form of seismic isolation and supplemental damping were evaluated for the retrofit of the Terminal building. Because the addition of supplemental damping devices would have involved the addition of braces or wall panels in the lower two stories of the building, a detailed retrofit design using supplemental dampers was not prepared. Two seismic isolation options were considered: base isolation of the entire building, and isolation of the roof trusses. The building isolation option was the preferred option of the two, but was rejected by the owner because of the advanced state of construction of the building. The installation of an isolation system immediately above the foundation would have required the demolition and reconstruction of the ground floor of the Terminal building, and the removal and reinstallation of the mechanical and baggage handling systems located in the first story of the building. The second isolation option was studied in detail, and was selected for the retrofit of the building by the owner. Information on this retrofit scheme is presented below.

Retrofit (Upgrade) of the Terminal Building

This scheme selected for the retrofit (or upgrade) of the Terminal building involved the isolation of the roof trusses to reduce the demand on the third story columns and the framing at the lower levels, the addition of shock transmission units to the roof trusses to lock the space-frame truss pods together during earthquake shaking so that the space frame would act as a diaphragm, and selected retrofit and strengthening of the reinforced concrete construction as summarized below.

Because of architectural constraints, the size of the third story columns could not be increased substantially, so the existing flexural strength of these columns as cantilever elements dictated the inertial force that could be developed at the roof level. Fuses in the form of Friction Pendulum (FP) isolation bearings were used to limit the lateral forces that could be imposed on the third-story columns. (FP bearings were used because such bearings can isolate light components and structures.) Preliminary calculations called for an isolated period of 3.00 seconds (based on the radius of the sliding surface), a design friction coefficient of 0.09, and a displacement capacity of approximately 260 mm.

The quarter and half columns around the perimeter of each pod were joined to the adjacent quarter and half columns respectively using reinforced concrete. Additional vertical reinforcement was placed in the joints between the part columns and around the perimeter of the joined columns to

further strengthen the columns. The objective of such strengthening was to eliminate the weak column-strong beam framing. These columns and the modestly strengthened interior square columns were then jacketed with circular steel casings to substantially increase the shear strength of all the columns and to provide confinement in potential hinge regions. Such column strengthening was implemented in the second and third stories. In addition, the expansion joints between the pods at the second and third floor levels were eliminated by tieing the pods together with reinforced concrete components to substantially increase the redundancy of the lateral-force-resisting system. No beams at either the second or third floors were strengthened.

The performance of the retrofitted building was checked by nonlinear static analysis of the frame described above. The resulting pushover curve for the modal load pattern is presented below in Figure 5 together with a sketch showing the sequence of plastic hinge formation (1 through 20). Note that some hinges form simultaneously. For a roof displacement less than 500 mm, hinges form in the beams, at the base of the columns above the foundation, and in the two-story columns at the underside of the third story only.

The retrofit design was further evaluated by nonlinear dynamic analysis using 20 ground motion records that matched on average the revised design spectrum described above. The mean maximum displacement at the roof level of 190 mm is indicated by the open-ended arrow on the pushover curve of Figure 5. The deformation demands on the beams and columns in the retrofitted building frame at this roof displacement were considered acceptable for the performance level of collapse prevention.

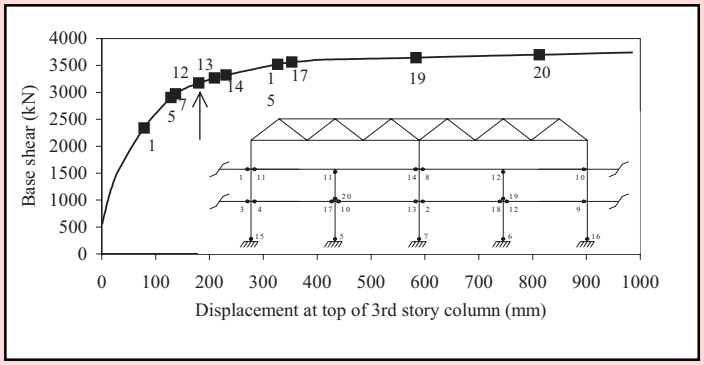

■ Figure 5. Pushover Analysis of the Retrofitted Frame

Two photographs of the retrofit work showing an installed FP bearing (before release) and a jacketed column (covered by an architectural treatment) are presented in

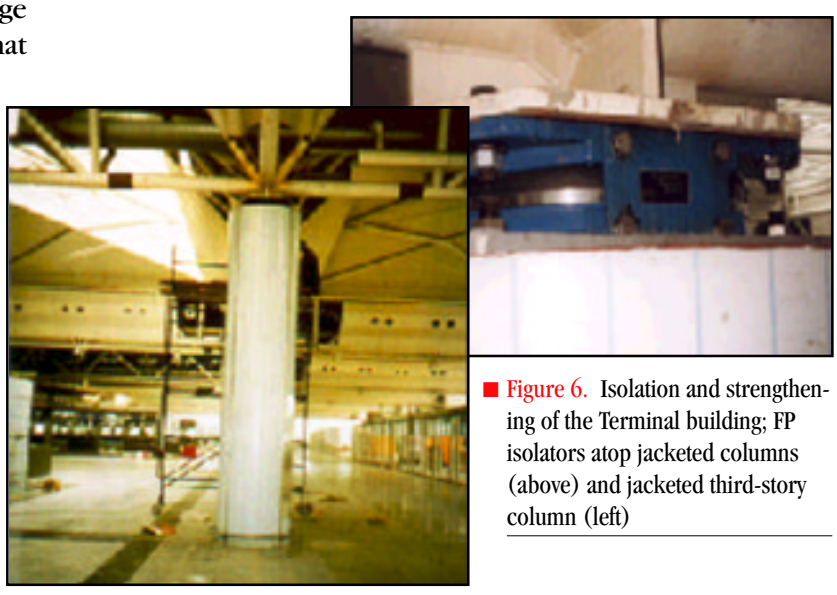

■ Figure 6. Isolation and strengthening of the Terminal building; FP isolators atop jacketed columns (above) and jacketed third-story column (left)

Figure 6. No retrofit work was undertaken in either the first story or to the foundations. The nonlinear static analysis and the nonlinear dynamic analysis indicated no inelastic action in the first story above the footings, in part because the columns in this story were substantially stronger and taller than the columns in the stories above. Retrofit of the footings beneath the existing columns was not feasible given the advanced state of the construction at the time the retrofit scheme was developed.

Summary and Conclusions

An innovative retrofit and upgrade scheme was developed and implemented for the new Ataturk International Airport Terminal building, which was damaged during the August 19, 1999, Izmit earthquake. The retrofit scheme involved the use of conventional strengthening and seismic isolation hardware to avoid building collapse in the event of a maximum earthquake. The efficacy of the retrofit scheme was demonstrated by nonlinear dynamic and static analysis. The studies of the existing building and the development of the retrofit schemes commenced in late September 1999, and the retrofit construction work was completed by the end of December 1999: a period of approximately 12 weeks.

References

FEMA, (1997), *NEHRP Guidelines for the Seismic Rehabilitation of Buildings*, Report No. FEMA 273, Federal Emergency Management Agency, Washington D.C. October.

Valles, R.E., Reinhom, A. M., Kunnath, S. K., Li, C and Madan, A., (1996), *IDARC2D Version 4.0: A Computer Program for the Inelastic Damage Analysis of Buildings*, Report No. NCEER-96-0010, National Center for Earthquake Engineering Research, University at Buffalo, June.

Estimating Earthquake Losses for the Greater New York City Area

by Andrea S. Dargush (Coordinating Author), Michael Augustyniak, George Deodatis, Klaus H. Jacob, Laura McGinty, George Mylonakis, Guy J.P. Nordenson, Daniel O'Brien, Scott Stanford, Bruce Swiren, Michael W. Tantala and Sam Wear

Research Objectives

The goal of the project is to use the federally sponsored loss estimation software, HAZUS (Hazards–U.S.), to project the magnitude of potential losses that might be experienced by the metropolitan New York City area as a consequence of a damaging earthquake. After modification of the default HAZUS datasets for soil and building characteristics, a more credible estimation of losses will emerge and be useful to metropolitan emergency personnel, as well as to other public and private stakeholders. It is hoped that the results will contribute to improved disaster mitigation and emergency response plans throughout the area.

The metropolitan New York-New Jersey region is vulnerable to several potential natural disasters. Ice storms, snow, and other severe weather events such as hurricanes, associated storm surges, and flooding, foot-and-mouth, and the West Nile virus are among those of current concern and prominent public attention. After adding such man-made disruptions as terrorism and hazardous materials releases, and the hazards posed by decaying infrastructure and aging buildings, earthquakes seem a dim prospect. But however unrecognized or unacknowledged the threat from earthquakes may be in New York City, seismic events have occurred and, until recently, no codes have existed to mandate earthquake strengthening of structures. Statistics indicate that potential losses to a large urban area such as New York would be considerable. According to Scawthorn and Harris (1989), the economic impact of a damaging earthquake (e.g., M6.0) in New York would be in the billions of dollars due to direct structural and architectural damage, and does not reflect additional impacts on building contents, business continuity, fire suppression and human safety. An earthquake in the greater New York area would thus be considered a low-probability, yet high consequence event. Credible estimates of future loss can be effective tools to encourage area stakeholders to mitigate against the possible future damaging consequences of earthquakes.

Hazards U.S. (HAZUS) is a standardized, nationally-applicable loss estimation tool, developed by the Federal Emergency Management Agency (FEMA) in cooperation with the National Institute of Building Sciences. The HAZUS software utilizes geographic information systems, such as

Sponsors

National Science Foundation, Earthquake Engineering Research Centers Program
Federal Emergency Management Agency
Federal Emergency Management Agency Region II
New Jersey Office of Emergency Management
New York State Emergency Management Organization

Research Team

***George Mylonakis**, **Walter Fish** and **Paul Spiteri**, The City College of the City University of New York*
***Bruce Swiren**, Federal Emergency Management Agency, Region II*
***Klaus Jacob**, **Noah Edelblum** and **Jonathan Arnold**, Lamont Doherty Earth Observatory*
***Andrea Dargush**, **Michael Kukla** and **Montree Polyium**, MCEER*
***Scott Stanford**, New Jersey Geological Survey*
***Michael Augustyniak**, New Jersey State Police Office of Emergency Management*

Research Team continued on page 2

Research Team (cont.)

***Dan O'Brien**, New York State Emergency Management Office*
***Dan Cadwell**, New York State Geological Survey*
***George Deodatis**, **Guy Nordenson**, **Michael Tantala** and **Amanda Kumpf**, Princeton University*
***Sam Wear**, **Laura McGinty** and **Andrea Albert**, Westchester County Geographic Information Systems, Department of Information Technology*

ArcView and MapInfo, to produce detailed maps and analytical reports that describe a community's potential losses. The current version applies a uniform engineering-based loss estimation approach to quantify damages, economic losses and casualties resulting from earthquakes. Future adaptations are intended to carry out similar analyses for hazards such as flooding and high wind.

Similar loss modeling studies have been conducted in the New York area in past years to examine the impact of flooding and hurricanes, and have been used to guide emergency plans. Recognizing the potential collective benefits of a regional study, mitigation specialists at FEMA Region II, the New York State Emergency Management Agency (NYSEMO), the New Jersey State Police Office of Emergency Management (NYOEM) and the New Jersey Geological Survey joined together to develop a similar loss estimate for earthquakes. With NYSEMO and NJOEM, a FEMA-supported project was initiated in 1998 to apply HAZUS to the greater New York City area. A regional consortium has been formed - the New York City-area Consortium for Earthquake-loss Mitigation (NYCEM). MCEER was selected to provide general coordination of the activities and to conduct outreach activities to promote the outcomes of the project. The purpose of the consortium is to help develop the necessary databases to effectively utilize the loss estimation program HAZUS to identify potential economic loss to the greater New York City area as a consequence of a damaging earthquake. In the latter stages of Year 2, increased attention was given to inclusion of information on critical facilities, to assess post-event functionality. The consortium consists of public agency officials, business owners, emergency managers, engineers and architects, utility owners and other area stakeholders. Researchers at Lamont–Doherty Earth Observatory, Princeton University, and the City College of New York work together to develop soils and building stock inventories which can be used to refine the default data contained within HAZUS. The data will be used in future executions of HAZUS and will assist researchers in refining their ultimate loss estimations for New York.

These studies are being complemented by information generated by similar studies for Westchester County, New York and for a number of counties in New Jersey. A generalized HAZUS analysis will provide a regional picture of potential earthquake damage and loss.

These assessments will ultimately be used to encourage and promote earthquake mitigation action at the local, regional and statewide levels.

Technical Summary

After preliminary explorations of available data and its transferrability

The users of this research include emergency responders, city planners, utility managers, building owners, design and construction engineers, critical facility managers, school and hospital administrators, the public at large and other researchers.

to a HAZUS format, the NYCEM team prioritized its efforts, focusing on the development of a database of geologic and building information for Manhattan below 59th Street. As the project progressed, additional stores of data became available that allowed expansion of the study to the entire borough. In the current Year 3 of the project, results of the Manhattan study will be merged with those of parallel studies being carried out in New Jersey and Westchester County, New York, for extrapolation to a larger region covering about 31 counties in New York and New Jersey. The respective activities of the team members and the parallel studies are described in the following section. Priorities, methodologies and progress of the NYCEM team have benefited from periodic technical advisement from a panel of experts in earthquake engineering and loss modeling.

Lamont Doherty Earth Observatory (LDEO)

Based on extensive prior research, the LDEO team, led by Klaus Jacob, realized from the outset that the default soils data within HAZUS did not accurately reflect the subsurface conditions of the Manhattan area. Near surface geologic differences can introduce local variations in shaking that can influence both the amplitude and spectral composition of ground motions, thus impacting structures and lifelines.

It would be a challenge to the team to upgrade the data to produce the needed NEHRP geotechnical site classes at an individual Manhattan census tract level (Jacob, 1999). Pre-existing geological studies were geographically limited and not specific enough to derive important information on depth to bedrock. Other subsurface data collected in the form of borehole logs, were collected by private developers or other entities, holding the data as proprietary.

Using information provided by the New York City Department of Design and Construction, data from 150 geotechnical borings for lower Manhattan were studied in the first year of the project. Using casing information and results from the standard penetration tests (SPT) conducted, it was possible to derive shear wave velocity profiles as a function of depth at each location, then translated into the appropriate NEHRP site class. Some 200 other older borings were available, but only offered information on depth to bedrock.

To classify the overlying soils, a shear wave velocity vs. depth function was derived from a subset of the initial 150 borings and applied to generate point values at the 200+ sites. The resultant classifications were primarily NEHRP soil types D and C. Surprisingly, no class A (very hard rock) sites emerged, although numerous B (firm rock) sites were identified. Several individual borings indicated class E conditions. However, the conditions were not sufficiently continuous throughout the census tract to merit assignment of E to the tract.

This may be a pervasive problem associated with the census tract approach to geological classification. These differences in soil type from the default assignments resulted in apparent reductions of the total loss estimations for buildings

Collaborative Partners

- *Metropolitan Transportation Authority/ New York Transit Authority*
- *New York City Department of Design and Construction*
- *New York City Department of Finance and Operations Research*
- *New York State Geological Survey*

NYCEM Technical Advisory Committee

***Dr. Carl J. Costantino**, Professor Emeritus, Department of Civil Engineering, City College of New York*

***Mr. Ronald T. Eguchi**, CEO, ImageCat*

***Mr. Ramon Gilsanz**, Gilsanz, Murray and Steficek*

***Dr. Jeremy Isenberg**, CEO, Weidlinger Associates, Inc.*

***Dr. Stephanie A. King**, Stanford University*

***Mr. Charles A. Kircher**, Principal, Charles Kircher and Associates*

***Dr. Joanne M. Nigg**, Professor of Sociology and Co-Director, Disaster Research Center, University of Delaware*

***Dr. Thomas O'Rourke**, Professor, School of Civil and Environmental Engineering, Cornell University*

***Mr. Maurice S. Power**, Vice President, Geomatrix Consultants, Inc.*

***Mr. Thomas Z. Scarangello**, Vice President, Thornton-Tomasetti Engineers*

Links to Current Research

- *The NYCEM project is primarily linked to MCEER outreach efforts to increase awareness and acknowledgment of earthquake risk and the value of loss estimation methodologies as mitigation tools.*
- *Data collected from the project may benefit ongoing projects focusing on earthquake risk to critical facilities in areas of low-to-moderate hazard but with high collateral damage.*
- *Future phases of the project will likely benefit from MCEER lifeline research which has led to improvements in HAZUS treatment of buried pipeline systems.*

by factors of 0.7, 0.72 and 0.8 for scenario events of M_w 5.0, 6.0, and 7.0, respectively. Additional refinement of the shear wave velocity functions made possible with added calibration borings may be reflected in future loss estimates.

In Year 2, additional refinement of the lower Manhattan study area was made possible by the inclusion of additional data provided by the Metropolitan Transportation Authority/New York City Transit Authority. The study area was also expanded to include the entire borough of Manhattan. In spite of the additional information, data density was greatest for midtown and lower Manhattan and sparse for areas north of 137th St..

Modifications were made to the methodology developed in Year 1 to reflect consideration of the NEHRP 10-foot rule, which assigns site category E to any soil profile that contains a continuous ten-foot thick layer of very soft soils (Jacob, 2000). Additional study also led to the increase in the calculated shear wave velocity for bedrock at the bedrock/soil interface, better reflecting the prevailing rock formations in the area. Site classes for all DDC borings in Year 1 were recalculated under these assumptions.

A primary product in Year 2 is a census-tract based soil map for the entire borough, which can be used in validating results, generated by HAZUS. Figure 1 describes the distribution of soil/rock types across the island, with higher elevations in uptown Manhattan on stiff rock/soil (Class B), intermediate type C in Midtown, and soft soil (Class D) in lower Manhattan, along the identified fault zones in Upper Manhattan and in low-lying, coastal areas. An anticipated product of this effort will be the development of a contoured soils map for Manhattan. This will allow more accurate extrapolation of census-tract specific geotechnical characteristics.

An important Year 2 activity was the coordination of approach to classification of soils among the New York City, New Jersey and Westchester County study areas. With input from members of the NEHRP Seismic Provisions Geotechnical Subcommittee and the Building Seismic Safety Council, a uniform methodology was derived to assure that assumptions used to assign NEHRP soil class types are, to the extent possible in agreement with the objectives of the NEHRP guidelines. There was

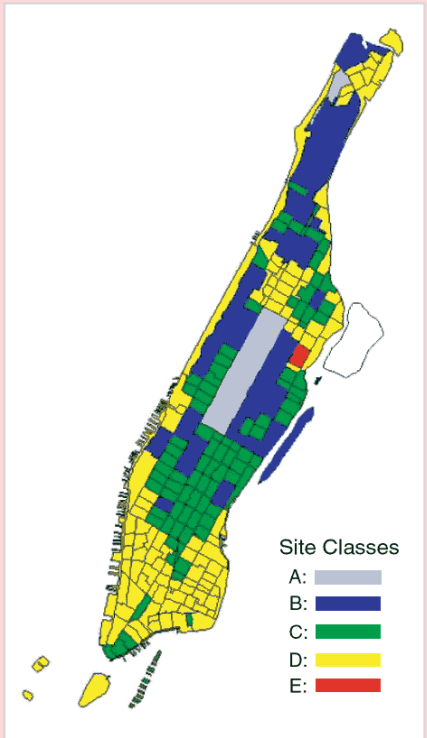

Figure 1. NEHRP Site Classes for Manhattan by Census Tracts

general consensus that the information needed to accurately assign NEHRP classes is often unavailable and that in view of other inherent uncertainties within the HAZUS algorithm, it should not unduly impact results.

The HAZUS algorithm is designed to execute loss estimations using both deterministic and probabilistic earthquake inputs. Using historical local seismic events, the LDEO team also provided the epicentral locations for scenario earthquake events to be used in the deterministic HAZUS executions.

Princeton University

New York City has one of the highest concentrations of high rise buildings per square foot than any other city. Unreinforced masonry structures housing businesses, architectural treasures, masonry fire stations, theaters and art galleries, apartment buildings, and more, stand shoulder to shoulder with these skyscrapers.

Many New York structures hold historical status and many more were constructed without the guidance of a seismic building code. Before 1996, earthquakes were not a design consideration although as construction progressed in the 20th century, wind load factors were being incorporated, thus addressing (albeit coincidentally) some of the horizontal displacements that might be experienced during an earthquake.

Even today, seismic statutes apply to new construction only. Consensus opinion is that retrofitting thousands of New York buildings to meet seismic standards is impractical and economically unrealistic. It is therefore even more important to accurately identify areas of highest potential vulnerability to earthquake ground shaking so that mitigation, emergency response and recovery approaches can be strengthened.

In HAZUS, the default building inventory is categorized by occupancy (commercial, residential, industrial, governmental, educational, religious, agricultural), model building type (e.g., steel, reinforced concrete, wood, masonry), structural configuration and height. HAZUS also makes other assumptions about typical percentage distribution of buildings within a census tract by age, quality (inferior, built to code, superior) seismic design level (low, moderate and high) and height. The NYCEM team at Princeton University (Guy J. P. Nordenson, George Deodatis, Michael Tantala and Amanda Kumpff) recognized the obvious disparities between the typical suburban building inventory presented in HAZUS and the actual structural characteristics of New York. Such disparities would ultimately affect the accuracy of damage and loss scenarios to be generated by the program.

One of the objectives of the studies being carried out at Princeton is to develop a credible building inventory for the New York City area, which will be more representative of its wide mix of structures. Various damage and loss scenarios would then be carried out, using both the improved building data and the soils data provided by the LDEO team.

In Year 1 of the study, the team used Sanborn fire insurance map data (building height, size, location, occupancy and type) and visual inspection to modify building inventories for two representative

Web Sites

New York City-area Consortium for Earthquake Hazard Mitigation:
http://www.nycem.org

Federal Emergency Management Agency HAZUS:
http:www.fema.gov/hazus

Westchester County GIS:
http://giswww.co.westchester.ny.us

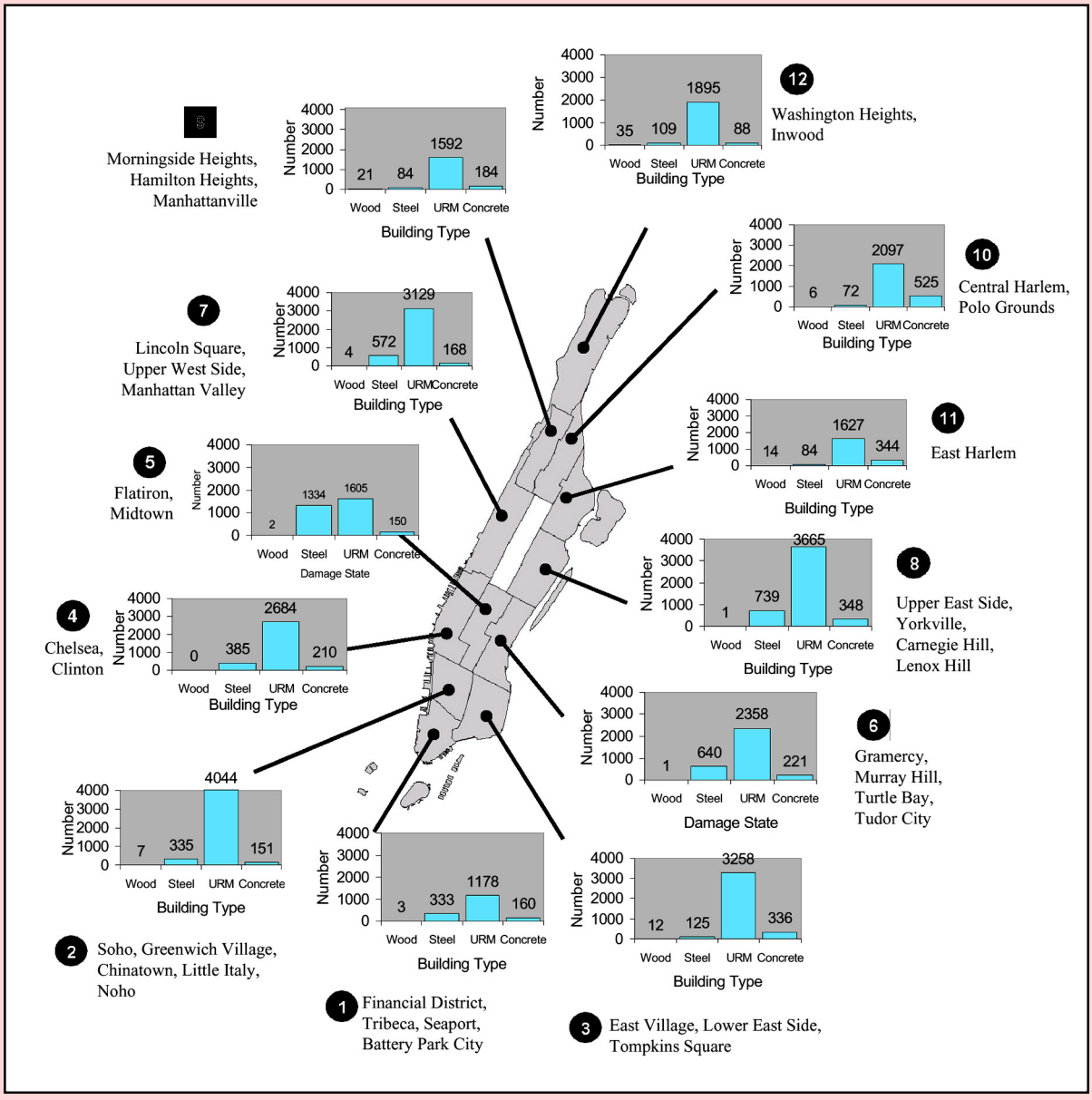

Figure 2. Building Count by Structural Type and Neighborhood

census tracts – Wall Street (primarily commercial) and Kips Bay (primarily residential) (Nordenson et al., 2000). Broader regional studies examined New York below 59th Street, and the 31 county, New York-New Jersey area. HAZUS runs were then carried out to assess the sensitivity of the methodology to changes in building inventory data. Dramatic differences in loss estimates emerged, particularly when using smaller magnitude earthquakes. Total loss estimates in the modified runs differed significantly from those of the default (in some cases more than a factor of ten). Based on the runs, it appears that the most sensitive building information for refined loss estimations might be square footage and height, and not structural type, as previ-

ously assumed. This will require further validation.

With assistance from Dr. Jack Eichenbaum, New York City Assessor, the Princeton team acquired valuable building data from the New York City Department of Finance. The Mass Appraisal System (MAS) data consists of over 2 million property entries for the entire city, including such information as parcel square footage, address, height, use, building footprint dimensions, construction year, quality, and architectural style (Tantala et al., 2001).

The year 2 studies used this information to further refine the building inventory, although geocoding of entries was needed to match information to the appropriate census tract. In addition the richness of the MAS data required simplification to fit into the HAZUS categorization scheme.

In contrast, the MAS construction type data required addition of more specific information. Field surveys were carried out with the City College team and were used to validate some of the existing data as well as some of the associated assumptions being made. Additional data sources from local engineers, Dun and Bradstreet business databases, aerial photography, existing structural drawings and other sources helped to further validate the new database.

After thorough modification, the resultant MAS database included records for more than 37,000 buildings, or over 2.2 billion square feet of area. Figure 2 shows the relative distribution of the number of buildings in each of four category types for twelve Manhattan neighborhood districts, illustrating that unreinforced masonry is the predominant building type. This is not, however, reflected in the amount of square footage occupied by unreinforced masonry, which is perhaps a more important variable.

In the end, the Princeton team was able to establish the building inventory for the entire island of Manhattan, with HAZUS-required information at the individual building level. This is a unique accomplishment for HAZUS applications. With the assistance of Princeton student Evan Schwimmer, the database has been further enhanced with the addition of critical facilities data (hospitals, schools, and police and fire stations). Several preliminary probabilistic and deterministic HAZUS runs have been carried out using the critical facilities data to generate projected functionalities of schools, hospitals, and police and fire stations, to assess their relative capabilities to provide shelter, provide emergency care and control conflagration. Casualties, population displacement and short- and long-term economic changes have also been projected. These are described in detail in the Year 2 report, which may be found at the NYCEM website.

These subsequent HAZUS (1999 and SR-16 versions) runs used the improved building inventory and further verified the need for improved data sources for buildings and soils to derive credible damage, loss and casualty estimates.

Westchester County, New York

Under sponsorship of the New York State Emergency Management Organization, a collaborative study was carried out in Westchester County, New York. The study evalu-

"It is important to accurately identify areas of high potential vulnerability to earthquakes so that mitigation, emergency response and recovery approaches can be strengthened.

ated the applicability of the HAZUS default datasets, and made appropriate modifications to the extent possible.

Considerable effort was dedicated to data collection and to the updating of the HAZUS datasets, in particular, additions of information on essential facilities (McGinty and Wear, 2001). Important new coverages were included for such facilities as day care centers and senior housing. Additional efforts were focused on the inclusion of information on essential facilities such as hospitals, schools, police and fire stations, and emergency medical services.

This led to the identification of shortfalls in county data availability and development of a strategy for future data creation. In the absence of borehole data, scientists at the New York State Geological Survey assisted by conducting seismic shear wave velocity tests on surficial soils within the county. Tests were conducted in locations of different NRC-defined soil types so that a larger scale surficial soils map could be developed. Data was then extrapolated to a census tract level for necessary seismic soil classifications.

The Westchester study culminated in a HAZUS execution based on three earthquake scenarios. The goal of the study is to provide loss estimation data to the sponsor to enable development of a statewide mitigation approach for potential future earthquakes.

New Jersey

Under the oversight of Michael Augustyniak at the New Jersey Office of Emergency Management, studies were carried out by the New Jersey Geological Survey to define areas of seismic hazard. Building inventory data was collected for selected areas to upgrade HAZUS inventory data.

Geologic data were acquired and analyzed in order to compile maps of seismic soil class and liquefaction susceptibility for Hudson County, New Jersey (Stanford, 1999). The soil class and liquefaction susceptibility data were entered into the HAZUS model for each census tract in the county.

The HAZUS model was run with the upgraded geologic data and with the default geologic data for earthquake magnitudes of 5, 5.5, 6, 6.5, and 7. The upgraded building inventory data has not yet been included in the runs but is presently being processed by the Princeton team.

The upgraded geologic information produced significant changes in both the spatial distribution of damage and the total damage estimates. This increased building damage was particularly notable in the Hudson waterfront and Hackensack Meadowlands areas of the county, where soils are softer and more liquefiable than HAZUS default soil.

Building damage was less on the Palisades Ridge and on uplands in Kearny and Secaucus, where soils are stronger than the default. Because most building construction in the county is concentrated on these ridges, the total estimated building damage is somewhat less with the upgraded geologic data than with the default data at all magnitudes. Additional mapping and scenario executions have also been carried out in Bergen county, with Essex County underway.

In addition to the HAZUS data upgrades and scenarios executions,

shear-wave velocities were measured on the three softest soil types at nine locations. These were conducted to validate the soil class assignments used in the scenario executions, which use test-drilling data as a proxy for shear-wave velocities. The measured velocities confirmed the assignments. An additional 13 shear wave velocity measurements completed in Bergen County on four soil types indicate once again that the SPT data accurately proxy for shear wave velocities, except in gravel rich areas. These have faster velocities than SPT values suggest. Soil classes were adjusted accordingly in these areas.

City College of New York

To support the ongoing activities and to add some additional validation checks, MCEER provided support to George Mylonakis, CUNY, and his team of undergraduate engineering students to conduct field surveys of building inventory data. Their objectives were to assess the accuracy of both the default HAZUS building inventory data and to verify and benchmark the MAS data for two of three representative census tracts.

After initial training in HAZUS, the team carried out walking surveys of the Rockefeller Plaza census tract and a portion of the Kips Bay census tract. Buildings over a 10-block area were photographed, with data collected on frame type, exterior wall type, basement grade, construction quality, exterior condition, existing damage, HAZUS building code, and occupancy. These categories correspond to the required data fields within HAZUS (Mylonakis, et al., 1999). A total of more than 600 buildings were surveyed by the CUNY and Princeton teams.

Survey data was input into an ACCESS database and compared against the default data. The differences between the default and actual data were quite evident for the number of buildings and for the percentage of residential buildings. There is also a significant difference between the actual data and default data for the number of commercial buildings. The HAZUS dataset depicts a greater variety of building types within a census tract than actually exists. These led to further differences in loss estimations carried out for these areas.

To further validate the data sensitivity, the CUNY team generated HAZUS loss estimates for Kips Bay, Rockefeller Center and Wall Street census tracts (Mylonakis, 2000). The Wall Street tract data were collected by the Princeton team. Using a fixed location (1884 Rockaway Beach) scenario earthquake at varying magnitudes, the default and modified datasets were used to generate costs of structural damage. The 1999 version of the HAZUS software was used. The Princeton group conducted similar analyses using HAZUS version '97. Good agreement existed between the results generated by different versions of HAZUS.

Outreach

Several years after the passage of seatbelt legislation, drivers and passengers still disregard the need for simple protective actions. Convincing the public, the government and the private stakeholders in the northeastern United States of the

"The goal of the Westchester County study was to provide loss estimation data to enable development of a state-wide approach to potential future earthquakes."

need to prepare for an earthquake is a challenge not easily met. It has been an important objective of this project to convey that a low-probability event is a potential reality, carrying with it consequences for which the metropolitan area may be ill prepared.

The NYCEM project has taken advantage of numerous media opportunities to disseminate this information and to explain the importance of accurate inventories and loss characterizations to the development of mitigation strategies. The work has been featured in several articles in the New York Times and other area newspapers, has been the subject of a news focus piece on WNBC-News and has recently been prominently broadcast in the Discovery Channel program, "Earthquakes in New York?" The awareness campaign was further augmented by a minor tremor that struck midtown Manhattan, January 17, 2001 (see Figure 3). This attention, combined with the leadership of Bruce Swiren of FEMA Region II and Dan O'Brien of New York State Emergency Management, has helped to open dialogues with City and metropolitan area emergency managers about the importance of earthquake hazard mitigation.

In addition, conventional outreach activities have been carried out, targeted toward regional stakeholders who can both assist in refining the model through data provision, and can benefit from the enhanced loss estimation model. Workshops and briefings have increased their interest in the project and have led to sharing of information and data necessary to refine the default HAZUS data. Metropolitan transportation engineers are interested in being part of possible future studies that would include transportation lifelines in the model.

Project results are made widely available. A NYCEM website has been established by MCEER, which serves as a repository for technical reports, data and maps generated by the team. NYCEM results are reported regularly through the MCEER Bulletin and on the web, and several additional information briefings will be featured throughout the final year of the program. At the completion of the program, all data will be publicly accessible through a central repository.

■ Figure 3. Epicenter of January 17, 2001 Manhattan Earthquake (courtesy of Dan O'Brien)

Conclusions and Future Research

The study has revealed variances in HAZUS default data that would, left uncorrected, compromise its ability to accurately project potential losses due to a damaging earthquake. Loss quantifications generated by HAZUS have been found to be sensitive to variations

in building inventory data, earthquake magnitude and local soil conditions.

In some cases, the damage and loss values generated were notably higher using default data than with the upgraded building and soils information. The data collection and modification activities have substantially enhanced the program's ability to become a credible forecast instrument of economic impact.

These activities have also significantly improved the general knowledge base about New York area geology and have led to the development of a more comprehensive building inventory that can be used by others. In fact, it is notably the first database where the building inventory has been described in a building-by-building manner, which is not only unique, but quite valuable to future regional studies. The ability of the NYCEM team to build this information base is notable, since available data for such a complex and large urban area was difficult to identify and obtain. Surmounting this initial obstacle has been an important achievement of the project. Reconciling this information to the census-tract based approach of HAZUS has also been an intensive and challenging effort.

In an area of such vast and vital economic activity, it is paramount that any estimation of potential economic impact be based in well-founded data and analysis. While both the methodology, its inherent uncertainties, and its associated datasets have come under question, HAZUS is being utilized in other large urban areas with higher levels of seismic hazard as a tool to assist area planners, responders, and other stakeholders.

The studies conducted have established a foundation for more complete loss estimation studies for the greater New York metropolitan area. Additional data collection and study of regional lifeline systems, including water, gas and highway systems, will significantly enhance the risk characterizations that HAZUS can provide for the New York City area.

Further involvement by emergency responders, planners, builders, and health and human services officials will help improve the effectiveness of these studies. Accurate and complete fingerprints of risk, enabled by more widespread participation by other stakeholders, will ideally lead to the development of an acceptable damage and loss indicator that can be embraced by responders, builders and the public.

This goal has been encouraged as this study has progressed into its third year, as several presentations of results to municipal agencies has led to greater coordination, in particular with the New York City Office of Emergency Management and with officials in Westchester County.

"The NYCEM project has taken advantage of numerous media opportunities to disseminate information and explain the importance of accurate inventories and loss characterizations."

Acknowledgements

The author would like to recognize and acknowledge the efforts of the following individuals: Bruce Swiren, FEMA Region II, and Dan O'Brien, New York State Emergency Management Office, for their sponsorship and leadership; Elizabeth Lemersal, FEMA, for overall support of the program; and Dr. Jack Eichenbaum, City Assessor, New York City Department of Finance, and Dr. A. N. Shah, Metropolitan Transportation Authority/New York City Transit Agency, for their generous assistance.

References

Cadwell, D. and Nottis, G., (2000), "Seismic Hazard Assessment Data, Westchester County, New York," New York State Museum, Albany, New York.

HAZUS 99: Estimated Annualized Earthquake Losses for the United States, Federal Emergency Management Agency Mitigation Directorate, FEMA 366, February 2001, 33 pages.

Jacob, K. H., (1999), "Site Conditions Affecting Earthquake Loss Estimates for New York City," Lamont-Doherty Earth Observatory of Columbia University, Palisades, NY, New York City Consortium for Earthquake Loss Mitigation (NYCEM): Earth Science Tasks, First Year Technical Report May 6, 1999, 35 pages.

Jacob, Klaus H., Edelblum, Noah, Arnold, Jonathan, (2000), "NEHRP Site Classes for Census Tracts in Manhattan, New York City," Lamont-Doherty Earth Observatory of Columbia University, Palisades, NY, New York City Consortium for Earthquake Loss Mitigation (NYCEM): Earth Science Tasks, Second Year Technical Report, December 31, 2000, 23 pages.

Jarvis, Hugh, (1999), "Disaster Damage: Cost Issues for the New York City Area," Annotated Bibliography, MCEER Information Service.

McGinty, Laura and Wear, Sam, (2001), "Initial Earthquake Loss Estimation Analysis for Westchester County, New York," Report to New York Emergency Management Organization, Westchester Counter Department of Information Technology, Geographic Information Systems, February, 2001, 53 pages.

Mylonakis, George et al., (1999), "Earthquake Loss Estimation for the New/York City Area," NYCEM-MCEER Progress Report.

Mylonakis, George, Fish, Walter, and Spiteri, Paul, (2000), "Development of a Building Inventory for Manhattan Region," NYCEM Preliminary Technical Report.

Nordenson, G., Deodatis, G., Tantala, M. and Kumpf, Amanda, (2000), "Earthquake Loss Estimation for the New York City Area," NYCEM First Year Technical Report.

Scawthorn, C. and Harris, S. K., (1989), "Estimation of Earthquake Losses for a Large Eastern Urban Center: Scenario Events for New York City," *Annals of the New York Academy of Sciences*, Volume 558, June 16, 1989, pages 435-451.

Stanford, S. D., Pristas, R. S., Hall, D. W., and Waldner, J. S., (2000), "Earthquake Loss Estimation Study for Bergen County, New Jersey: Geologic Component," prepared for the New Jersey State Police Office of Emergency Management by the New Jersey Geological Survey, 8 p. plus appendices and plates.

Stanford, Scott, Pristas, Ronald S., Hall, David W. and Waldner, Jeffrey S., (1999), "Geologic Component of the Earthquake Loss Estimation Study for Hudson County, New Jersey," Final Report.

Stanford, S. D., Pristas, R. S., (1998), "Earthquake Loss Estimation Study for Newark, New Jersey: Geologic Component," prepared for the New Jersey State Police Office of Emergency Management by the New Jersey Geological Survey, 2 p. plus appendices and plates.

Tantala, Michael W., Nordenson, Guy J.P., and Deodatis, George, (2001), "Earthquake Loss Estimation Study for the New York City Area," NYCEM Year 2 Technical Report, 1999-2000.

Production Staff

Jane E. Stoyle, Editor
Michelle A. Zuppa, Layout and Design
Hector A. Velasco, Illustration

Acknowledgements

This report was prepared by the Multidisciplinary Center for Earthquake Engineering Research through a grant from the National Science Foundation Earthquake Engineering Research Centers Program, a contract from the Federal Highway Administration, and funding from New York State and other sponsors.

The material herein is based upon work supported in whole or in part by the National Science Foundation, Federal Highway Administration, New York State and other sponsors. Opinions, findings, conclusions or recommendations expressed in this publication do not necessarily reflect the views of these sponsors or the Research Foundation of the State University of New York.

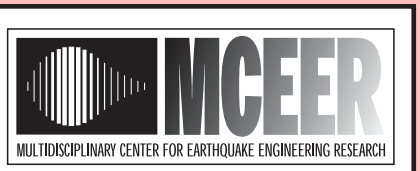

MULTIDISCIPLINARY CENTER FOR EARTHQUAKE ENGINEERING RESEARCH

A National Center of Excellence in Advanced Technology Applications

University at Buffalo, State University of New York
Red Jacket Quadrangle ▪ Buffalo, New York 14261-0025
Phone: 716/645-3391 ▪ Fax: 716/645-3399
E-mail: mceer@acsu.buffalo.edu ▪ WWW Site: http://mceer.buffalo.edu

Headquartered at the University at Buffalo